Università degli Studi di Cagliari

PhD DEGREE

Earth and Environmental Sciences and Technologies

Cycle XXXI

TITLE OF THE PhD THESIS

CONVENTIONAL BIOLOGICAL AND BIOELECTROCHEMICAL METHODS FOR THE TREATMENT OF MARINE SEDIMENTS POLLUTED BY ORGANIC COMPOUNDS

Scientific Disciplinary Sector

ICAR/03

PhD Student: Claudia Camedda

Coordinator of the PhD Programme Prof. Aldo Muntoni

Supervisor Prof.ssa Alessandra Carucci

Co-Supervisor Dr. Stefano Milia

Final exam. Academic Year 2017 – 2018
Thesis defence: January-February 2019 Session

Acknowledgements

First, I would like to thank sincerely my advisors, Prof. Alessandra Carucci and Dr. Stefano Milia, for their continuous support and encouragement. Throughout my PhD, they provided constructive criticism and valuable advices that helped me to develop this thesis. Moreover, I would also like to acknowledge Prof. Aldo Muntoni, coordinator of the PhD course in Earth and Environmental Sciences and Technologies, for providing useful comments and suggestions during the yearly revisions. I am also grateful to Dr. Bernardino Virdis, who supervised my traineeship at the Advanced Water Management Centre (AWMC) at The University of Queensland (Australia) and generously shared his knowledge in bioelectrochemistry with me.

For the helpful discussions and technical feedback, I am thankful to Giovannimatteo Erby (Dept. of Civil-Environmental Engineering and Architecture, DICAAR, University of Cagliari, Italy) and Dr. Michele Mascia (Dept. of Chemical Engineering, University of Cagliari, Italy), who also gave me access to a potentiostat and other instrumentation useful for my electrochemical tests. For providing the inoculum used in the of bioaugmentation tests, and for the helpful discussions on the microbiological aspects involved in my thesis, I am grateful to Dr. Elena Tamburini (Dept. of Biomedical Sciences, University of Cagliari, Italy).

Dr. Martina Piredda (DICAAR) is acknowledged for supplying technical support with analytical methods. I am also thankful to Prof. Giovanna Cappai, Giorgia de Gioannis and Angela Serpe, for kindly providing their advises and opinion on scientific matters.

Special thanks go to Giaime Tocco and Dr. Daniela Spiga, with whom I shared not only the office and lab space, but also the whole PhD experience, including doubts about experiments as well as less technical issues. All other staff and PhD students at DICAAR are acknowledged for the support.

Finally, I would like to thank the University of Cagliari, which funded my scholarship, the Globusdoc Programme of the University of Cagliari that offered a mobility grant that allowed my stay abroad, and the AWMC, which provided financial support to my research in Australia.

Abstract

Polycyclic aromatic hydrocarbons (PAHs), mainly derived from human activities and mostly found in soils and sediments, pose a serious worldwide concern, since they are hazardous contaminants. Aerobic bioremediation approaches are usually applied, due to their fast kinetics: in this framework, two sediment slurry sequencing batch reactors, namely SBR-C and SBR-EK, treated, in 5-days cycles, marine sediments spiked with 4-mixed PAHs (fluorene, phenanthrene, fluoranthene and pyrene) and coming, respectively, from Cagliari (Italy) and El Kantaoui (Tunisia) ports. Both systems achieved the best performances (and in parallel met threshold levels of Italian regulations) when the solid-to-liquid ratio (S/L) was set at 0.1, PAHs concentration at 200 $mg_{PAHtot}\,kg_{dw}^{-1}$ (dw = dry weight) and the volumetric organic loading rate at 0.4 $mg_{PAHtot}\ L^{-1}\cdot d^{-1}$. Increasing these parameters resulted in worsening the process performances; bioaugmentation was not useful to recover good process performances in SBR-C.

An alternative approach could be the use of bioelectrochemical systems (BES). Sediment microbial fuel cells (SMFCs) were used for preliminarily assess phenanthrene (Phe) removal from marine sediments: glass bottles (anodic compartments, anaerobic) were batch-fed with a slurry (S/L=0.05) contaminated up to 150 mg kg_{dw}^{-1}; cathodes were placed in a PVC tube inserted in the bottle cap and the compartments were separated by a cation-permeable membrane; both anode and cathode consisted of a piece of conductive graphite felt. BESs were operated under mechanical stirring and in static conditions, though mixing accelerated Phe removal (which was almost completed in 20 days). Since high Phe removals were achieved also in the open circuit controls, the role of sulphate (which was part of the sediment and of the culturing medium adopted) was investigated: although sulphate had a putative role in Phe degradation, the presence of the anode fastened the degradation, hence indicating the successful development and maintenance of a Phe degrading biomass on the anodic surface. However, SMFCs reached low current outputs, due to the low biodegradability of Phe and to the limited *radius of influence* of the bioelectrochemical treatment in the specific configuration adopted. To solve these problems, a model soil (quartz sand, density ≈ 1.5 kg dm^{-3}) was amended with 2,000 mg kg_{dw}^{-1} of graphene oxide (GO) that, once electrochemically reduced to rGO (for 60 hours), increased the electric conductivity of the soil not amended with GO by four orders of magnitude. These percolating anodes, supplemented with an inoculum of electroactive microorganisms and acetate, outperformed the controls by delivering >30 times higher current, indicating that probably a much larger volume of soil contributed to the catalytic current

production. Promising results were achieved also in preliminary tests of toluene and Phe degradation and encourage further investigations for future applications to real contaminated soils and sediments.

Keywords

Bioremediation, polycyclic aromatic hydrocarbons, marine sediments, sediment-slurry sequencing batch reactors, sediment bioelectrochemical systems, reduced graphene oxide, percolating bioanodes

Table of contents

List of figures

List of tables

List of abbreviations

AC	Alternate current
AOPs	Advanced oxidation processes
ATP	Adenosine triphosphate
AWMC	Advanced Water Management Centre
BMFC	Benthic microbial fuel cell
BTEX	Benzene, toluene, ethylbenzene and xylene
CAC	Citric acid cycle
CE	Counter electrode
CEM	Cation exchange membrane
CFSTR	Continuous flow stirred tank reactor
COD	Chemical oxygen demand
CV	Cyclic voltammetry
Cyt	Cytochrome
DC	Direct current
DICAAR	Department of Civil-Environmental Engineering and Architecture
DNA	Deoxyribonucleic acid
DO	Dissolved Oxygen
DOC	Dissolved organic carbon
EAB	Electroactive bacteria
EEA	European Environment Agency
EET	Extracellular electron transfer
EIS	Electrochemical impedance spectroscopy
EMF	Electromotive force
ET	Electron transfer
EU	European Union
EuDA	European Dredging Association
FAs	Fulvic acids
$FADH_2$	Flavin adenine dinucleotide (reduced form)
GC	Gas chromatography
GO	Graphene oxide
HAs	Humic acids
HDB	Hydrocarbon degraders bacteria
HMW	High molecular weight (PAHs)

HPLC	High performance liquid chromatography
HRT	Hydraulic retention time
IMO	International Maritime Organization
ISTD	*In situ* thermal desorption
LMW	Low molecular weight (PAHs)
LSV	Linear sweep voltammetry
MES	Microbial electrosynthesis
METs	Microbial electrochemical technologies
MFC	Microbial fuel cell
MS	Mass spectrometry
NAD^+	Nicotinamide adenine dinucleotide (oxidised form)
NADH	Nicotinamide adenine dinucleotide (reduced form)
NADPH	Nicotinamide adenine dinucleotide phosphate
NAPLs	Non-aqueous phase liquids
OCV	Open circuit voltage
OMC	Outer membrane cytochrome
PAHs	Polycyclic aromatic hydrocarbons
PBS	Phosphate buffer solution
PVC	Polyvinyl chloride
rGO	Reduced graphene oxide
RHD	Ring-hydroxylating dioxygenase
RO	Reverse osmosis
RVC	Reticulated vitreous carbon
SedNet	Sediment Research Network
S/L	Solid-to-liquid ratio
SBES	Sediment bioelectrochemical system
SCE	Saturated calomel electrode
SEM	Scanning electron microscope
SHE	Standard hydrogen electrode
SMFC	Sediment microbial fuel cell
SRB	Sulphate reducing bacteria
SS-SBR	Soil/sediment slurry sequencing batch reactor
TCA	Tricarboxylic acid

TEC	Total extractable carbon
TOC	Total organic carbon
TPH	Total petroleum hydrocarbons
TS	Total solids
UNESCO	United Nations Educational, Scientific and Cultural Organization
UV	Ultraviolet
VER	Volumetric exchange ratio
vOLR	Volumetric Organic Loading Rate
VS	Volatile solids
WE	Working electrode
WFD	Water Framework Directive

GENERAL INTRODUCTION

This PhD thesis is the product of a three-year work at the Department of Civil-Environmental Engineering and Architecture (DICAAR), University of Cagliari (Italy); during the third year, a six months traineeship (October 2017-April 2018) was performed at the Advanced Water Management Centre (AWMC), The University of Queensland (Brisbane, Australia). The focus of the thesis is the use of bioremediation (which exploit the biodegradative capability of microorganisms and is often preferred to physico-chemical treatments due to its lower costs) for the treatment of marine sediments polluted by organic compounds, specifically polycyclic aromatic hydrocarbons (PAHs): in particular, this work evaluate the process performance of a conventional approach, based on sediment-slurry sequencing batch reactor technology (SS-SBR), and of a bioelectrochemical treatment, operated with two different configurations of sediment bioelectrochemical systems (SBESs).

Nowadays, pollution of soils and sediments, mainly derived from anthropogenic sources (*e.g.*, rapid industrialisation, intensive agricultural practices, but also residential heating and transports) poses a serious worldwide concern, and often requires a proper remediation of polluted sites. In this framework, given their recalcitrant nature, potential hazard for the human health, accumulation onto solid particles owing to their hydrophobicity, and also given the high occurrence of global emissions, PAHs became the target of this research. The first Chapter of this thesis outlines the main characteristics of these contaminants, their diffusion and fate into the environment, and focuses, in particular, on the biodegradation processes that, once into the environment, PAHs can undergo. As to sediments, the preservation of the ecological and chemical water quality status coupled with practical aspects (*i.e.* the necessity to maintain suitable water depth in areas such as harbours, following an excessive sedimentation) lead to the dredging of large volumes of sediments worldwide every year. These dredging activities become extremely complicated and more expensive in the presence of a contamination. However, after proper management and treatment (necessary if a contamination is detected), sediments can be considered more a resource than a waste, in a vision of circular economy. In Chapter 2, a general introduction of the main processes behind the formation and the transport of sediments, a summary of the main regulations for the management of dredged materials coming from marine environments (with an insight on the Italian perspective), and an overview

of the most common treatments available for sediments contaminated by organic compounds, will be given.

Chapter 3 and 4 firstly review basic principles and the state of the art of both treatments adopted in this PhD thesis, secondly outline results achieved with the experimental work. SS-SBR technology, described in Chapter 3, is a well-established technique for the treatment of recalcitrant fluxes. Here, sediments, contaminated by a mixture of four PAHs (namely fluorene, phenanthrene, fluoranthene and pyrene), were treated with biostimulation (*i.e.*, the adjustment of nutrients, oxygen and the addition of co-substrate or surfactants). Moreover, biostimulation was also coupled with bioaugmentation. The purpose of this experimental part was to assess which process parameters can guarantee the best process performances, coupled to the compliance with threshold levels taken from Italian regulations. Instead, Chapter 4 delves into the feasibility of bioelectrochemical degradation of phenanthrene. In the first experiment, a double-chambered sediment microbial fuel cell (SMFC), obtained burying the anode into the sediment slurry and separating the cathode, placed in a polyvinyl chloride (PVC) cathodic compartment, by a cation exchange membrane (CEM), was adopted. The traineeship at AWMC was useful for the development of innovative percolating bioanodes obtained by reducing graphene oxide (GO) into reduced GO (rGO) within the pores of a model soil, hence inducing electrical properties to an otherwise insulating matrix; once back to Cagliari, this configuration, whose biodegradation capacity had been already tested on acetate and, briefly, on toluene, was used for a preliminary assessment of phenanthrene degradation.

In the last part of this thesis, performances of each approach will be shortly summarised in order to evaluate the efficacy of the treatments applied and try to figure out future outcomes.

1 POLYCYCLIC AROMATIC HYDROCARBONS: CHARACTERISTICS, FATE IN THE ENVIRONMENT, BIOLOGICAL DEGRADATION

Polycyclic aromatic hydrocarbons, also named polyarenes and polynuclear aromatic hydrocarbons, represent a class of organic pollutants composed by two or more fused benzene rings and/or pentacyclic molecules, arranged in diverse structural configurations, mainly produced by anthropogenic activities. These compounds, which can also originate from natural sources, are the product of incomplete combustion, *e.g.* creosote, diesel, cigarette smoke, and forest fires (Bamforth and Singleton, 2005; Wick *et al.*, 2011).

Due to their hydrophobicity, low water solubility, and affinity to the organic matter, PAHs are highly recalcitrant and persistent compounds. Although mostly found in soils and sediments, they are ubiquitous in the environment. Strong associations with solid matrix, in addition to contaminants physico-chemical properties, influence their availability and, as a consequence, their degradability (Couling *et al.*, 2010). Moreover, most PAHs exert toxic effects and have mutagenic and carcinogenic properties, hence they may have a harmful effect on both aquatic ecosystems and human health (Bamforth and Singleton, 2005). For these reasons, USEPA decided to include16 PAHs in the USEPA Priority Pollutant list (USEPA, 2014); they are reported in Table 1.2.

The aforementioned characteristics together with the high occurrence of global PAHs emissions (which will be better addressed below) pose a serious worldwide concern, and often require a proper remediation of polluted sites.

Once in the environment, polycyclic aromatic hydrocarbons may undertake processes of adsorption, volatilization, photolysis, chemical degradation, and microbial degradation. The latter mechanism, which naturally occurs because PAHs can be generated from natural sources, is directly related to contaminant bioavailability and catabolic activity of autochthonous microbial populations, and is considered one of the most important for the removal of PAHs from soils and sediments (Haritash and Kaushik, 2009; Couling *et al.*, 2010; Wick *et al.*, 2011). Therefore, between established technologies for remediate contaminated sites, bioremediation, which exploits the ability of microorganisms to remove contaminants, is often preferred to physical and chemical treatments (*e.g.,* incineration, chemical oxidation, and soil washing) since it is less expensive. Moreover, using microbial metabolism, compounds may be transformed to less hazardous or non-hazardous forms, whilst some physico-chemical

processes such as soil washing may cause the movement of contamination from one phase to another, without effectively solve the problem (Haritash and Kaushik, 2009).

Due to the potential hazard associated to polycyclic aromatic hydrocarbons contaminations, several studies have delved into this topic. In this scenario, for the purposes of this PhD thesis, that is to evaluate the performances of different bioremediation techniques suitable to decontaminate marine sediments polluted by organic compounds, PAHs have been chosen as target compounds.

Considering these preliminary remarks, this chapter provides an overview on polycyclic aromatic hydrocarbons chemistry, behaviour and fate in the environment, as well as contaminant bioavailability; afterwards, it focuses on microbial (particularly bacteria) metabolism of PAHs.

1.1 SOURCES OF CONTAMINATION AND ANALYSIS ON GLOBAL AND EUROPEAN ATMOSPHERIC EMISSIONS

Polycyclic aromatic hydrocarbons are mainly formed during the thermal decomposition and the following recombination of organic molecules (Haritash and Kaushik, 2009). Pyrogenic PAHs derive from incomplete combustion at high temperatures (350-1,200 °C), and are formed under low oxygen or no oxygen conditions (*e.g.*, processes like distillation of coal into coke and coal tar, or thermal cracking of petroleum residues into lighter hydrocarbons); they are mainly concentrated in urban areas (Abdel-Shafy and Mansour, 2016). Petrogenic PAHs are associated with crude oil maturation or similar processes and are formed through subjection of organic material at low temperatures (100-300 °C) for a long period of time (Haritash and Kaushik, 2009; Abdel-Shafy and Mansour, 2016). PAHs can also be also synthesized biologically by plants (Abdel-Shafy and Mansour, 2016). As for pyrogenic PAHs, higher combustion temperatures (*e.g.*, coking processes) form simple PAHs[1], while lower combustion temperatures (*e.g.*, smouldering) result in contaminants which possess a higher complexity (Wick *et al.*, 2011). Because they are sourced from alkylated parents[2], pyrogenic residues contain a greater number of 4 to 6 ring PAHs than petrogenic ones (Kuppusamy *et al.*, 2017).

[1] Simple PAHs include 2 or 3 rings compounds, the so-called low molecular weight PAHs (LMW), whereas high molecular weight PAHs (HMW) contain more than 4 rings.

[2] Alkylated compounds include, in their structure, a substitution with an alkyl group, *i.e.*, an alkane which lacs of a hydrogen atom (general formula C_nH_{2n+1}).

An easier way to classify PAHs sources, is distinguishing in natural or anthropogenic sources. Natural sources can be biogenic and geochemical, and include forest and rangeland fires, oil seeps, volcanic eruptions, exudates from trees, pyrolysis (*i.e.*, a petrogenic process that involves the submission of sediments to high temperatures when diagenesis occurs). Anthropogenic sources include the combustion of fossil fuels (*e.g.*, motor vehicle emissions and power generation), wood, coal tar, municipal and industrial waste incineration, petroleum spills and discharge, coal liquefaction and gasification during coke production (creosotes, which are by-products of coking, are formed up to 85% from PAHs). Minor sources are cigarette smoke and burnt food (Bamforth and Singleton, 2005; Haritash and Kaushik, 2009; Wick *et al.*, 2011). Human activities generate the biggest quantity of PAHs; the majority of PAHs production, in fact, is associated to energy and industrial production processes (Zhang and Tao, 2009).
The combustion of fossil fuels, wood and vegetation induces air pollution and the following transport of contaminants over long distances, but point sources of PAH contamination, like oil spills, pose the major concern, despite the relatively small size of compromised areas: here, polycyclic aromatic hydrocarbons are often associated with co-contaminants (*e.g.,* benzene, toluene, ethylene and xylene (BTEX), and heavy metals) and are generally present at high concentration, thus making remediation more difficult (Bamforth and Singleton, 2005).

A global atmospheric emission inventory, published by Zhang and Tao (2009) and concerning the diffusion of 16 PAHs (*i.e.*, the contaminants listed by USEPA in the Priority Pollutant List), estimated the global emissions in 2004 as 520 Gg. Asian countries (China and India were the main producers) covered the 55% of the total PAHs production, whereas Europe contributed to the 9.5%. As reported in Figure 1.1 A, biofuel combustion and wildfires (*i.e.*, biomass burning) lead to 56.7% and 17% of emissions, respectively, whereas the major industrial activities cover less than 10% of the total emissions. In a following survey, Shen *et al.* (2013), found that the emissions of the same 16 PAHs in 2007 corresponded to 504 Gg, equivalent to 76 g per capita per year. Figure 1.1 B shows the global distribution of emissions for the main sources of release: biomass fuels, *i.e.*, burning of firewood and crop residues, represents the 60.5% of the whole diagram, followed by emission from motor vehicles, and deforestation/wildfire. Not surprisingly, both surveys showed that the distribution of emissions changes depending on the status of development and the vegetation covering of each country: while indoor biomass burning (*i.e.*, use of biomass for cooking and heating) was the most important source in developing countries, motor vehicle exhaust emissions and consumer product use had particular influence in many developed countries.

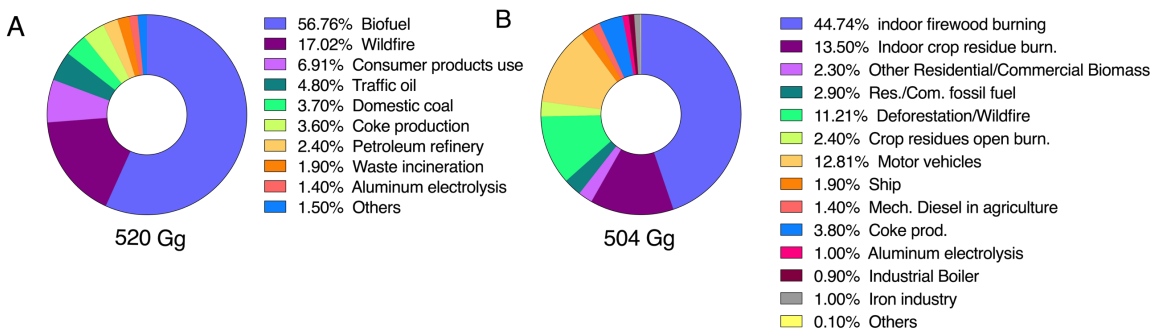

Figure 1.1 *Global PAHs emission sources A) in 2004, redrafted after: Zhang and Tao (2009), and B) in 2007, redrafted after: Shen et al. (2013).*

As for Europe, the 2007 survey determined that emissions from residential/commercial fuel consumption and from transportation generated the major impact, accounting, respectively, for the 47.5% and the 23.8% of the total emissions in the country. The major contributors to the industrial sources were coke production, primary aluminium production and iron and steel industry (13.6% of the total emissions for the considered sector).

The general trend of emissions in 2007 resulted in the highest levels of contamination for developing countries because of the fast population growth and the increasing energy demand; in developed countries, due to the strict legislations on the emissions generated by motor vehicles and industries, and the available processes and technologies, airborne PAHs levels were lower: total European emissions resulted in 33,918 ton, higher than countries such has North America (17,840 ton), but definitely lower than countries like South and Southeast Asia (139,256 ton). It should be noted that, when looking at these data, the population density and the extent of the country must be considered.

Emissions of HMW carcinogenic PAHs were higher for developing countries than for developed countries, due to the high contribution of residential fuel consumption, industrial emissions, and non-organized waste burning. Moreover, the burning of biomass posed a particular concern due to the direct human exposure to this source.

In the same study, Shen *et al.* (2013) considered also historical time trends and future trends. The first ones were evaluated between 1960 and 2008. The peak of PAHs emissions for developed countries dated back to 1970s and decreased gradually thanks to the general better control of emissions (see above). In developing countries, the total PAHs emissions for transportation sector increased continuously, due to the increasing number of motor vehicles present in the traffic system; PAHs emissions from residential, commercial and industrial sources started to decrease around 1995, for several reasons (*e.g.*, the promotion of centralized heating systems), so this is considered as the peak year for emissions. Moreover, because

developing countries contributed to the majority of global emissions, both, developing countries and the globe reached their peak in the same year. As for future trends, emissions have been estimated to decrease in both, developed and developing countries, due to the reduction of worldwide emissions from residential sources, better laws on emissions abatement, and the utilization of cleaner burning fuels. Duran and Cravo-Laureau (2016) indicated the decrease in the PAHs levels of sediments after the 1960s as due to the application of measurements to limit emissions, such as the transition from coal to oil to gas energy sources. Despite these previous studies and the emission trends described above, Kuppusamy *et al.* (2017) reported a general increase of PAHs concentration in soils during the last 30 years, which particularly important in industrialized regions; moreover, according to this study, concentrations will increase in the next years because of the increasing atmospheric emissions. With regard to Europe, through the European Union emission inventory report (EEA, 2018), the European Environment Agency (EEA) analysed the total emission trends of several pollutants between 1990 and 2016, for EU-28[3] States. The major contribution to European emissions, represented in Figure 1.2 for 2016, came from industrial processes and product use, followed by commercial, institutional and households' sectors, and agriculture; the indication is totally in line with the previous considerations about developed and developing countries. Also, coherently with trends reported by Shen *et al.* (2013), as shown in Table 1.1, which lists total polycyclic aromatic hydrocarbons emissions for single States and their sum, the total emissions decreased of 83% along the period considered in the survey (even if, between 2015 and 2016 there was an increase by 3.4 %, due to the increased emissions of Portugal, Germany, Poland and Spain); this improvement was associated to the targeted legislation, coupled with improved controls and abatement techniques.

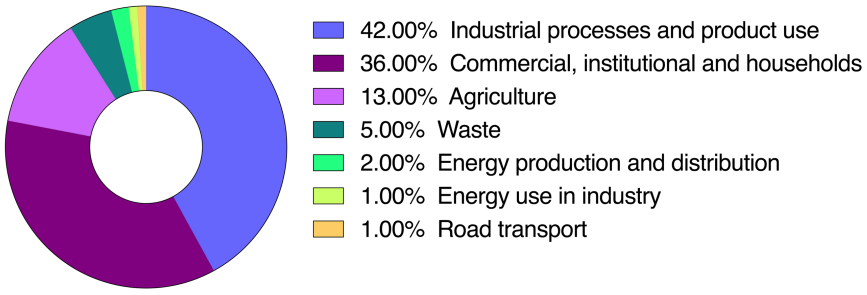

Figure 1.2 *Total PAHs emissions in the EU, 2016: sectoral trend emissions. Redrafted after: EEA (2018).*

[3] EU-28: refers to the 28 Member States of the European Union (from 1 July 2013) listed in Table 1.1.

Table 1.1 *Member State contributions to EU total emissions of PAHs. Redrafted after: EEA (2018).*

	Change in Total PAHs (%)	
Member State	**1990-2016**	**2015-2016**
Austria	-59	0.8
Belgium	-83	10.2
Bulgaria	-54	6.8
Croatia	-71	-14.9
Cyprus	-95	-23.7
Czech Republic	-84	-2.8
Denmark	38	2.2
Estonia	-15	-1.0
Finland	44	9.2
France	-59	2.0
Germany	-51	7.7
Greece	-59	-39.5
Hungary	-60	2.1
Ireland	-69	-6.0
Italy	-17	-0.2
Latvia	-56	-0.5
Lithuania	-58	0.4
Luxemburg	-86	10.7
Malta	-26	10.8
Netherlands	-76	0.7
Poland	0	4.9
Portugal	41	5.2
Romania	0	-2.9
Slovakia	-7	-7.8
Slovenia	-35	2.2
Spain	-96	3.9
Sweden	-26	2.1
United Kingdom	-98	-2.1
EU-28	**-83**	**3.4**

1.2 GENERAL CHEMISTRY OF POLYCYCLIC AROMATIC HYDROCARBONS

Polycyclic aromatic hydrocarbons come as colourless, white/pale yellow solids (Haritash and Kaushik, 2009). They present different structures and sizes, hence different molecular weights (the difference between LMW and HMW PAHs has been already elucidated above). As a consequence, physical and chemical properties are variable for each PAH compound; however, they have typically low solubilities, low vapor pressures and high melting and boiling points. Physical and chemical properties exert a direct influence on the fate of these compounds in the

environment (Wick *et al.*, 2011), because they can affect, for instance, contaminant availability and, therefore, degradability in soils (Couling *et al.*, 2010).

As an example, Table 1.2 lists selected properties for USEPA's 16 priority pollutant PAHs: number of rings, molecular weight, solubility in water, vapor pressure and logarithm of octanol-water partition coefficient (K_{ow}[4]).

Table 1.2 *USEPA's 16 priority pollutant PAHs and selected properties at 25°C. Redrafted after: Wick et al. (2011).*

PAH name	Number of rings	Molecular weight [g mol^{-1}]	Solubility in water [mg L^{-1}]	Vapor pressure [Pa]	Log K_{ow}
Naphtalene	2	128.17	31	11.866	3.37
Acenaphtene	3	154.21	3.8	0.500	3.92
Anthracene	3	178.23	0.045	3.40×10^{-3}	4.54
Phenanthrene	3	178.23	1.1	9.07×10^{-2}	4.57
Fluorene	3	166.22	1.9	0.432	4.18
Fluoranthene	4	202.26	0.26	1.08×10^{-3}	5.22
Benz[a]anthracene*	4	228.29	0.011	2.05×10^{-5}	5.91
Chrysene	4	228.29	0.0015	1.04×10^{-6}	5.91
Pyrene	4	202.26	0.132	5.67×10^{-4}	5.18
Benzo[a]pyrene*	5	252.32	0.0038	6.52×10^{-7}	5.91
Benzo[b]fluoranthene*	5	252.32	0.0015	1.07×10^{-5}	5.80
Benzo[k]fluoranthene*	5	252.32	0.0008	1.28×10^{-8}	6.00
Dibenz[a,h]anthracene*	6	278.35	0.0005	2.80×10^{-9}	6.75
Benzo[g,h,i]perylene*	6	276.34	0.00026	1.33×10^{-8}	6.50
Indeno[1,2,3-cd]pyrene*	6	276.34	0.062	1.87×10^{-8}	6.50

*Classified by USEPA as possible human carcinogens.

Considering the chemical structure, it is possible to distinguish between alternant and nonalternant PAHs: alternant structures contain only rings constituted of six carbon atoms, whereas nonalternant PAHs contain also rings formed by less or more carbons and derive from lower and less efficient combustion temperatures. The chemical structures of the four PAHs used during the experimental work described in this thesis are represented in Figure 1.3. The solubility in water, which changes when parameters such as temperature, pH, and ionic strength (*i.e.*, concentration of soluble salts) change, can be estimated looking at chemical structure and octanol-water partition coefficients. Observing Table 1.2, it is evident that, in general, when PAHs molecular weight increases, solubility in water and vapor pressure decrease. However, solubility depends also on symmetry, planarity, and substitutions in the compounds structure:

[4] K_{ow}: ratio between the amount of the organic chemical in octanol, and the amount of the organic chemical in water. The coefficient expresses the affinity of a considered compound for organic matter.

solubility increases in linearly-fused PAHs when the number of rings increases (weaker bonds), while the behaviour has not been confirmed in angularly fused PAH; planar PAHs are less soluble, and less biologically toxic. In general, alternant PAHs, planar and symmetrical, are less soluble but, when they drift from planarity and symmetry, they become more soluble in organic solvents. As for the octanol-water partition coefficient, the higher is K_{ow}, the lower is the solubility in water (Wick *et al.*, 2011). Moreover, by increasing PAHs molecular weight, melting and boiling points increase (Haritash and Kaushik, 2009).

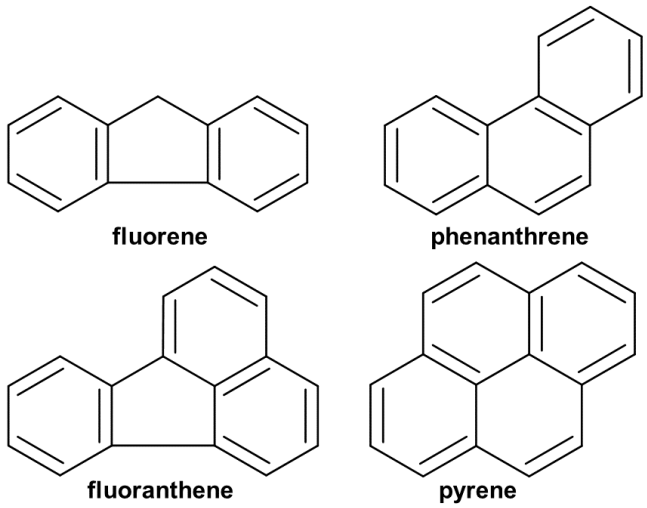

Figure 1.3 *Structures of the four polycyclic aromatic hydrocarbons used during the experimental work.*

1.3 ROUTES AND FATE IN THE ENVIRONMENT

As already mentioned above, PAH compounds have a ubiquitous distribution in the environment, because they are continuously emitted in the atmosphere, and they can be deposited around the site of emission or, after transport (short or long-range), in another site; hence, they reach soils and surface water. The arrival to surface water can occur also directly through oil spills, wet deposition, municipal wastewater discharge or indirectly through runoff. Moreover, percolation allows contaminants to reach, eventually, the groundwater. Figure 1.4 gives a schematic example of sources (they have been already mentioned in the previous paragraph), and some typical routes and repositories of pollutants in the ecosystem.

Atmosphere represents a temporary receptor; the highest concentrations of PAHs in the atmosphere are recorded in urban areas, and emissions are usually higher in winter, due to residential heating. Once compounds are released to the atmosphere, they can be found associated with particulate matter, or in vapor phase, depending on their vapour pressure: the higher is the vapour pressure, the bigger quantity of emitted PAHs is found as vapour. The

phase also depends on temperature: PAHs generally condense at temperatures lower than 150°C, and the majority of two- and four-ring compounds, as well as two-ring nitrated compounds, are found in the gaseous phase associated with particulate at ambient temperatures. Based on the phase in which PAHs are in the atmosphere, they can be transported, as long as no rain causes wet deposition. Evaporation (*i.e.*, volatilization) from soils, plant or aquatic ecosystems is a secondary mechanism by which compounds can arrive to the atmosphere (Wick *et al.*, 2011).

Compounds that reach water bodies through the various mechanisms already introduced, are hydrophobic and therefore they are mostly found associated to sediments (in concentration ranging from μg kg^{-1} to g kg^{-1}); thereby, a very low concentration is found in water (Wick *et al.,* 2011).

The main source of PAHs found in soils is the deposition from the atmosphere, unless contamination is not directly related to industrial activities; when natural processes occur, concentrations range between 1-10 μg kg^{-1}, while they can reach more than 10,000 mg kg^{-1} in industrial areas (Wick *et al.*, 2011). As detailed in Kuppusamy *et al.* (2017), if the PAHs content is under 0.2 – 0.6 mg kg^{-1}, the soil is considered 'unpolluted', while it is regarded as 'slightly polluted' between 0.6 and 1.1 mg kg^{-1}, 'polluted' in the range 1.1 – 5.5 mg kg^{-1}, 'heavily polluted' above the last value (while it is 'very heavily polluted' over 10 mg kg^{-1}). Depending on the source of contamination, soils can reach contamination higher than 300,000 mg kg^{-1} (Bamforth and Singleton, 2005). The Italian 'Decreto legislativo 3 aprile 2006, n. 152 Norme in materia ambientale' (*i.e.*, 'Legislative Decree 152/2006' or 'Regulations concerning the Environment'), and its subsequent amendments, in Table 1, Annex 5 to the Fourth part (which involves regulations about contaminated sites and wastes management), defines contaminants threshold levels in soils, subsurface and groundwaters: limits related to the sum of 10 PAHs are, respectively, 10 mg kg_{dw}^{-1} for the reuse in residential areas and 100 mg kg_{dw}^{-1} for the reuse in industrial sites (the acronym *dw* means 'dry weight', *i.e.*, the dry content of sediments, measured according to published protocols (IRSA-CNR, 2005)).

PAHs can accumulate in plants due to atmospheric deposition, or through plants roots. Type of plants, environmental conditions, type of compounds, influence PAHs concentration in plant's tissues; of course, concentrations are higher in urban and industrialised areas than in rural areas (Wick *et al.*, 2011).

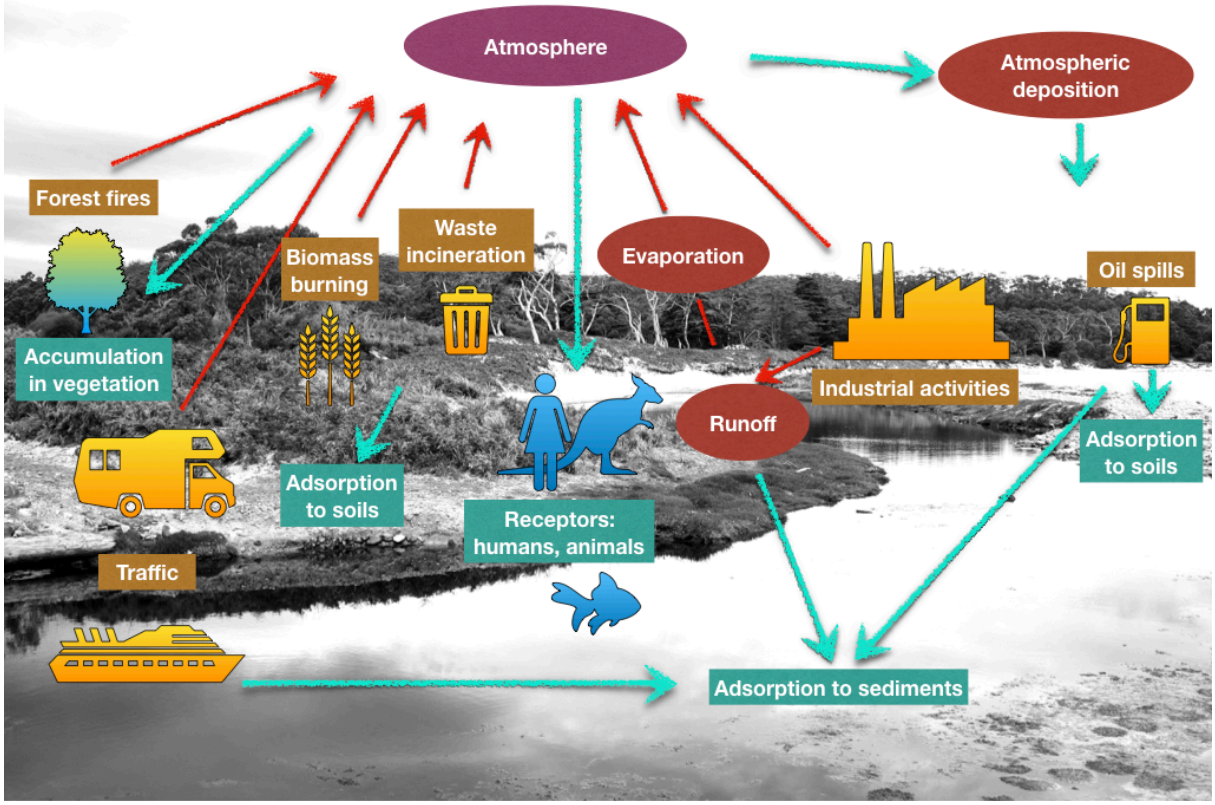

Figure 1.4 *Diagram of sources, transfer and receptors of polycyclic aromatic hydrocarbons in the environment: yellow objects represent sources of contamination (caption in light brown); pale blue objects are the receptors (caption in teal); red arrows indicate the path of emissions and go to circled text in dark pink, which represents a temporary receptor or to circled text in dark red, which is a mechanism of transport for contaminants; ice blue arrows indicate the route towards the final receptors.*

1.3.1 PAHs in marine environments

Since this thesis concerns the treatment of marine sediments contaminated by PAHs, it is important to focus on the behaviour of these compounds once they reach marine environments. The last definition covers a broad variety of ecosystems, such as coastal zones, estuaries, surface and deep oceans.

According to Duran and Cravo-Laureau (2016), pyrogenic PAHs, considered responsible of chronic pollution, reach marine environments with the mechanisms already described of direct deposition from the atmosphere and fluvial runoff (whose contribution decreases in distal areas, *e.g.*, oceans). Conversely, petrogenic PAHs, that enter the marine environment due to oil spills, generate acute pollution; however, they represent less than 10% of the total petrogenic compounds found in marine ecosystems: natural oil seeps cover about the half of the whole contribution of crude oil in oceans, meanwhile transportation gives the remaining input. Old natural oil seeps are considered like another example of chronic pollution. However, petrogenic

PAHs are more bioavailable than pyrogenic PAHs: interestingly, the contamination level associated to this source is able to generate particular habitats for benthic microorganisms and to promote the selection of the microbial community.

The global fluxes of PAHs in marine environments are determined by microbial degradation and the biological pump[5], which, coupled with compounds characteristics, influence the uptake of PAHs in sediments. Considering as example coastal areas, the most contaminated sediments are found in urbanised areas, *e.g.*, estuaries, where PAHs levels can exceed 100 ng g_{dw}^{-1}. LMW PAHs enter the environment generally via diffusive gas exchanges, while HMW PAHs, due to deposition of soot and black carbon particles. Grain size, temperature and salinity have an influence on PAHs distribution in sediments.

Once in sediments, environmental conditions, practices such as shipping or biological processes, the removal of sediments (*i.e.*, dredging) or their relocation, may cause the remobilisation of PAHs. Resuspension and remobilisation processes can exert an effect on benthic microorganisms since oxygen is provided to deeper sediments, but also PAHs become suddenly available for biodegradation, which can be operated by bacteria, fungi and algae (insights on biodegradation will be provided below).

1.4 PAHS TOXICITY IN HUMANS

Many PAHs show acute mutagenic, teratogenic and carcinogenic properties. If such compounds are ingested, they are rapidly absorbed to the gastrointestinal tract, because of their high solubility in lipids (Samanta *et al.*, 2002). Also, the passage of PAHs through skin constitutes one of the most important ways to humans, which, according to Bamforth and Singleton (2005), represents the 75% of the total amount absorbed. Since absorption is a rapid process, it may lead to biomagnification in the food chain. Human exposure usually comes from working environments, but atmospheric emissions give an important contribution, as well as tobacco smoke. Other sources of ingestion are represented, for instance, from drinking water, leafy vegetables, and grilled and smoked meats (Wick *et al.*, 2011).

PAHs are not necessarily genotoxic. However, genotoxicity is due to a specific mechanism of activation operated by mammalian enzymes: cytochromes P_{450} play a determinant role on

[5] Biological pump: biologically driven process by means of which marine phytoplankton transport carbon from the ocean's surface layers to the deep ocean and convert dissolved inorganic carbon and nutrients into organic matter through photosynthesis, sequestrating it in sediments (https://definedterm.com/biological_pump).

metabolism of PAHs, by forming reactive epoxides and quinones, which can combine with and/or attack deoxyribonucleic acid (DNA). Oxidation or hydroxylation[6] constitute the first step of the metabolization: it can produce detoxification products, or the so-called bay- and K-region epoxides[7], which are highly reactive and, in turn, can be carcinogenic. Bay- and K-regions are exemplified in Figure 1.5 for phenanthrene, the smallest PAH to possess them.

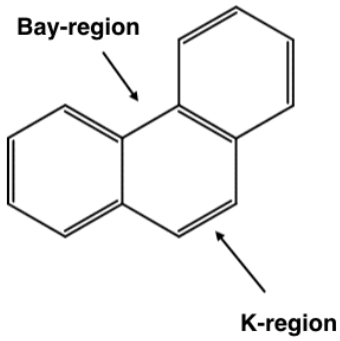

Figure 1.5 *Example of bay- and K-regions for phenanthrene.*

Samanta *et al*. (2002) described the effect of naphthalene and phenanthrene in humans: while the first one can lead to haemolytic anaemia and nephrotoxicity, the latter is a photosensitizer of human skin. Generally, PAHs toxicity increases as the number of benzene rings increases (Bamforth and Singleton, 2005). Unfortunately, PAHs are usually encountered as mixtures in the environment, whereby their toxic effect can be even enhanced (Samanta *et al*., 2002).

1.5 PERSISTENCE OF PAHS IN THE ENVIRONMENT AS A FUNCTION OF BIOAVAILABILITY

Bioavailability, which exerts a great influence on the persistence of PAHs in the environment, is the possibility of a substance to affect an organism, in a positive or in a negative way (Wick *et al.*, 2011); hence, it represents the chance for humans and ecological receptors to be exposed to contaminants, influencing and controlling toxicity of compounds (Shuttleworth and Cerniglia, 1995). The last concept, *i.e.* the risk for human receptors to be reached by contaminants, strictly influences decisions on the clean-up of a contaminated matrix (Ehlers and Luthy, 2003). Bamforth and Singleton (2005) describe bioavailability as a factor related to the rate and extent of degradation, which can occur through the action of physico-chemical and microbiological factors.

[6] Hydroxylation is the process of introduction of a hydroxide group (-OH) into an organic compound.
[7] Epoxides constitute cyclic ethers with a three-atom ring

Once in the soil, these compounds are mostly degraded through microbial activity, though volatilization of LMW PAHs may happen. Persistence in the environment and, therefore, bioavailability (*i.e.*, the possibility to obtain microbial degradation), are influenced by the physico-chemical properties of compounds, their concentration, type of soil (organic matter content, texture, aggregation, heterogeneity), type of microorganisms, and pH, temperature and other parameters which regulate mechanisms of microbial degradation (Bamforth and Singleton, 2005; Wick *et al.*, 2011).

In general, petrogenic PAHs are more bioavailable than pyrogenic ones (Duran and Cravo-Laureau, 2016), and also, to an increasing molecular weight is associated a greater persistence in the environment (Bamforth and Singleton, 2005): LMW PAHs can be removed faster by biological and physico-chemical processes, due to their properties and to their possibility to act as a sole carbon source for microbial metabolism, whereas the slower microbial degradation of HMW PAHs may be related to the necessity of cometabolism[8] or inducible catabolism (Couling *et al.*, 2010) (much more details on microbial degradation will be given below in the chapter). Moreover, the 'age' of contaminants (*i.e.*, their persistence) in soils and sediments is thought to decrease their bioavailability (and toxicity), because it increases the strength of associations with solid particles, especially with soil organic matter, clay and silt fractions. PAHs 'aging' starts with partition into and onto humic and fulvic acids (HAs and FAs), then the second step is the diffusion into soil micropores. Generally, if a soil or a sediment contain a high proportion of HMW PAHs, it means that the contamination is 'old', because LMW PAHs have been already depleted (Wick *et al.*, 2011). As reported from Johnsen *et al.* (2005), however, some bacteria are able to access the 'unavailable' fractions and promote the diffusion back out of micropores. Another factor known for ravelling decontamination is the association of PAHs with co-pollutants or heavy metals.

Between various definitions of bioavailability, Semple *et al.* (2007) introduce the concept of accessibility of contaminants with a mild extraction, which is coupled with the possibility for physico-chemical processes of diffusion, sorption and partitioning to occur. When PAHs are sequestrated, *i.e.*, stored for long periods of time, without alterations of their structure, they are considered no more bioavailable. Sequestration mechanisms are distinguished between adsorption to soils and sediments (highly influenced by clay and organic matter content, clay type and moisture), and diffusion into soil micropores not accessible for microbial degradation

[8] This is the process that microorganisms use to transform simultaneously organic compounds, although they are not able to use only one compound for growth and energy; product of cometabolism are accumulated as carbon that could be available for other microbial groups or that could persist in the environment (Wick *et al.*, 2011).

(depending on the hydrophobic nature of micropores and PAHs). Conversely, the transfer processes described above, do not influence compounds bioavailability but only relocate PAHs without altering their structure. Therefore, when transfer happens, the possibilities for biological or chemical degradation are not compromised (Wick *et al.*, 2011). In the next paragraph, degradation mechanisms, with a particular emphasis on biological processes, will be described.

1.6 DEGRADATION MECHANISMS

Once organic contaminants, such as PAHs, have entered the environment, different degradation processes can enhance the removal of contamination. The aim of degradation is to achieve mineralization to carbon dioxide, water and other inorganic compounds. In particular, degradation can be a physicochemical or a biological process. The latter mechanism will be better analysed in the next paragraphs, while some information on non-biological degradation will be given below.

As already described, the possibility to achieve degradation highly depends on the availability of compounds: Wick *et al.* (2011) distinguish between water extractable-phase, slow molecular diffusion of PAHs into microsites, and sequestered residual phase (requiring solvent extraction); phases are ordered with respect to the higher degree of availability.

Non-biological degradation comprises three known oxidation pathways, *i.e.*, direct photooxidation (the oxidation after direct absorption of sunlight), radical oxidation reactions and oxidation reactions which are promoted by atoms having a high oxidation state, as well as thermal oxidation. As it can happen for biological degradation, chemical processes can lead to products more toxic than their parent compounds.
Oxidation processes involve the removal of electrons from a molecule that becomes oxidized, and the addition of them to another molecule that becomes reduced. Since polycyclic aromatic hydrocarbons have a highly recalcitrant nature, advanced oxidation processes (AOPs) based on the formation of free radicals from reagents such as the Fenton's reagent, activated persulphate, hydrogen peroxide, or ozone, can be used to achieve oxidation: free radicals have, in fact, oxidation potentials higher than PAHs and are, therefore, able to attack this class of compounds. Another possibility is the use of the electrokinetic degradation. Electrodes are placed around the zone of contamination and connected to a power supply, which generates a low intensity electric field that results in the movement of water, charged molecules contained in the soil

solution, and charged colloidal particles, towards anodic and cathodic zones. This movement allows the transport of not charged PAHs, that are then collected through direct extraction from the contaminated soil for further treatment (Wick *et al.*, 2011).

1.6.1 Introduction to the concept of bioremediation

The bioremediation is a process by which organic compounds are degraded to a less toxic or innocuous state; the world 'bio' indicates that microorganisms are the responsible for contaminants removal and/or conversion in less toxic compounds (Bamforth and Singleton, 2005). Microbial degradation of polycyclic aromatic hydrocarbons was recognized to occur mostly by means of bacteria, but also fungi (ligninolytic and non-ligninolytic) and algae. Since microorganisms use carbon sources as substrate for accomplishing their respiration (which is a metabolic function that naturally occurs), pollutants may constitute this substrate, hence promoting the microbially mediated degradation processes of organic compounds. Therefore, bioremediation aims to enhance the natural microbial activity by stimulating the microbial metabolism under controlled conditions, through the adjustment of water, air and nutrient supply.
PAHs-contaminated sediments, soils and water can be bioremediated by using a wide range of techniques (which will be discussed in the following chapters), that can be categorised in methods implemented *in situ*, *i.e.*, without the need of extracting or excavating contaminated matrixes, and *ex-situ* (*e.g.*, using bio-reactors, or composting).

From now on, this thesis will refer exclusively to degradation operated by bacteria.

1.6.1.1 Description of bacterial respiration: some thermodynamic aspects

Bacterial respiration can be aerobic (*i.e.*, occurs in the presence of molecular oxygen), or anaerobic (*i.e.*, occurs in the absence of molecular oxygen). The process is composed by a certain number of redox reactions: in fact, chemotrophic organisms satisfy their energy requirements by moving electrons from a low redox potential molecule, or electron donor, to a high redox potential molecule, or electron acceptor (Madigan *et al.*, 2017). Non-halogenated organic compounds can serve as electron donors in the electron transport chain for both, aerobic and anaerobic respiration. As reported by Creasey *et al.* (2018), a wide range of water-soluble electron acceptors, first of all oxygen, 'the strongest electron acceptor of any significance in nature' (Madigan *et al.*, 2017), but also insoluble minerals (particularly iron and manganese), can serve for the bacterial respiration. In the absence of molecular oxygen, other acceptors *e.g.*

inorganic compounds, such as nitrate, sulphate and ferric iron, are used. In subsurface soil and groundwater environments, oxygen may be limiting, because it is rapidly consumed by aerobic microorganisms and the atmosphere recharge proceeds slowly. Moreover, considering the presence of organic contaminants and their biodegradation, the consumption of oxidants is even faster: the heterotrophic mineralization of organic compounds will depend on the microbial use of these different electron acceptors (McFarland and Sims, 1991), which in turn may be depleted. Therefore, conventional bioremediation treatments provide continuous replenishments, thus entailing important operational costs and energy investments (Zhang *et al*., 2010).

All chemical reactions occurring in a bacterial cell are coupled with exchanges of energy, hence it is important to consider the thermodynamic aspects of respiration. In order to evaluate these aspects, first it is necessary to know which half-cell reactions of oxidation and reduction are involved in the overall reaction. Table 1.3 and Table 1.4 report, respectively, examples of the most common half-cell reactions of reduction for electron acceptors usually found in natural environments, and of oxidation for some representative PAHs.

The Gibbs free energy is a measure of the maximal energy available to do work at certain conditions; this value can be associate to each half-cell reaction. The number is expressed in kilojoules (kJ) and indicated with ΔG_r (where 'Δ' indicates the variation, and the subscript 'r' is associated with the single reaction):

Equation 1. $$\Delta G_r = \Delta G_r^0 + RT ln K$$

where ΔG_r^0 is the free energy of formation at standard conditions (pH 7, T=298.15 K, 1 atmosphere of pressure, and all reactants at 1 M concentration), R is the universal gas constant (8.3145 J mol^{-1} K^{-1}), T is the absolute temperature (K), and K is the equilibrium constant[9]. If ΔG_r^0 is negative, the reaction (that is called in this case exergonic) proceeds spontaneously and generates a net energetic advantage for cells; the energy produced during reactions is stored as adenosine triphosphate (ATP). Table 1.3 and Table 1.4 contain values of ΔG_r^0 associated to each half-cell reaction listed. Due to the different energy content of each PAH, half-cell reactions are not directly comparable; instead, values of ΔG_r^0 reported on an electron equivalent basis (kcal eeq^{-1}) allow to compare mineralization reactions.

[9] Considering a generic reaction $\nu_A A + \nu_B B \rightarrow \nu_C C + \nu_D D$, the constant K corresponds to the ratio $\frac{a_C{}^{\nu_C} \cdot a_D{}^{\nu_D}}{a_A{}^{\nu_A} \cdot a_B{}^{\nu_B}}$, where a_i are the activities of the species involved in the reaction; the activities are elevated to their relative stoichiometric coefficients. In diluted systems activities can be replaced with the species concentrations.

Table 1.3 *Free energy change in the reduction of electron acceptors under aqueous conditions (at 25°C, pH 7 and concentration of reactants 1 M). ΔG_r^0 (kJ) and E_0' have been calculated from McFarland and Sims (1991).*

Electron acceptors	Stoichiometric equation	ΔG_r^0 [kcal eeq^{-1}]	ΔG_r^0 [kJ]	$E^{0'}$ [V]
Oxygen	$^1/_4\,O_2 + H^+ + e^- \rightarrow {}^1/_2\,H_2O$	-18.675	-313	0.82
Nitrate	$^1/_5\,NO_3 + {}^6/_5\,H^+ + e^- \rightarrow {}^1/_{10}\,N_2 + {}^3/_5\,H_2O$	-17.128	-358	0.74
Manganese (oxide)*	$^1/_2\,MnO_2 + {}^1/_2\,HCO_3^- + {}^3/_2\,H^+ + e^- \rightarrow {}^1/_2\,MnCO_3 + H_2$	-12.130	-102	0.53
Manganese (soluble sp.)**	$^1/_2\,Mn^{4+} + e^- \rightarrow {}^1/_2\,Mn^{2+}$	-28.32	-237	1.23
Ferric iron (oxide)*	$FeOOH + HCO_3^- + 2H^+ + e^- \rightarrow FeCO_3 + 2H_2O$	1.091	5	-0.05
Ferric iron (soluble sp.)**	$Fe^{3+} + e^- \rightarrow Fe^{2+}$	-17.78	-74	0.77
Sulphate	$^1/_8\,SO_4^{2-} + {}^{19}/_{16}\,H^+ + e^- \rightarrow {}^1/_{16}\,H_2S + {}^1/_{16}\,HS^- + {}^1/_2\,H_2O$	5.085	170	-0.22
Carbon dioxide	$^1/_8\,CO_2 + H^+ + e^- \rightarrow {}^1/_8\,CH_4 + {}^1/_4\,H_2O$	5.763	193	-0.25

*Assumes a bicarbonate concentration of 10^{-3} M, which is more typical of aquatic environments.
**Assumes a soluble species is available at neutral pH.

Table 1.4 *Stoichiometry and free energy change in the half-cell oxidation of four selected PAHs under aqueous conditions (at 25°C, pH 7 and concentration of reactants 1 M). ΔG_r^0 (kJ) and E_0' have been calculated from McFarland and Sims (1991). Standard potentials are given as oxidation potentials ($E_0'_{ox}$).*

Electron donors	Stoichiometric equation	ΔG_r^0 [kcal eeq^{-1}]	ΔG_r^0 [kJ]	$E^{0'}{}_{ox}$ [V]
Naphtalene	$({}^1/_{48})C_{10}H_8 + ({}^{20}/_{48})H_2O \rightarrow ({}^{10}/_{48})CO_2 + H^+ + e^-$	-6.75	-1356	0.29
Anthracene	$({}^1/_{66})C_{14}H_{10} + ({}^{28}/_{66})H_2O \rightarrow ({}^{14}/_{66})CO_2 + H^+ + e^-$	-6.70	-1851	0.29
Phenanthrene	$({}^1/_{66})C_{14}H_{10} + ({}^{28}/_{66})H_2O \rightarrow ({}^{14}/_{66})CO_2 + H^+ + e^-$	-6.60	-1823	0.29
Pyrene	$({}^1/_{74})C_{16}H_{10} + ({}^{32}/_{74})H_2O \rightarrow ({}^{16}/_{74})CO_2 + H^+ + e^-$	-6.49	-2010	0.28

Microorganisms can survive only in the presence of a net energy yield able to satisfy cell's maintenance requirements. Therefore, by evaluating free energy changes associated with the presence of some specific electron donors and acceptors at the particular site conditions, it is possible to conclude which conditions make heterotrophic mineralization possible (McFarland and Sims, 1991). ΔG_r of the overall reaction can be obtained as the sum of the half-cell reactions of oxidation and reduction.

The reaction can be also evaluated in terms of electromotive force (E_{emf}), concept particularly useful when talking about bioelectrochemical systems. E_{emf} is expressed in Volts (V); E_{emf} is related to ΔG_r as reported in Equation 2:

Equation 2. $$-\Delta G_r = QE_{emf} = nFE_{emf}$$

where Q is the charge transferred in the reaction (C), that is in turn equal to the number n of electrons exchanged in the reaction (mol) multiplied by the Faraday's constant F (9.64853 x 10^4 C mol^{-1}). Hence, the electromotive force can be obtained as reported in Equation 3:

Equation 3. $$E_{emf} = -\frac{\Delta G_r}{nF}$$

Equation 3 can be written for standard conditions, obtaining Equation 4:

Equation 4. $$E^0_{emf} = -\frac{\Delta G^0_r}{nF}$$

where E^0_{emf} is the electromotive force at standard conditions.

Combining Equation 1 and Equation 4, it is possible to obtain Equation 5, which corresponds to the Nernst law, or the electromotive force associated to a given redox reactions for specific conditions:

Equation 5. $$E_{emf} = E^0_{emf} - \frac{RT}{nF} \ln K$$

Because the equation of E_{emf} contains in its expression the contrary of ΔG_r, positive values of E_{emf} indicate a spontaneous process. As described for ΔG_r, E_{emf} of the overall reaction can be obtained as the sum of the half reaction of oxidation and reduction: in particular the value is the difference between the half-cell reduction potentials (*i.e.*, the half-cell reduction potential associated to reduction minus the half-cell reduction potential associated to oxidation). Electrons, as already said, naturally flow from lower to higher redox potential; to more negative values of reduction potential are associated stronger reductants, whereas to more positive values of reduction potential are associated stronger oxidants. Therefore, to major differences in reduction potentials between electron donor and acceptor are associated larger releases of energy. Alternatively, E_{emf} can also be given as the sum of the half-cell reduction potential associated to reduction plus the half-cell oxidation potential associated to oxidation. The half-cell oxidation potential can be easily obtained by switching the sign of the reduction potential, under the hypothesis that the reaction associated to a given redox couple is reversible (this condition is not always applicable for the reactions listed, in some cases the reversibility is only theoretical).

Observing Table 1.3 it is evident that redox reactions taking place in the presence of oxygen are the most favourable in terms of energy gain. When different electron acceptors are present

in natural environments, bacteria will use first the oxidant which can guarantee the highest metabolic advantage; once the compound is depleted, they will use the other compounds based on the energy supplied.

Generally, half-cell potentials are reported as reduction potentials (*i.e.*, associated to electron consuming reactions) in comparison with the standard hydrogen electrode (SHE), conventionally set to zero at 25°C, pH 0, partial pressure 1 atmosphere (atm), 1 M concentration. For biological purposes, the redox potentials are referred to 25°C and pH 7, and are indicated with $E^{0'}$. However, coherently with the reactions listed in Table 1.4 (*i.e.*, half-cell oxidation reactions), in this particular table standard potentials are reported as oxidation potentials.

In addition, for clarity and simplicity of exposition, Table 1.5 supplies here other examples of some important half-cell redox reactions typical of biological respiration, and some cases of half-cell redox reactions concerning compounds other than PAHs and used in the experiments of this thesis, which will be talked about below.

Table 1.5 *Examples of some redox reactions typical of biological systems and their standard redox potentials at 25°C and pH 7. Values are taken from (Madigan et al., 2017). Redox couples are ordered from the top to the bottom from the strongest reductant (most negative reduction potential) to the strongest oxidant (most positive reduction potential).*

Redox reaction	$E^{0'}$ [V]
$6CO_2+24H^++24e^-\rightarrow Glucose+6H_2O$	-0.43
$2H^++2e^-\rightarrow H_2$	-0.42
$NAD^++H^++2e^-\rightarrow NADH$	-0.32
$2CO_2+8H^++8e^-\rightarrow Acetate+2H_2O$	-0.28
$Pyruvate^-+2H^++2e^-\rightarrow Lactate^-$	-0.19
$FAD^++2H^++2e^-\rightarrow FADH_2$	-0.180
$Fumarate^{2-}+2H^++2e^-\rightarrow Succinate^{2-}$	+0.03
Cytochrome b $(Fe^{3+})+e^-\rightarrow$ Cytochrome b (Fe^{2+})	+0.035
$Ubiquinone+2H^++2e^-\rightarrow UbiquinoneH_2$	+0.11
Cytochrome c $(Fe^{3+})+e^-\rightarrow$ Cytochrome c (Fe^{2+})	+0.25
$Fe(CN)_6^{3-}+e^-\rightarrow Fe(CN)_6^{4-}$	+0.36
Cytochrome a$(Fe^{3+})+e^-\rightarrow$ Cytochrome a (Fe^{2+})	+0.39

It is important to note that free energy calculations give only information about the energy that is possible to release or that is required in a given reaction, but they do not allow to estimate the rate of a reaction; in fact, thermodynamics indicates the potential for a reaction to occur in specific environmental conditions, but do not say anything about the presence of favourable kinetic conditions, which are needed for the reaction in order to proceed at a certain rate. The key concept is the existence of the so-called activation energy, which is the energy required by

molecules to be changed in a reactive state. The energy jump may be large, but in the presence of a proper catalyst (*i.e.*, enzymes for microbial degradation), this barrier can be reduced, and more easily overcome. Catalysts affect only the rate of reactions, not the energetics or the equilibrium (Madigan *et al.*, 2017). Temperature is another important parameter that must be considered when evaluating kinetics (McFarland and Sims, 1991).

1.6.1.2 Other parameters influencing bioremediation

Bioremediation is promoted by two main mechanisms: biostimulation, which is the addition of nutrients, such as nitrogen, phosphate and potassium, and/or bulking agents (*e.g.*, wood chips), and bioaugmentation, *i.e.*, the addition of an inoculum of microorganisms that possess the capability to remove the contaminants to be treated (Bamforth and Singleton, 2005). In particular, nutrient availability is one of the key parameters exerting a direct influence on the good quality of a bioremediation process. Together with electron acceptors, nutrients can be depleted as well in a contaminated site. The amount of nitrogen and phosphate required to have optimal microbial growth and achieve bioremediation have been estimated, in previous studies, from ratios of C:N:P in microbial biomass ranging between 100:15:3 and 120:10:1 (Bamforth and Singleton, 2005). Another important parameter is temperature: since it changes according to the season, is more difficult to achieve control of bioremediation *in situ*. While higher temperatures enhance compounds solubility increasing their availability, they decrease oxygen solubility, which is against microorganisms' activity. Although PAHs have been shown to be metabolised at extreme temperatures, the mesophilic ones are the most suitable (Bamforth and Singleton, 2005). pH conditions have been found to be optimal around the neutrality (between 6-8) for bacteria, and under 5 for fungi (Wick *et al.*, 2011), thus requiring adjustments in several contaminated sites (*e.g.*, by using lime and elemental sulphur for increasing and decreasing the pH, respectively); however, biodegradation has been still recorded in sub-optimal conditions. Soil pH exerts an influence on the mobility of nutrients and metals; the last ones can be toxic for some microorganisms and reduce their ability to biodegrade contaminants. The optimal moisture content of soils has been reported in the range 50 - 75% of field capacity (Wick *et al.*, 2011). Moreover, high degrees of salinity can negatively affect decontamination (Wick *et al.*, 2011). As already highlighted, bioavailability plays a very important role in the possibility of microorganisms to reach and exert an effect on contaminants: releases of PAHs from soils' or sediments' surface can be achieved by using surfactants, which promote desorption and transfer of hydrophobic compounds in the liquid phase; some microorganisms are able to produce biosurfactants (Bamforth and Singleton, 2005).

Once the bioremediation has been concluded, it is important to regard degradation products, because they can be more toxic than the parent compounds (Shuttleworth and Cerniglia, 1995): examples are represented from oxy-PAHs, quinones and coumarins (Bamforth and Singleton, 2005).

1.6.2 Details on bacterial growth and degradation pathways of PAHs

Biodegradation processes are influenced by the different factors listed in the previous paragraphs, *i.e.* oxygen content, temperature, pH, nutrient availability, etc. Aerobic processes are usually preferred to anaerobic ones because they are thermodynamically favoured: as already explained, the energy conservation in the presence of molecular oxygen is the highest achievable. Moreover, aerobic degradations are fast and, considering the complexity of the reactions involved with PAHs removal, their degradation pathways could be identified easier than anaerobic ones. However, the removal of 2- and 3-ring PAHs under methanogenic, iron-reducing and sulphate-reducing conditions (*i.e.*, anoxic conditions) has been reported (Wick *et al.*, 2011).

Nowadays, a number of bacteria species are known for their ability to remove PAHs: examples reported from Wick *et al.* (2011) are *Alcaligenes* (active on phenanthrene, fluorene and fluoranthene), *Pseudomonas* (that work on phenanthrene, fluoranthene, fluorene and benzo[a]pyrene), *Arthrobacter* (identified for benzene, naphthalene and phenanthrene); actually, a lot of PAHs contaminated soils and sediments contain active PAH-degrading bacteria populations (Bamforth and Singleton, 2005).

Johnsen *et al.* (2005) described bacteria PAHs degradation as limited by the bioavailability of compounds, *i.e.*, by the amount of PAHs dissolved in water phase, whereas PAHs dissolved in non-aqueous phase liquids (NAPLs), or sorbed, or crystalline, result unavailable to microorganisms. According to the authors, bioavailability is related to the double effects of 1) the rate of the substrate mass-transfer to microbial cells, and 2) bacteria catabolic activity. If the mass-transfer rates are high, the metabolic activity of bacteria (influenced by population density and specific activity of the cells) controls biodegradation rate; instead, a lower mass-transfer rate is related to a lower transport of substrate or to the continuous growth of bacteria population. The condition in-between is obtained when the biodegradation rate depends equally on both, physical transport and microbial activity.

In the same study, the authors showed the behaviour of the bacterial growth when the substrate is present in excess in aqueous solution and as crystalline phase, while bacteria grow in suspended and shaken cultures; in this ideal scenario, microorganisms' growth follows three steps: 1) exponential phase, 2) pseudo-linear growth, and 3) pseudo-stationary phase. In phase 1) specific growth rate has the maximum value and is stationary until the phase 2), in which the decay is constant; phase 3) corresponds to the lowest specific growth rate, maintained equal during the whole phase. Until PAHs consumption does not exceed the PAHs dissolution rate, their dissolved concentration is stable at the saturation value, and exponential growth continues (phase 1); then both, dissolved concentration and bacterial growth decrease. Instead, when dissolved PAHs do not saturate the bacterial uptake capability, the exponential growth maintains a sub-maximum rate, and the dissolved PAHs concentration is constant as long as the PAHs surface is not covered by attached bacteria. During phase 3), the entire flux of contaminants serves for the maintenance of bacteria cells.

In the real situation of a soil or a sediment, which is complicated by the adsorption of PAHs to the organic matter and the diffusion of compounds into micropores, the mass transfer constitutes the rate limiting step; the diffusion occurring in this phase can be modelled by Fick's First Law of diffusion[10]. Also, in real soil conditions, bacteria may utilize more than one carbon source for their growth, hence it is possible the threshold limit of PAHs concentration below which their biodegradation stops is not reached. Johnsen *et al.* (2005) propose that, in this situation, bacterial growth stays at phase 3).

Considering the aerobic bacterial metabolism of PAHs, that is shown in Figure 1.6, degradation starts thanks to the action of ring-hydroxylating dioxygenase (RHD) enzymes with the initial oxidation of benzene ring to form *cis*-dihydrodiols. In order to start degradation, the cells must be able to incorporate PAHs (Johnsen *et al.*, 2005). *cis*-dihydrodiols are then dehydrogenated to form dehydroxylated intermediates that can be further metabolised through catechols (thanks to the action of a dehydrogenase enzyme): a catechol dioxygenase performs the aromatic ring fission by *ortho*- or *meta*-cleavage, thus producing aliphatic products that enter the tricarboxylic acid (TCA) cycle; in the end, carbon dioxide and water can be produced. A restricted number of bacteria can oxidize PAHs by the action of P_{450} monooxygenase enzyme, to form *trans*-

[10] Fick's first Law of Diffusion: $\frac{Q}{t} = -DA\frac{C_0 - C_x}{x}$, where Q is the quantity of substrate (mol), t is the time (s), D is the diffusion coefficient ($m^2\ s^{-1}$), A is the area (m^2), $C_0 - C_x$ (mol m^{-3}) is the concentration gradient between source (C_0) and sink (C_x).

dihydrodiols; monooxygenases are responsible of detoxification pathways, rather than assimilation processes. Some enzymes can introduce one oxygen atom into the aromatic ring, hence giving as intermediate an arene oxide; this is then transformed to a dihydrodiol by an epoxide hydrolase or a phenol, through non-enzymatic rearrangement.

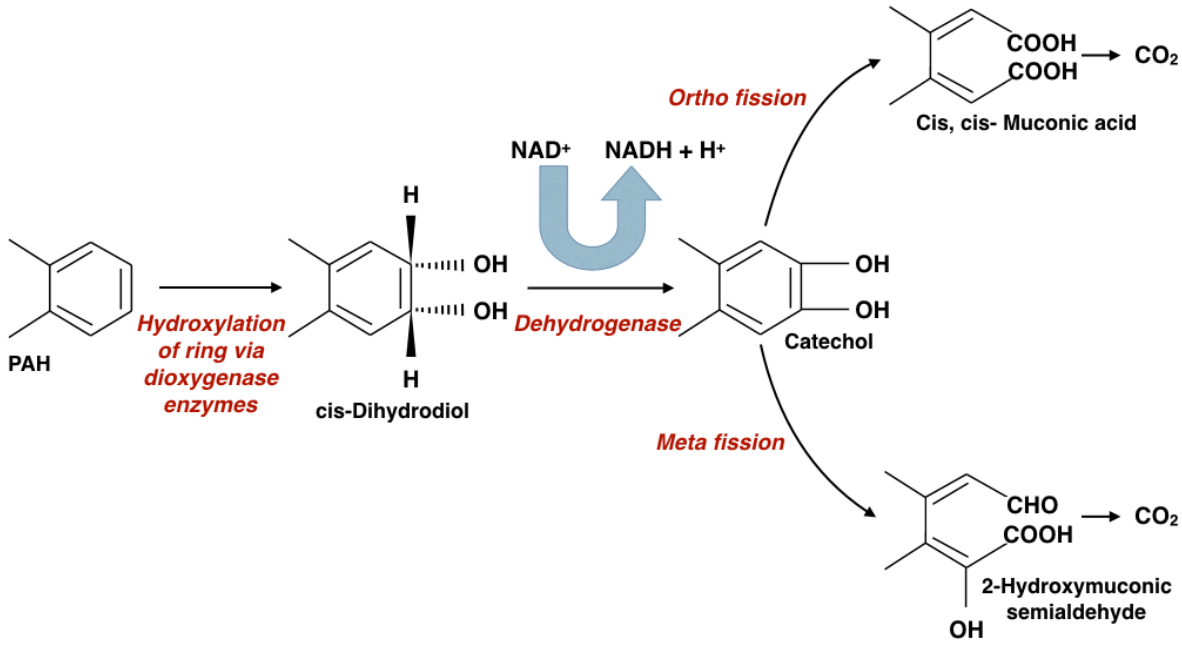

Figure 1.6 *Bacteria pathway for polycyclic aromatic hydrocarbons degradation. Redrafted from: Bamforth and Singleton (2005); Haritash and Kaushik (2009).*

When molecular oxygen is absent, aromatic compounds can be still oxidized in the presence of alternative electron acceptors, such as nitrate, ferrous iron and sulphate (Bamforth and Singleton, 2005). The anaerobic degradation process is slower than the aerobic one, but this mechanism is particularly important because of the presence of natural anoxic environments, such as sediments. When considering contaminated sediments, Haritash and Kaushik (2009) reported that the sediments containing low PAHs levels can be adapted for anaerobic degradation, if they are exposed to high PAHs levels, thanks to an increase of anaerobic PAH-degraders. Meckenstock *et al.* (2016) indicated several attempts of PAHs degradation under anoxic conditions. LMW PAHs were in general degraded as the sole source of carbon and energy under anoxic conditions (*i.e.*, sulphate-reducing, methanogenic and nitrate-reducing). The transformation of larger PAHs was studied in microcosms and occurred, for instance in the case of pyrene, under the three mentioned conditions; moreover, HMW PAHs were degraded under sulphate-reducing conditions in petroleum-contaminated marine sediments. However,

degradation of PAHs containing more than 4 rings is not attributable with absolute certainty to the use of these PAHs as sole carbon sources or to cometabolism mechanisms.
As an example of these processes, Coates *et al.* (1997) found an efficient anaerobic degradation of a mixture of PAHs and alkanes under sulphate reducing conditions. The study, developed in microcosms containing petroleum-contaminated marine harbour sediments, was conducted by inoculating a scarcely contaminated sediment with active PAH-degrading sediments coming from heavily contaminated sites. The authors confirmed the efficacy of the anoxic process since degradation was stopped after the amendment of molybdate, a specific inhibitor of sulphate reduction.

The growth of PAH-degraders in anoxic conditions is very slow: doubling times were found to range between 1-2 weeks up to months, putatively due to the little energy conservation (*i.e.*, little ΔG_r) derived from oxidation in the absence of molecular oxygen (Meckenstock *et al.*, 2016). Here the case of phenanthrene is considered as a representative example and Equation 6 reports the stoichiometric equation of heterotrophic mineralization in sulphate reducing conditions:

Equation 6. $$C_{14}H_{10} + 8.25\, SO_4^{2-} + 9H_2O \rightarrow 14\, HCO_3^- + 8.25\, HS^- + 5.75\, H^+$$

$C_{14}H_{10}$ exchanges sixty-six electrons with SO_4^{2-}, therefore the free energy change associated with the half-cell reduction of the sulphate ion was multiplied by a stoichiometric coefficient of 8.25 in order to obtain a balanced reaction. Considering standard conditions, the ΔG_r^0 of the overall reaction is obtained as the sum of the ΔG_r^0 associated with the half-cell reduction reaction (170 kJ, Table 1.3) and the ΔG_r^0 associated with the half-cell oxidation reaction (-1823 kJ, Table 1.4), and results in -417 kJ. This value, according to previous considerations, is about seventeen times lower than the value calculated for the oxidation of phenanthrene using oxygen as electron acceptor (-6984 kJ). The mineralization under methanogenic conditions results even more difficult; in general, the heterotrophic biodegradation of PAHs in environments in which carbon dioxide or sulphate are the major electron acceptors is less favourable and may be not suitable to enhance microbial maintenance requirements (McFarland and Sims, 1991). In accordance to Monod kinetics[11], the little energy conservation achieved in the absence of molecular oxygen leads to small growth yields, which are directly proportional to slow growth

[11] The Monod equation can be written as: $\mu = -Y \cdot {}^{dS}/_{dt} \cdot {}^{1}/_{X_0}$, where μ is the growth rate, Y is the growth yield, S is the substrate, X_0 represents the initial biomass and t the time of observation.

rates. Based on the previous considerations, Meckenstock *et al.* (2016) proposed that biodegradation of PAH compounds is most likely controlled by kinetics than by thermodynamics.

Although knowledge about the anaerobic degradation of polycyclic aromatic hydrocarbons is still poor, Haritash and Kaushik (2009), analysing previous studies made on compounds like phenols, creosols, benzene, nitroaromatic compounds, proposed that anaerobic bacteria follow a strategy similar to aerobic bacteria: according to their study, the aromatic compounds degradation would pass through transformation in a few central intermediates; then activation and cleavage of aromatic ring would occur, and the obtained cycling compounds would become central metabolites. The authors also suggested that the major intermediates can be benzoate (or benzoyl-CoA), resorcinol and phloroglucinol.
In particular, two main mechanisms have been described for PAH molecule activation (Meckenstock *et al.*, 2016). They involve direct methylation[12] followed by direct addition to fumarate, or carboxylation[13] (Duran and Cravo-Laureau, 2016). Considering methylation, Meckenstock *et al.* (2016) proposed that the process would proceed through the enzyme methyl-transferase; after aromatic ring methylation, a naphthyl-2-methyl-succinate synthase, which is a glycyl-radical-containing enzyme, would catalyse the addition to fumarate. Instead, the enzyme proposed to be active for carboxylation is a carboxylase belonging to the UbiD-like proteins family. Other possible mechanisms proposed for activation are hydroxylation, reduction, reductive dehydroxylation, deamination[14], dechlorination, aryl ether cleavage, and lyase[15] reactions (Haritash and Kaushik, 2009).

Cometabolism is another possible way by which PAHs can be degraded. Examples of cometabolism generally involve more than 4-ring PAHs, due to the scarce bioavailability if compared with other PAH compounds. Alexander (1999) explained cometabolism as related to three main reasons: 1) the transformation of substrate in an organic product no further transformed by the same microorganism; 2) the transformation into organic products which inhibit enzymes or suppress growth; 3) the requirement of an additional substrate suitable for the degradation of both substrates, not available at the time of the reaction. An example of this

[12] Methylation is the addition of a methyl group on a substrate, or substitution of an atom (or group) by a methyl group.
[13] Carboxylation is a reaction of a substrate with carbon dioxide, which leads to production of a carboxylic group.
[14] Deamination is the process of removal of an amine group from a molecule.
[15] The enzyme lyase catalyze the braking of various chemical bonds.

metabolic function reported by Johnsen *et al.* (2005) involves cometabolization of benzo[a]pyrene by bacteria growing on pyrene. Moreover, the authors reported as only few bacteria that can grow in pure cultures by using PAHs with five or more rings have been isolated; in fact, recalcitrant compounds are thought to be oxidized in several steps by consortia of microbes.

1.7 Conclusions

The experiments object of this thesis and herein presented involve both, the aerobic degradation of a mixture of polycyclic aromatic hydrocarbons, and the anaerobic degradation of phenanthrene; PAHs were artificially spiked to marine sediments and degradation was operated by the community of autochthonous microorganisms living in the sediments adopted.

Of course, the degradation of a mixture of PAHs add a certain level of complication to the considerations made above, which are mostly generic for the degradation of a single compound. In fact, considering a mixture of two PAHs, it is possible to observe a preferential degradation of one PAH or the reduced degradation rates of both compounds that indicates metabolic competition (Johnsen *et al.*, 2005). Moreover, Johnsen *et al.* (2005), through lab tests made in the presence of a non-mineralizable compound together with an oxidizable one, described as possible scenarios, apart from the option of cometabolism, the unaffected degradation of the biodegradable PAH without cometabolism of the second one, or the inhibition of the degradation of the oxidizable PAH.

However, it is not redundant to observe that lab experiments made artificially spiking sediments with contaminants (such as the experimental works that will be presented herein) do not consider the important factor represented by the 'ageing' of the contamination, which complicates biodegradation; moreover, the use of pure cultures described in some studies can add another element of simplification, therefore indicating the necessity to evaluate carefully the results achieved.

In this context, the experiments that will be presented in this thesis, rather than reproduce the complexity of a real contaminated site, aim to improve knowledge about conventional and innovative bioremediation processes applied to the removal of PAHs from marine sediments, whose properties and biodegradation mechanisms have been extensively described above.

2 MARINE SEDIMENTS MANAGEMENT

Sediments represent a highly dynamic part of a river or marine system: they are formed by loose particles of sand, clay, silt, organic matter, solid particles that are released from wastewater treatment plants, and also by decomposing plants, animals and other living organisms (Bortone, 2007). Sediments originate typically in river basins through erosion mechanisms and are then transported to the coast, where they settle to the bottom of oceans that constitute their final repository (Salomons and Brils, 2004). Topography, climate, hydrology, geology, but also the land use exert an influence on sediments' formation and movement: materials can be temporarily deposited in the river bed, then they can be transported again; dams, which are often present in regulated rivers, may artificially trap sediments, hence reducing their supply downstream (Salomons and Brils, 2004); sediments can also be deposited in floodplain areas or lake beds (Bortone, 2007). Due to the action of wind, water and ice, transport of particles is not restricted to a single area of the river basin (Bortone, 2007); therefore, downstream areas such as deltas, wetlands and harbours may be highly impacted by sediment movement (Salomons and Brils, 2004).

Geographic origin, physico-chemical properties of the aquatic environments and their complex hydrodynamics that regulate transport or deposition, highly influence sediments chemical and geochemical heterogeneity (*i.e.*, grain size and chemical composition), contributing to determine their quality, which affect the ecological status of waterways. Indeed, according to MAPMED (2015), sediment quality in marine environments may possess a great variability based on the physical parameters of the overlaying water (*e.g.*, temperature, salinity, oxygen, pH) that in turn depend on the considered season; therefore, if the aim is to determine the physico-chemical characteristics of a sediment collected at specific geographic coordinates and at a certain depth, the same assessment may give different results throughout the same year.
Sediment quality plays an important role in biodiversity preservation: in fact, sediments constitute habitat for several microorganisms, supply food and interact with the overlaying water, *e.g.*, regulating the nutrient cycling (Bortone, 2007). However, events of contamination can threaten these important ecologic functions, hence affecting also the ecological or chemical water quality status: mostly due to anthropic activities, such as industrial activities, transportations, and accidents which lead to oil-spills, hazardous chemicals (*e.g.*, PAHs, whose properties, diffusion and removal mechanisms have been described in Chapter 1) have entered the aquatic environment for many decades, and they have been typically found tied to fine clay

particles (Salomons and Brils, 2004).

Moreover, considering practical aspects, contamination adversely affects sediment management because of the high costs involved in handling contaminated material: in fact, due to excessive sedimentation and in order to maintain suitable water depths, areas such as harbours are often subjected to dredging. Dredging helps also in flood prevention, because it may guarantee a correct drainage capacity (Bortone, 2007).
Since large amounts of inorganic and organic pollutants may be released to the water column during dredging operations (Bortone, 2007), and since large volumes are dredged worldwide every year, a proper management of dredged sediments constitutes a serious environmental issue. Moreover, in a vision of circular economy, in which dredged sediments can be considered more as a resource than a waste, proper dredging constitutes also a social and economic issue. The volume of dredged material in Europe has been estimated at 200 million cubic meters per year (Salomons and Brils, 2004). Nevertheless, despite these large volumes, an integrated approach directly addressing sediments management does not exist at the international and European level; the Water Framework directive (WFD) rather aims to the maintenance of a good water quality status, hence promoting operations such as the reduction of pollution sources, which in the long term can lead to a cleaner sediment (Salomons and Brils, 2004). Wherever international and European regulations are not specific, often national regulations intervene: in the following paragraphs the Italian perspective on marine sediment management will be presented as the reference regulation used in this PhD thesis. Moreover, in this chapter an overview of the most common treatments available for sediments contaminated by toxic organic compounds will be given.

2.1 SEDIMENT FORMATION AND CLASSIFICATION

According to Nichols (2009), sediments can be classified, considering their origin, in terrigenous clastic, biogenic, chemical and volcanogenic, as shown in Figure 2.1; principal components found in sedimentary environment can be divided in:

- mineral grains: including quartz, mica, feldspar, calcite, etc.;
- lithic fragments: formed by limestone, mudrock, volcanic rock, metamorphic rock, chert, etc.;
- biogenic material: comprising shells, skeletal material, plant debris, algae/bacteria, bone, etc.;

- chemical precipitates: examples are carbonates, chlorides, sulphates, silica, etc.

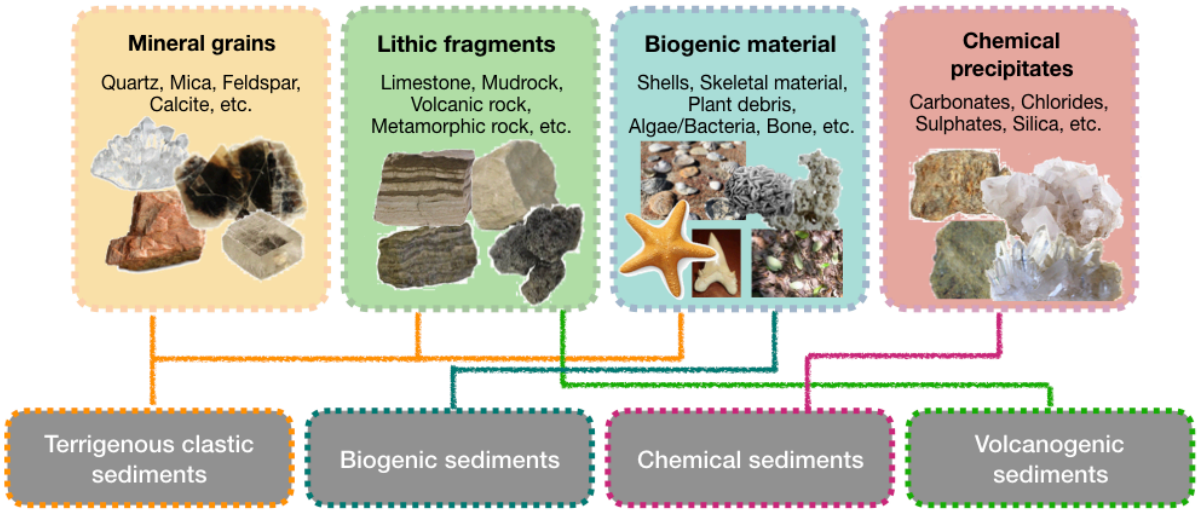

Figure 2.1 *Classification of different sediments present in sedimentary environments (grey rectangles at the bottom) and their principal components (rectangles at the top). Redrafted after: Nichols (2009).*

Particles that are often originated in continents can be transported through glacial and aeolian environments to rivers, lakes and marine environments. Marine environments are differentiated in shallow or deep environments; coastal environments are instead considered transitional environments and are subjected to very complicated dynamics because they represent the junction between continental and marine environment. Deposition can occur in continental and marine environments where materials accumulate, and eventually give origin to sedimentary rocks due to cementation (*e.g.*, volcanoclastic, terrigenous clastic, carbonates, evaporites, coal, ironstones).

Terrigenous clastic sediments are those originated from weathering erosion of pre-existing rocks. They are mostly formed by minerals, lithic fragments and biogenic material and classified according to the size of particles (or clasts), and to their composition. Clasts are commonly composed by silicate minerals. Particles' size ranges from microns (clay particles) to metres (boulders): according to grain size, it is possible to distinguish between gravel (clasts > 2 mm in diameter), sand (clasts between 63 μm and 2 mm) and mud, including sand and silt (< 63 μm).

Sands, formed by weathering and erosion of pre-existing rocks, are mostly composed by minerals and lithic fragments. The commonest minerals associated with terrigenous clastic sediments are quartz, feldspars, micas, other silicate minerals, glauconite, calcite, dolomite; minerals can be found in associations because they derive from the breakdown of original rocks.

Moreover, sands can be composed by oxides (such as iron oxide hematite), sulphides, and heavy minerals. Fragments of broken shells of molluscs and other organisms formed by calcareous hard parts originate the biogenic fragments of sands and are common in materials deposited in shallow marine environments. Wood, seeds and other parts of land plants can be found in both, continental and marine environments.

Clay, silt and mud represent the larger volume of terrigenous clastic sediments: silt indicates material between 4 and 62 μm, while clay is everything under 4 μm; clay and silt particles, mixed together in unknown proportions, constitute the mud. Silt particles, mostly formed by quartz, can be found in air as dust and be transported for long periods before deposition; once in water, silt deposits when the flow is very slow and in the presence of little waves. However, the possibility of contaminants to attach and be adsorbed to sediments is determined by the presence of clay minerals, characterised by very high specific surface and a net surface negative charge deriving from the presence of incomplete bonds in the mineral structure. Clay minerals are aluminosilicates constituted by a layered structure and commonly formed from feldspars and other silicate minerals: crystal layers contain silica, aluminium and magnesium ions and sheets are linked by oxygen atoms. According to the different patterns of layering, it is possible to distinguish between kaolinite group (kaolinite is the most common member) formed by two layers, one layer of silica tetrahedra and one layer of alumina octahedra, and smectite group (*e.g.*, montmorillonite and illite) composed of blocks of three layers, two layers of silica tetrahedra and one inner layer of alumina octahedra, separated by interlayer ions; montmorillonite, formed by interlayer calcium ions, can absorb water within his structure and expand, instead illite contains interlayers of potassium, hydroxide, iron and magnesium ions. Clay particles are cohesive because of the presence of thin films of water between layers that generate strong surface tension effects, and because of electrostatic effects given by the surface charges originated by incomplete bonds in the mineral structure; hence, when they come into contact with each other, they tend to stick. In solution they usually flocculate due to chemical effects (especially in salt waters) or due to biological effects (because bacteria and plankton can produce exopolymers that glue the particles) (Wang and Andutta, 2013a), hence forming small aggregates, with a greater settling velocity than single clay particles.

Biogenic (or biogenous) sediments are ubiquitous in the marine environment and are formed by plants and animal residues, including shell's fragments or corals; size particles is < 0.005 mm and the major components are calcium carbonate ($CaCO_3$) and silica (SiO_2).

Calcium carbonate constitutes hard parts such as shells, that animals leave behind once they die, and can be formed by animals such as molluscs and gastropods, or by plants such as algae or cyanobacteria. Biogenic sediments can be classified according to relative quantities of $CaCO_3$ and SiO_2, and to the depth of water at which sediments are found (shallow or deep). The dominant deposits of this kind of sediments are deep-sea sediments. Lithification processes in the presence of high percentages of calcareous deposits lead to limestones.
Deposits with a high proportion of organic matter are termed carbonaceous: in particular, in order to be considered carbonaceous the proportion of the organic material must be higher than 2% for mud, higher than 0.2% for calcareous deposits, and higher than 0.05% for sand. After deposition, organic matter derived from death of plants or animals, is decomposed and preserved in anaerobic conditions in environments such as stratified lakes and marine waters, hence generating, after diagenetic alterations[16], coal, oil and gas.

Chemical sediments are those formed after chemical processes of precipitation of ions. Volcanogenic sediments originate from solidified material and particulate matter coming from volcanic eruptions: the two major components of volcanogenic sediments are pyroclastic debris, which derive from aerial and subaerial volcanic explosions, and volcanoclastic materials or reworked fragments of volcanic rocks, derived from chemical and mechanical processes (Kennish, 2000).

2.2 TRANSPORT PROCESSES, DEPOSITION AND EFFECTS ON DEPOSITIONAL ENVIRONMENTS

Sediments generation can occur due to the up-lift of pre-existing bedrocks, through their exposition to weathering; bedrocks represents, in fact, the ultimate source of loose materials in the environment. This phenomenon is quite spread: Oldeman *et al.* (1991) estimated that European land areas subjected to soil erosion represent about the 17% of the total land areas. The erosion mechanism is worldwide enhanced by phenomena such as deforestation, urbanisation, agricultural practices, leading in extreme cases to desertification (*e.g.*, in some Mediterranean areas) (Salomons and Brils, 2004). Eroded materials are then transported as dissolved or particulate matter.

[16] Process involving physical, chemical and biological changes in sediments: diagenesis occurs after deposition and before metamorphism, and between deposition and weathering.

Particles movement can occur due to gravity (*e.g.*, rock falls) or to the flux in water, air, ice or in dense mixtures of sediments and water: water flowing through river channels, currents generated by wind, tides and oceanic recirculation are the main mechanisms of sediment transport. According to the strength of the water flow, coarser materials can be moved along the base of the flux while the finer particles are transported in suspension. Considering transport in river systems, particles does not travel very far apart from during extreme floods or in mountain catchments (Salomons and Brils, 2004); river bed incision is an important secondary source of river sediments. If the concentration of sediment in water is very high, the mixture formed is called 'debris flow' and it has the consistence of a slurry (Nichols, 2009). Instead, wind is mainly responsible for the transport of dust that can cover long distances. Sediments found in estuarine and delta zones in areas with little or no offshore currents and with limited tidal range, such as the Mediterranean Sea, have generally river origin, whereas river estuaries, that possess large tide, trap a net amount of seabed particles, thus requiring quite often dredging operations to guarantee the availability of waterways. Only small portions of river sediments can reach open seas (Salomons and Brils, 2004).

The velocity of water flow is important since it regulates the possibility of loose particles to move: in fact, once a grain has settled, a greater amount of energy is required to start it moving; also, because of the cohesive behaviour of clay particles (especially when they have been compacted), fine-grained sediments need a higher velocity to be transported. Protected environments such as ports and artificial harbours are particularly subjected to deposition, due to slower water flow if compared with the open sea: these human artefacts, which are useful for reasons such as facilitating ships' trade, and structures associated with harbours (*e.g.*, breakwaters and seawalls or other shoreline structures) can change the wave characteristics close to the shore and hinder the possibility of water to naturally adjust cycles of deposition and resuspension.

A proper control of sediment deposition is very important due to the generation of possible environmental impacts: too much sediment can lead to the obstruction of channels, rivers fill and flood, smothering of reefs and turbidity; on the contrary, too little sedimentation has the consequence to erode beaches, riverbanks, degrade river profiles and lead to the loss of wetlands (Salomons and Brils, 2004). Therefore, an excessive deposition or erosion require the already mentioned dredging operations (much more details will be given in the next paragraph) or other interventions (Walker, 2012).

Moreover, streams, marine environments, groundwaters, lakes, wetlands constitute habitat for an enormous variety of species. In particular, sediment biota plays an important role in the mediation of biogeochemical transformations of global significance, in the maintenance of clean water, in the decomposition of organic material, in the uptake and transfer of materials and also in primary production[17]. Quite often organisms stay confined within the deep sediments, therefore they can be affected by sediments deposition (and resuspension). Moreover, in the presence of a high concentration of sediments close to the surface, the sunlight penetration in the water column is decreased, hence the formation of mud flocks and the possibility of their deposition is slowed down because the reduced lighting influences the formation of plankton, which in turn contributes to biological flocculation. Types of sediments and flocculation processes may influence the profile of vertical distribution of suspended sediment concentration. Vertical profile can lead to a well-mixed distribution, a smooth increase of concentration with depth, or a high depth concentration when vertical mixing is hindered (Wang and Andutta, 2013b).

In addition, coastal infrastructure (even when built using natural materials such as stones) and their interaction with the sedimentation process, may influence habitats and key ecological processes, determining which kind of species can establish populations on it. Shoreline infrastructures change illumination, water flow, rates of sedimentations, therefore, they can generate harmful effects on organisms; they create artificial slopes that constrain species in small portions of the intertidal habitat, hence the density of population is increased, and sometimes they may put in contact species that normally would have lived separately. Sometimes, unnatural materials may provide an environment totally unsuitable for colonization. On the other hand, built structures often represent sheltered habitats (whereas some rocks can be naturally exposed), therefore they might promote the development of several different species (Bulleri and Chapman, 2010).

2.3 DREDGING TYPOLOGIES AND MAJOR IMPACTS THAT OCCUR DURING DREDGING OPERATIONS

According to the European Dredging Association (EuDA), dredging involves operations such as ‘bringing up, fishing up or clearing away or out material and/or any object from the bed of a

[17] Primary production is the biological synthesis of organic compounds from inorganic carbon. The process occurs in the euphotic zone of the upper ocean.

river, sea, etc.' and 'transporting it to a relocation site'. Dredging operations made in order to render waterways suitable for shipping are called 'maintenance dredging'; they have been already introduced above and are different from capital, mineral and remediation dredging. Maintenance dredging impacts are generally limited, but they can increase when sediment is contaminated.
'Capital dredging' involve building new civil engineering works such as harbours and the deepening of existing waterways or approach channels. Capital dredging generally concern unpolluted soil, so that the environmental effects are restricted to habitats and ecosystems existing underwater; sediments are only temporarily removed from their environment.
'Mineral dredging' include the activity of extraction of minerals having an economic value, but also sand, gravel and clay. The non-valuable materials are in general put back underwater. Effects on the environment are similar to the ones generated from capital dredging.
'Remediation dredging' involve the removal of polluted sediments from environments such as harbour basins and rivers. They are considered as a particular typology of maintenance dredging. Environment can be highly impacted from this kind of dredging operations, since they involve the management of contaminated sediments.

Mechanical operations such as excavation, transport and deposition, which constitute basic steps of dredging activities, can easily affect the surrounding environment and originate impacts, *e.g.*, the decrease of invertebrate species, the increase of oxygen demand due to the re-suspension of sediments and the associated increase of turbidity levels, alterations of the seabed surface, the formation of dredging plumes and the exposure of organisms to contamination (Manap and Voulvoulis, 2015). In fact, each step is made up by using mechanical instruments: excavation is made thanks to hydraulic and/or mechanical cutters, and dredging is often executed at port basins by anchor dredgers, which move by anchor and/or hydraulic spud; hoppers or pipelines are used for collecting sediments and for transporting them to a disposal site.

As mentioned in the introduction, sediment can often act as sinks retaining contaminants that have settled at the bottom of an aquatic environment. Organic and inorganic contaminants coming from rural, urban, and industrial and mining areas can enter river systems and aquatic environments in general as direct or indirect inputs. Considering the contributions from rural areas, waste dumps that arrive first to the groundwater, and then reach surface waters, represent an example of indirect input, as well as geogenic background, agriculture and atmospheric

depositions that reach soils and afterwards surface waters as the result of soil erosion, runoff, etc.; atmospheric deposition can also constitute an example of direct input. Traffic, building materials, industry and households releases represent indirect inputs from urban areas, and reach surface waters passing through paved areas or are discharged first to sewer systems and then proceed through wastewater treatment plants. Contaminant releases coming from shipping, or industrial and mining activities effluents are instead classified as direct inputs (Salomons and Brils, 2004). Sediments constitute also repository for nutrients generated by microorganisms or human activities (*e.g.*, the usage of fertilizers in agriculture), and for metals, such as zinc and cadmium that can be originated from sedimentary and volcanic rocks.

All these compounds can be released when sediments are disturbed and moved, hence the choice of the correct management option (*e.g.*, during dredging operations) is fundamental (Manap and Voulvoulis, 2015): even if contaminants are hazardous, they may exert only a negligible risk if they are strongly bounded to sediments and sediments are not moved from their original position; on the contrary, the risk for ecological and chemical water status is higher if contaminants become bioavailable (*e.g.*, when sediments are resuspended). However, the actual effects generated by sediments contamination are difficult to predict due to the complex interactions existing between sediments and the surrounding environment. For example, contaminants such as PAHs, described in the Chapter 1, which tightly bond with sediments, can fast sink in association with sediment particles and then accumulate at the bottom of the water body, constituting an important source of contamination in the marine environment when sediments are resuspended in the water column during dredging operations (Vagge *et al.*, 2018); they can also diffuse due to the release of interstitial water from bottom sediments, to the transport of resuspended material that have absorbed PAHs, and to the action of processes such as erosion and runoff, or PAHs desorption and degradation. Sediment contamination may exert toxic effects on living organisms, whose abundance can be reduced, and more susceptible species can even disappear; therefore, the food availability for higher organisms can decrease. Moreover, microbes altered by pollution can be consumed by higher organisms, hence causing bioaccumulation and biomagnification, affecting all the food chain and negatively influencing the natural ecosystem (Salomons and Brils, 2004).

Therefore, in order to protect the surrounding environment, the characterisation before, during and after dredging operations becomes fundamental (Vagge *et al.*, 2018). Once the material has been dredged, in the presence of uncontaminated sediments open water disposal is widely adopted, thus requiring adequate barriers in order to avoid diffusion of suspended sediments;

conversely, management options different than open water disposal become particularly important when sediments are contaminated (Manap and Voulvoulis, 2015). Further information about management options consequent to dredging operations and examples of suitable remediation will be given in the following paragraphs.

2.4 MAIN REGULATIONS FOR THE MANAGEMENT OF DREDGED MATERIALS COMING FROM MARINE ENVIRONMENTS: INTERNATIONAL, EUROPEAN AND ITALIAN PERSPECTIVES

Thus far, International laws have specifically addressed soils, wastes and waters management, rather than directly regulate sediments dredging and the management of dredged materials. Moreover, sediments have been often mentioned in International conventions and protocols regarding marine environment protection and recovery, only sometimes considering aspects related to dredging. Nevertheless, International regulations indicate three main principles of general validity, easily applicable to the specific case of the management of dredged materials:

- precautionary principle: water disposal is allowed only after a proper sediment characterisation that considers also environmental impacts and the subsequent monitoring;
- polluter-pays principle: the polluter is considered responsible of bearing the cost of environment remediation;
- integrated management of coastal zones: socio-economic and environmental aspects must be integrated when dealing with marine environments.

Therefore, nowadays the general tendency is to consider the resulting materials as resources more than wastes: a beneficial reuse of dredged sediments alternative to water disposal is certainly the preferred choice.

The ‘Convention on the Prevention of Marine Pollution by Dumping of Wastes and Other Matter 1972’ of the ‘International Maritime Organization’ (IMO), also called ‘London Convention’, in force since 1975, is one of the first global conventions that have considered the marine environment protection from human activities by promoting the control of sources of marine pollution and preventing contamination. 87 States are currently Parties to this Convention. In 1996 the ‘London Convention’ was updated in the ‘London Protocol’ (50 States are Parties to the Protocol) that forbade dumping, except for some wastes listed in the Protocol

(http://www.imo.org/en/OurWork/Environment/LCLP/Pages/default.aspx). Other global regulatory guidelines have been developed from 'United Nations Educational, Scientific and Cultural Organization' (UNESCO) or from 'PIANC, The World Association for Waterborne Transport Infrastructure' (PIANC); the latter proposed guidelines for the disposal of dredged material.

In the same way, European regulations do not address directly dredging activities; they rather give suggestions and inputs useful for regulations afterwards adopted by single States considering their own site-specific conditions. The main legislative reference is the 'Directive 2000/60/EC of the European Parliament and of the Council of 23 October 2000 establishing a framework for Community action in the field of water policy', called 'Water Framework Directive (WFD)'. The WFD aims to protect and improve the aquatic environment, by adopting, between the others, 'specific measures for the reduction of discharges, emissions and losses of priority substances' and for the 'cessation or phasing-out of discharges, emissions and losses of the priority hazardous substances' (art. 1, letter c). The WFD distinguishes between 'ecological status' and 'chemical status'. Ecological status is classified in all water bodies in terms of five classes (*i.e.*, high, good, moderate, poor or bad) and is assessed with respect to biological, physico-chemical and hydromorphological elements (*e.g.*, using numeric measurements of communities of plants and animals, evaluating temperature and nutrient content, water flow, sediment composition and movement). Chemical status considers the quality standards established for chemical substances at the European level (http://ec.europa.eu/environment/water/water-framework/info/intro_en.htm). In this scenario, dredging activities are considered compatible with the environmental protection when the requirements of water preservation and maintenance of a high standard of the water quality are met.

Sediments are also mentioned in the European soil legislation and European waste legislation. For example, 'Soils protection Acts' (in force in some European countries) establish actions such as avoiding to release excessive quantities of particulate matter in the water bodies in order to prevent soil erosion; the 'European Waste Directive' (or 'Directive 75/442/EEC') includes treatment and safe disposal of sediments as measures appropriate to avoid waste production and re-use profitably wastes; the 'European Landfill Directive' (or 'Directive 1999/31/EC') is applied when dredged material is disposed on lands.

Other minor regulations mentioning sediments that are useful in the European context are the 'Council Directive 92/43/EEC of 21 May 1992 on the conservation of natural habitats and of

wild fauna and flora' (or 'Habitats Directive'), or conventions written by organizations such as 'OSPAR Commission Protecting and conserving the North-East Atlantic and its resources' (OSPAR Commission) and 'HELCOM, Baltic Marine Environment Protection Commission' (HELCOM) (Salomons and Brils, 2004).
Considering the fragmentariness of the European Legislation, the organization 'European Sediment Research Network' or 'SedNet', supported by the European Commission, was formed in order to help actions at the river basin scale, with a major focus on the sustainable management of contaminated sediments. According to SedNet, any decision regarding sediment management should consider the impacts exerted by sediment contamination on the chemical or ecological water status (as defined from the WFD) (Salomons and Brils, 2004; Bortone, 2007).

The main Italian regulation for the environmental protection is the 'Decreto legislativo 3 aprile 2006, n. 152 Norme in materia ambientale' (*i.e.*, 'Legislative Decree 152/2006' or 'Regulations concerning the Environment') and its subsequent amendments. In particular, article 109 transferred the power to take decisions regarding the seawater disposal of materials excavated from the seabed, and the laying of cables and pipelines underwater, to local authorities (except for particular cases). Therefore, until 2016, in the absence of specific regulations, the 'Manuale per la movimentazione dei sedimenti marini' (*i.e.*, 'Manual concerning the movement of marine sediments', written by the 'Agency for the environmental protection and for the management of technical services' (the Italian APAT) and by the 'Central Institution for the Scientific and Technological Research applied to the Sea' (the Italian ICRAM) in 2008, herein indicated as ICRAM Manual) was used as the main reference for the characterization of sediment quality. In 2016 the 'Decreto 15 luglio 2016, n. 173 Regolamento recante modalità e criteri tecnici per l'autorizzazione all'immersione in mare dei materiali di escavo di fondali marini' (*i.e.*, 'Ministerial Decree No. 173/2016' or 'Regulation concerning technical criteria for the seawater disposal of materials excavated from the seabed') was approved.
This regulation involves:

- procedures for obtaining the permission for the seawater disposal of materials excavated from the seabed, according to the article 109 of the Legislative Decree 152/2016;
- homogeneous criteria for the Italian territory in order to maintain an adequate water status quality (as required by the WFD), regarding the beneficial reuse of dredged materials (*e.g.*, use for replenishments operations) and also the characterization of the sediment quality and its classification procedures;

- management of materials dredged in port and marine coastal areas not comprised in sites of national concern (specifically regulated);
- management of materials coming from sites of national concern, in areas located outside from these sites.

This Decree is directly connected to the Ministerial Decree No. 172/2016 that regulates, instead, dredging operations within sites of national concern.

2.5 CHARACTERISATION AND MANAGEMENT OF MARINE SEDIMENTS ACCORDING TO THE MINISTERIAL DECREE NO. 173/2016

Sediments quality standards defined as threshold values according to the current legislation may be overcome in harbour and port areas, due to anthropic activities but also due to natural causes (*e.g.*, the erosion from rocks containing a high percentage of hazardous compounds). As already explained above, sediments interact with the water column and living organisms, strongly influencing the marine ecosystem quality; therefore, a common approach for the assessment of sediment contamination is to consider the sum of different aspects (Salomons and Brils, 2004):

- chemical analysis can serve to determine the concentration of pollutants; contamination is assessed by the comparison with standard or guidelines values;
- bioassays can be used to evaluate the toxicity to organisms;
- field inventories can help in investigations regarding the long-term impact on sediment biota.

Sediment characterisation includes also physical characteristics and chemical composition of the sediment itself. Moreover, temporal and spatial aspects must be considered when evaluating the effectiveness of remediation treatments or when planning monitoring actions: a characterisation should be representative of the whole surface and volume to be excavated and moved, and the choice of sampling points should be based on historical data and information about the most vulnerable areas and probably contaminated zones. In Figure 2.2 the procedure for the characterisation, classification and management of dredged materials is schematised, as indicated in the Technical Annex of the Ministerial Decree No. 173/2016. The schematisation is divided into three main parts: the first section is dedicated to the collection of information

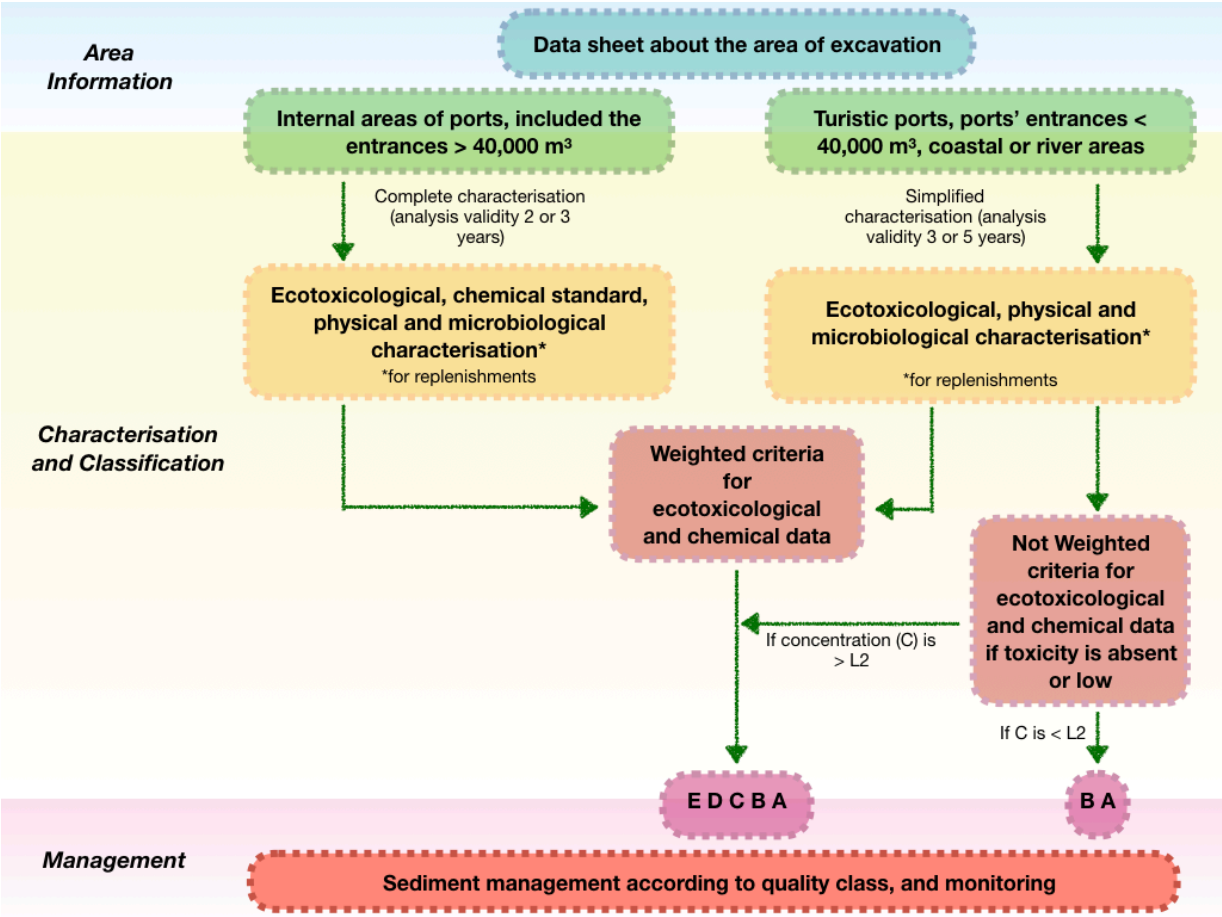

Figure 2.2 *General framework for dredged material characterisation, classification and management: the first step is represented by the area information, the second one by the characterisation and classification of the sediment quality, the last one is the management; letters indicate each Quality Class. Redrafted after: Technical Annex of the Ministerial Decree No. 173/2016.*

about the area of excavation, the second to the characterisation and classification and the third to the choice of the best management option. The collection of information about the area proposed by the Ministerial Decree includes pre-existing information and has to be reported in a default data sheet. The characterisation of dredged material is made after a proper sample collection: the number of samples is decided in advance overlapping a square grid, whose size changes according to the position in the area of excavation (*e.g.*, more samples close to artefacts). In addition, according to the size and typology of the area of excavation it is possible to adopt the normal or the simplified procedure: for instance, touristic ports are subjected to simplified procedure. The normal procedure includes ecotoxicological, chemical standard, physical and microbiological characterisation for each sample collected, whereas the simplified procedure generally requires the analysis of some specific chemical parameters (however, if the information collected for a particular sample are scarce or absent, or the sample has been

classified for mean or high toxicity, all chemical standard analyses become compulsory). Chemical standard characterisation is made analysing each chemical parameter listed in Table 2.4 of the Technical Annex (*e.g.*, a specific list of metals, PAHs, polychlorinated biphenyls); national chemical levels of the chemical parameters are reported in Table 2.5 of the same document; chemical levels are the same previously adopted in ICRAM Manual. Levels, expressed per kg of dry sediment (dw), are distinguished between lower levels (L1) and higher levels (L2). The chemical levels of the four PAHs used in the experimental work object of this thesis are indicated in Table 2.1.

Table 2.1 *National chemical levels for the PAHs used in the experimental work object of this thesis and taken from Table 2.5 of the Technical Annex of the Ministerial Decree No. 173/2016. Low and high levels (L1 and L2) are reported.*

PAHs used in the experiments	L1 [µg $kgDS^{-1}$]	L2 [µg $kgDS^{-1}$]
Fluorene	21	144
Phenanthrene	87	544
Fluoranthene	110	1494
Pyrene	153	1398

In some cases, it is possible to add compounds to the list of chemical standard parameters. Moreover, according to the normal procedure, analyses are valid in the range between two or three years, whereas, according to the simplified procedure, between three or five years. At the end of the characterisation, dredged materials can be classified in five different 'Quality Classes' (A, B, C, D, E) each one related to specific management options: the better quality of dredged materials is related to class A, the worst to class E. For example, when sediment quality is high, possible options are replenishments or seawater disposal, whereas when sediment belongs to Quality Class E, material must be safely removed from the marine environment after a proper risk evaluation, in accordance to the current legislation. For the normal procedure of characterisation, the attribution to a specific 'Quality Class' is always made by integrating chemical and ecotoxicological characterisations and applying weighted criteria; only in specific situations weighted criteria are adopted also for the simplified procedure. Once the Quality Class has been determined, a physical characterisation is important for the decision of the specific management option. Biological characterisation is unavoidable in areas intended to aquaculture and bathing. The process indicated in Figure 2.2 is concluded with the choice of the best management option and of a proper monitoring.

2.6 TREATMENTS SUITABLE FOR SEDIMENTS CONTAMINATED BY ORGANIC COMPOUNDS

The possibility to remediate contaminated sediments and the risk associated with contaminants are highly related to the processes used to control contaminant release and their movement towards aquatic organisms, which in turn depends on the volume of sediments that is going to be managed: according to Majone *et al.* (2015) this volume, at certain sites, can exceed one million cubic meters and is associated with large volumes of water. Contaminated sediments are generally managed in Europe and the USA through dredging and dump site accumulation: this is the easiest way to handle large volumes, sometimes characterised by a complex contamination, whereas treatment and re-use are generally encouraged on a small scale, due to the higher costs compared to disposal and the higher difficulty to sell this material. It is generally possible to distinguish between physico-chemical and biological treatments (bioremediation) (Alvarez and Illman, 2005).

Sediment washing is a physico-chemical technique that is employed for a wide range of organic contaminants (the treatment is suitable also for inorganic compounds): the first step involves the removal of metals; clay and silt particles, which constitute the most contaminated fractions, are separated from sand and generally disposed, because they represent a little portion and their treatment could be too expensive; gravel and sand are washed apart. If contaminants are not present as a separate phase, they are generally detached through physical actions such as scrubbing and scraping, or through washing agents that can be applied individually or as mixtures (*e.g.*, surfactants, organic solvents, acids, bases or chelating agents used with water). Units of sludge and water treatment are necessary (Todaro *et al.*, 2016). Sediment washing is quite effective for HMW PAHs that are strongly bonded to solid particles (Kuppusamy *et al.*, 2017).

Incineration and *in situ* thermal desorption (ISTD) can be applied for sediments containing organic contaminants that volatize below 650 °C (*e.g.*, polychlorobiphenyls, PAHs and mineral oils). Incineration is usually operated at temperatures ranging between 900 and 1,200 °C. Dewatering pre-treatment is generally required. ISTD uses heat to separate organic compounds, but no excavation is required; the treatment is considered safe because contaminants are volatised in a carrier gas or vacuum system and then transported to a gas treatment system (Kuppusamy *et al.*, 2017).

Vitrification is another physical process that applies electricity to electrodes inserted into sediments in order to heat them at about 1,600°C, hence destroying organic compounds and immobilising inorganic contaminants within sediments particles. When treating marine sediments, in order to avoid volatilisation and the consequent corrosion of the system, salts must be removed before to apply this process; moreover, dewatering is necessary (Todaro *et al.*, 2016).

Chemical oxidation acts through the injection of an oxidant (*e.g.*, commonly Fenton's reagent and ozone, but also potassium permanganate, hydrogen peroxide, sodium or iron activated persulphate and peroxy-acid) in soils: it is an effective *in situ* treatment on both LMW and HMW PAHs. A pre-treatment of extraction is required in order to increase contaminants availability (Kuppusamy *et al.*, 2017).

Although physico-chemical treatments are effective and faster than biological ones, the former are more expensive due to the large employment of chemicals and to the high energy requirements (Daghio *et al.*, 2017): in the last few decades natural attenuation processes, mediated by microorganisms and applied to the treatment of sediments contaminated by organic pollutants, have received a rising attention (Majone *et al.*, 2015).

Landfarming is an example of bioremediation process in which contaminated sediments are spread on the soil surface (or enclosed in biotreatment cells) and are regularly turned over to allow aeration. The treatment involves the use of common agricultural practices. The moisture content is controlled by irrigating or sparging, pH is buffered around neutrality (*e.g.*, amending agricultural lime), and bulking agents and nutrients in the form of fertilisers (to allow biostimulation) are added. The fact that the process is limited to the top soil (between 10 – 35 cm from the soil surface), the possibility of contaminants to move from the treatment area, the possible influence of weathering (*e.g.*, rainfalls) and the possibility for PAHs degraders to lack in the natural environment are between the major drawbacks of landfarming. The last issue can be overcome by adopting the practice of bioaugmentation of an acclimatised biomass deriving from sites that possess an old contamination and/or highly contaminated: degradation can be facilitated adding both aerobic or anaerobic degraders (Todaro *et al.*, 2016; Kuppusamy *et al.*, 2017).

Composting is another biological process in which, under both, aerobic or anaerobic conditions, indigenous microorganisms can degrade organic contaminants to less toxic or innocuous by-products. Composting technology include the use of blowers to aerate the 'aerated piles', the use of mobile equipment in order to periodically mix the 'windrows' (*i.e.*, long piles of

compost), or the employment of closed reactors. Temperature (between 54 and 65°C), water, oxygen and nutrients content must be controlled to established values (Todaro *et al.*, 2016).
Phytoremediation is a degradation process enhanced by plants, that can be applied to organic or inorganic contaminants: plants can accumulate/sequester/chemically transform contaminants present in soils; moreover, they can secrete enzymes that act as surfactants hence increasing the bioavailability of contaminants and improving the nutrient status of the soil (Kuppusamy *et al.*, 2017). Metabolic processes can be promoted in the rhizosphere (*i.e.*, the area immediately close to the plant roots): roots facilitate contaminants movement in the rhizosphere and their uptake by plants; they also exert an indirect effect by providing nutrients in the form of exudates; moreover, dead roots represent an important biodegradable carbon input in soils able to promote the microbial activity. Another way to promote contaminants removal is their translocation into the plant shoots, where they can be accumulated, transformed and transpired from the plant (Hutchinson *et al.*, 2011). Drawbacks of phytoremediation are the length of the processes (for example, according to Straube *et al.* (2003), PAHs treatment can exceed one year), and the limited application due to presence of phytotoxic contaminants.
Slurry bioreactors represent one of the most important and well-established *ex-situ* processes for the treatment of highly recalcitrant organic compounds, such as PAHs, under controlled environmental conditions (Robles-González *et al.*, 2008), though these processes can be effectively applied only to small sediment volumes (Wick *et al.*, 2011). The slurry phase (*i.e.*, the mixture of a certain low percentage of solid in liquid) promotes the contact between microorganisms and contaminants, a complete mixing and a better oxygen diffusion (if the process requires aeration), thereby fastening the process; moreover, the technology is easy-monitored thanks to the use of a close reactor.

From the points raised in the first part of this chapter, it is evident that contaminated sediments represent a serious threat for the human health and the ecosystem protection. They also constitute a recognised social and economic problem due to the large quantities of materials deposited close to strategic points (such as ports), that require periodical dredging and a proper management. Therefore, although the treatment presented above are conventionally used and widely applied, there is a continuous need for improving consolidated processes and finding new and better technologies, which could be less expensive and more effective. In this regard, some emerging technologies have been recently studied in the lab-field.

Electrokinetic remediation (see section 1.6) is a physicochemical treatment used for treating low hydraulic permeable soils. Until now attempts to remediate PAH-contaminated sediments by using this technology have been done only in the lab-scale; however, the removal with the traditional treatment is difficult due to their hydrophobicity and slow desorption rates, therefore solubilizing agents such as surfactants, co-solvent and cyclodextrins have been used to enhance compounds removal (Kuppusamy *et al.*, 2017).

Photocatalytic degradation is a process that uses photocatalysis to destroy organic contaminants through oxidising reactions in the presence of light radiation. As electrokinesis, the technique is well-established for the treatment of wastewater, but has been only recently applied to contaminated soils and sediments (Gan *et al.*, 2009). The use of titanium dioxide under ultraviolet (UV) light was demonstrated to accelerate photodegradation of PAHs; the process rate was different under different wavelengths and the process was also affected by pH; moreover, the presence of humic acids was shown to oxidise PAHs through sensitising radicals (Zhang *et al.*, 2008).

Bioelectrochemical processes are an innovative and promising technology in the field of soils and sediment biological remediation (Majone *et al.*, 2015): the addition of soluble electron acceptors or donors is not required, because this technology employs solid state electrodes that can be used by certain microorganisms thanks to extracellular electron transfer (EET), *i.e.*, the capability to move electrons outside the cell membrane. Electrodes can be conveniently tuned at the desired electrochemical potential, thereby promoting biodegradation of contaminants whilst producing electrical energy and/or useful chemical products according to the spontaneity or not of the process. The production of an electric signal makes the technology particularly smart due to the possibility to monitor process operation from remote fields site locations; moreover, the process can be operated in completely anaerobic conditions, hence it does not involve energy requirements for aeration. Sediment microbial fuel cells or electrolysis cells are prototypes of bioelectrochemical systems (BESs) used for sediment remediation (SBESs).

With the aim to improve techniques for the treatment of marine sediments polluted by organic compounds, this experimental work explores in particular the use of aerobic conventional bioremediation adopting slurry bioreactors and of microbial electrochemical technologies (METs) for the treatment of a PAHs contamination. A better detail on these technologies will be given in Chapters 3 and 4.

3 TREATMENT OF MARINE SEDIMENTS CONTAMINATED BY PAHs IN BIOREACTORS USING THE SEDIMENT SLURRY SEQUENCING BATCH REACTOR TECHNOLOGY

3.1 THEORETICAL PRINCIPLES AND LITERATURE REVIEW

The slurry bioreactor technology, as introduced in section 2.6, is an *ad site* or *ex-situ* biological treatment, useful for the bioremediation of soils and sediments contaminated by recalcitrant pollutants such as polycyclic aromatic hydrocarbons, and in situations in which an *in situ* treatment is not convenient, *e.g.*, in the case of little accessible sites or areas that present extreme conditions unsuitable for the microorganisms activity (*e.g.*, low temperatures).

Bioreactors can be operated as batch reactors (also in semi-batch), Continuous Flow Stirred Tank Reactors (CFSTRs) or Sequencing Batch Reactors; moreover, reactors can be operated in aerobic, anoxic or anaerobic conditions.

As shown in Figure 3.1, treatments in slurry bioreactors generally comprise an installation for the contaminated soils handling and conditioning, the bioreactor itself, installations for the treated soils management and disposal and an equipment for the further treatment of process by-streams. Treating soils or sediments in percentages that typically range between 10 to 30% w/v of solids in aqueous suspension is the hallmark that distinguish slurry treatments from other bioremediation technologies such as composting and landfarming; the slurry is maintained in suspension by providing pneumatical or mechanical mixing (predominant for aerobic bioreactors). Therefore, in contrast to solid phase biotreatments, bioslurry reactors give the advantage to increase mass transfer rates whilst increasing the contact microorganisms/pollutants/nutrients and enhance the rates of contaminants biodegradation; as a consequence, treatment times can be significantly shortened. Moreover, engineered close reactors give the possibility to use electron acceptors different than oxygen (although aerobic treatments have been mostly applied), allow an easy and strict control over operational conditions, such as temperature (generally maintained between 25 and 30°C) and pH (usually kept between 6.75 and 7.25), and over processes evolution; biostimulation and bioaugmentation can be effectively applied, and contaminants bioavailability can be increased by amending surfactants and solvents. However, this technology requires soil excavation, handling and

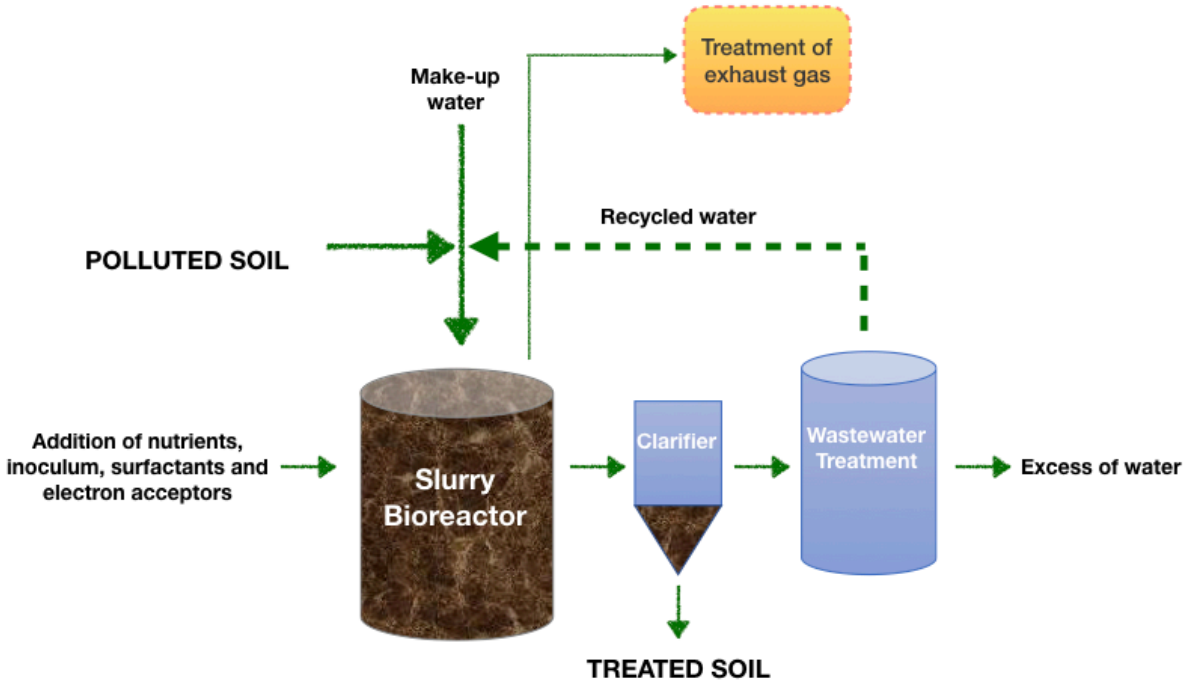

Figure 3.1 *Scheme of typical slurry bioreactor installation: polluted soils or sediment, nutrients, inoculum, possibly surfactants, electron acceptors and make-up water enter the reactor; slurry can optionally pass through a clarifier where treated soil is collected separately from water that go to a wastewater treatment phase. An excess of water is discharged, whereas clean water is recirculated to the slurry bioreactor. Another line exists for the treatment of exhaust gas. Redrafted after: Robles-González, Fava and Poggi-Varaldo (2008).*

conditioning before the treatment, and each step, from the building of each installation to the operation of the bioreactor, is more expensive if compared to other biological treatments (Robles-González *et al.,* 2008).

According to Cassidy *et al.* (2000), two main factors exert an influence on bioslurries performances: the kinetics of contaminants biodegradation and foaming. For example, design and operation of slurry reactors are highly dependent on the rate and extent of contaminants degradation. Generally Monod kinetics are assumed as valid (Eweis *et al.*, 1998) but, due to the difficult measurements of biomass in the presence of soils or sediments and to the association of contaminants to solid particles, attributing a specific kinetic to a degradation process is not that easy (Cassidy *et al*. 2000). Foaming has been related by Cookson Jr (1995) and Eweis *et al.* (1998) to the formation of biosurfactants in bioslurry reactors, which can be associated to the more difficult microbial growth in the presence of low soluble substrates (Miller, 1995). This problem can be solved by reducing aeration rates and/or mixing velocity. However, biosurfactants may give the beneficial effect to improve the biodegradation because they can promote the passage of contaminants in the water phase (Miller, 1995).

Moreover, according to Chiavola *et al.* (2010), the volumetric exchange ratio (VER) (*i.e.*, the volume of slurry replaced at the end of each cycle relative to the total volume of slurry), the hydraulic retention time (HRT) (*i.e.*, the cycle length divided by the volumetric exchange ratio), the solids concentration (often described as weight of solids over volume of liquid), the volumetric organic loading rate (vOLR) (or slurry loading rate, *i.e.*, the quantity of contaminants fed to the system, per unit of volume, per unit of time) and the mixing speed are fundamental operating factors influencing the efficacy of the process in a bioreactor.

The slurry bioreactors technology has been largely used in field applications for soils, sediments and slurries bioremediation (USEPA, 1990): the technology was, in fact, successfully employed for the treatment of petroleum hydrocarbons, solvents, polycyclic aromatic hydrocarbons, pesticides, pentachlorophenol and chlorinated aromatic compounds used for wood preservation (USEPA, 1990; Cookson Jr, 1995; Eweis *et al.* 1998). In particular, some examples of laboratory or pilot-scale tests treating PAHs-contaminations are herein reported: the largest number of tests were conducted using batch mode *(*Zappi *et al.*, 1996*;* Launen *et al.,* 2002; Dean-Ross, 2005; Lei *et al.*, 2005; Abbondanzi *et al.,* 2006); Cassidy *et al.* (2000) compared the PAHs biodegradation obtained in CSTR and SBR reactors; instead some studies explored the treatment in SBR (Giordano *et al.*, 2005; Prasanna *et al.*, 2008; Venkata Mohan *et al.*, 2008; Chiavola *et al.*, 2010); recently, Lee *et al.* (2017) compared the treatment of PAHs-contaminated soils using batch mode and SS-SBR mode. In general, studies indicated that PAHs biodegradation efficiency was influenced by several parameters, such as the organic loading rate, the quantity and quality of surfactants amended, and the 'ageing' of the contamination. The presence of PAH-degraders in contaminated soils or sediments can also influence the process: according to Lei *et al.* (2005) autochthonous PAH-degraders living in a contaminated sediment were able to biodegrade PAHs ranging between two and five rings; Chiavola *et al.* (2010) found the total absence of removal for six-ring PAHs. Moreover, Dean-Ross (2005) and Johnsen *et al.* (2005) indicated the possibility to enhance degradation with the bioaugmentation.

The experimental work described in this PhD thesis focuses, in particular, on the improvement of the SS-SBR technology.

The major advantage of SBR systems, when compared to other technologies, is their flexibility: they give the possibility to combine through a timeline, in the same tank, multiple steps that normally would have been spatially segregated in different tanks; therefore, in an SBR, feeding,

reaction, settling and drawing (plus a possible idle phase between drawing and the further filling phase) occur in sequence in the same vessel. Through a proper regulation of the time interval required to complete a certain task, SBRs enable a precise distribution of the volumes dedicated to each function. Each phase can be operated in different conditions (*e.g.*, filling can be mixed and aerated, or static; reaction can be mixed and aerated, or only mixed) according to different operating aims: for example, an aerated filling promotes the beginning of aerobic reactions whilst reducing the time necessary for the following reaction phase. In an SBR, once filling and reaction phases have been completed, the biomass is separated from the liquid and preserved inside the tank for the next cycle. The settling phase occurs instead in undisturbed conditions. Nevertheless, according to Chiavola *et al.* (2010), in SS-SBR the settle phase is not expected; rather, a known volume of slurry is discharged and then replaced from a new volume when a further working cycle is starting. SBR systems used at the field scale include multiple reaction vessels.

In particular, for the purposes of this thesis work, two SS-SBRs treating sediments collected in the touristic ports of Cagliari (Italy) and El Kantaoui (Tunisia) and spiked with fluorene, phenanthrene, fluoranthene and pyrene, have been operated in different conditions in order to achieve degradation of the PAHs mixture.

3.1.1 State of the art

A short review of the state of the art regarding the treatment of PAH-contaminated soils and sediments with bioslurry reactors will be given in this paragraph.

The study of Dean-Ross (2005) is useful to understand the effect that the solid concentration in the slurry phase exerts on biodegradation. A batch reactor was used to assess the PAHs-removal from river sediments. Two selected microorganisms, capable to grow, respectively, on pyrene and anthracene (used as the sole carbon and energy sources), were inoculated to achieve the biodegradation on a contaminated sediment and on a pristine sediment spiked with anthracene, phenanthrene, fluoranthene and pyrene. Factors such as sediment loading, the presence of surfactants, ageing of contamination and strain selection were identified as responsible for the biodegradation efficiency. The author tested sediment loadings of 5, 10 and 20 % w/v: interestingly, the worst biodegradative efficacy was obtained for a loading of 20% w/v, whereas no significant differences existed between tests performed at 5 and 10% w/v. As a consequence, a loading of 10% w/v was used in the following experiments since it was the best compromise between process efficacy and quantity of sediment treated time by time. The next step was to

assess the effect exerted by different surfactants on the PAHs-degrading microorganisms. Tween 80 did not exert inhibitory effects, even if amended at high concentrations, but also it did not affect positively contaminants degradation. According to Rouse *et al.* (1994) both microbial stimulation and inhibition can be observed in the presence of surfactants, hence suggesting a complex and case-specific interaction that would require tests applied on a case-by-case basis.

Irvine *et al.* (1993) and Eweis *et al.* (1998) widely discussed about advantages and disadvantages of SS-SBR and CFSTR technologies. CFSTR dilutes the contaminants' concentration in the reactor entrance and, therefore, reduce biodegradation rates if the kinetics are related to concentration; conversely dilution is useful in the presence of toxic compounds. Moreover, even if the CFSTR system generally requires a single tank, it needs for continuous and therefore expensive pumping, which determines high operating and maintenance costs due to the abrasion of mechanic parts, whereas SS-SBR systems allow an intermittent pumping, that is necessary only when a working cycle has been completed. In addition, in SS-SBRs the volume of slurry to be replaced can be regulated in order to provide an optimal concentration of contaminants and microorganisms for the reaction phase. However, a major complexity characterises SS-SBR systems due to the presence of multiple reaction tanks (Cassidy *et al.,* 2000).

In particular, in their study, Cassidy *et al.* (2000) compared the performance of an SS-SBR and a CFSTR while treating a soil contaminated by diesel fuel; the best performance was obtained with the SS-SBR. The enhancement of the degradative process was attributed to the presence of biosurfactants produced by microorganisms during SS-SBR operation; nevertheless, microorganisms generated also foams. Both, biosurfactants production and foaming were directly related to the diesel fuel concentration fed to the system: reducing the diesel fuel added per cycle resulted, in fact, in their decrease. This observation proved an important correlation between biosurfactants formation and diesel concentration, which makes the phenomenon of foaming easier to control. Moreover, the authors observed that the maximum foaming production occurred after the surfactant concentration in the system reached a maximum, in the presence of free biosurfactant (*i.e.*, not bound to diesel fuel) molecules temporary accumulated in the reactor. Conversely, biosurfactant production was not observed in CFSTR system, since the influent was less concentrated.

Prasanna *et al.* (2008) and Venkata Mohan *et al.* (2008) investigated the decontamination of soils contaminated by one single PAH by adopting SS-SBR technology.
The study of Prasanna *et al.* (2008) explored the bioremediation of a soil spiked with anthracene in five slurry sequencing batch reactors; the solid concentration composing the slurry fed to the systems was 10%. Sole autochthonous microorganisms' activity with or without the inoculum of domestic sewage was investigated under an alternatively anoxic-aerobic microenvironment (*i.e.*, air was supplied only during reaction phases). A control reactor showed a negligible degradation of anthracene due to the absence of microbial activity; in the other reactors, anthracene degradation was dependent on both, substrate loading rate and bioaugmentation: the best performances were achieved in bioaugmented reactors, meanwhile the worst performances were related to the highest loading substrate rates. The same experimental setup was used by Venkata Mohan *et al.* (2008) for determining the influence of bioaugmentation in the bioremediation of soils spiked with pyrene. Various substrate loading rates were applied. The same considerations made by Prasanna *et al.* (2008) were valid also in this second study: higher substrate loading rates corresponded to worst process performances; the bioaugmentation achieved the highest removal efficiencies.

The studies of Giordano *et al.* (2005), Chiavola *et al.* (2010) and Lee *et al.* (2017) concerned the degradation of a mixture of PAHs in contaminated sediments and soils.
According to the higher efficiencies achieved by Cassidy *et al.* (2000) by using SS-SBR compared to the use of CFSTR, Giordano *et al.* (2005) choose to operate 8 lab-scale SS-SBR in order to evaluate the reactors' performance when treating Venice (Italy) lagoon sediments contaminated with 17.1 $mg_{PAHtot}\ kg_{dw}^{-1}$ (that were classified as wastes according to the Italian law). The slurry phase contained 10% of solids concentration, VER corresponded to 0.10 and the reactors worked in aerated conditions. The cycle length was set initially at 14 days, then shortened to 7 days and finally set at 3.5 days. As to the PAHs removal, the global efficiency resulted close to 55%, showing the highest values for two- and three-ring PAHs (average removal efficiency of 70%), whereas the efficiency decreased for more than three-ring PAHs (64% for four-ring PAHs and close to 43% for five- and six-ring PAHs). The removal was almost completely attributed to the microbial activity (volatilization had only negligible effects). Moreover, the process was not influenced by changes of HRT and by the addition of an external carbon source to the slurry: the microbial community used the PAHs mixture as primary substrate even when the cycle length was shortened. Chiavola *et al.* (2010) used the SS-SBR technology due to its possibility to treat fluxes characterised by the presence of highly

toxic and biorecalcitrant contaminants. Sediments were spiked with a mixture of fluorene, anthracene, pyrene and chrysene, and the solid concentration was 10 % w/v, in accordance with the results obtained by Dean-Ross (2005). The reactor was aerated. PAHs concentrations were decided in order to simulate a real contamination: starting from a first range of values (30 ÷ 40 $mg_{PAHtot}\,kg_{dw}^{-1}$), the concentration of spiked contaminants was changed in successive feedings based on the reactor performances observed during the experiments (the last concentrations applied ranged between 70 and 110 $mg_{PAHtot}\,kg_{dw}^{-1}$). Moreover, different HRTs and cycle lengths were tested. Biostimulation was chosen as the only treatment. Following the promising results achieved by the reactor, the cycle length, initially set at 20 days, was reduced gradually to 7 days. The overall PAHs removal efficiency reached values higher than 90%; three-ring PAHs were degraded faster than four-ring compounds and the best results were achieved for fluorene degradation. Low PAHs concentrations were found in the supernatant (separated by the slurry phase in the end of the experiments), hence confirming the typical behaviour of these compounds, characterised by low solubility and high hydrophobicity. The authors considered microbes as the main responsible of degradation; nevertheless, since microorganisms were not able to use chrysene as the sole source of carbon and energy, cometabolism was suggested as a solution in order to promote its degradation. Moreover, the results suggested that the highest microbial activity was condensed in the first three days of each working cycle; afterwards an endogenous respiration phase started.

Lee *et al.* (2017) investigated the removal of a mixture of PAHs, composed by phenanthrene, anthracene and pyrene (initial concentration of 1,000 $mg_{PAHtot}\,kg_{w}^{-1}$), from an artificially spiked soil, by adopting a 2 L two-phase partitioning bioreactor. The same reactor, filled with a slurry composed by the 30% (w/v) of soil, was operated at first in batch mode (approx. 7 days) and then in SS-SBR mode (2 cycles of 7 days). Two water-immiscible liquids, *i.e.*, silicon oil and paraffin oil, were used to desorb PAHs from soils, hence facilitating the contact between a selected bacterium (*Sphyngomonas* sp. 3Y) and contaminants. After the transfer of PAHs into the water-immiscible liquid phase, that occurred in the first 24 hours, both reactors lead to similar results: while pyrene was only transferred into the water-immiscible liquid phase, but was not degraded, phenanthrene and anthracene were degraded by approximately 90 and 80%, respectively. Moreover, the degradation of phenanthrene was higher in silicon oil than in paraffin oil; instead, since the initial anthracene concentration was higher than its solubility in silicon oil, it was completely transferred only into the paraffin oil. However, since in SS-SBR, water-immiscible liquid phase and inoculum were supplied only at the start-up of the system (without the need for refilling or change them at each working cycle, as instead required when

the reactor was operating in batch mode), the first operational mode was suggested as the most economical.

In their research, Shuttleworth and Cerniglia (1995) focussed on environmental aspects regarding bacterial degradation of PAHs. The authors highlighted some common behaviours adopted by bacteria in the presence of this class of recalcitrant compounds but described also situations in which is difficult to standardise behaviours. In fact, as already explained in Chapter 1, starting from the characteristics proper of the contaminants themselves, several factors may influence degradation, even more in the presence of a complex matrix like a soil or a sediment. Moreover, it must be noted that each degradation process is strictly related to the specific case study (different sites possess different characteristics) and to the system adopted (Shuttleworth and Cerniglia, 1995). Considering degradation rates, the authors explained that initial values, after any lag phase, are usually faster than later rates. They also suggested that degradation rates decrease if nutrients or oxygen becomes severely limiting, or as soon as the most bioavailable substrates is removed, leaving only the recalcitrant fraction. Moreover, the authors indicated (as already described in section 1.5) that, the older is the contamination, the more difficult is the decontamination; therefore, laboratory studies would probably overestimate the degradation potential in real soils or sediments (unless a spill has recently occurred). In the same study, the authors reported a list of bacteria isolated from contaminated sites and cultivated on PAHs as the sole carbon and energy sources. They observed as the scarce compounds' bioavailability leads, in general, to low growth rates: values of growth rate reported by the authors ranged, in fact, from 0.0003 h^{-1} for a mixed culture grown on anthracene (concentration not given) (Volkering *et al.*, 1992) to 0.23 h^{-1} for *Beijerinckia* sp. grown on phenanthrene (concentration not given) (Stucki and Alexander, 1987). Only two species were recognised to grow on fluorene as the sole carbon and energy source: *Pseudomonas vesicularis* (Weissenfels *et al.*, 1990) and *Arthrobacter* sp. (Grifoll *et al.*, 1992). Several species did the same with phenanthrene, *e.g.*, *Mycobacterium* sp. (Boldrin *et al.*, 1993), *Flavobacterium* sp. (Stucki and Alexander, 1987), *Pseudomonas paucimobilis* (Weissenfels *et al.*, 1990), *Arthrobacter polychromogenes* (Keuth and Rehm, 1991), and also an example of a mixed culture was reported (Volkering *et al.*, 1992). *Mycobacterium* sp. resulted quite versatile because it could grow also on fluoranthene and pyrene (Boldrin *et al.*, 1993). In addition, fluoranthene and pyrene acted as sole carbon and energy sources, respectively, for *Alcaligenes denitrificans* (Weissenfels *et al.*, 1990) and *Rhodococcus* sp. (Walter *et al.*, 1991). Naphthalene, likewise anthracene and phenanthrene, was used as a growth substrate by a mixed culture (Volkering *et al.*, 1992).

Dean-Ross *et al.* (2002) described microbial interactions in the presence of a PAHs mixture: in this case, the rate of utilisation of individual PAHs can either increase or decrease. In particular, the authors investigated the ability of bacteria *Mycobacterium flavescens* and *Rhodococcus* sp., isolated from sediments, to use mixtures of PAHs: the first one was able to use fluoranthene in the presence of pyrene, even if pyrene was degraded more slowly than in the absence of fluoranthene; the latter was able to use fluoranthene together with anthracene but, also in this case, the presence of fluoranthene slowed the rate of utilisation of the other compound. This study demonstrated the cometabolism of fluoranthene (*i.e.*, the secondary substrate), thanks to the presence of metabolites of the contaminant: in both strains, fluoranthene metabolism occurred on the fused ring of the fluoranthene molecule and led to the production of 9-fluorene-1-carboxylic acid; moreover, *Rhodococcus* sp. produced also a second metabolite, a (carboxymethylene)fluorene-1-carboxylic acid; therefore, the strain was able to metabolise fluoranthene via *ortho* and *meta* cleavage. Moreover, through analyses of the enzymatic kinetics, the authors measured the maximum velocity associated to the degradation of the primary substrates, pyrene and anthracene. They observed slower kinetics (*i.e.*, higher half saturation constants) of both primary substrates when the secondary substrate fluoranthene was present, whereas maximum velocities were identical in the presence and in the absence of fluoranthene, therefore indicating that fluoranthene could be considered as a competitive inhibitor. Similarly, Stringfellow and Aitken (1995) noted a competitive metabolism in phenanthrene degradation when naphthalene, methylnaphthalenes and fluorene were present.

Yuan *et al.* (2000) explored the ability of an aerobic mixed culture (composed by six isolates) to biodegrade polycyclic aromatic hydrocarbons by using phenanthrene as the sole carbon source; the mixed culture was able to degrade phenanthrene (5 mg L^{-1}) after 28 h, following 3-5 hours lag phase and was more effective than the single strains. Mueller *et al.* (1989) had already suggested that individual organisms have the ability to metabolise only a limited range of substrates, hence mixed cultures can probably better degrade complex PAH mixtures. The removal efficiencies decreased when phenanthrene concentrations were higher, putatively due to an increased level of toxicity. The mixed culture could also efficiently degrade pyrene and acenaphthene as single PAHs but could not degrade anthracene and fluorene. In samples which contained a mixture of the five compounds, degradation rates were increased for fluorene and anthracene, but delayed for acenaphthene, phenanthrene and pyrene. This may indicate the necessity of cometabolism for the degradation of anthracene and fluorene. Moreover, the

authors obtained negative effects when amending systems with some specific non-ionic surfactants: degradation was, in fact, inhibited or slowed down.
Experiments testing the effect of two different nitrogen sources (*i.e.*, sodium nitrite and ammonia chloride) and of individual carbon sources (*i.e.*, yeast extract, acetate, glucose or pyruvate) on phenanthrene degradation, showed that nitrogen sources did not affect the process, whereas better performances were shown when the system was amended with each one of the carbon sources (added individually).

While the studies reported above focussed on tests made with pure cultures or enrichments, and in the presence of freshly spiked PAHs, Lei *et al.* (2005) explored the decontamination of a sediment characterised by an aged contamination, mediated by indigenous bacteria. Sediment was contaminated by over 1,000 mg_{PAHtot} kg_{dw}^{-1}, and phenanthrene had the highest concentration (approximately 190 mg kg_{dw}^{-1}). The vicinity of the sampling site to estuarine areas made salinity and sulphate concentration of the water comparable to that of seawater. Aerobic studies were conducted by adjusting oxygen, inorganic N and P, and adding a non-ionic surfactant to a sediment/water slurry (20% of solid concentration) prepared mixing sediment with the overlaying water collected in the same contaminated site at the same depth. Moreover, experiments were performed under sulphate reducing and denitrifying conditions, adjusting inorganic nutrients, in the presence and absence of co-substrates (*i.e.*, acetic acid and ethanol).
Aerobic tests with and without nutrients and with and without surfactants did not suggest any significant enhancement due to the presence of N and P; during the 24 experiments weeks, a considerable degradation of PAHs ranging between two and five rings was achieved, while controls remained basically unchanged. Except for few compounds present initially in very low levels, the lower levels were achieved for compounds with less benzoic rings; a great number of compounds reached their steady residual level after 9 weeks. Two-ring PAHs naphthalene and 2-metylnaphthalene, and three-ring PAH acenaphthylene remained in the sediment in considerable amount, probably due to their low initial concentration. Moreover, the authors suggested that putatively a major portion of the concentration initially present was sorbed strongly into the organic fraction, that it was not available for degradation (this effect was markedly higher for the highest molecular weight PAHs), and that the degradation achieved was smaller than in the case of sediments freshly spiked with PAHs. Tests with nutrients led to a considerable increase in sulphate concentration with respect to the initial values (assuming sulphide as initial reduced form): in fact, the metabolism of indigenous sulphur oxidising

bacteria accounted for the greatest amount of oxygen amended to the system (about 60%), which in turn indicates the necessity of an extra oxygen addition compared to the quantity that would have been used for the sole PAHs removal. Sulphur oxidation leads also to extremely acidic conditions, thus requiring a contemporary pH adjustment.

Considering sulphate reducing conditions, phenanthrene started to be degraded after a lag phase of 14 weeks in the presence of co-substrates and was the only compound subjected to a noteworthy removal. However, tests with and without co-substrate were not comparable because they were executed in different periods of time: tests with co-substrate started from a significantly lower contamination, after 7 months than tests without co-substrate; therefore, it is not possible to conclude that the presence of co-substrate enhanced degradation. This difference, which was observed only in the case of phenanthrene, was putatively due to the slow degradation of phenanthrene in the storage buckets where sediments were stocked, which was hypothetically mediated by an autochthonous population of sulphate reducing bacteria probably living within the sediment (thanks to the high presence of sulphate in the pore water). Contamination decreased significantly within 19 weeks. PAHs degradation was coupled to loss of sulphate, hence confirming that it was the main terminal electron acceptor in the presence of a probable sulphate reducing autochthonous population; moreover, the addition of specific inhibitor to sulphate reducing bacteria showed a very low PAHs biodegradation, hence indicating that indigenous sulphate reducers were probably the main degraders in those conditions.

As for the last experiment made in the presence of nitrate (spiked to the system because they were not originally present in the sediment), PAHs were not easily degraded in denitrifying conditions.

The most remarkable conclusions of this study are that 1) indigenous microbial communities could effectively mediate the degradation of PAHs, even if the contamination was aged and if the concentration of contaminants was high, and that 2) the degradation of phenanthrene in anoxic conditions was lower than the degradation in aerobic conditions (both degradations were evaluated during the same period of time), confirming the general higher efficiency of aerobic PAHs-degradations.

3.2 EXPERIMENTAL WORK

3.2.1 Effects of different operating conditions on sediment slurry sequencing batch reactors treating two marine port sediments contaminated by PAHs: Part 1

3.2.1.1 Introduction

In this study, two SS-SBRs were used to biologically degrade a mixture of PAHs (namely fluorene, phenanthrene, fluoranthene and pyrene) from marine sediments dredged from Cagliari (Italy) and El Kantaoui (Tunisia) ports. National chemical levels taken from Table 2.5 of the Technical Annex of the Ministerial Decree No. 173/2016 and reported in Table 2.1 (section 2.5), herein indicated as L_2 limits, were used as the target environmental quality standards for both sediments.

To enhance PAHs removal by biostimulation, nutrients were added in both sediments, acetate was used as co-substrate (El Kantaoui, SBR-EK), and saponins were used as surfactants (Cagliari, SBR-C), based on the good results achieved in previous batch tests (Erby *et al.*, 2014). Different PAHs concentrations (up to 200 $mg_{PAHtot}\ kg_{dw}^{-1}$ in SBR-EK; up to 400 $mg_{PAHtot}\ kg_{dw}^{-1}$ in SBR-C) and solid-to-liquid ratios (S/L, up to 0.2 in SBR-EK; up to 0.1 in SBR-C) were tested in each reactor, in order to determine the optimal operating conditions and maximize process performance.

3.2.1.2 Materials and methods

Marine sediments. Sediments were collected from Cagliari (Sardinia, Italy) and El Kantaoui (Tunisia) ports, wet sieved in order to eliminate particles greater than 2 mm in diameter, and stored at 4 °C in a dark container, in order to prevent the occurrence of photo- and bio-oxidation. Grain size analysis were done in previous studies on raw sediments, before wet sieving under 2 mm (MAPMED, 2015a,b): analysis was performed by dry sieving, estimating the silt-clay ratio (% silt and clay) using the pipette method, according to Buchanan (1984), and the classification followed the Wentworth chart; sediments from Cagliari and El-Kantaoui differed in terms of carbon content (4 and 10% w/w, respectively), as well in terms of silt-clay, sand and gravel composition (65/35/0 and 50/50/0 % w/w, respectively).

SS-SBR configuration. Both SS-SBRs consisted of an amber Pyrex water-jacketed vessel with 5 L working volume (7.3 L total volume; height 32 cm; working height 22 cm; working diameter 17 cm). A picture of SBR-C and a schematization of the SS-SBRs configuration are shown in Figure 3.2. A stainless-steel flange ensured reactors sealing. Reactors were run under temperature-controlled conditions (25 °C) by a circulating water bath. Air was supplied through a porous stone placed at the reactors bottom and connected to an external aeration system (Schego Optimal). Before entering the reactors, air was forced to pass through a humidifier in order to avoid humidity losses within the vessels. Moreover, a condenser was used in order to minimize evaporation phenomena. Siemens LOGO! 12/24 RCE was used for process timing. Main process parameters were controlled by M300-ISM transmitter (Mettler Toledo): oxygen was monitored through an O_2 sensor (Mettler Toledo, InPro 6850i) and maintained above 2 mg L^{-1}; pH was monitored by a pH sensor (Mettler Toledo, InPro 4260i) and maintained between 6.8 and 7.3 by adding acid (HCl 1.5 M) or base (NaOH 1.5M) solution.

PAHs degradation assessments. The reactors were operated in 5-day cycles, each cycle comprising a short feeding and effluent withdrawal phases (5 minutes each). No settling phase was implemented, as described by Chiavola *et al.* (2010). Feed was provided manually, from the top of the reactor. Mixing (125 rpm) was ensured during the reaction phase by a mechanical shaft mixer (IKA RW 20). The effluent was manually drawn from a port located at 19.8 cm from the bottom (the corresponding volumetric exchange ratio was 0.1). Before feeding, sieved sediments were spiked using an acetone-based stock solution prepared with equal amounts of 3-ring (fluorene, Flu; phenanthrene, Phe) and 4-ring PAHs (fluoranthene, FlA; pyrene, Pyr); specific compounds and their concentrations were chosen according to Chiavola *et al.* (2010) with the aim to simulate a real-case contamination. PAHs solution was pipetted over the sediment, meanwhile mechanical stirring was provided. Artificial seawater was produced by adding 35 g L^{-1} of sea salts (Sigma Aldrich) in distilled water and used to prepare the sediment slurry with different solid-to-liquid ratios (S/L).

Initial operating conditions for both SS-SBRs were derived from a previous study (Erby *et al*., 2014). In particular, nutrients (N, P) were added in both sediments to maintain the C:N:P ratio at 100:10:1; readily degradable sodium acetate (10x the feeding PAHs content, in terms of organic carbon, according to Yuan *et al.* (2000)) was added as co-substrate in El Kantaoui sediments (SBR-EK), since it was proved to accelerate phenanthrene degradation more than other carbon sources, such as glucose or pyruvate, in the same study; saponins were used as biodegradable surfactants (up to 1% of dry weight sediment content) in SBR-C (Cagliari).

Different PAHs concentrations ($mg_{PAHtot}\ kg_{dw}^{-1}$), S/L and volumetric organic loading rates ($mg_{PAHtot}\ L^{-1}\cdot d^{-1}$) were applied to each reactor, as summarized in Table 3.1.

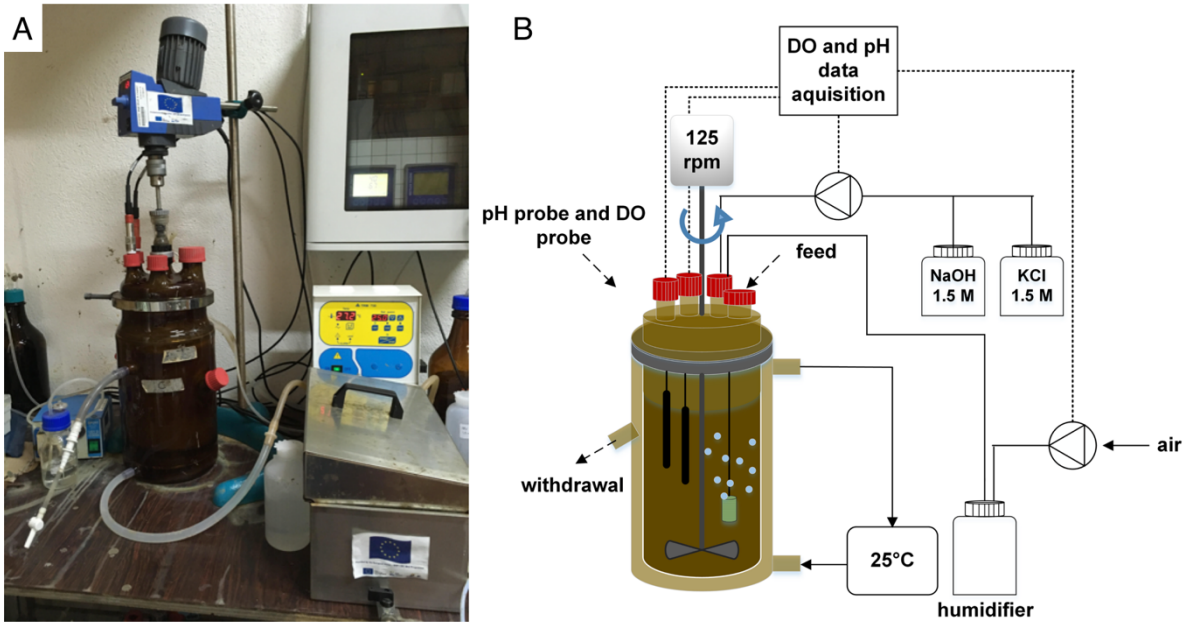

Figure 3.2 *A) SBR-C used in this study (SBR-EK, not shown, was identical), and B) scheme of the whole SS-SBR system.*

Table 3.1 *Synthesis of the main process parameters applied to each experimental phase in SBR-EK (El Kantaoui) and SBR-C (Cagliari), cycles range and length of each phase (each working cycle was 5 days long).*

Reactor	SBR-EK					SBR-C		
Phase	A	B(*)	C	D	E	A	B	C
Cycles	1÷7	8÷13	14÷26	27÷37	38÷57	1÷13	14÷29	30÷57
Length [d]	35	30	65	55	100	65	80	140
Total PAHs concentration [$mg_{PAHtot}\ kg_{dw}^{-1}$]	200	100	150	150	200	200	400	200
S/L	0.1	0.1	0.13	0.2	0.2	0.1	0.05	0.1
vOLR [$mg_{PAHtot}\ L^{-1}d^{-1}$]	0.4	0.2	0.4	0.6	0.8	0.4	0.4	0.4

(*) = sediment was spiked only with fluorene and phenanthrene.

Analytical methods. For PAHs determination, samples were periodically collected and centrifuged at 4,000 rpm for 15 minutes; the solid phase was dried by adding diatomaceous earth (1:1 w/w) and exposed to accelerated solvent extraction (Dionex, ASE 150) by using a solvent phase formed by hexane:acetone (2:1); the extracting cycle was set approximately at 24 minutes. Before analysis, the liquid extracts were dried by adding anhydrous sodium sulphate (Na_2SO_4) and filtered at 0.20 µm. Analysis were performed by high performance liquid chromatography (Dionex, HPLC P680) equipped with an UV detector at 220 nm and an Agilent Zorbax Eclipse PAH column. The compounds were eluted using a linear gradient (from 60/40

to 100/0 (% v/v) acetonitrile/demineralized water) over 10 min at 1.5 ml min^{-1}. The detection limit of each PAH was 0.01 ppm.

PAHs removal efficiency (*E*, %) was calculated using the theoretical inlet concentration (C_{INth}, μg g^{-1}) (which was considered a good approximation of the actual inlet concentration C_{INac}, since sediments were artificially contaminated in our laboratories), and the effluent concentration (day 5, C_{OUT}, μg g^{-1}) as reported in Equation 3.1:

Equation 3.1
$$E=100\cdot(C_{INth}-C_{OUT})/C_{INth}$$

Volatile solids (VS, % w/w) were determined according to published protocol (IRSA-CNR, 2005). Dissolved organic carbon (DOC) was measured on filtered samples (0.45 μm) using a total organic carbon (TOC) analyser (SHIMADZU, mod. TOC-V CSN). All the analyses were performed in duplicate on both influent and effluent samples. DOC removal efficiency (*DOC*, %) was calculated using the inlet concentration (DOC_{IN}, mg L^{-1}) and the effluent concentration (day 5, DOC_{OUT}, mg L^{-1}) as reported in:

Equation 3.2
$$E=100\cdot(DOC_{IN}-DOC_{OUT})/DOC_{IN}$$

3.2.1.3 Results and discussion

<u>*PAHs removal in SBR-EK.*</u> As to SBR-EK, Table 3.2 shows the average removal efficiencies calculated in each Phase for the total PAHs and for each compound used in this experiment, whereas removal efficiencies calculated for each cycle are displayed in Figure 3.3.

Table 3.2 *Average PAHs removal efficiencies for each PAH compound and for the total PAHs, calculated in each experimental Phase (SBR-EK).*

Average PAHs removal efficiency of SBR-EK [%]					
Phase	A	B(*)	C	D	E
Fluorene	99.7±0.2	99.8±0.1	99.95±0.09	99.9±0.1	99.95±0.04
Phenanthrene	99.7±0.2	99.78±0.09	99.9±0.3	99.7±0.3	99.9±0.1
Fluoranthene	98.5±0.4	-	98.5±0.2	98.8±0.4	98.8±0.5
Pyrene	99.0±0.6	-	99.2±0.5	99.1±0.2	96±4
Total PAHs	99.3±0.2	99.8±0.1	99.4±0.2	99.4±0.2	99±1
Cycles	1÷7	8÷13	14÷26	27÷37	38÷57

(*) = sediment was spiked only with fluorene and phenanthrene.

Although total PAHs removal efficiency was very high during the whole experimental campaign (98.5±3%), the best process performance was achieved during Phase A (99.3±0.2%; cycles #1-4), C and D (both equal to 99.4±0.2%). As shown in Figure 3.3, initial high PAHs removal efficiencies (99.3±0.2%) dropped down to 93 and 71% for 3- and 4-ring PAHs,

respectively, as an accumulation of 4-ring PAHs occurred in the second half of Phase A (total PAHs concentration was set to 200 mg_{PAHtot} kg_{dw}^{-1}), starting from cycle #5, due to a failure in the aeration system. As a consequence, no compounds complied with L_2 limits (Figure 3.4).

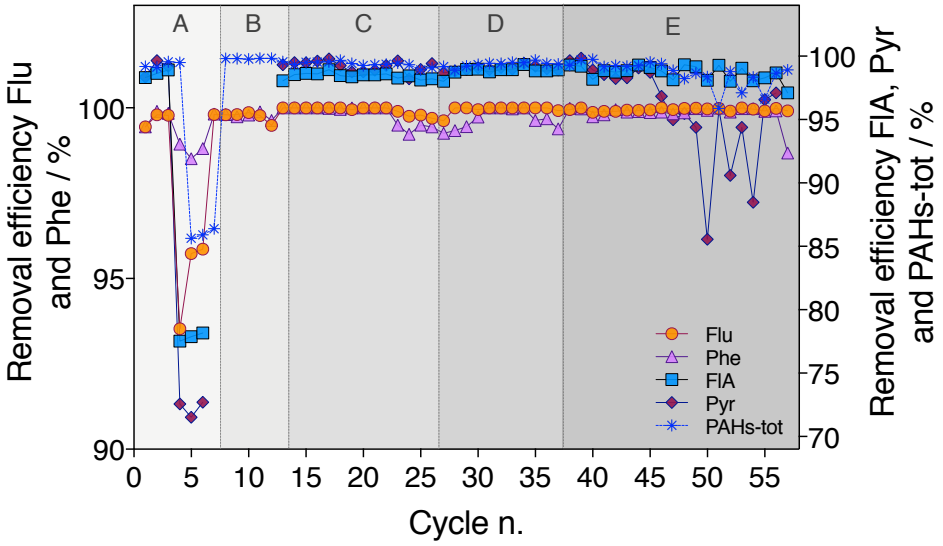

Figure 3.3 *Removal efficiency of each PAH and of the total PAHs, calculated for each working cycle (SBR-EK).*

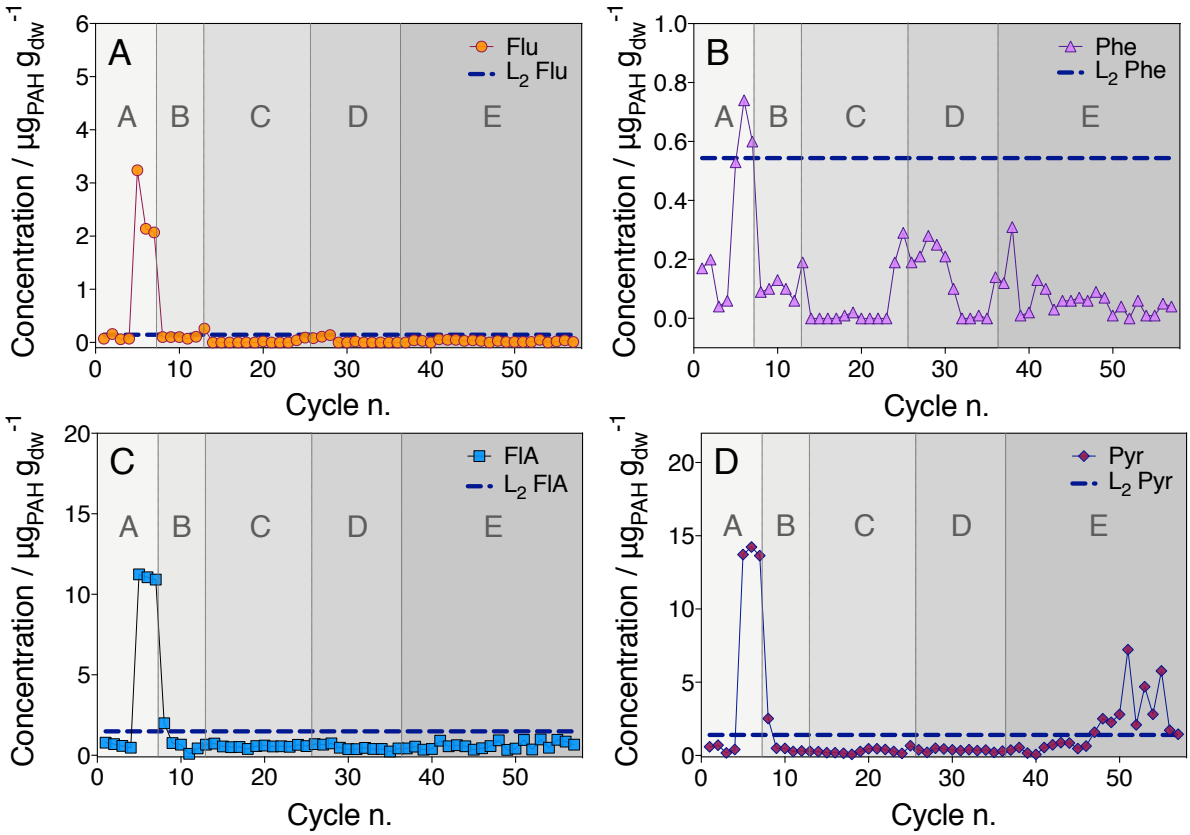

Figure 3.4 *Concentration of A) fluorene, B) phenanthrene, C) fluoranthene and D) pyrene measured in SBR-EK effluent vs the corresponding L_2 limit (blue dotted line).*

In order to recover process performance, the vOLR was reduced by decreasing total PAHs concentration to 100 $mg_{PAHtot}\ kg_{dw}^{-1}$ (Phase B), using the same operating strategy described by Chiavola *et al.* (2010). Only 3-ring PAHs were spiked and, as a consequence, residual concentrations of 4-ring PAHs (which accumulated into SBR-EK during Phase A) decreased below L_2 limits. Coherently, total PAHs removal efficiency increased up to 99.8±0.1%, indicating complete process recovery.

During Phase C, all PAHs were spiked again (total PAHs concentration was 150 $mg_{PAHtot}\ kg_{dw}^{-1}$), and the vOLR was set at 0.4 $mg_{PAHtot}\ L^{-1}\cdot d^{-1}$ (the same as Phase A) by increasing S/L from 0.1 to 0.13. High total PAHs removal efficiency was achieved (99.4±0.2%) and all compounds complied with L_2 limits, despite some negligible fluctuations in Flu and Phe removal efficiency observed in cycles #24-26.

In Phase D, S/L was set to 0.2 in order to increase the applied vOLR (from 0.4 to 0.6 $mg_{PAHtot}\ L^{-1}\cdot d^{-1}$), without changing total PAHs concentration. Some fluctuations in Flu and Phe removal efficiencies were observed also at the beginning of Phase D (until cycle #31), and Phe removal efficiency slightly decreased at the end of the Phase (cycles #36 and #37). Despite the higher vOLR, no decrease in process performance occurred (the total PAHs removal efficiency was 99.4±0.1%), and PAHs residual concentrations were below the L_2 limits during the whole experimental Phase.

During Phase E, total PAHs concentration was increased to 200 $mg_{PAHtot}\ kg_{dw}^{-1}$ (same as Phase A), resulting in a vOLR of 0.8 $mg_{PAHtot}\ L^{-1}\cdot d^{-1}$. Although total PAHs removal efficiency was still high (99±1%), significant fluctuations in pyrene removal (between 85 and 98%) were observed in the second half of Phase E (cycles #47-57), indicating a less stable process behavior (Figure 3.3). As a consequence, L_2 limit for pyrene was exceeded. A similar toxic effect due to high PAHs concentrations was previously observed by Yuan *et al.* (2000). Since total PAHs concentration was the same as in Phase A (which run smoothly until a system malfunction occurred, as previously described), such unstable behavior may be rather ascribed to a delayed effect of the high vOLR applied in Phase E.

For all the above mentioned, the results achieved are promising since SBR-EK was able to satisfy the L_2 limits with only few exceptions, as previously described.

PAHs removal in SBR-C. As to SBR-C, the vOLR was always kept at 0.4 $mg_{PAHtot}\ L^{-1}\cdot d^{-1}$. Working conditions were the same in Phases A and C (200 $mg_{PAHtot}\ kg_{dw}^{-1}$ and S/L=0.1), whereas in Phase B the total PAHs concentration was doubled (400 $mg_{PAHtot}\ kg_{dw}^{-1}$) and the solid-to-liquid ratio was halved (0.05). Average PAHs removal efficiencies, calculated in each

Phase for each compound and for the total PAHs, are reported in Table 3.3. Total PAHs and removal efficiencies for each compound, calculated for each cycle, are displayed in Figure 3.5. Figure 3.6 shows, instead, the effluent concentrations for the single PAH, compared to the corresponding L_2 limits.

Table 3.3 *Average PAHs removal efficiencies for each PAH compound and for the total PAHs, calculated in each experimental Phase (SBR-C).*

Average PAHs removal efficiency of SBR-C [%]			
Phase	A	B	C
Fluorene	99.8±0.2	99.96±0.07	99.8±0.2
Phenanthrene	99.7±0.3	99.92±0.07	99.8±0.2
Fluoranthene	98.1±0.5	99.0±0.3	97.9±0.7
Pyrene	99.4±0.6	99.8±0.1	99.0±0.9
Total PAHs	99.3±0.2	99.7±0.1	99.1±0.4
Cycles	1÷13	14÷29	30÷57

The total PAHs removal efficiency was above 98% during the whole experimental campaign (Figure 3.5). The highest averaged total PAHs removal efficiency was achieved during Phase B (99.7±0.1%), when the highest PAHs concentration was applied; however, FlA and Pyr removal efficiencies slightly and gradually decreased from cycle #22 onward (Figure 3.5), likely due to the delayed effect of the higher (double) total PAHs concentration, compared with Phases A and C. The subsequent reduction of total PAHs concentration (Phase C) did not stabilize the process, and slight fluctuations in FlA and Pyr removal efficiencies (between 96 and 100%) were observed (from cycle #35 to #57). Despite such negative trend, L_2 limits were generally met for each compound (Figure 3.6), apart from few exceptions observed for Flu in Phases A and B, in correspondence to some slight fluctuations of its removal efficiency, and in the second half of Phase C, when Flu limit was always exceeded from cycle #48 to #56; instead, Pyr limit was exceeded only once (in cycle #52). Phe and FlA always complied with limits.

Degradation profiles in SS-SBRs. PAHs degradation profiles in both reactors showed (Figure 3.7 and Figure 3.8) that 3-ring PAHs were degraded completely, and faster than 4-ring PAHs, according to the first order kinetic constants (k) of the nonlinear regression used for modelling the profiles, and in agreement with the results achieved by Chiavola *et al.* (2010) and Giordano *et al.* (2005). As an exception, incomplete 3-ring PAHs removal was observed in SBR-EK during Phase A (Figure 3.7 B), due to a system malfunction; at the same time, an accumulation of FlA and Pyr occurred. For this reason, 4-ring PAHs were not fed in the following Phase: degradation profiles and k displayed in Figure 3.7 C clearly show the enhancement of PAHs

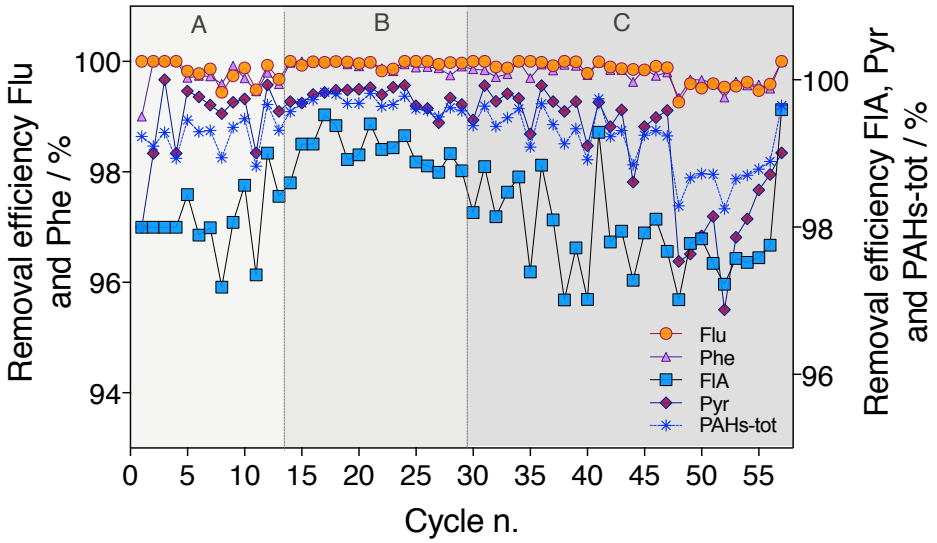

Figure 3.5 *Removal efficiency of each PAH and of the total PAHs, calculated for each working cycle (SBR-C).*

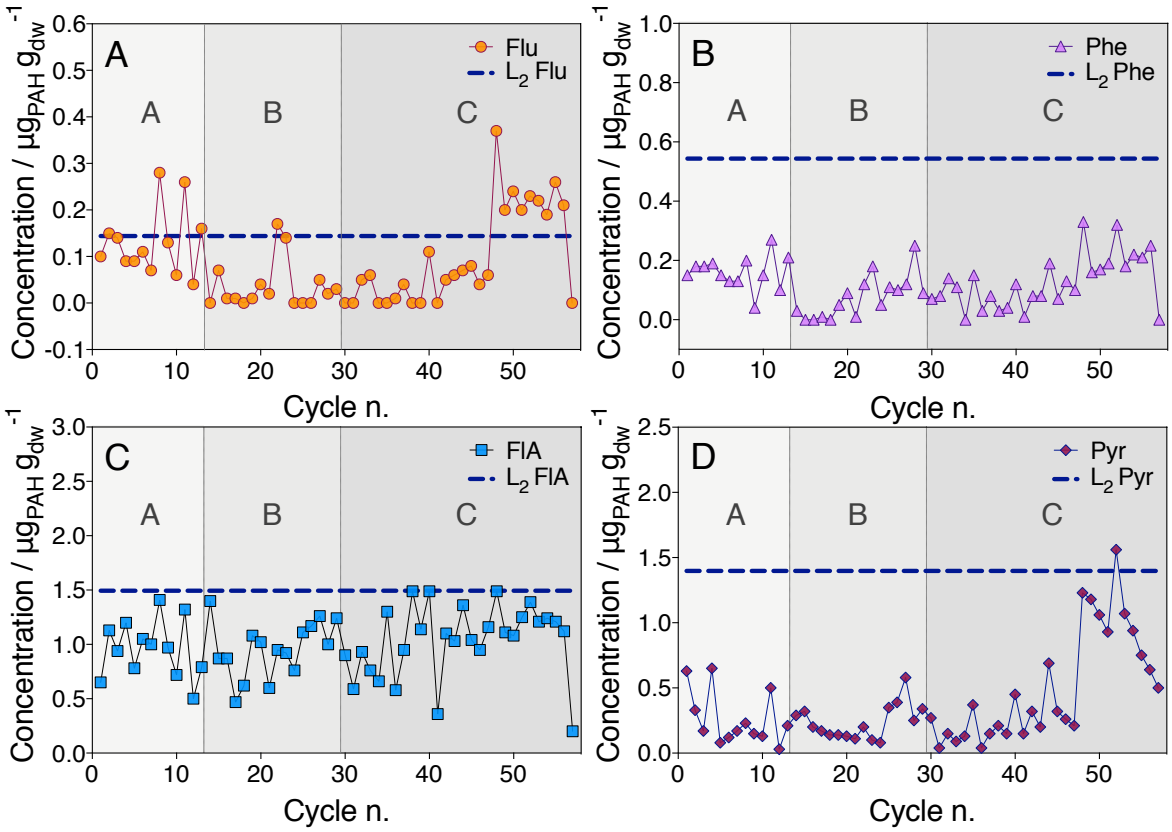

Figure 3.6 *Effluent concentration of A) fluorene, B) phenanthrene, C) fluoranthene and D) pyrene vs the L_2 limit reported for each compound (blue dotted line), in SBR-C.*

depletion achieved during Phase B; as FlA and Pyr were spiked again in Phase C, an increase in FlA removal rate was observed, as shown from its k value (Figure 3.7 D); despite the increased vOLR, the degradation profiles of each PAH in Phase D had steep slopes and showed low residual levels at the end of the cycle (Figure 3.7 E), confirming the excellent process

performance achieved; as a confirmation of process instability in the last part of Phase E, Pyr degradation profile determined on cycle #50 (Figure 3.7 F) showed a very low k with a corresponding high residual Pyr concentration (C C_0^{-1} > 35%).

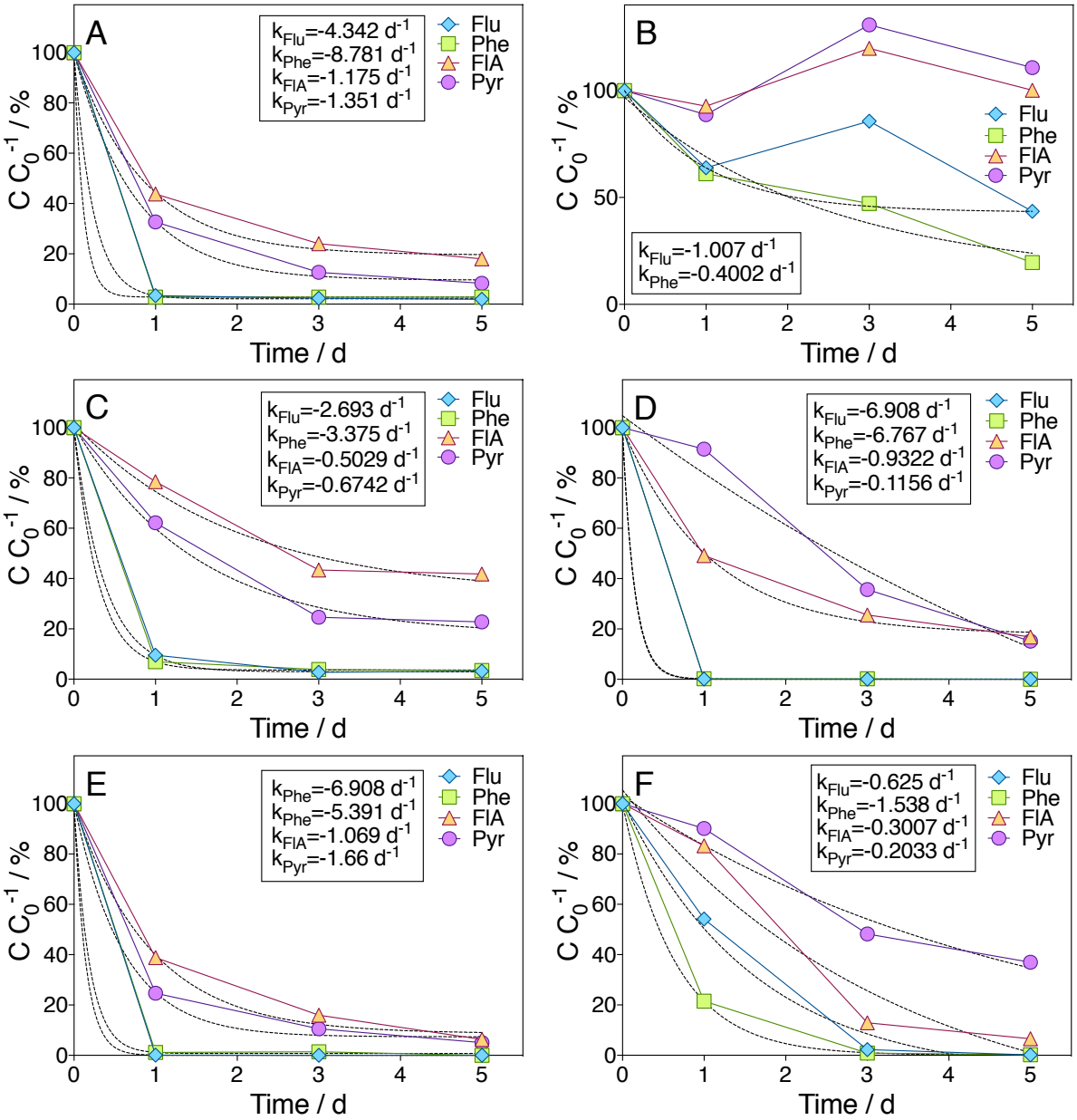

Figure 3.7 *Degradation profiles of PAH compounds for SBR-EK in A) cycle #1 and B) cycle #6 (Phase A), C) cycle #9 (Phase B), D) cycle #21 (Phase C), E) cycle #33 (Phase D), and F) cycle #50 (Phase E); C_0 is the PAHs concentration at day 0 (μg g^{-1}). Dashed black line: nonlinear regression; k (d^{-1}) indicates the first order kinetic constant of the nonlinear regression used for modeling degradation profiles.*

As to SBR-C, Pyr removal was faster in Phase A (Figure 3.8 A, cycle #9), than in B (Figure 3.8 B, cycle #21) and C (Figure 3.8 C, cycle #47) confirming the better process performance observed during Phase A, when PAHs concentration was 200 $mg_{PAHtot}\,kg_{dw}^{-1}$ (in Phase B, total

PAHs concentration was doubled). The lowest FlA removal rate was determined during Phase C, as indicated by its kinetic constant k, in agreement with the slight fluctuations in removal efficiency observed during this Phase (from cycle #35 to #57), and previously described.

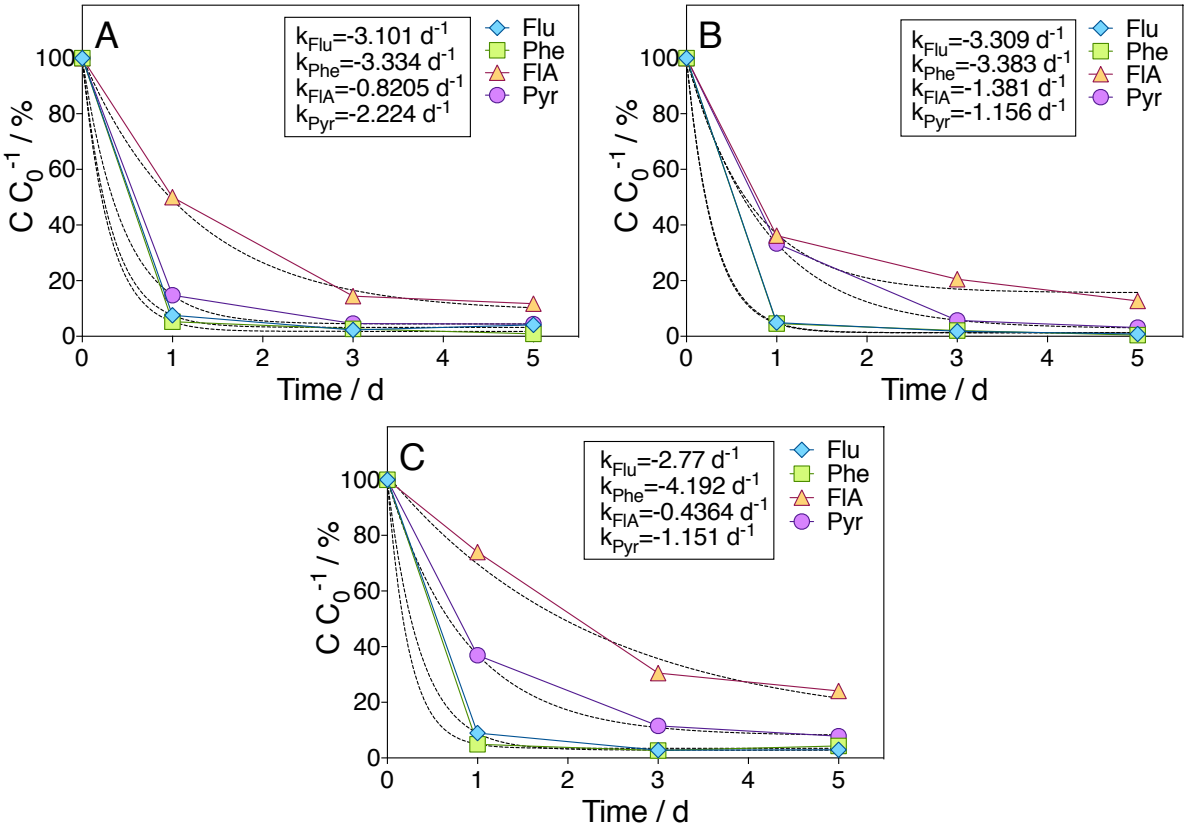

Figure 3.8 *Degradation profile of PAH compounds for SBR-C in A) cycle #9 (Phase A), B) cycle #21 (Phase B), and C) cycle #47 (Phase C); C_0 is the PAHs concentration at day 0 (μg g^{-1}). Dashed black line: nonlinear regression; k (d^{-1}) indicates the first order kinetic constant of the nonlinear regression used for modeling degradation profiles.*

VS and TOC. According to Chiavola *et al.* (2010), comparing the influent and effluent VS helps in quantitatively evaluate biomass evolution in the reactor.

As to SBR-EK, despite the system malfunction observed in Phase A and the fluctuations in Pyr removal efficiency observed in the last part of Phase E (between cycles #47 and #57, Figure 3.3), VS measured in the sediments at the end of each cycle were always higher than those measured in the inlet (Figure 3.9). This observation is in accordance with the quite high total PAHs removal efficiencies achieved during the whole experiment and might indicate an intense biodegradation activity, related with an increase of the microbial population in the reactor.

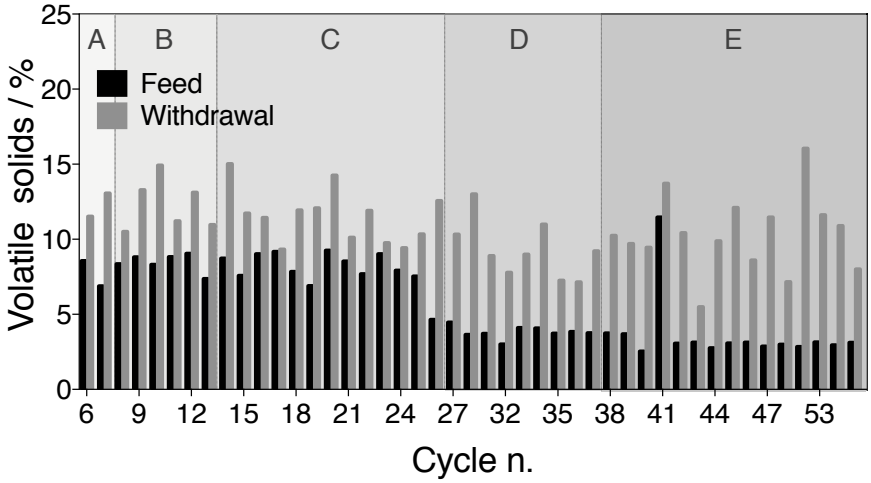

Figure 3.9 *Volatile solids content measured in the influent and in the effluent during each cycle (SBR-EK).*

As to SBR-C, although PAHs removal efficiencies were high during the whole experimental campaign (Figure 3.5), Figure 3.10 clearly indicates an opposite behavior in terms of VS content, between cycles #20 and #44 (almost in each cycle): due to the probable toxic effect generated by the high PAHs inlet concentration (400 mg_{PAHtot} kg_{dw}^{-1}), VS in the effluent were lower than those measured in the influent, hence indicating a possible decrease in biomass concentration. Moreover, this observation may be considered in line with the slight fluctuations of FlA and Pyr removal efficiencies observed at the end of Phase B and along Phase C. Despite these fluctuations, biomass was likely recovering in the last cycles of Phase C, as indicated from the restoration of the condition of higher VS in the outlet than in the inlet sediment.

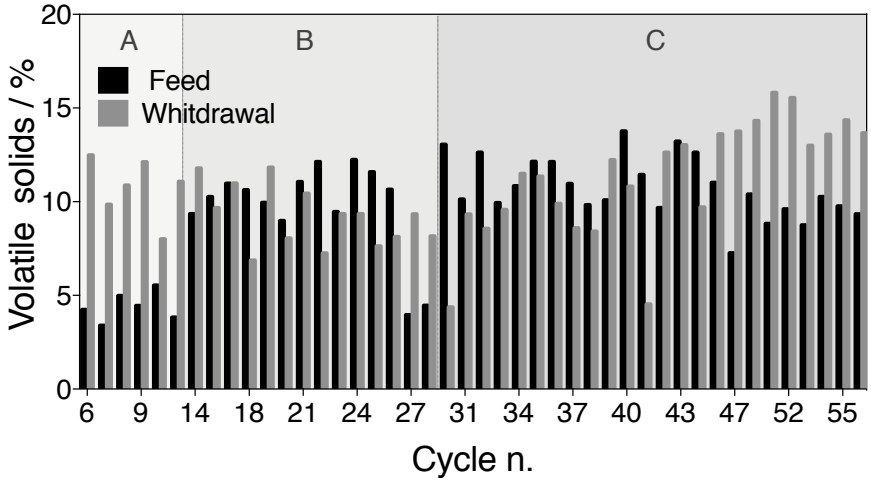

Figure 3.10 *Volatile solids content measured in the influent and in the effluent during each cycle (SBR-C).*

Since the quantities of sodium acetate and saponins supplied to SBR-EK and SBR-C, respectively, were much higher than the feeding PAHs content (see section 3.2.1.2), and due to

the very low solubility of PAHs, calculations of DOC removal efficiencies provided a direct indication of the effective removal of these compounds within each cycle length. As shown in Figure 3.11 (SBR-EK) and in Figure 3.12 (SBR-C), both reactors were able to degrade the added co-substrate and biosurfactant almost completely (average DOC removal efficiencies higher than 90%).

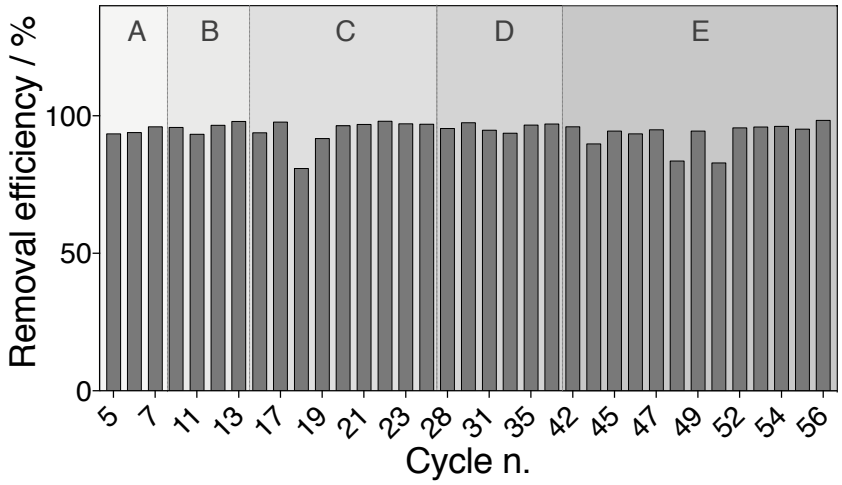

Figure 3.11 *Removal efficiency of the dissolved organic carbon measured in representative cycles for each Phase (SBR-EK).*

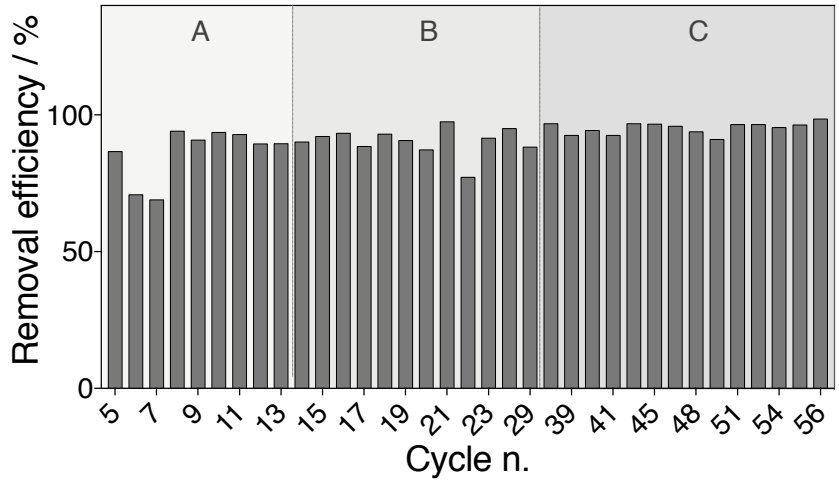

Figure 3.12 *Removal efficiency of the dissolved organic carbon measured in representative cycles for each Phase (SBR-C).*

3.2.1.4 Conclusions

In this study, two SS-SBRs were run with different operating conditions to bioremediate PAHs-contaminated marine sediments from El-Kantaoui (Tunisia) and Cagliari (Italy) ports. Although high PAHs removal efficiencies were achieved in both reactors, L_2 limits for specific sediment

reuse or disposal were not always satisfied. As to SBR-EK, the best results were achieved at vOLR up to 0.6 $mg_{PAHtot}\ L^{-1}\cdot d^{-1}$ (Phases A, first half, C and D), when L_2 requirements were always satisfied. In particular, when the vOLR was further increased to 0.8 $mg_{PAHtot}\ L^{-1}\cdot d^{-1}$ (Phase E) a clear worsening of overall process performance was observed; indeed, according to Prasanna *et al.* (2008) and Venkata Mohan *et al.* (2008) higher substrate loading rates corresponded to worst process performances.

Considering SBR-C, the best results were achieved during Phase A, when high total PAHs removal efficiencies were observed and L_2 limits were always satisfied (with the exception of Flu on cycles #8 and #11). Although the limits were always met during Phase B, the slight but progressive decrease in FlA and Pyr removal efficiencies (from cycle #22 onward) indicated a delayed, negative effect of the higher total PAHs concentration applied. Restoring the initial operating conditions in Phase C was not enough to restore process stability, and L_2 limit for Flu was exceeded in the second half of the Phase (from cycle #48 to cycle #56).

Interestingly, very good process performances were achieved in both SS-SBRs when the same total PAHs concentration (200 $mg_{PAHtot}\ kg_{dw}^{-1}$), S/L (0.1) and vOLR (0.4 $mg_{PAHtot}\ L^{-1}\cdot d^{-1}$) were applied, despite the significant differences in sediments characteristics and initial operating conditions. According to Dean-Ross (2005) the solid-to-liquid ratio affects process performances: the author found that an S/L of 0.1 was the best compromise between process efficacy and the quantity of sediment treated time by time. This result was clearly confirmed in the current study.

As to PAHs degradation profiles, the first order kinetic constants of the nonlinear regression used for modelling the profiles in this study indicated that 3-ring PAHs were degraded completely and faster than 4-ring PAHs, in agreement with Giordano *et al.* (2005) and Chiavola *et al.* (2010). Moreover, according to Shuttleworth and Cerniglia (1995), degradation profiles confirmed that initial degradation rates were usually faster than later rates, that decreased when the most bioavailable substrates had been removed.

Such promising results, already published as proceedings of the 15th International Conference of Environmental Science and Technology (Milia *et al.*, 2017), suggested the possibility to evaluate the effects of other important process parameters on process performance.

3.2.2 Effects of different operating conditions on a sediment slurry sequencing batch reactor treating marine port sediments contaminated by PAHs: Part 2

3.2.2.1 Introduction

In the previous study, the effect of different process parameters on two SS-SBRs treating PAHs contaminated-sediments from El Kantaoui (Tunisia) and Cagliari (Italy) ports was investigated. In particular, the treatment of biostimulation with nutrients and saponins achieved good results in SBR-C (treating Cagliari sediments). In the current study, after an increase of the vOLR fed to the system (from 0.4 mg_{PAHtot} $L^{-1} \cdot d^{-1}$ to 0.54 mg_{PAHtot} $L^{-1} \cdot d^{-1}$), which led to a general worsening of the process performance (in particular evident in Pyr degradation), the effect of bioaugmentation (applied in parallel with biostimulation) was investigated. Interestingly, previous bioaugmentation batch tests revealed very good removal efficiencies on 4-ring PAHs when the strain *Amaricoccus* sp. C286, isolated from Cagliari sediments at the Dept. of Biomedical Sciences (University of Cagliari, Italy), was inoculated to the same sediments (Erby *et al.*, 2015). In this study, new bioaugmentation + biostimulation batch tests were executed in order to confirm previous results and before to proceed to bioaugmentation in SBR-C.

3.2.2.2 Materials and methods

Marine sediments. Cagliari sediments were the same used in the previous experiment (see section 3.2.1.2).

Batch tests configuration. Aerobic batch tests (Figure 3.13) were performed in Duran® glass bottles (600 mL working volume). Sediments were pre-conditioned by supplying air for 24 h through a porous stone placed at the reactors bottom and connected to an external aeration system (Schego Optimal). Thereafter, batch tests started when the porous stone was removed, and the air was provided in the headspace in order to avoid volatilization. Before entering the reactors, air was forced to pass through a humidifier in order to avoid humidity losses within the reactors. Moreover, a condenser was used in order to minimize evaporation phenomena. Oxygen concentration was measured with a DO probe (WTW oxi 197i) and was maintained above 2 mg L^{-1}. During experiments, reactors were covered with aluminum foil in order to avoid photo-oxidation of the contaminants.

Figure 3.13 *Example of batch tests performed in the current study. Each reactor was covered with aluminium foil in order to avoid photo-oxidation effects.*

SS-SBR configuration. SBR-C configuration was the same previously described (see section 3.2.1.2). In the current study, working volume and working height were, respectively, 5 L and 22 cm for Phase C, and 5.2 L and 22.9 cm for Phases D and E.

PAHs degradation assessments in batch tests. The reactors were operated for 7 days. Sediments were spiked with the same stock solution of PAHs described in section 3.2.1.2, reaching 200 $mg_{PAHtot}\,kg_{dw}^{-1}$ (50 $mg_{PAHtot}\,kg_{dw}^{-1}$ for each compound). Stock solution was pipetted directly in the reactors after the 24 h sediments pre-conditioning with the aerating porous stone placed at the reactors bottom. Mixing (120 rpm) was provided during the reaction phase by a direct current (DC) geared motor (Crouzet 0.5 Nm ovoid 3.9 W). Samples were manually drawn from a port located at one side of the reactors. Artificial seawater was produced as described in section 3.2.1.2, and added in order to reach a S/L ratio of 0.1.

The following treatments were performed:

1) control tests without amendments or bacterial biomass addition (test N.A.);

2) biostimulation with nutrient regulation (C:N:P ratio of 100:10:1) and addition of saponins (up to 1% of dry weight sediment content) as biodegradable surfactants (test Sap+N,P; the C:N:P ratio was calculated considering the organic carbon provided with PAHs and saponins);

3) bioaugmentation by inoculating the selected bacterial strain C286 into the slurries at an initial concentration of $1 \cdot 10^5$ cell mL^{-1}, adding nutrients and saponins, reaching a C:N:P ratio of 100:10:1 (test C286+Sap+N,P).

Tests Sap+N,P and C286+Sap+N,P were performed four times, while test N.A. was performed in duplicate. The isolation of C286 is described in Erby *et al.* (2015).

PAHs degradation assessments in SS-SBR. The SBR-C was operated as described in section 3.2.1.2. Different vOLR ($mg_{PAHtot}\ L^{-1} \cdot d^{-1}$) were obtained by changing the volume fed to the reactor (V_{IN}); S/L ratio and feeding PAHs concentration were constant in the whole experimental campaign, as summarized in Table 3.4. Initial operating conditions for SBR-C were derived from the previous experiment (see section 3.2.1.2). The effluent was manually drawn from a port located at 19.8 cm from the bottom (the corresponding VER was 0.1 in Phase C, and 0.135 in Phases D and E). Before feeding, sieved sediments were spiked using the same acetone-based stock solution described in section 3.2.1.2. In this study, instead of being pipetted, PAHs solution was nebulised over the sediment whilst manual mixing was provided, 5÷10 days before feeding the reactor; thereafter, contaminated sediments were stored at 4°C in the dark in order to prevent photo- and bio-oxidation phenomena. This contamination method was expected to increase the contact between PAHs and sediment particles.
Artificial seawater was produced as described in section 3.2.1.2 and used to prepare the sediment slurry, according to S/L ratios reported in Table 3.4.

Table 3.4 *Synthesis of the main process parameters applied to each experimental phase in SBR-C, cycles range and length of each phase (each working cycle was 5 days long).*

Reactor	SBR-C		
Phase	C	D	E(*)
Cycles	58÷81	82÷121	122÷137
Length [d]	120	200	80
Total PAHs concentration [$mg_{PAHtot}\ kg_{dw}^{-1}$]	200	200	200
S/L	0.1	0.1	0.1
V_{IN} [mL]	500	700	700
vOLR [$mg_{PAHtot}\ L^{-1}d^{-1}$]	0.4	0.54	0.54

(*) = bioaugmentation with C286.

Analytical methods. For PAHs determination, samples were periodically collected and treated as described in section 3.2.1.2. The liquid extracts were stored in sealed vials and analyzed by gas chromatography–mass spectrometry (GC-MS) (Agilent 6890N, 5975C) equipped with an

autosampler (Agilent, 7863B) and a capillary column (Agilent, VF-5ms, 30 m x 0.25 mm x 0.25 μm).

Since analysis of the feeding PAHs concentrations revealed fluctuations compared to the expected values, here removal efficiency (*E*, %) was calculated using the actual inlet concentration (C_{INac}, μg g^{-1}) and the effluent concentration (day 5, C_{OUT}, μg g^{-1}) as reported in Equation 3.3:

Equation 3.3

$$E = 100 \cdot (C_{INac} - C_{OUT}) / C_{INac}$$

This phenomenon was observed especially for Flu concentration. According to Madrid *et al.* (2016) different abiotic losses could affect the attenuation of Flu: among them, volatilization is a possible explanation, which could be justified considering the semi-volatile nature of this compound. Moreover, fluctuations could be also related to the contamination method adopted in this study.

Volatile solids (VS, % w/w) and dissolved organic carbon (DOC) were measured according to section 3.2.1.2.

3.2.2.3 Results and discussion

PAHs removal in batch tests. Average degradation profiles of PAH compounds revealed, in each test, the faster degradation of 3-ring PAHs than 4-ring PAHs (Figure 3.14), and confirmed the easier degradation of LMW PAHs than HMW PAHs, widely discussed in section 1.5. In particular, Flu was the only compound completely or almost completely removed in each experiment and it was characterized by the fastest degradation rate: residual concentrations at day 3 were already 14±6%, 6±6% and 2±2% in the control (N.A., Figure 3.14 A), Sap+N,P (Figure 3.14 B) and C286+Sap+N,P (Figure 3.14 C) tests, respectively. Phe showed a similar degradation profile, but with a slower removal rate. Moreover, this compound was not completely removed in N.A. test (30.9±0.5% of residual concentration at day 7). As to FlA and Pyr, these compounds were not degraded in the control test; conversely, only Pyr was almost completely removed at day 7 and day 5 in Sap+N,P and C286+Sap+N,P, respectively; residual FlA at day 7 was 29±14% in Sap+N,P test and 31±9% in C286+Sap+N,P test. Both FlA and Pyr degradation profiles showed a lag phase until day 3, in both Sap+N,P and C286+Sap+N,P tests, hence indicating that 4-ring PAHs degradation started only when 3-ring PAHs were almost completely degraded, as already observed in Erby *et al.* (2015).

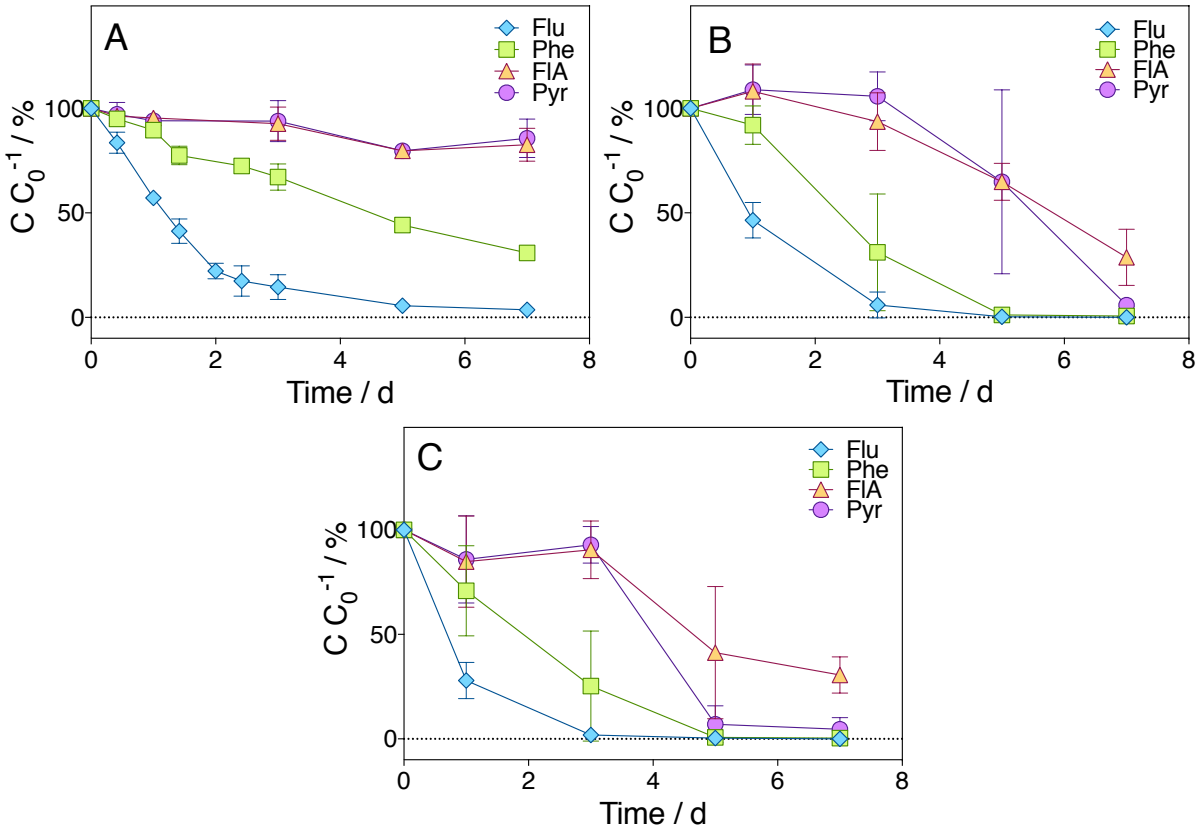

Figure 3.14 *Average degradation profiles of PAH compounds for different batch test carried out using Cagliari sediments: A) N.A., B) Sap+N,P; C) C286+Sap+N,P. Concentration were reported as C* C_0^{-1} *(*C_0 *is the concentration measured at day 0,* $\mu g\ g^{-1}$*).*

A comparison among the average degradation profiles for each compound is displayed in Figure 3.15. Flu degradation showed the same trend in each test (Figure 3.15 A), therefore indicating an easy removal of this 3-ring PAH even in the control test (without biostimulation). No significant differences among Sap+N,P and C286+Sap+N,P treatments were observed in Phe (Figure 3.15 B) and FlA (Figure 3.15 C) degradation profiles; conversely, Pyr degradation was fastened by the addition of the strain C286, in the presence of biostimulation (Figure 3.15 D).

Results of these batch tests indicated that, even if the bioaugmentation did not enhanced removal performances of Flu, Phe and FlA (in fact, both, Sap+N,P and C286+Sap+N,P tests led to similar degradation profiles), it was more effective in Pyr degradation. Therefore, since the removal of this compound was often difficult in SBR-C (as it will be better described later), these results suggested that bioaugmentation may be a possible operating strategy to accelerate Pyr degradation.

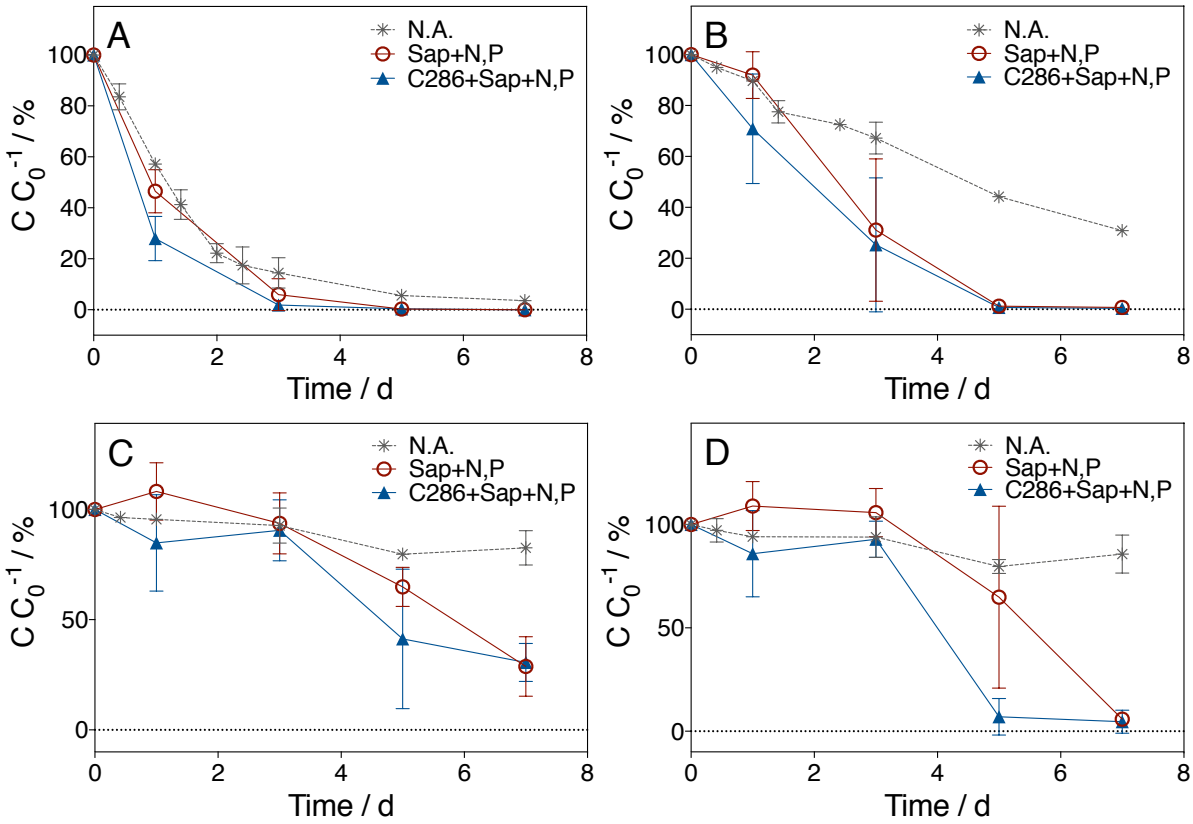

Figure 3.15 *Average degradation profiles of A) Flu, B) Phe, C) FlA, and D) Pyr, determined through batch tests carried out on Cagliari sediments.*

PAHs removal in SBR-C. In this study, the inlet PAHs concentration and the S/L ratio were kept, respectively, at 200 mg_{PAHtot} kg_{dw}^{-1} and 0.1 along the whole experimental campaign (as reported in Table 3.4). Phase C, which started in the previous study, was continued until cycle #81. In Phase D, the vOLR was increased to 0.54 mg_{PAHtot} $L^{-1} \cdot d^{-1}$ by increasing the V_{IN} from 0.5 L to 0.7 L. This more severe condition was maintained constant until the end of the experimental work.

In Table 3.5 are indicated the average removal efficiencies of the total PAHs and of each compound, calculated in the three Phases C, D and E. Considering only the part of Phase C analysed in the current study (from cycle #58), average removal efficiency was 97±2%. A general worsening of the process performance was indicated, in Phase D (when the vOLR was increased), from the lower values of average PAHs removal efficiencies, if compared with the previous Phase: in particular, average Pyr removal efficiency and total PAHs removal efficiency reached, respectively, 88±14% and 93±5%. The bioaugmentation, applied in Phase E, was not useful to recover the process performance: average removal efficiencies of each

compound decreased and, accordingly, the total PAHs removal efficiency was slightly lower than in the previous Phase (92±5%).

Table 3.5 *Average PAHs removal efficiencies for each PAH compound and for the total PAHs, calculated in each experimental Phase (SBR-C).*

Average PAHs removal efficiency of SBR-C [%]			
Phase	C	D	E(*)
Fluorene	97 ±2	94±3	90±7
Phenanthrene	98±1	97.3±0.9	97.7±0.5
Fluoranthene	96±2	94±3	93±4
Pyrene	96±3	88±14	86±13
Total PAHs	97±2	93±5	92±5
Cycles	58÷81	82÷121	122÷137

(*) = bioaugmentation with C286.

This behavior is also evident observing Figure 3.16 and Figure 3.17, which display, respectively, removal efficiencies of each compound and of the total PAHs, and the effluent concentration of each PAH compared with the L_2 limit, both represented in each cycle.

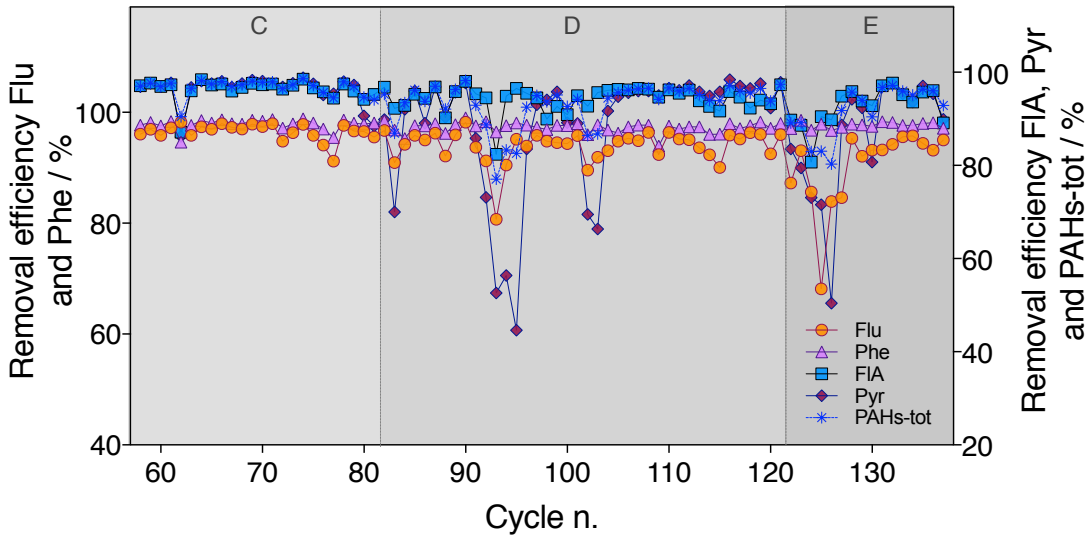

Figure 3.16 *Removal efficiency of each PAH and of the total PAHs, calculated during each cycle and in each Phase (SBR-C).*

Phe was the only compound to have reached an almost stable degradation along the whole experimental campaign (Table 3.5 and Figure 3.16). However, despite the high removal efficiencies, the compound never complied with threshold levels in the three Phases (except in few cycles, Figure 3.17 B). Flu removal efficiency worsened passing from Phase C, to Phase D and E, according to the general worsening observed in SBR-C: indeed, this compound never

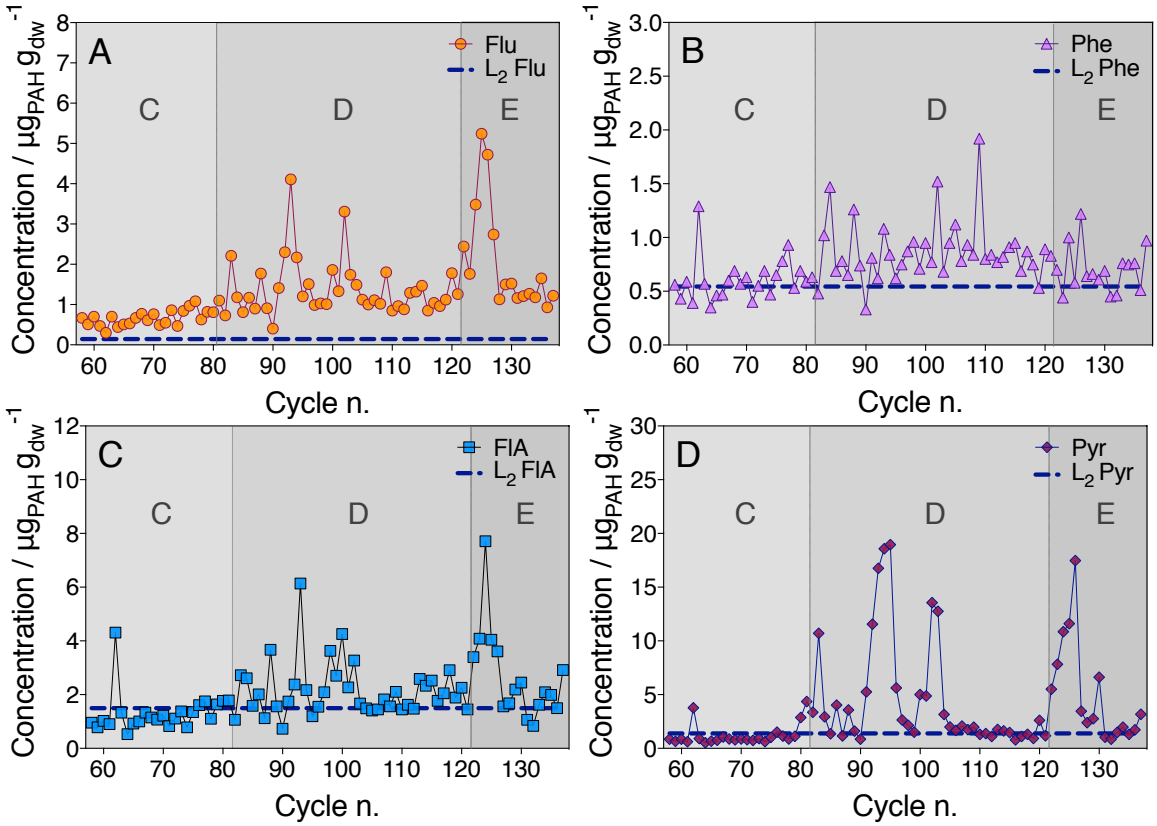

Figure 3.17 *Effluent concentration of A) fluorene, B) phenanthrene, C) fluoranthene and D) pyrene vs the L_2 limit reported for each compound (blue dotted line), in SBR-C.*

met its L_2 limit in the current study (Figure 3.17 A; the negative trend of Flu started, in the previous study, from cycle #48 onward, see section 3.2.1.3). As to FlA and Pyr, these compounds generally met the threshold levels in the whole phase C (L_2 limits were exceeded only in few cycles). In Phase D, according to the overall worsening of the process performance, high fluctuations of FlA and Pyr (observed also for Flu) and of the total PAHs removal efficiencies (more pronounced up to cycle #105) were observed (Figure 3.16): in particular, Pyr removal efficiency dropped to 45% in cycle #95 and again to 66% in cycle #103. Considering L_2 limits, FlA and Pyr always met the threshold levels (except in few cases) from cycle #103 and #106, respectively, to the end of Phase D.

Since, during Phase D, Pyr degradation showed the more unstable behaviour, the strain C286 was inoculated in Phase E in order to test the effect of bioaugmentation on the degradation process. Nevertheless, as already described above, despite the good results achieved in previous batch tests, the inoculum resulted ineffective in SBR-C (Table 3.5). As shown in Figure 3.16, the worst performances were recorded in the first half of Phase E, immediately after the inoculum, putatively indicating a temporary inhibition of the autochthonous biomass (which was already acclimated to work with the PAHs used in this study). Instead, higher degradations

were observed, for each compound, from cycle #128 onward. This behaviour could indicate three options: 1) the added biomass did not survive and disappeared after few cycles (in fact, biomass was inoculated only once), while the autochthonous biomass slowly recovered its previous activity; 2) the inoculated biomass survived and started to work with autochthonous biomass as a consortium, but a longer period of adaptation would have been required in order to have a more positive effect; 3) the inoculated biomass survived and was competitive with the autochthonous biomass, therefore, after autochthonous biomass disappeared, the inoculated biomass was slowly adapting to the operating conditions. Of course, these options could have been confirmed only by DNA analysis. However, effluent concentrations measured in Phase E, confirmed that the treatment of bioaugmentation + biostimulation was not effective in bringing again values under L_2 limits: Phe, FlA and Pyr met law levels only in few cycles, until the end of this experimental work. Actually, slurry samples were collected for microbiological analysis before and after the inoculum, but they were not immediately analysed given the negative results achieved after the bioaugmentation; therefore, they remain still available for trying to explain why the bioaugmentation was not useful in the process described.

If compared to batch tests, this behaviour can be explained considering the different initial conditions of the two systems: while SBR-C process performances had been bad for a long time (before the addition of the inoculum), in batch tests C286 was spiked to fresh sediments. Moreover, in SBR-C the inoculum could have been in competition with the autochthonous biomass (probably abundant and well-selected after a long period of activity on the 4 PAHs used in this study).

Degradation profiles in SBR-C. Comparing degradation profiles of Phase C and Phase D, the worst operating conditions noticeably affected degradation profiles (Figure 3.18).

According to previous considerations, Phe was the only compound that was immediately degraded at the maximum rate (even if never completely). Flu, which is generally easier degraded than HMW PAHs, showed degradation rates comparable or slower than 4-ring PAHs (as displayed in cycle #82, Figure 3.18 D), following a scarce degradation started in the last cycles of the previous study. This behaviour indicated that when the reactor was compromised, it was not able to bring Flu concentration below its threshold level. After the increase of vOLR, in Phase D, confirming the previous discussion, Pyr showed the lowest k (Figure 3.18 D and F, cycles #82 and #95), or was not degraded (Figure 3.18 E, cycle #93). From cycle #105 onward

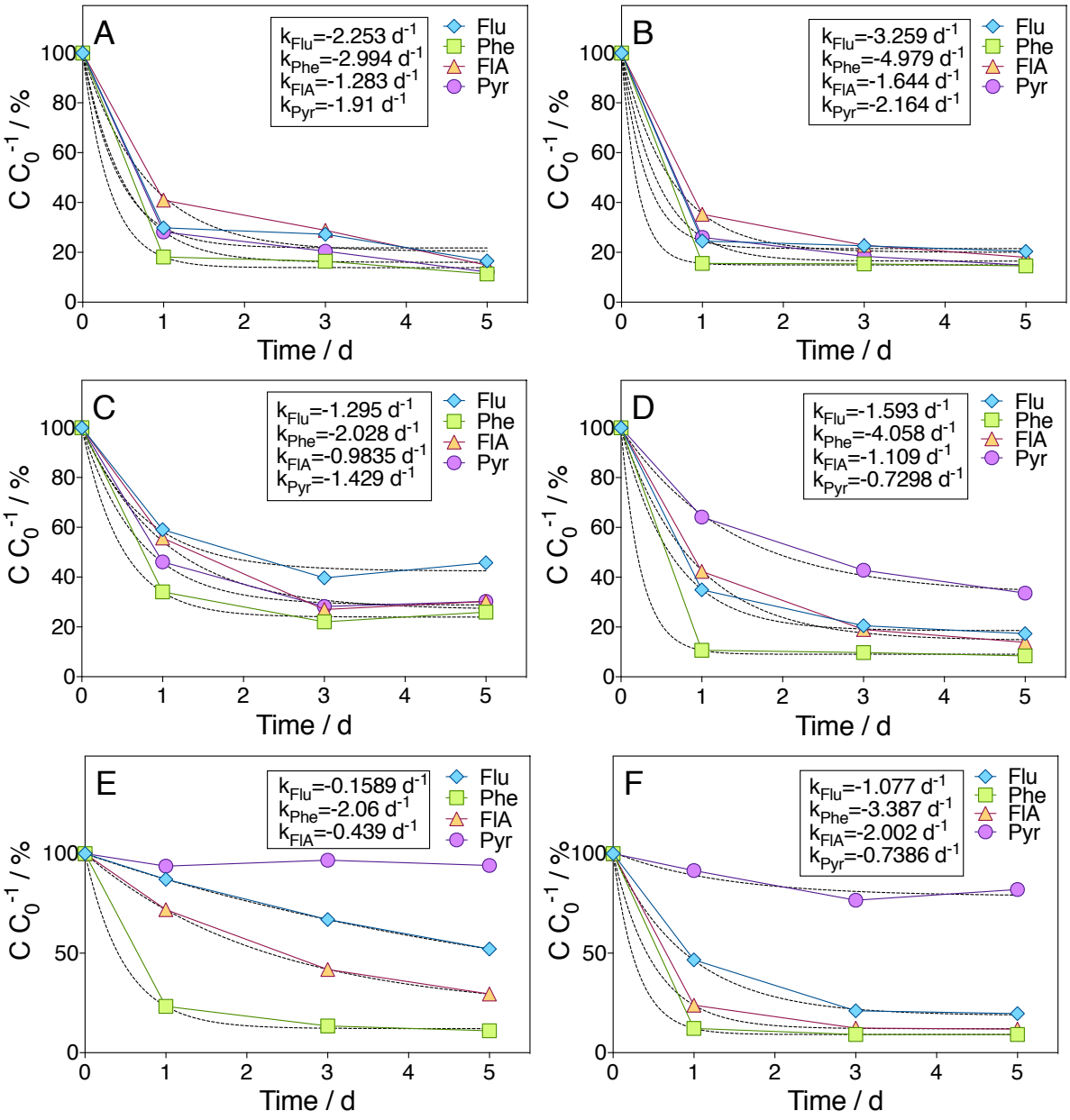

Figure 3.18 *Degradation profiles of PAH compounds for SBR-C in A) cycle #65, B) cycle #68 and C) cycle #79 (Phase C), D) cycle #82, E) cycle #93 and F) cycle #95 (Phase D); C_0 is the PAHs concentration at day 0 (μg^{-1}). Dashed black line: nonlinear regression; k (d^{-1}) indicates the first order kinetic constant of the nonlinear regression used for modeling degradation profiles.*

(Figure 3.19), 3-ring PAHs were again degraded faster than 4-ring PAHs (as an exception, in cycle #132, Figure 3.19 D, Flu was degraded more slowly than the other compounds). In general, Figure 3.19 A and B indicate a slightly enhancement of process performances that occurred in the second part of Phase D, before the inoculum was added. Analysing the first representative cycle of Phase E (cycle #123, Figure 3.19 C), the inhibitory effect to the autochthonous biomass exerted by the bioaugmentation is clear in degradation profiles of Pyr (not removed), FlA (slowly removed until 50%, after a lag phase of 32 h) and Flu (that reached

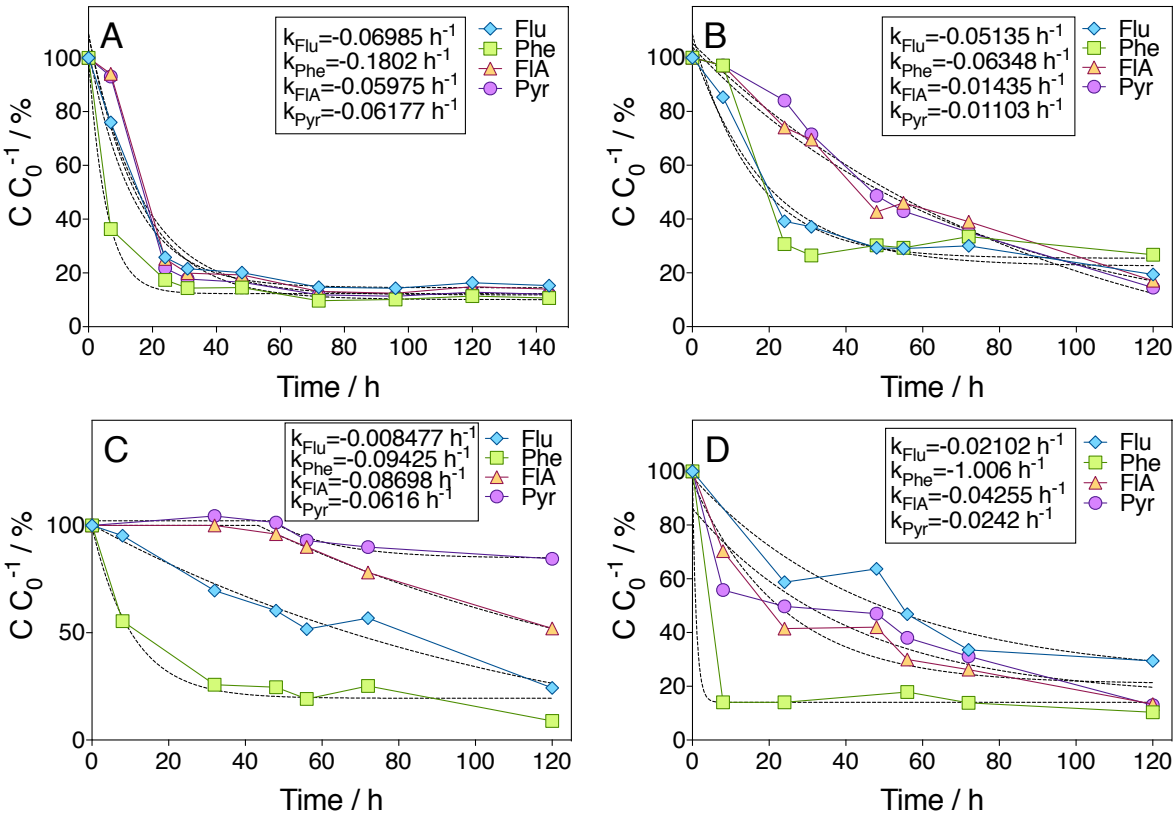

Figure 3.19 *Degradation profiles of PAH compounds for SBR-C in A) cycle #111 and B) cycle #121 (Phase D), C) cycle #123 and D) cycle #132 (Phase E); C_0 is the PAHs concentration at day 0 (μg g^{-1}). Dashed black line: nonlinear regression; k (d^{-1}) indicates the first order kinetic constant of the nonlinear regression used for modeling degradation profiles.*

25% of residual concentration at day 7). In cycle #132 (Figure 3.19 D), when a slow adaptation to the new conditions (after inoculum) had already occurred, degradation rates of each compound, apart from Flu, improved. Despite this improvement, and according to considerations made in the previous section about the negative performances achieved during Phase E, residual concentrations at the end of this representative cycle were still high (never under 10%, and equal to 30% of C_0 in the case of Flu).

SV and TOC. Coherently with observations made in the previous study (see section 3.2.1.3), in this study, in Phase C, VS in the withdrawal were usually higher than VS in the feed (Figure 3.20). Albeit this behaviour did not change when vOLR was increased, the difference among inlet and outlet VS decreased, therefore suggesting a probable general decrease of the biomass in the reactor, due to the severe conditions imposed to SBR-C. In Phase E, the difference among feed and withdrawal VS was oscillating between higher and lower values, suggesting a difficult adaptation of the biomass to the new conditions.

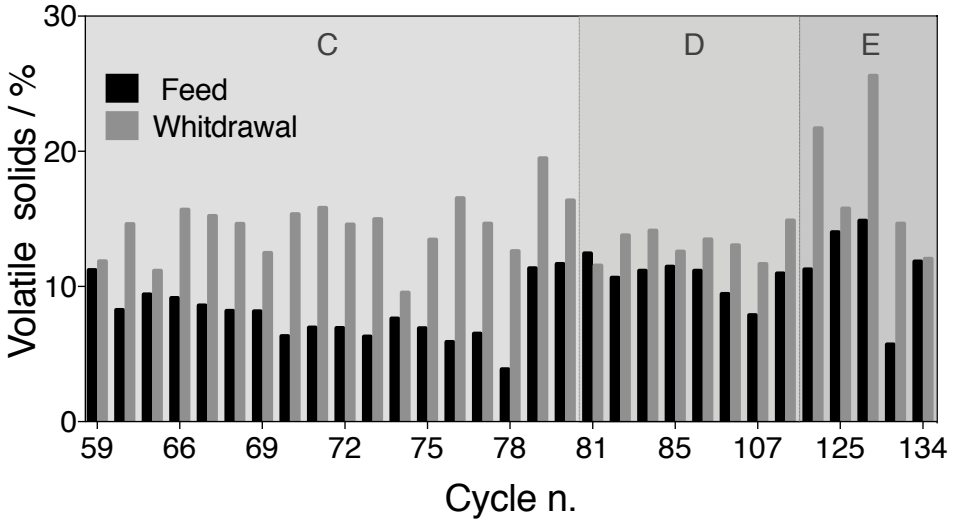

Figure 3.20 *Volatile solids content measured in the influent and in the effluent during each cycle (SBR-C).*

As to DOC, trend observed in Figure 3.21 indicated that the complete removal of saponins from SBR-C occurred within each cycle (see also section 3.2.1.3).

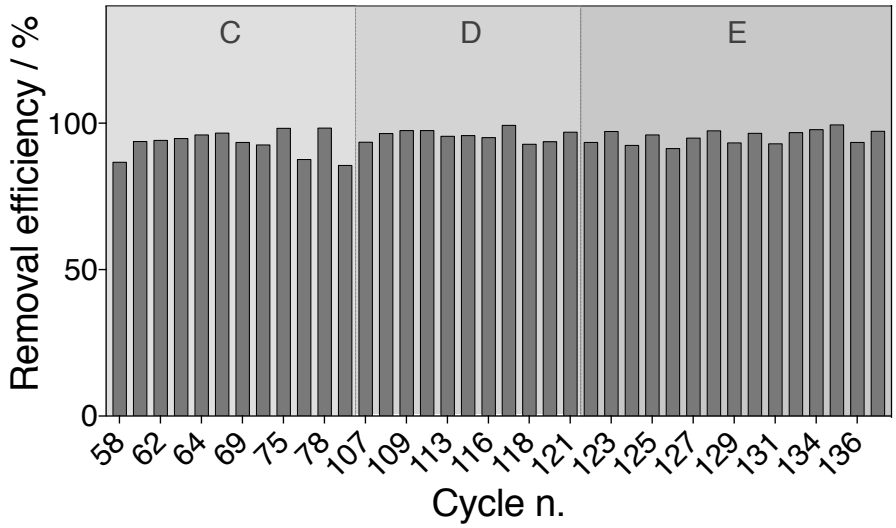

Figure 3.21 *Removal efficiency of the dissolved organic carbon measured in representative cycles for each Phase (SBR-C).*

3.2.2.4 Conclusions

In conclusion of this study, bioaugmentation resulted not useful to recover a reactor which was already compromised after the previous increase in vOLR; in general, the achieved results suggested that an increase in vOLR over a certain limit (to be determined on a case by case basis, since the best process conditions can depend from the specific sediment to be treated) is against process performances. In fact, despite the high removal efficiencies (often higher than 90%), PAHs complied with threshold levels only in few cases, hence sediments were not

suitable to specific reuse or disposal (see section 2.5). In this study, Pyr was the compound that showed the highest recalcitrance; the difficulty to degrade over 3-ring PAHs and to degrade mixed PAHs was already discussed in section 1.6.
However, given the contradictory results achieved in batch tests with respect to SS-SBR, results obtained in SBR-C cannot be considered conclusive about the ineffectiveness of a hypothetical bioaugmentation treatment: in fact, the inoculum of the C286 strain positive influenced the degradative process in batch tests and enhanced Pyr removal efficiency; the conditions pre-inoculum have probably played a significant role in the positive results achieved in batch tests (bioaugmentation was here applied to fresh sediments) and in the negative ones achieved in SBR-C. The higher vOLR applied to SBR-C in Phase D had already resulted, in fact, in a decrease of the PAHs removal efficiency (from 97±2% to 93±5%), in the overall worsening of the process performances and in the consequent lack of compliance with L_2 limits.

Therefore, the eventual application of a bioaugmentation treatment should be carefully evaluated, since too many variables, such as the sediment used, the microorganism inoculated, the conditions pre-inoculum, the quantity and number of PAHs contaminating the sediment, can influence the final result.

4 TREATMENT OF MARINE SEDIMENTS CONTAMINATED BY PAHs BY USING MICROBIAL ELECTROCHEMICAL TECHNOLOGIES

4.1 THEORETICAL PRINCIPLES AND LITERATURE REVIEW

As extensively described in Chapter 1, contamination of soils and sediments represents a worldwide issue that could be faced by applying treatments that include physico-chemical and biological processes. While the first are typically fast and easy to control, biological processes are increasingly preferred even for the treatment of toxic organic compounds due to their lower cost, although they require a longer treatment time (Friman *et al.*, 2012). As already explained, bioremediation relies on the microbial destruction of pollutants: microorganisms use their metabolic functions to convert the contaminants into less toxic forms (this is not always true in the case of compounds such as PAHs) and to reduce their concentration (Friman *et al.*, 2012). The use of conventional bioremediation treatments has been investigated in Chapter 3, where SS-SBR technology was described.

However, although biological degradation of recalcitrant organic compounds is achievable under aerobic and, to a lesser extent, anaerobic conditions (Coates *et al.*, 1996, 1997), conventional remediation systems suffer from a certain number of drawbacks. While oxidants and reductants (required for degradation of compounds such as non-halogenated hydrocarbons, or chlorinated hydrocarbons, respectively) can be both available in the environment, degradation typically results in their depletion; therefore, addition of chemicals is necessary to achieve complete decontamination. For example, conventional bioremediation treatment of petroleum organic hydrocarbons, such as BTEX and PAHs, usually requires the addition of oxygen as terminal electron acceptor, since it could be present at low levels in natural soils. Often, nutrients and co-substrates are added as well, in order to promote microorganisms cell growth and, hence, bioremediation capacity (Kronenberg *et al.*, 2017). These chemicals additions entail important operational costs and energy investments (Zhang *et al.*, 2010). Moreover, unwanted side reactions (such as the reaction of oxygen with elements like Fe^{2+}, whose oxidation can cause clogging phenomena, or the production of H_2S), a limited dispersion of chemicals through the soil matrix, their diffusion away from the contaminated area, and eutrophication consequent to nitrates and phosphates addition to an aquifer, constitute other common problems associated with conventional bioremediation techniques (Daghio *et al.*,

2017, Kronenberg *et al.*, 2017). These problems, together with usually high operating costs, make the process implementation and monitoring of *in situ* treatments quite difficult. On the other hand, *ex-situ* treatments, such as sediment slurry sequencing batch reactors process, impose higher costs for aeration than *in situ* treatments, apart from pre-treatments and chemical supply costs (Pisciotta and Dolceamore Jr, 2016).

Alternatively, microbial electrochemical technologies, and their technological platform, the bioelectrochemical systems, can potentially overcome such drawbacks and may therefore represent a valid replacement to conventional processes. By employing a specific ability of certain microorganisms to use solid state electrodes as electron acceptors or donors through the extracellular electron transfer, BESs can achieve the oxidation or reduction of a wide range of groundwater and soil contaminants, *e.g.* nitrates (Virdis *et al.*, 2009), BTEX (Zhang *et al.*, 2010), PAHs (Lu *et al.*, 2014), chlorinated aliphatic hydrocarbons (Aulenta *et al.*, 2009). In addition, by acting as an inexhaustible sink or source of electrons, the electrodes overcome the requirement for expensive chemical dosing. Another advantage of BESs is the low energy demand.

Considering the operating principles of the most common types of BESs, they couple biological and electrochemical processes to remove organic compounds and simultaneously generate electricity in microbial fuel cells (MFCs), or produce hydrogen or other chemicals of interest, in microbial electrolysis (MECs) and electrosynthesis cells (MESs). An MFC and a MEC are schematised in Figure 4.1. Considering specifically MFCs, the chemical energy contained in soluble organic molecules can be directly recovered as electric energy suitable, in principle, to power electrical devices. An MFC usually consists of two chambers containing the electrodes (the anode and the cathode), separated by an ion-selective membrane and electrically connected via an external electric circuit containing an electrical load. Bacteria oxidize organic matter in the anodic chamber (under anaerobic conditions), thereby liberating electrons and protons. Electrons are transferred to the anode and through the electric circuit towards the cathode. Instead, protons migrate to the cathode compartment through the electrolyte and the ion-selective membrane. At the cathode, protons and electrons combine to reduce biotically or abiotically a terminal electron acceptor at a high electrochemical reduction potential, usually oxygen to generate water (Logan *et al.*, 2006). Conversely, for MECs, whose ultimate goal is the production of chemicals having an economic value, both compartments must be completely anaerobic: the cathode stays at a lower electrochemical reduction potential value than the anode,

which implicates the use of an external energy input (in terms of a low and fixed external voltage, or a fixed current) in order to push reactions that normally would not be favoured (Logan *et al.*, 2008).

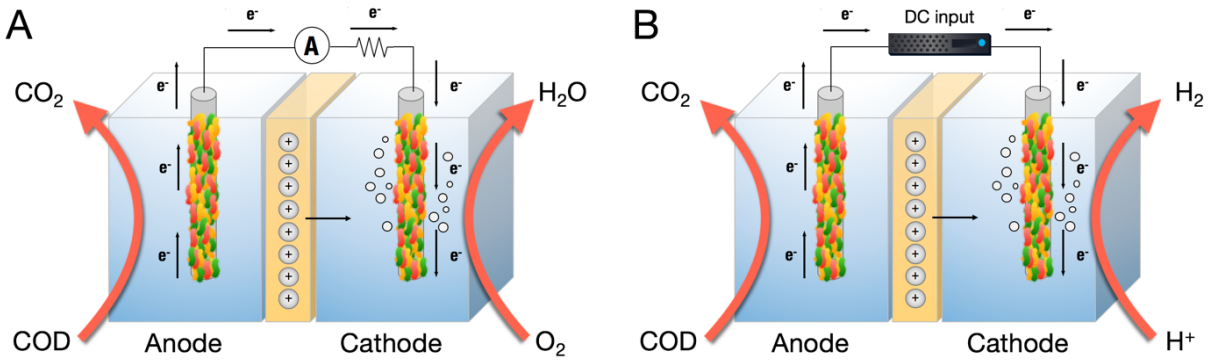

Figure 4.1 *Schematic representation of the most common bioelectrochemical systems: A) microbial fuel cell (MFC) and B) microbial electrolysis cell (MEC). Systems are examples of two chamber BES: the anodic chamber is the site of oxidation, whereas the cathodic chamber is the site of reduction. The organic substance represented as chemical oxygen demand (COD) is oxidised to CO_2 by bacteria. Microorganisms transfer the electrons taken from the substrate to the anode. At the cathode, oxygen or protons, considering respectively MFC or MEC, are reduced abiotically or biotically by using the electrons transferred from the anode, through an external circuit, hence producing water or gaseous hydrogen, respectively. To maintain electroneutrality within the system, positive charges migrate from the anodic chamber to the cathodic chamber passing through an ion-permeable separator (a CEM in this schematisation). While the first process occurs spontaneously in the presence of an external load, hence producing an electrical current, the second process is not spontaneous and a potentiostat (DC input) imposes a fix voltage, or a fix current.*

Although the mechanisms behind BESs used for bioremediation purposes can be the same described above, their main goal is the removal of contaminants rather than the generation of current or useful chemicals, which are considered merely secondary aspects.

For example, recent studies have shown that SMFCs treating contaminated sediments can accelerate bioremediation rates in anoxic environments while providing a stable permanent electron acceptor (Pisciotta and Dolceamore Jr, 2016). So far, only few studies investigated the ability of SMFCs to remediate sediments contaminated by PAHs: for example, an SMFC was proven to enhance the removal efficiency of phenanthrene and pyrene in freshwater sediments (Yan *et al.*, 2012); Sherafatmand and Ng (2015) investigated degradation of naphthalene, acenaphthene and phenanthrene in lake sediments. Recently, Hamdan *et al.* (2017) carried out the first attempt to assess the performance of an SMFC treating PAH-contaminated marine sediments.

In this framework, here SMFCs were deployed to assess the applicability of these non-conventional treatment technology to the bioremediation of marine sediments contaminated by phenanthrene. Tubular cathode compartment-SMFCs were operated in slurry phase, comparing

static and well mixed conditions (*i.e.*, by adopting mechanical stirring). Promising results in terms of high removal efficiencies of Phe, which encouraged further investigations on this field, were achieved in well mixed conditions.

However, current outputs associated to the SMFCs deployed in this study were low. The last one is a typical drawback of sediment bioelectrochemical systems: currents are often hindered by the generally limited mass transport of contaminants towards the electrode surface (Tender *et al.*, 2002), and by limited interfacial and long-range electron transfer kinetics, which altogether translate in a limited *radius of influence* of the bioelectrochemical treatment. The distance at which the decontamination is still effective plays an important role in defining the effectiveness of the bioelectrochemical remediation. Water content, soil or sediment type, conductivity, and matrix porosity highly influence the mass transport. In addition, an electrode is usually spatially confined, hence long-range electron transport is restricted to the thickness of the biofilm attached to the electrode: degradation is typically restricted to a few centimetres close to it (Wang *et al.*, 2012; Lu *et al.*, 2014). Apart from these considerations, the intrinsic characteristics of soil contamination *per se* can be related to low current outputs; for example, contaminants such as BTEX and PAHs, which are slowly biodegradable and poorly soluble in water, are also, due to their hydrophobic nature, very easily adsorbed to soil particles. Moreover, contrary to processes occurring in liquid phase, the presence of soil particles and the absence of mixing conditions, contribute to generate strong concentration gradients around the electrodes, which limit the kinetics of the remediation process. Typical current outputs from MFCs used for decontamination of soils and sediments from contaminants such as total petroleum hydrocarbons, PAHs, n-alkanes, and normalised for the projected anodic surface, are within the range 2 – 30 μA cm^{-2} (Sherafatmand and Ng, 2015, Li *et al.,* 2016). The consequent low signal-to-noise ratio makes it difficult to couple current output to the removal of a specific contaminant; hence, the bioelectrochemical process loses his characteristic to be easy-to-monitor, which constitutes instead one of his main strengths.

In order to solve the outlined problems, the microbial kinetics at the electrode need to be improved. Possible solutions are: 1) use of materials suitable for catalysing bacteria activity, 2) increase of ionic conductivity, hence improving the mass transport, 3) increase of specific surface that constitutes the site for reactions, hence extending long-range electron transfer distance (*i.e.*, increase of the soil conductivity). For example, carbon fibre added to polluted soils achieved a current output 110% higher than soil without amendment (Li *et al.*, 2016); in a soil supplemented with silica colloids (added in order to increase the ionic conductivity) power production was enhanced by 10 times (Domínguez-Garay *et al*., 2013). Moreover, the

incorporation of conductive nanomaterials within soils and sediment particles may be a solution that helps improving the conductivity of porous soils and therefore may resolve the drawbacks of traditional SBESs configurations. Along these lines is the use of graphene, a two-dimensional carbon material characterized by an outstanding electric conductivity, excellent mechanical properties (Dreyer *et al.*, 2010), high specific surface area (Zheng *et al.*, 2016), and biocompatibility (Syama and Mohanan, 2016). Previously, Virdis and Dennis (2017) have demonstrated that graphene produced by the biological reduction of graphene oxide, self-assembles with microbial cells to form thick biofilms with superior electrocatalytic properties due to the large packing of cells and the increased conductivity resulting from the inclusion of graphene within the biofilm structure.

Here, under a similar rationale, two different reduction methods were compared: 7 lab-scale systems were amended with increasing GO concentrations and inoculated with electroactive microorganisms to promote the *in situ* microbial reduction of GO to rGO, which deposited within the pores of the soil, hence providing a significant increase in the soil electric conductivity; furthermore, the same GO concentrations were dosed to the same lab-scale system configuration, in order to test electrochemical reduction, without the inoculum of electroactive microorganisms.

Promising results obtained with these experiments suggested that reducing *in situ* graphene oxide represents an easy-to-apply and cost-effective method to induce electrical properties to otherwise insulating soils. Moreover, bioelectrodegradation capacity was significantly enhanced in comparison to systems not amended with GO.

Based on these good performances, the action of rGO-sediment composite electrodes on decontamination of marine sediments spiked with Phe was investigated: specifically, taking the hypothesis that rGO-sediment composite electrodes account for the largest phenanthrene removal, the performance of one bench scale reactor operated under closed circuit was compared to the activity of an open circuit control and an abiotic control built with the same criteria of the first two reactors.

4.1.1 Occurrence of EET in electroactive biofilms and description of oxidative processes

4.1.1.1 EET as mechanism for anaerobic respiration in natural environments

Bacteria and Archea possess a higher respiratory flexibility if compared to higher animals and plants, whose respiration relies instead totally on the use of oxygen as terminal electron acceptor

(Richardson, 2000; Creasey *et al.*, 2018): a wide range of water-soluble electron acceptors and insoluble minerals (particularly iron and manganese) can, indeed, serve for the microbial respiration (Creasey *et al.*, 2018). Soils and aquatic environments are reach of dissimilatory metal-reducing microorganisms, such as *Geobacter metallireducens* GS-15 and *Shewanella oneidensis* MR-1, that in the absence of molecular oxygen and other respiratory terminal electron acceptors can oxidise organic matter or hydrogen using minerals containing Fe(III), Mn(III) or Mn(IV) (Shi *et al.*, 2016) as electron acceptors, and coupling this process with energy conservation (Shi *et al.*, 2009).

Microbial cell envelope of Gram-negative bacteria is a non-conductive structure formed by a cytoplasmic membrane, other external components such as peptidoglycan and the S-layer, and an outer membrane (peptidoglycan is located between internal and external membranes). Because of the insoluble nature of Fe and Mn, they cannot get through this non-conductive barrier, hence electrons are transferred via EET on the external environment. In fact, albeit structural components of the cell envelope are non-conductive and physically impermeable to minerals, membrane proteins, able to transport electrons, are anchored to the cell envelope (Shi *et al.*, 2016).

Different mechanisms are involved in EET: microorganisms such as the Gram-negative bacteria *Shewanella oneidensis* MR-1 and *Geobacter sulfurreducens,* that are two of the most studied dissimilatory-metal reducing bacteria for the reduction of metal oxides, have developed some specialized mechanisms for the exchange of electrons such as the metal-reducing pathway for *S. oneidensis* MR-1 and the use of porin-cytochrome proteins for *G. sulfurreducens* PCA (Shi *et al.*, 2016). Multiheme[18] *c*-type cytochromes (*c*-Cyts), located in the outer membrane, represent their major electron transport carrier proteins. Hypothetically, trans-outer membrane proteins act as sheaths; the redox proteins are embedded inside the sheaths and allow the electron transfer from the quinone/quinol pool (for further details see section 4.1.1.2) in the inner membrane, to the periplasm and then to the outer membrane; through *c*-Cyts, electrons can be transferred to metal oxides directly, indirectly or both (Shi *et al.*, 2009).

Besides the transport of electrons to Fe and Mn oxides used as terminal electron acceptors, EET can serve for microbial interspecies electron transfer when semi-conductive particles such as iron-oxide nanoparticles act as conductors bridging electrons between different cells *(Kato et al.*, 2012). Some organisms are able to perform EET by self-producing soluble redox-active

[18] This is the iron-containing portion of cytochromes; cytochromes carry electrons and the iron atom constitutes the redox site, and alternate between Fe^{2+} and Fe^{3+} oxidation states (Madigan *et al.*, 2017).

molecules to facilitate EET, hence they overcome the need for a physical connection between the intracellular metabolism and the extracellular space (Creasey *et al.*, 2018).

Moreover, some microorganisms are able to make long-range electron transfer of electrons to minerals or to other cells that are distant nanometres from the cell surface: for example, *G. sulfurreducens* PCA can employ nanowires for these purposes. Nielsen *et al.* (2010) evidenced an interesting phenomenon of long-range electron transfer thanks to the presence of microbially driven electric currents able to connect spatially separated biogeochemical processes over distances of 10 mm: the authors observed that the rapid oxidation of hydrogen sulphide in the sulphidic zone (deprived of oxygen) was promoted, whilst oxygen in the overlying sea was reduced. Further studies demonstrated that electrons were transported over centimetres by 'cable bacteria' of the family *Desulfobulbaceae*, a particular type of filamentous bacteria (Pfeffer *et al.*, 2012; Schauer *et al.*, 2014).

Thanks to the described behaviours, microorganisms can also exchange electrons with other extracellular substrates, such as humic acids, soluble metal ions, dimethyl sulfoxide and electrically conductive nanomaterials.

Interestingly, the movement of electrons towards Fe and Mn oxides, that occurs in subsurface environments deprived of oxygen molecules, is the same movement underpinning the exchange of electrons with a solid-state electrode in bioelectrochemical systems. In particular, bacteria which can perform extracellular electron transfer with an electrode without the addition of exogenous mediators are indicated as 'electrochemically active bacteria' (EAB) (Chang *et al.*, 2006).
Considering as example the case of an MFC, thanks to the ability to reduce insoluble electron acceptors, dissimilatory metal-reducing bacteria are capable to form a multi-layered aggregation (or microbial biofilm) attached to the electrode (the anode) and to transfer through this biotic-abiotic interface electrons that derive from the oxidation of the substrate (Millo, 2012). Both pure cultures and mixed communities of bacteria able to directly transfer electrons to the anode can form electroactive biofilms (*i.e.*, biofilms able to make extracellular electron transfer). A variety of organic substrates, such as acetate, propionate, lactate, glucose and domestic wastewater were proven to be oxidised by pure or enriched mixed cultures *(Kim et al.*, 1999; Bond and Lovley, 2003, 2005; Chaudhuri and Lovley, 2003; Gil *et al.*, 2003). Even if the mechanism of electron transfer is the same, there is a fundamental difference between the use of insoluble minerals and electrodes: while the ability of insoluble minerals to accept or

donate electrons is eventually depleted, electrodes provide a surface with long-term electron accepting or donating capacity. Therefore, the relation between microbes and electrodes, and microbes and minerals is different: for example, *Geobacter* spp. are planktonic when oxidising organic compounds using minerals as terminal electron acceptors; conversely, they firmly attach to electrodes forming thick metabolically active biofilms (Lovley, 2012).

4.1.1.2 Description of oxidative processes

According to section 1.6.1.1, a certain number of redox reactions compose aerobic and anaerobic respiration processes of chemotrophic organisms, and the net energy gain associated with the reactions is determined by the potential gap between a low redox potential molecule (*i.e.*, the electron donor) and a high redox potential molecule (*i.e.*, the electron acceptor) (Madigan *et al.*, 2017). Thanks to the synthesis of energy-rich compounds, such as ATP, cells store energy that has been released from catabolic reactions occurring along the electron transport chain. Considering anodic oxidation of an organic substrate, the mechanism of energy generation proper of microorganisms growing on an insoluble electrode is a form of respiration similar to molecular oxygen or O_2 substitute respiration: anodic oxidation requires, in fact, the TCA cycle and the electron transport chain; the net products are water, carbon dioxide and ATP (Freguia, 2009).

Together with fermentation, respiration represents a major strategy for energy conservation in chemoorganotrophs (Madigan *et al.*, 2017).
In the case of fermentation, which is a form of anaerobic catabolism, an organic compound is both an electron donor and an electron acceptor. Conversely, respiration is the form of aerobic or anaerobic catabolism in which an electron donor is oxidized with O_2 or an O_2 substitute, such as oxygen linked compounds like nitrates and sulphates, as the terminal electron acceptor. As already mentioned in section 1.6.1.1, molecular oxygen is the best electron acceptor existing in the environment. A major metabolic pathway for microbial fermentation and respiration is represented by the catabolism of glucose in glycolysis (Figure 4.2), which breaks down glucose into pyruvate.

In fermentation, ATP is synthesized by substrate-level phosphorylation directly from energy-rich intermediates. Conversely the mechanism that occurs in respiration is the oxidative phosphorylation: ATP is synthesized thanks to the use of the proton motive force; if pyruvate

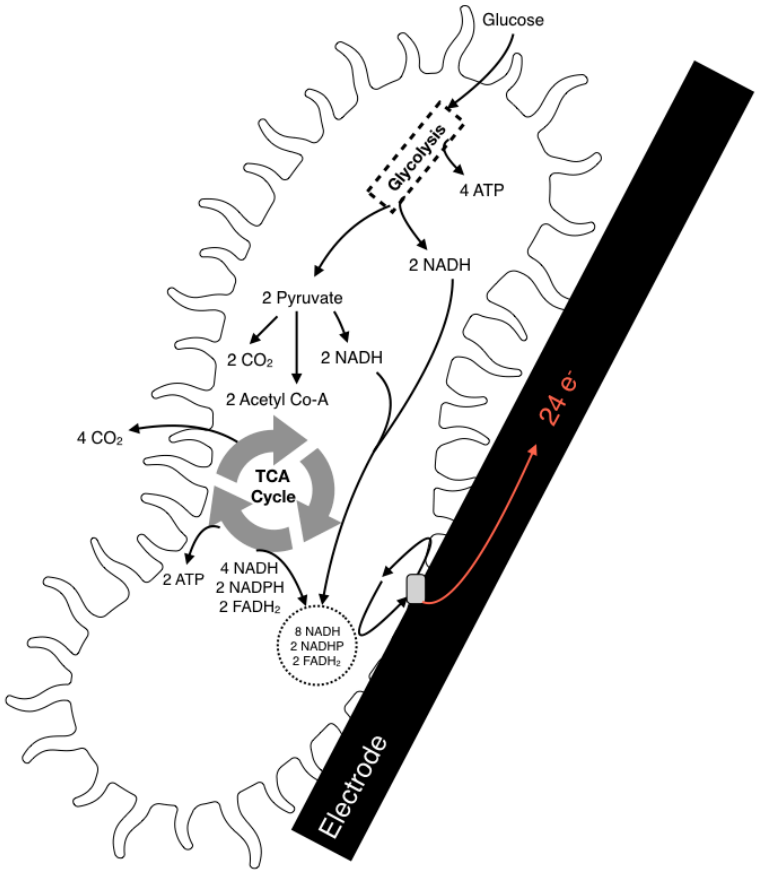

Figure 4.2 *Schematic representation of the pathways of oxidation of glucose in respiratory metabolism of EAB in the presence of an anode. Glucose is firstly converted by glycolysis into pyruvate and acetyl Co-A; the last one enters the TCA cycle where it is converted into CO_2, ATP and reducing equivalents nicotinamide adenine dinucleotide (NADH), nicotinamide adenine dinucleotide phosphate (NADPH), flavin adenine dinucleotide ($FADH_2$), which transfer electrons firstly to the electron transport chain, and then to the electrode. Redrafted after: Freguia et al. (2012).*

is fully oxidized to CO_2 rather than reduced to some fermentation product, a far higher production of ATP is possible (Madigan *et al.*, 2017). Oxidative phosphorylation forms two NADHs, deriving from the coenzyme NAD^+ (*i.e.*, the oxidised form of nicotinamide adenine dinucleotide).

The proper respiration pathway starts with the TCA cycle or citric acid cycle (CAC). Here the pyruvate produced from glycolysis is first decarboxylated, forming CO_2, NADH, and the energy-rich substance acetyl-CoA. Citric acid, which is a six-carbon compound, is produced when the acetyl group of acetyl-CoA combines with the four-carbon compound oxaloacetate. After a series of reactions two additional CO_2 molecules are produced; moreover, electrons released during the oxidation of intermediates in the TCA are transferred to NAD^+ to form NADH (four in the end of the TCA cycle), or in one reaction, to FAD (oxidised form of flavin adenine dinucleotide) to form $FADH_2$ (reduced form), or form NADPH. Eventually, the cycle is completed when oxaloacetate is regenerated and returns as an acetyl acceptor.

NADH, NADPH and $FADH_2$ produced in TCA cycle are then fed to the electron transport chain. Here, carriers are organised in order of increasing redox potential (with NADH dehydrogenase first and cytochromes last), and there is an alternation of electron-only and electron-plus-proton carriers in the chain. Redox reactions of common compounds responsible for electron transport in electron transport chain are reported in Table 1.5. Electron transport occurs in the membrane, and several types of oxidation–reduction enzymes participate. NAD^+ is a common redox intermediary of respiration also proper of mitochondria of higher plants' and animals' respiration (Richardson, 2000), able to carry both electrons and protons, whilst being reduced to NADH. Then, electrons move through a range of redox cofactors bound to the cell membrane or constituting membrane-associated protein complexes, such as flavoproteins, iron–sulphur proteins, cytochromes and nonprotein electron carriers called quinones, hence NADH is further oxidised to NAD^+.
Quinones typically participate as links between iron–sulphur proteins and the first cytochromes in the electron transport chain; since they are small and hydrophobic, they are free to move within the membrane. Like the flavins, they accept both, electrons and protons, but only donate electrons. They form the quinone pool, to which electrons are sent from NADH and $FADH_2$.
All electron transport chains are associated with the release of free energy: as reported above, the electrons movement is coupled to the generation of a proton motive force (H^+ derives from water dissociation and from NADH).

The combined reactions of the TCA cycle and electron transport chain allow the complete oxidation of glucose to CO_2. Aerobic respiration of glucose ends with the conservation of a greater amount of energy than fermentation: in fact, the former produces 38 ATP, whereas 2 ATP are generated from the latter (Madigan *et al.*, 2017).

Like aerobic respiration, anaerobic respiration requires electron transport, generates a proton motive force, employs ATP-ase to make ATP, and is the basis for anodic oxidation. As a consequence, acetate, lactic acid and ethanol, which can enter the TCA cycle through pyruvate or acetyl-CoA by using one or two enzymatic steps (whereas glycolysis, required for more complex carbohydrates before entering the TCA cycle, is divided in ten steps), can be used directly by EAB as electron donors for electricity production (Bond and Lovley, 2003). According to White (1995), the maximum theoretical ATP yield for prokaryotes, also known as respiration ratio, is 3 ATP per NADH molecule. However, its actual value is reduced by the utilization of proton motive force for other cell activities, such as motility or solute transport,

or due to 'shortcut' in the electron transport chain: in fact, considering bacteria attached to a solid anode, soluble mediators or cytochromes (aligned or not in nanowires) constitute the last electron carriers able to physically establish an electrical contact with the electrode; since they might possess a potential not sufficiently electronegative to receive electrons from further components in the electron transport chain, less protons would probably be extruded from the cell membrane and the maximum ATP yield would be accordingly reduced. Therefore, considering the growth of electroactive bacteria in the presence of an anode, as the bacterial growth depends on the availability of intracellular ATP, it will be related to the mechanism of electron transfer, which is in turn dependent on the anodic potential: in synthesis, the potential of the anode ultimately regulates the growth yield of bacteria (Schröder, 2007).
Between the broad range of biodegradable material serving as electron donor in BESs, acetate has been frequently used in BESs studies as the preferred substrate by EAB; this readily biodegradable substance may generate very high Coulombic efficiencies[19], and is inert to alternative biochemical conversions such as fermentations (fermenters can, in fact, syntrophically interact with electroactive bacteria) (Freguia *et al.*, 2007).

4.1.1.3 Transport of electrons through electroactive biofilms in BESs

When an organic substrate comes into contact with electroactive microorganisms in the presence of an electrode several steps occur. Carbon uptake into the cell, cellular metabolism and the consequent energy generation at the bacterial inner membrane have been widely described in sections 4.1.1.1 and 4.1.1.2. The next step, herein described, is the transfer of electrons through the biofilm matrix that ends with transfer of electrons to the electrode (Zacharoff and El-Naggar, 2017).

Although biofilms are commonly considered as electronic insulators (*i.e.*, no free electrons can flow under ordinary thermal conditions) (Dheilly *et al.*, 2008), direct conductivity measurements, as well as modelling studies (Kato Marcus *et al.*, 2007) and cyclic voltammetry (CV)[20] measurements (Torres *et al.*, 2008; Snider *et al.*, 2012), have revealed that biofilms

[19] It is given as the percentage of electrons which are actually transferred to a solid electrode in a BES, considering the total number of electrons which are expected to be exchanged for achieving full oxidation of an organic substrate.
[20] Cyclic voltammetry is an electrochemical technique used for the analysis of electrochemical processes: the potential applied to the working electrode is varied linearly with time, and the resulting current is plotted *versus* the applied potential; the signal is composed of a backward and forward scan. From the correct application of the technique important information for the electrochemical process is derived, including thermodynamics, interfacial kinetics, identification of mass-transfer regime and rate-limiting process.

formed by a pure culture of *G. sulfurreducens* (Malvankar *et al.*, 2011) or mixed cultures derived from wastewater (Malvankar *et al.*, 2012) are electronically conductive when they grow on the anodes of MFCs.

Electronic conductivity is a property of the material thanks to which electrons can flow within the material itself; in fact, in an electron transport process, electrons are carried in multiple steps through a molecule bridge between donor and acceptor. In the case of biofilms, electronic conductivity means that microorganisms have the capability of long-range electron transport, *i.e.*, to access electron acceptors that are even many cell lengths away, over distances of ten angstroms (Malvankar and Lovley, 2015). Conductivity can occur through three different modes, *i.e.*, tunnelling, hopping and delocalisation. According to Malvankar and Lovley (2015), these processes can arise simultaneously, and each one can dominate at different values of the applied electric field or at different temperature range. Tunnelling is a mechanism related to the "wave" nature of electrons: hypothesizing to direct electrons towards an electrode/insulator interface, they will cross with a finite probability the barrier only if this barrier is very thin (< 5nm); in fact, the wavefunction decays rapidly with depth of penetration from the electrode/insulator interface. Tunnelling depends on the magnitude of the applied voltage and on the similarity of materials put in contact.

Electron hopping occurs between one reduced molecule and an adjacent oxidised molecule via physical displacement. In this case, conductivity is proportional to the concentration of redox species. Albeit in both mechanisms the electron moves through one or more sites to migrate over long distances, tunnelling and hopping are differentiated because hopping involves a nuclear motion over the cell barrier by rearrangement of the molecule, tunnelling does not. Moreover, tunnelling is dominant for small distances, while hopping for large distances.

Metallic conductivity, instead, derives from a process of electron delocalisation or spreading of electron wavefunctions: electrons are free throughout the material. The phenomenon is due to the overlapping of molecular orbitals: when energies are very close together, molecular orbitals merge in a continuous band forming electronic bands, which originate conductivity when are partially populated (Malvankar and Lovley, 2015).

For the last step of electron transport, which is necessary to cross the barrier constituted by the outer membrane of the microbial cell and reach the electrode, bacteria can use two different strategies: mediated electron transfer and direct electron transfer. The former requires soluble

redox mediators able to shuttle electrons between the bacteria and the electrode, while, thanks to the latter, bacteria establish a direct contact with the electrode. Mediated electron transfer was the first mechanism recognised for the transport of electrons between the microbial cell and the electrode surface in the first MFCs applications. In particular, electrons movement was promoted thanks to the addition of soluble redox mediators, such as neutral red (Park and Zeikus, 2000), well known for the ability to be reversibly oxidised and reduced, the resistance to biological degradation, the fast kinetics of oxidation at an electrode, the ease of diffusion through bacterial membranes and the non-toxicity towards microbial consortia. Soon, it was reported that redox active compounds serving as endogenous mediators (*e.g.*, pyocyanin and phenazine-1-carboxamide) could be also self-produced by bacteria (e.g., by *Pseudomonas aeruginosa*) (Rabaey *et al.*, 2005). Direct electron transfer is suggested to occur either through conducting proteinaceous nanowires or through multiheme redox proteins referred to as outer membrane cytochromes (OMCs) (Millo, 2012; Dennis *et al.*, 2016). In particular, OMCs were proven to promote the transfer at the biofilm/electrode interface, but also to promote the long-range electron transfer (ET), which occurs across the biofilm. In fact, considering as example a biofilm formed by *G. sulfurreducens*, it can reach a thickness of more than 100 μm (Virdis *et al.*, 2016); inside the biofilm, multiheme *c*-type cytochromes are located on the outer membrane and periplasmic space (as explained above), along extracellular filaments, and are dispersed in the extracellular polymeric substance. Models proposed for *Geobacter* biofilm conductivity are redox conduction and metallic-like conductivity: redox conduction occurs through electron hopping between discrete redox cofactors bound to the extracellular matrix of biofilms (Boyd *et al.*, 2015, Virdis *et al.*, 2016), while metallic-like conductivity happens through intrinsic conducting properties of nanowires which are specific for *G. sulfurreducens* (Virdis *et al.*, 2016). According to a proposed model, redox conduction consists of a fast-heterogeneous electron transfer at the biofilm/electrode interface, which is coupled with a slower long-range homogeneous electron transfer; the former is governed by electron tunnelling, the latter by hopping. Electron transfer occurs to a given direction thanks to a redox gradient. Bonanni *et al.* (2013) suggested that redox conduction takes place thanks to the action of both, OMCs and nanowires. According to the same study, electron transfer may be different in mixed culture biofilms, due to the presence of multiple species that may complicate the interactions with the anode; however, multi-layered biofilms formed by a mixed community of electroactive microorganisms are able to produce current densities comparable with those of pure *G. sulfurreducens*. *Shewanella* sp., instead, build a three-multiheme *c*-type cytochromes complex that conducts electrons originated in the cytoplasm from the inner membrane through the

periplasm and outer membrane; outside the cell, as *G. sulfurreducens*, they generate pili and microbial nanowires that have a nanometre scale diameter and are micrometre scale length (Snider *et al.*, 2012). Pirbadian and El-Naggar (2012) model described filaments lengthwise conductivity as a multistep electron hopping involving redox cofactors apparently associated with these filaments. However, also in the case of *Shewanella* sp., a number of c-type cytochromes was found in the extracellular matrix.

4.1.2 Suitability of marine sediments as contaminated media for application

Electron acceptors are naturally depleted in the environment due to the activity of microorganisms able to degrade organic matter by using available oxidised compounds; alternatively, given the ability of EAB to use insoluble terminal electron acceptors, electrodes might be usefully provided as inexhaustible sinks for electrons.

In particular, when considering the sediment-water interface and moving from the interface to the bottom within the sediment, it is common to find different redox horizons (*i.e.*, reduction-oxidation gradients), which are generated from spatially separated reactions of reduction and oxidation mediated by microorganisms (Girguis *et al.*, 2009). As shown in Figure 4.3 A, starting from the sediment-seawater interface, the dominant process is aerobic respiration due to the presence of oxygen. Suddenly, passing from this level to deeper sediments oxygen is depleted, and leave place to other microbially mediated processes supporting the organic matter degradation such as nitrate, iron and manganese reduction. Below nitrate-reduction level, sediments are dominated by microbial sulphate reduction, fermentation and methanogenesis. The order in which electron acceptors are consumed is dictated by the different redox potential: higher redox potential acceptors are consumed before than lower ones; in an idealised system: $O_2 > NO_3^- > Fe^{3+} > SO_4^{2-} > CO_2$. As already described in section 1.6.1.1, the first process occurring, *i.e.*, aerobic degradation yields the highest free energy.

Natural redox gradient distribution, coupled with microbial degradation of organic matter, can be usefully exploited in bioelectrochemical systems such as benthic microbial fuel cells (BMFCs), which rely on the potential gradient at a sediment-water interface. BMFCs are analogous to SMFCs, but specific for marine environments: in both systems the anode is buried in the sediment and the cathode is suspended in the overlaying water, as shown schematically in Figure 4.3 B. Electrodes are connected *via* an external load or a potentiostat (for research

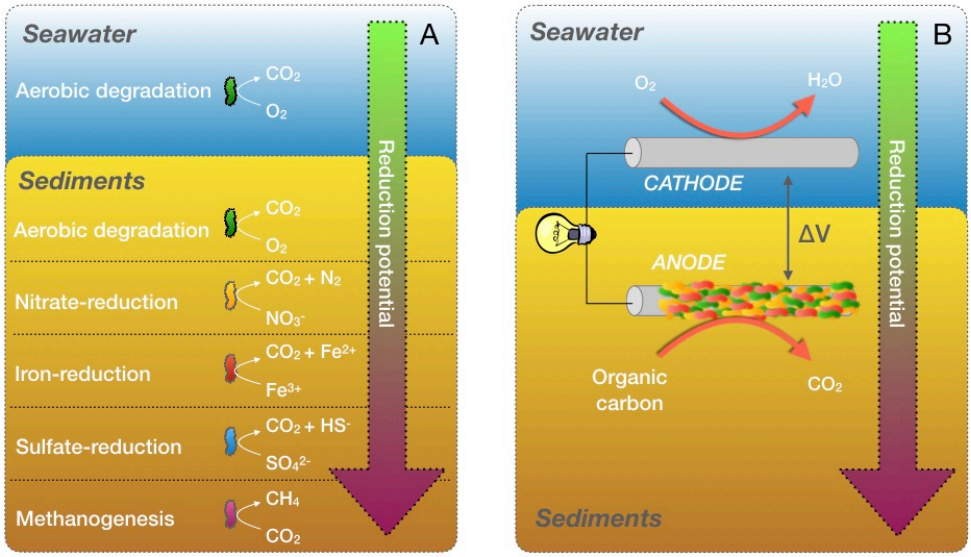

Figure 4.3 *A) Redox horizons in marine sediments: starting from the overlaying seawater and the seawater-sediment interface, where aerobic reactions take place (green portion of the arrow), deeper in the sediment anoxic and anaerobic degradation become the prevalent mechanisms (red-violet portion of the arrow).The arrow indicate the direction of the reduction potential from the higher to the lower levels: the electron acceptors with higher redox potential are consumed close to the sediment surface. Redrafted after: Daghio et al. (2017); B) Example of a microbial fuel cell deployed in marine environments: the anode is buried in the sediment and connected through an external load or through a sensor to the cathode, in the overlaying water (a voltage difference is naturally present between anode and cathode); due to the ΔV, at the anode organic carbon is microbially degraded to CO_2 while oxygen present in the seawater is reduced at the cathode to H_2O.*

purposes), or *via* a sensor system (used in field applications, sensors are geared to understand marine biogeochemical processes, harvest electricity from natural systems, monitor the marine environment also in remote applications); moreover, the presence of solid particles that hinder mass transport through sediments provides the separation between anode and cathode, with no need for membranes. First prototypes of SBESs were deployed in marine sediments with the purpose to harvest power from the natural microbially established voltage gradients between marine sediments and seawater interface (Reimers, 2001; Bond *et al.*, 2002; Tender *et al.*, 2002; Holmes *et al.*, 2004). Albeit the theoretical difference in redox potential between the oxic seawater and the sulphide-reach sediment horizon should be approximately between 0.86 and 0.91 V at the conditions found *in situ* (Stumm and Morgan, 1996), the actual values recorded from BMFCs were lower due to environmental heterogeneity (*e.g.*, variation in the concentration of redox species, mixing of pore water and bioturbation), but still advantageous for this kind of application, and comprised between 0.7 and 0.8 V (Schulz, 2006). The possibility to use BMFCs is, indeed, supported by the presence of a widespread community of electroactive microorganisms living in marine sediments (see section 4.1.1).

Beyond the effective application of BMFCs, the presence of a large electroactive community and the anoxic conditions that are common under the sediment surface have pave the way for the potential use of BESs for the bioelectrochemical degradation of toxic compounds in aquatic environments, hence solving the drawbacks common in conventional treatments, allowing monitoring from far away locations and potentially avoiding the presence of operators *in loco*. The "Oil-Spill Snorkel" is a representative example of how a bioelectrochemical approach can be effective for bioremediating marine sediments contaminated by hydrocarbons (Viggi *et al.*, 2015). A segment of electrode (the snorkel) was buried within the sediment, hence creating an electrochemical connection between the anoxic contaminated sediment (anodic portion) and the oxic overlaying water (cathodic part): the electrons flow-up to the aerobic environment was promoted; there, through oxygen reduction, water was produced. The presence of the snorkel allowed, through the easy establishment of an electrical connection, the development of a bioelectrochemical reaction not entailing excessive costs or intensive energy requirements and capable to effectively decontaminate the sediment fastening the process that typically occurs in the absence of electrodes.

4.1.3 From the anaerobic degradation of PAHs in conventional treatments to the anaerobic degradation in SBESs

Proof of anaerobic degradation of PAHs, whose mechanism has been already described in section 1.6.2, was given by Coates *et al.* (1997) and Mcnally *et al.* (1998, 1999). The first study described the degradation of a PAHs mixture (naphthalene, phenanthrene, methylnaphthalene, fluorene and fluoranthene) in heavily e poorly contaminated marine sediments under sulphate reducing conditions. Degradation was promoted by the active PAH-degrading bacteria that were exposed to the heavy and chronical contamination, whereas decontamination did not occur in the less contaminated site, unless an inoculum from the heavily contaminated site was added. The second and third studies compared biodegradation of a PAHs mixture containing anthracene, phenanthrene and pyrene (Mcnally *et al.,* 1998), and naphthalene, phenanthrene and pyrene (Mcnally et al. 1999), under nitrate-reducing and aerobic conditions; degradation was carried out by pure cultures of *Pseudomonas putida* and *Pseudomonas stutzeri*, respectively: the first culture was slower in anaerobic conditions than in aerobic conditions, whereas the activity of the second culture was similar in both conditions. Ambrosoli *et al.* (2005) investigated degradation, under denitrifying conditions, of biphenyl, fluorene, phenanthrene and pyrene spiked to soils. A mixed population of microorganisms from a paddy

soil was incubated; the authors tested also the effect of two co-substrates, glucose and acetate, individually supplied. In this study, all hydrocarbons showed similar degradation trends for each condition tested: molecular structure was suggested as the factor that influenced PAHs removal the most, and degradation was poor when PAHs were fed as the only carbon source. In addition, Zhang and Lo (2015) found that the supply of acetate and methanol as co-substrates was effective in the removal of total petroleum hydrocarbons (TPH)[21] from marine sediments: methanogenesis and sulphate reduction were the mechanisms involved when both co-substrates were added, but acetate was the most-effective for TPH degradation, whereas methanogenesis was the prevalent mechanism in the methanol-added sediments. As proved by Johnson and Ghosh (1998) only LMW PAHs are degraded under methanogenic conditions, while HMW PAHs cannot be effectively removed. In addition, the presence of different microorganisms involved in the degradation could be related to different behaviours observed in the presence of sulphate reduction or methanogenesis.

Besides the degradation of PAHs under anaerobic conditions, the possibility to use PAH-compounds as carbon sources in BESs was explored long after and, so far, only few studies investigated the potential for PAH-degradation in bioelectrochemical systems: Kronenberg *et al.* (2017) listed a total of 25 studies specifically treating PAHs or treating hydrocarbons mixtures containing PAHs in the 2010-2016 time lapse. In particular, Zhang *et al.* (2010) provided the first insight on the aromatic hydrocarbon removal using a BES: initial tests proved that *Geobacter metallireducens* could oxidise toluene with a graphite electrode polarised at +500 mV vs SHE, with a potenstiotat electrically connected to a cathode. Then the study moved on the stimulation of the anaerobic degradation of aromatic hydrocarbons in contaminated marine sediments where naphthalene was bioelectrochemically reduced in the presence of the natural community. The bioelectrochemical process was faster than a conventional anaerobic process occurring in the absence of a solid electrode, hence suggesting that recalcitrant compounds such as PAHs may be more easily transformed to less complex compounds if the metabolism of degraders is directly or indirectly boosted by bioelectrochemical activity occurring close to electrodes (Chandrasekhar and Venkata Mohan, 2012). In addition, graphite electrodes had the advantage to adsorb naphthalene (and in general organic compounds) thus

[21] TPH are a mixture of hydrocarbons found in crude oil: the number of chemicals that composes the mixture is high, thereby measuring each compound separately is not practical. Chemicals that occur in TPH include hexane, benzene, toluene, xylenes, naphthalene, fluorene and other petroleum products.

co-localizing the contaminants and the microorganisms able to grow on the electrode surface. Mohan and Chandrasekhar (2011) found a further evidence of PAHs removal in BESs: while conventional anaerobic treatment was effective only for 2-3 ring PAHs, an MFC operating on petroleum sludge was capable of attacking aromatic compounds containing up to 6 rings.

Among the studies which used SBES for the biodegradation of mixed hydrocarbons containing PAHs, the already cited studies of Zhang *et al.* (2010) and Viggi *et al.* (2015) represent two examples of deployment of METs in marine sediments, which is crucial for this thesis work. Moreover, Morris and Jin (2012) investigated TPH removal from marine sediments, by using a 100 mL glass test tube in which the anode was buried in about 70 mL of sediment, and the cathode was fully submerged in the overlaying water: TPH, starting from 16000 mg kg_{dw}^{-1}, after 66 days were removed in percentages of 24% and 2% in the closed circuit and in the open circuit control, respectively. Voltages, measured across 1 kΩ resistance, were as high as 190 mV, equivalent to 2.2 mA m^{-3} of sediment volume.

To the knowledge of the author of this thesis work, until now, the only study specifically addressing the application of METs to the removal of PAHs in marine sediments is the recent study of Hamdan *et al.* (2017). In this study, removal of a naphthalene, 2-methylnaphthalene and phenanthrene mixture were evaluated under different conditions (*i.e.*, by using sediment sulphates, commonly enriched in marine sediments, as terminal electron acceptors without anode; by using a single anode under inhibited sulphate reducing bacteria activity; by using both, anode and sediment sulphates). Tests were conducted in 900-mL Plexiglass reactors filled with composite samples of 1:1 (v/v) sediments/seawater. Sediments were spiked with the PAHs to achieve an initial concentration of 60 mg kg_{dw}^{-1} (20 mg kg_{dw}^{-1} for each compound), which is a relatively high contamination for marine sediments. In each SMFC, anode and cathode consisting of carbon fiber brushes twisted around a titanium wire were placed at 3.5 cm below and above the water-sediment interface, respectively.

Considering the example of phenanthrene, the compound was significantly removed in 28 weeks experiment in the closed circuit SMFC either when the anode acted as the only terminal electron acceptor (93.8±1.7%) and under combined anode and sulphate reduction conditions (88.5 ± 1.3%), whereas a much lower removal (40.4 ± 3.2%) was achieved in the open circuit control operating with sulphate as major terminal electron acceptor. In the closed circuit SMFC with combined effects of anode and sulphate reduction, the voltage reached a maximum value of 0.33 mV after 4 weeks of operation. Slightly higher voltages (up to 0.57 mV) were observed after 4 weeks of incubation in the SMFC where sulphate reducing bacteria (SRB) were inhibited

and the anode was used as the only terminal electron acceptor. Consistently, sulphate depletion was the lowest when SRB were inhibited (although sulphates were still depleted, probably due to a temporary effect of the inhibitor). Moreover, the highest depletion of sulphates was associated to the open circuit control. Interestingly, microbiological analysis revealed the enrichment of *Geoalkalibacter* and *Desulfuromonas* (genera with potential exoelectrogenic capability) on the anode of the closed circuit SMFC under inhibited SRB activity. Conversely, they were absent in the open circuit control and in the closed circuit operating without SRB inhibition; in fact, in both the last cases, the anodic community was the same, also in terms of relative abundance, with the highest relative abundance of *Pseudomonas*. Results clearly indicated that the presence of the anode as terminal electron acceptor highly enhanced PAHs degradation with respect to the control; moreover, only a slightly improvement was recorded when SRB activity was inhibited in the closed circuit SMFC, with respect to the closed circuit SMFC working without SRB inhibition, thus suggesting that inhibition had not a crucial role in the functionality of the community, although it influenced the taxonomy. Results were consistent with the observed phenanthrene removal, sulphate consumption and with the voltages recorded during the experiments.

Comparing performances of BESs such as MFCs working on liquids and SBESs, which work by definition on solids, current densities and power densities may be quite different, especially when SBESs are used for decontamination of recalcitrant compounds; in fact, the nature of the contaminant *per se* and the presence of solid matter complicate mass transfer and long-range electron transfer kinetics significantly (drawbacks of the application of SBESs for bioremediation purposes have been already described in the introduction of this chapter).
Considering MFCs, typical maximum power densities are about 2 or 3 W m^{-2} of projected electrode (usually the cathode), assuming temperature optimum conditions of about 30°C, solution conductivities of about 20 mS cm^{-1}, and well-buffered solutions at neutral or slightly alkaline pH (Logan and Rabaey, 2012). Such values change according to the complexity of the substrate.
When using complex substrates such as TPH, power densities are much lower: for example, the highest power density reported for a synthetic wastewater contaminated with petroleum sludge (*i.e.*, containing TPH) was 21 mW m^{-2} (Chandrasekhar and Venkata Mohan, 2012), hence significantly lower than typical values reached in MFCs.
A common strategy attempting to overcome this drawback, and also mass transfer and long-range electron transfer kinetics issues observed in the presence of solids, is to increase the

electrode surface with the aim to obtain high currents and power densities, and to allow degradation to occur beyond a certain distance. Zhou *et al.* (2016) adopted a high surface carbon cloth thus achieving power densities as high as 220 mW m^{-2}; Li *et al.* (2014) used multi-anodes, hence achieving higher degradation levels than in natural attenuation; Lu *et al.* (2014) used a pilot scale of 50 L, where biochar and graphite granules surrounding a tubular air cathode (a simple PVC tube with holes) served as anode material: degradation had an extended *radius of influence* of 34 cm.

In addition to these aspects related to the build-up of a proper BES suitable for bioremediation purposes, Logan and Rabaey (2012) observed that the complex nature of organic wastes requires a diverse microbial community. For example, although in the specific case of *Geobacter metallireducens* reported above, they showed the ability to grow on toluene, benzene and naphthalene as sole carbon sources (Zhang *et al.*, 2010), the presence of *Geobacteraceae* in the anodic community is generally associated with the use of a limited number of substrates, being acetate the most common substrate among different strains (*Geobacter* spp. can achieve current densities of 1 mA cm^{-2} in the presence of acetate). Syntrophic interactions may therefore be required in order to achieve degradation of complex organic matter into simpler substrates that can be used by exoelectrogens. Kronenberg *et al.* (2017) suggested that, during PAHs bioremediation, the positive effect of electricity is probably related to bioelectrochemical catalysis in which hydrocarbon degraders (HDB) are favoured by the presence of EAB. Syntrophic interaction between HDB and EAB should be deeply investigated in order to understand the mechanisms behind the use of PAHs as carbon source in BESs, but these examinations go beyond the purposes of this thesis work.

4.2 EXPERIMENTAL WORK

4.2.1 Preliminary evaluation of SMFC applicability to bioremediate marine sediments contaminated by PAHs

4.2.1.1 Introduction

This experimental part reports a preliminary evaluation of SMFCs applicability to the bioremediation of marine sediments contaminated by phenanthrene. The anodic compartments of two SMFCs were batch-fed with a slurry (5% w/w real dry sediment in artificial seawater) contaminated with phenanthrene (150 mg kg_{dw}^{-1}), while the corresponding cathodic compartments were filled with 0.5 M $K_3(Fe(CN)_6)$. Both anode and cathode consisted of a piece of conductive graphite felt (4 cm^2). A cation-permeable membrane was used to separate the compartments. SMFC-1 was operated in static conditions, whereas mechanical stirring was applied in SMFC-2, in order to test their effectiveness in accelerating Phe degradation, due to the putative capability of electroactive microorganisms to promote removal at the anodes.

4.2.1.2 Materials and methods

Marine sediments. Sediments were collected from the port of Cagliari (Sardinia, Italy), sieved in order to eliminate particles greater than 2 mm in diameter, and stored at 4°C. The main sediment characteristics are reported in Table 4.1.

SMFC configuration. Both SMFCs consisted of a modified 500 mL Duran-glass bottle (Figure 4.4 A). The bottle cap was modified to accommodate the tubular cathode compartment, a PVC tube (thickness, 1 mm; length, 10 cm; diameter, 3 cm), sealed with an o-ring and lid. A cation exchange membrane (CMI 7000S, Membrane International Inc., USA) was glued at the bottom of the PVC tube to separate the cathode and anode compartments. Both anode and cathode consisted of a conductive graphite felt (thickness, 0.5 cm; area, 4 cm^2; Figure 4.4 B, C); titanium wires (diameter, 0.75 mm) were used to connect both anode and cathode to a voltmeter and data acquisition system (PicoLog 1012, Pico Technology; Figure 4.4 D). The anodic chamber was equipped with a saturated calomel reference electrode (SCE, 0.2412 V *vs* the standard hydrogen electrode, Amel, 303/SCG/12). All potentials herein are reported with respect to this reference electrode. The cells were operated at ambient temperature (20°C).

Table 4.1 *Main characteristics of sediments from the port of Cagliari.*

Parameter	Value
Silt – Clay [%]	65
Sand [%]	35
Total organic carbon (TOC) [% w/w]	3.3
Total extractable carbon (TEC) [% w/w]	1.3
Humic and fulvic acids (HAs+FAs) [% w/w]	0.4
Total solids (TS) [% w/w]	55
Volatile solids (VS) [% w/w]	8.3

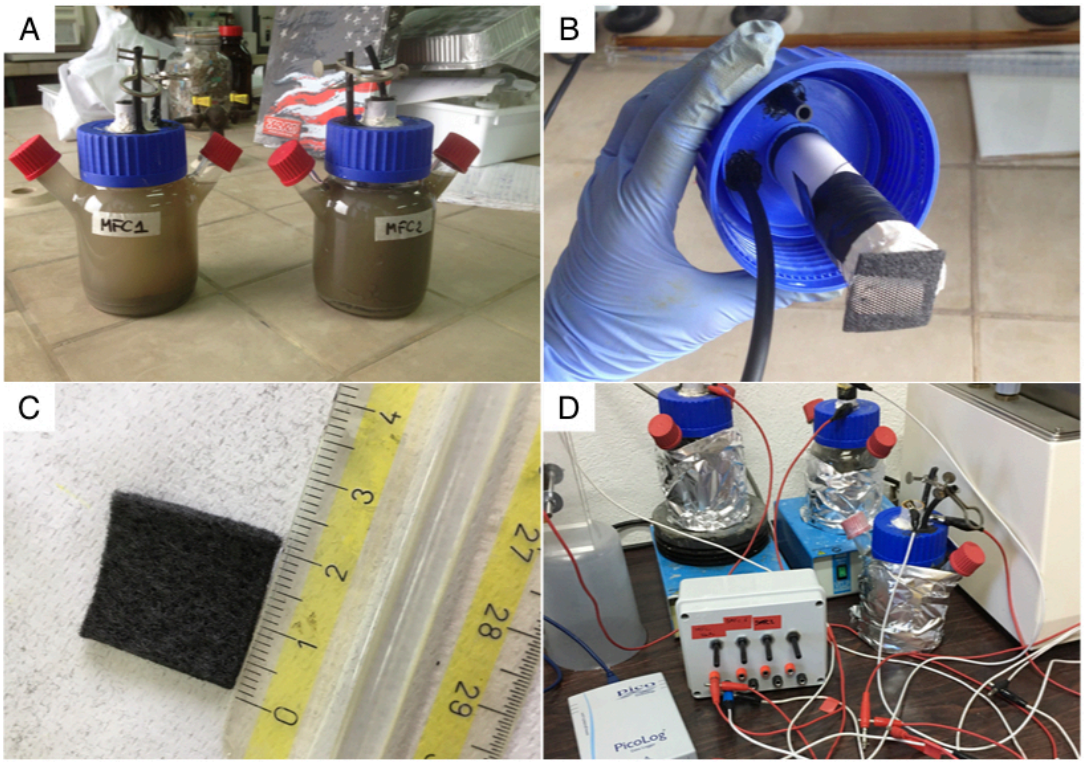

Figure 4.4 *A) SMFCs used in the study; B) Cathodic compartment (PVC tube) inserted in the bottle cap. The anode was placed at the bottom, while the cathode is placed inside the PVC tube; C) 4 cm² graphite felt anode; D) SMFCs connected to the data acquisition system.*

Phenanthrene degradation assessment. Table 4.2 represents a summary of the experimental Phases described herein. SMFC-1 was operated in static conditions (anode suspended in the sediment supernatant), whereas mechanical stirring was applied in SMFC-2.

Both SMFCs were operated in batch mode. In Phase 1 (20 days), they were started-up with phenanthrene spiked sediments (50 mg_{Phe} kg_{dw}^{-1}, 5% w/w real dry sediment in artificial seawater, 650 mL slurry volume; seawater was obtained by adding 35 g L^{-1} Sea Salts to distilled water, Sigma-Aldrich) and inoculated with 30 mL of slurry drawn from a lab-scale SS-SBR treating PAHs at DICAAR laboratories, which was working on the same sediment. The anolyte

solution had the following composition: K_2HPO_4, 0.35 g L^{-1}; KH_2PO_4, 0.27 g L^{-1}; NH_4Cl, 0.1 g L^{-1}; $MgSO_4 \cdot 7H_2O$, 0.1 g L^{-1}. Trace elements (1 mL L^{-1}) were prepared according to Rabaey *et al.* (2005b). In order to sustain the development of an electrochemically active biomass, 0.41 g L^{-1} of readily degradable sodium acetate (5 mM) were initially fed to the anodic compartment. The composition of the catholyte solution was: $Na_2HPO_4 \cdot 12H_2O$, 7.56 g L^{-1}; KH_2PO_4, 1.5 g L^{-1}; $K_3(Fe(CN)_6)$, 164.8 g L^{-1} (0.5 M). The external resistance was initially set to 400 Ω, and progressively reduced to 200 Ω using a variable potentiometer.

In the second run (Phase 2), half of the slurry in both SMFCs was replaced by fresh spiked sediment (150 mg_{Phe} kg_{dw}^{-1}, 5% w/w real dry sediment in artificial seawater, 650 mL slurry volume), and sodium acetate was not added to the anolyte solution. The external resistance was set again at 400 Ω, and gradually reduced to 250 Ω. Phenanthrene removal was monitored for 20 days. In order to better evaluate the extent of Phe degradation in SMFC-1 (since, after 20 days, the removal resulted lower than in SMFC-2), as well as to assess biocatalytic activity in both SMFC-1 and -2, Phase 2 was prolonged until day 90.

A Control test (150 mg_{Phe} kg_{dw}^{-1}, 5% w/w real dry sediment in artificial seawater) was performed under open circuit in both conditions, static and well-mixed, in order to quantify the extent of Phe removal not associated to the bioelectrochemical process. In addition, an abiotic control was run under open circuit conditions using a sediment previously heated at 560°C for 24 hours and spiked with phenanthrene (150 mg_{Phe} kg_{dw}^{-1}, 5% w/w real dry sediment in artificial seawater), in order to evaluate its adsorption on uncolonized graphite felt electrode.

Table 4.2 *Description of the experimental Phases.*

Experimental Phase	Duration [d]	External resistance [Ω]	Contamination [mg_{Phe} kg_{dw}^{-1}]	Objective
Phase 1	20	From 400 to 200	50	Start-up*
Phase 2	20**	From 400 to 250	150	Quantifying Phe removal associated to the bioelectrochemical process
Control test	20	- (open circuit)	150	Quantifying Phe removal not associated to the bioelectrochemical process
Abiotic control	20	- (open circuit)	150***	Evaluating the adsorption on uncolonized electrode

*Readily degradable sodium acetate was added to promote biofilm formation; **Prolonged until day 90 to better evaluate Phe-degradation and to assess biocatalytic activity; ***sediment previously heated for 24 hours at 560°C.

Analytical methods. For phenanthrene quantification, samples were periodically collected from the anode compartment, and centrifuged at 4,000 rpm for 15 minutes; the solid phase was dried by adding diatomaceous earth (1:1 w/w) and exposed to accelerated solvent extraction (Dionex, ASE 150); the liquid extracts were stored in sealed vials and analyzed by GC-MS (Agilent

6890N, 5975C) equipped with an autosampler (Agilent, 7863B) and a capillary column (Agilent, VF-5ms, 30 m x 0.25 mm x 0.25 µm). Total organic carbon (TOC, % w/w), total extractable carbon (TEC, % w/w), humic and fulvic acids (HAs+FAs, % w/w) were determined according to published protocols (ANPA, 2001). Biocatalytic activity was assessed by linear sweep voltammetries (LSVs) using an Autolab potentiostat-galvanostat (PGSTAT302N), whereby the cell voltage was ramped linearly between the open circuit voltages (OCVs) and 0 (recorded over a period of 5.4 min for SMFC-1 and 6 min for SMFC-2), at the scan rate of 2 mV s^{-1}. Current I (A) was calculated using the Ohm's law:

Equation 4.1 $$V=R\cdot I$$

where R is the external resistance (Ω) and V is the measured voltage (V). Power P (W) was calculated as:

Equation 4.2 $$P=V\cdot I$$

Current density (A m^{-2}) and power density (W m^{-2}) were calculated dividing I and P by the nominal anodic surface area (4 cm^2), in order to allow comparison between different systems.

Total solids (TS, % w/w) and volatile solids (VS, % w/w) were determined according to published protocols (IRSA-CNR, 2005).

4.2.1.3 Results and discussion

Degradation of phenanthrene in SMFCs, voltage and current densities. The biodegradation of phenanthrene was monitored for 20 days during each Phase. At the end of Phase 1 (start-up), phenanthrene removal efficiency in SMFC-1 and -2 was high (89.6% and 96.8%, respectively), indicating the successful development and maintenance of phenanthrene degrading biomass in the system. Although SMFC-2 showed higher phenanthrene removal efficiencies, the degradation was initially slower than in SMFC-1 (Figure 4.5): such result suggests a contradictory role of mechanical shear stress, which might have hindered the attachment and formation of the electrochemically active biofilm on the anode in the early start-up, but then promoted phenanthrene degradation rates as soon as biomass colonized the anode.

In Phase 2, readily degradable sodium acetate was not added to the anolyte, and phenanthrene concentration was raised to 150 mg_{Phe} kg_{dw}^{-1}. Despite the lower phenanthrene removal efficiencies observed at the end of Phase 2 (61% and 88.5% in SMFC-1 and -2, respectively), the results suggest that phenanthrene degradation can be carried out even without the supply of

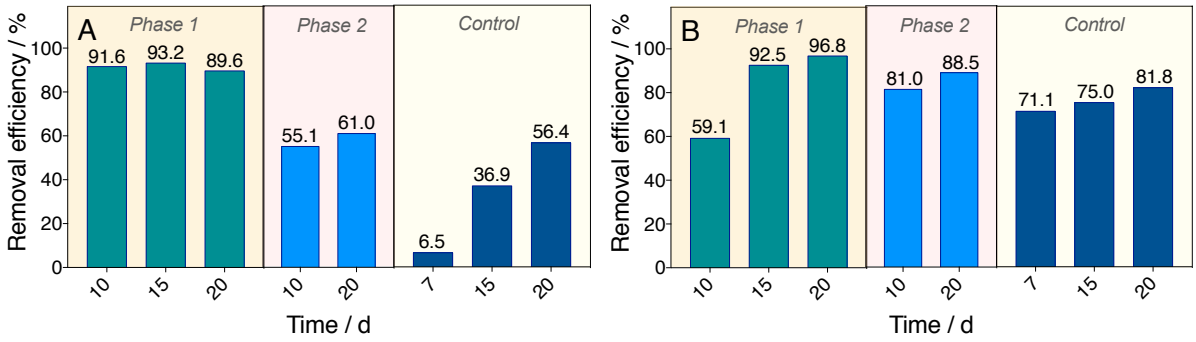

Figure 4.5 *Removal efficiencies of Phe in A) SMFC-1 and B) SMFC-2, during each working cycle, compared to the Control test with open circuit.*

an external carbon source, thus reducing the operating costs significantly. Moreover, phenanthrene degradation in SMFC-2 was higher than in SMFC-1 (Figure 4.5), confirming that mechanical stirring accelerates phenanthrene removal if a well active biofilm is attached to the anode, by promoting the contact between biomass and substrate.

Such conclusion was supported by the profiles of current density *vs* time, reported in Figure 4.6, measured in SMFC-1 and -2 during the second part of Phase 2, with an external resistance of 350 and 250 Ω (in the first part of Phase 2 the external resistance was 400 Ω, data not shown).

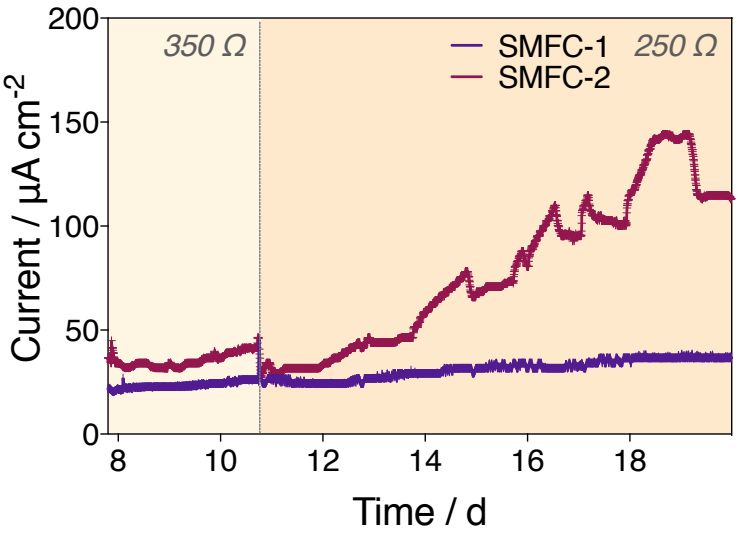

Figure 4.6 *SMFC-1 and -2 current density profiles during Phase 2, with an external resistance of 350 and 250 Ω.*

As to SMFC-1, current density was fairly stable, reaching a maximum of 38.5 µA cm^{-2} and a net voltage production of 38.5 mV, under an external resistance of 250 Ω. Such values are higher than those reported in previous studies (Yan *et al*. 2012, Sherafatmand and Ng, 2015), in not stirred conditions. A completely different electrical behavior was observed in SMFC-2, compared with SMFC-1, as the external resistance was reduced to 250 Ω: current density

increased up to 144.2 μA cm^{-2} (day 19) (the corresponding net voltage production was 144.2 mV).

The current densities achieved in this study are certainly lower than those obtained when more readily biodegradable substrates were used (Liu and Logan, 2004): assuming a graphite felt specific surface of 220 cm^{-1} (González-García *et al.*, 1999) and considering that the anodic surface was 4 cm^2 and that the electrode was 0.5 cm thick, the surface available for the bioelectrochemical process would have been 440 cm^2; therefore, the actual current densities associated to this anodic surface would have been 0.35 and 1.31 μA cm^{-2} for SMFC-1 and -2, respectively. However, the constant presence of an electrical activity in both SMFCs suggested that an electroactive biomass had developed at the anode. Moreover, the improvement of SMFC-2 electrical performance was coherent with the acceleration in phenanthrene degradation observed during Phase 2, suggesting that electroactive biomass played an important role in its removal.

In order to evaluate the extent of achievable phenanthrene degradation in SMFC-1, the duration of Phase 2 was extended: as expected, phenanthrene degradation proceeded slowly, and complete removal was achieved on day 60, in agreement with other studies reported in literature (Yan *et al.*, 2012; Sherafatmand and Ng, 2015; Hamdan *et al.*, 2017).

To better estimate the role of bioelectrochemical removal, a Control test was performed under open circuit conditions (*i.e.*, without an electrical load applied between anode and cathode) and using the same Phe concentration as in Phase 2. After 20 days of operation, the Phe removal efficiency was 56.4% and 81.8% in SMFC-1 and -2, respectively, that is lower than in the closed circuit systems (Figure 4.5). Confirming previous considerations, phenanthrene degradation was remarkably slower in SMFC-1 (static conditions). Furthermore, phenanthrene removal under anaerobic conditions (*i.e.*, excluding the bioelectrochemical effect) was slower than in Phase 2, although the removal efficiency achieved after 20 days was similar. Such results are in agreement with those reported by Yan *et al.* (2012).

The degradation of PAHs observed under open circuit conditions was probably related to the presence of alternative electron acceptors, or to the activity of anaerobic microbial populations diverse than biofilm attached to the anode, as previously demonstrated by Hamdan *et al.* (2017) and Sherafatmand and Ng (2015). The same interferences in Phe degradation should be taken into account in closed circuit conditions, requiring further investigations in order to assess the actual extent of the bioelectrochemical process.

The additional abiotic control showed no removal of phenanthrene in the absence of microbial communities, nor the adsorption on uncolonized graphite felt.

Biocatalytic activity assessment. In order to characterize the microbial electrocatalysis, LSVs were recorded considering the whole SMFCs. Results of polarization and power curves generated by the SMFCs are presented in Figure 4.7. Maximum power densities and optimal current densities achieved in SMFC-1 and -2 were 9.2 and 38.4 µW cm^{-2}, and 26.2 and 142.7 µA cm^{-2}, respectively. Maximum OCVs were 0.62 and 0.69 V; anodic potential measured at OCV were -0.31 and -0.47 V, respectively. Anodic potentials showed an increased catalysis in SMFC-2, in accordance with higher removal efficiencies obtained in that cell. At the same time, SMFC-2 polarization curve shape showed higher activation losses than SMFC-1: higher overpotentials were required to start the electron transfer in SMFC-2. As expected, the internal resistance *(i.e.*, the slope of the polarization curves in the "ohmic polarization region", where voltage decreases linearly with current) of SMFC-2 was lower than SMFC-1 (0.5 and 3.1 kΩ, respectively), confirming the better overall performances under stirred conditions, but the presence of mass transfer limitations under this range of currents in both cases.

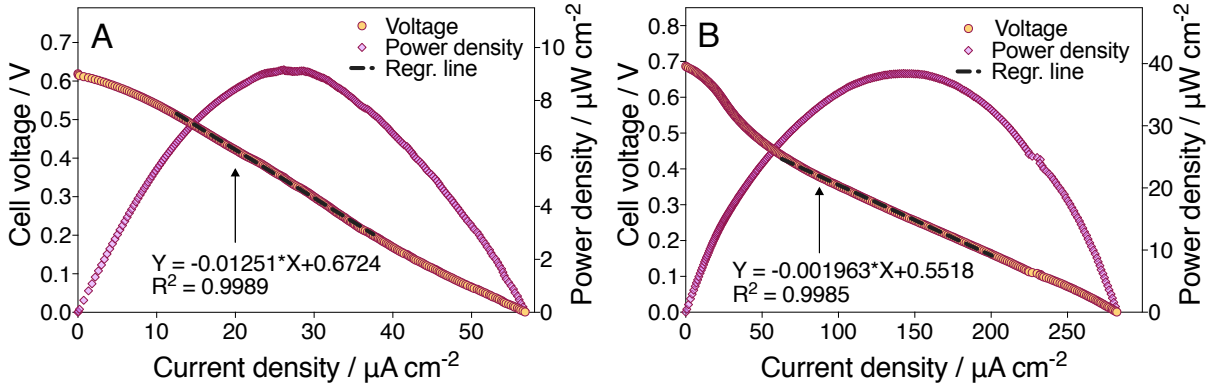

Figure 4.7 *Polarization curves (orange) and power curves (violet) of A) SMFC-1 and B) SMFC-2. Reported straight linear equations indicate the slope of polarization curves.*

4.2.1.4 Conclusions

The results achieved in this preliminary study suggest that SMFCs can support the development of a bio-electroactive, Phe-degrading biofilm at the anode, accelerating Phe degradation: good phenanthrene removals were achieved in both experiments after 20 days of operation. The observed electrical performances were in line with the internal resistances of the system and with the complexity of the substrate that was treated. The peculiar geometrical configuration of these SMFCs makes them particularly suitable for their integration in *on-site* slurry bioreactors.

Biocatalytic activity was higher in SMFC-2 than -1: mechanical stirring (SMFC-2) was proved to hinder the attachment and development of an electrochemically active biofilm on the anode in the early start-up, and to enhance phenanthrene degradation rates as soon as biomass colonizes the anode.

With such premises, the experiments confirmed that the use of electrodes as electron sink in bioelectrochemical remediation of contaminated slurries might represent a cost-effective alternative to conventional treatments requiring energy-intensive aeration. Moreover, tests suggested the necessity to evaluate the possible interference of alternative electron acceptors (*e.g.*, sulphate) with the bioelectrochemical process and the need for overcoming typical drawbacks of SMFCs used for bioremediation (*e.g.*, testing new static SMFCs configurations, in order to assess process performance for *in situ* applications).

Such results were already published as proceedings of the 15th International Conference of Environmental Science and Technology (Milia *et al.*, 2017b).

4.2.2 Evaluation of SMFC applicability to bioremediate marine sediments contaminated by PAHs in the presence of an initial and temporary sulphate reduction inhibition

4.2.2.1 Introduction

This experimental part reports a supplement to tests described in section 4.2.1.
Since this thesis work involves the treatment of PAHs-contaminated marine sediments, and sulphate can be abundant in seawater, it appeared important to consider its possible influence as terminal electron acceptor in the process: sulphate reducing bacteria have been previously found to be responsible of PAHs degradation in marine environments (Rothermich *et al.,* 2002; Townsend *et al.*, 2003) and according to Laufer *et al.* (2016) this ion is the main terminal electron acceptor in marine sediments rich in it. Moreover, several studies documented a decrease of PAHs degradation after SRB inhibition by molybdate (Coates *et al.*, 1996; Zhang and Young, 1997; Townsend *et al.*, 2003; Hamdan *et al.*, 2017). In particular, Hamdan *et al.* (2017) found that electrical behavior and biomass composition on the anode surface changed in the presence of an initial and temporary inhibition of SRB activity (which was recovered during the experiment). Moreover, PAHs removal was similar with and without inhibition. Within this framework, in order to evaluate how temporary SRB inhibition could affect Phe removal and if the use of sulphate as terminal electron acceptor could interfere with the bioelectrochemical process, two SMFCs (batch-fed with a slurry composed by 5% w/w real dry sediment in artificial seawater and contaminated with 50 mg kg_{dw}^{-1} of phenanthrene), namely SMFC-a and SMFC-b, were operated respectively without and with SRB inhibition (addition of 0.3 mM of molybdate at system start-up). SMFC-a run *vs* an open circuit Control test. System configuration was the same adopted in the previous study (see section 4.2.1.2) and well mixed conditions were applied.

4.2.2.2 Materials and methods

Marine sediments. Sediments were the same used in the previous experiment (see section 4.2.1.2).

SMFC configuration. For the description of SMFC configuration see section 4.2.1.2. Here, TS content was 39.1% (values changed according to the manual wet sieving).

Phenanthrene degradation assessment. Table 4.3 represents a summary of the experimental work described herein. Both, SMFC-a and -b were operated under mechanical stirring conditions and in batch mode.

In the closed circuit test, SMFCs were started-up with phenanthrene spiked sediments (50 mg_{Phe} kg_{dw}^{-1}, 5% w/w real dry sediment in artificial seawater, 650 mL slurry volume) and inoculated with 30 mL of slurry drawn from a lab-scale SS-SBR treating PAHs at DICAAR laboratories, which was working on the same sediment. The artificial seawater had the following composition, readapted from Kester *et al.* (1967): NaCl, 23.926 g L^{-1}; Na_2SO_4, 4.008 g L^{-1}; KCl, 0.677 g L^{-1}; $NaHCO_3$, 0.196 g L^{-1}; KBr, 0.098 g L^{-1}; H_3BO_3, 0.026 g L^{-1}; NaF, 0.003 g L^{-1}). The anolyte solution had the same composition reported in section 4.2.1.2; 0.42 g L^{-1} ammonium heptamolybdate tetrahydrate (*i.e.*, 0.3 mM of molybdate, equivalent to the 1% of the sulphate expected in the SMFC) known inhibitor of sulphate reduction (Nemati *et al.*, 2001), were added to SMFC-b, in order to test the effect of an initial inhibition of sulphate reduction activity; previously, de Jesus *et al.* (2015) showed that the same ratio of molybdate *vs* sulphate guaranteed the inhibition of SRB activity for 168 hours. In order to sustain the development of an electrochemically active biomass, 0.41 g L^{-1} of readily degradable sodium acetate (5 mM) were fed to the anodic compartment initially and after 10 days (day 9) of operation. The composition of the catholyte solution was the same described in section 4.2.1.2. The external resistance was initially set to 400 Ω, and progressively reduced to 350 Ω using a variable potentiometer. Phenanthrene removal was monitored for 20 days.

A Control test (50 mg_{Phe} kg_{dw}^{-1}, 5% w/w real dry sediment in artificial seawater) was performed under open circuit conditions without SRB inhibition in order to quantify the extent of Phe removal not associated to the bioelectrochemical process, and putatively associated to sulphate reduction. Control test was performed under mechanical stirring for 20 days.

Analytical methods. For phenanthrene determination, see section 4.2.1.2. Sulphates were extracted from sediments according to published protocol (UNI EN 15105, 2011); the concentration of SO_4^{2-} (mg L^{-1}) was determined on filtered samples (0.45 μm) by ion-chromatography, using a DIONEX chromatograph (mod. ICS -90) equipped with an Ion-PAC AS14A-5 μm column (DIONEX). All the analysis were performed in duplicate. Biocatalytic activity was assessed by LSVs and CVs using an Autolab potentiostat-galvanostat (PGSTAT302N): LSVs were performed ramping the cell voltage linearly between the OCV and 0 (recorded over a period of 1.5 hours for SMFC-a and 2.1 hours for SMFC-b), at the scan rate of 0.1 mV s^{-1}; CVs were performed at the scan rate of 1 mV s^{-1} and the anode potential was

varied from -0.8 V to 0 V vs SCE. Current density and power density were calculated as described in section 4.2.1.2.

Table 4.3 *Description of each test.*

Tests	Duration [d]	External resistance [Ω]	Contamination [mg_{Phe} kg_{dw}^{-1}]	Objective
Closed circuit	20	From 400 to 300	50	Start-up and assess Phe removal associated to the bioelectrochemical process with and without SRB inhibition*
Control test	20	- (open circuit)	50	Quantifying Phe removal not associated to the bioelectrochemical process

*Readily degradable sodium acetate was added to promote biofilm formation at day 0 and after 10 days (day 9).

4.2.2.3 Results and discussion

Degradation of phenanthrene in SMFCs, voltage and current densities. The biodegradation of phenanthrene was regularly monitored for 20 days in each test.

Closed circuit tests were dedicated to the start-up of the systems and to the quantification of Phe removal associated to the bioelectrochemical process, with and without initial SRB inhibition (Table 4.3). In fact, results of previous assessments indicated high removal efficiencies of Phe in the open circuit Control test, which, according to the study of Hamdan *et al.* (2017), might be associated to the use of sulphates as terminal electron acceptors; moreover, the same option could not be excluded in the closed circuit tests (see section 4.2.1.3). In this study, phenanthrene removal efficiency was measured along the working phase for SMFC-a and -b, and values achieved at the end of the phase were compared with the removal efficiency of the open circuit Control test measured after 20 days, as shown in Figure 4.8. In addition, sediments were characterized for the presence of sulphates at day 0 and 19, as summarized in Table 4.4.

High Phe removal efficiencies were achieved after 3 days (72.5 and 70% respectively, for SMFC-a and -b), as shown in Figure 4.8 A, therefore suggesting that the presence of the anode, together with the addition of readily biodegradable sodium acetate, stimulated the prompt development of Phe-degrading bacteria. After 3 days passed, removal efficiencies slightly increased until the end of the phase, and reached, at day 19 (*i.e.*, after 20 days), values as high as 91.5% and 95.7% in SMFC-a and -b, respectively. Therefore, the successful maintenance of

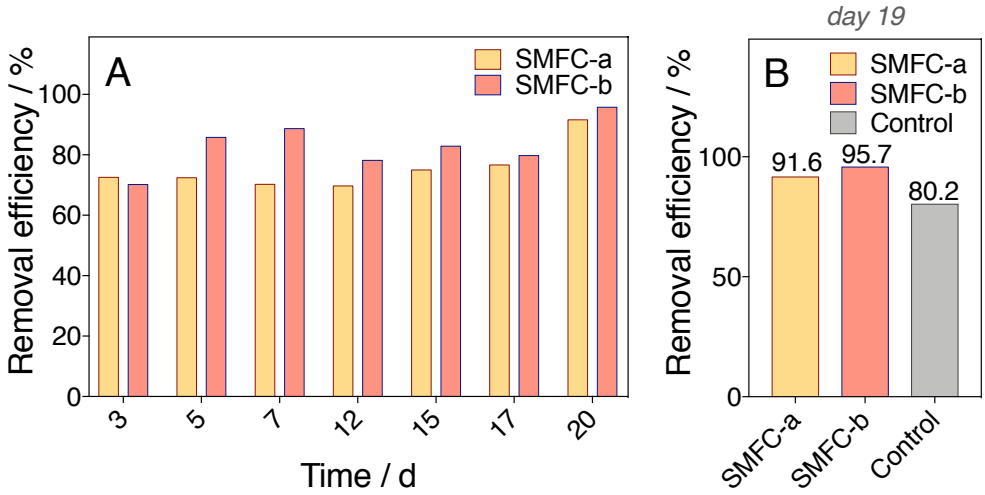

Figure 4.8 *A) Removal efficiencies of Phe in SMFC-a and -b, during the closed circuit test; B) Removal efficiencies of Phe in SMFC-a and -b, compared to the open circuit Control test, at the end of the same phase (after 20 days).*

a phenanthrene degrading biomass in the system was confirmed. Such good removals were in accordance with results obtained under mechanical stirring in the previous experiment (see section 4.2.1.3).

As expected, the addition of molybdate influenced sulphate concentration: sulphate consumption was, in fact, higher in SMFC-a than SMFC-b (44 mg g_{dw}^{-1} *vs* 36 mg g_{dw}^{-1}, respectively); consumption measured in SMFC-b can be ascribed to the only temporary effect of molybdate on inhibition (Predicala *et al.*, 2008, de Jesus *et al.*, 2015, Hamdan *et al.*, 2017). However, despite the differences in sulphates consumption, the inhibition lead to quite similar Phe-degradation trends and removal efficiencies in both SMFCs, therefore indicating that the initial inhibition did not influence significantly Phe-removal under closed circuit conditions. The use of sulphate as terminal electron acceptor is clear in the open circuit Control test. Phe-removal after 20 days was, in fact, high and removal efficiencies reached 80.2% (Figure 4.8); correspondingly, sulphate consumption was higher than consumption measured in SMFC-a and SMFC-b (61 mg g_{dw}^{-1}, Table 4.4).

Table 4.4 *Sulphate consumption measured in this experimental work, recorded for each test.*

Test	Sulphate (day 0) [mg g_{dw}^{-1}]	Sulphate (day 19) [mg g_{dw}^{-1}]	Sulphate consumption [mg g_{dw}^{-1}]
SMFC-a	62	18	44
SMFC-b	63	27	36
Control test	68	7	61

Effects of SRB inhibition were more evident comparing the profiles of current density *vs* time measured in both SMFC-a and -b (Figure 4.9).

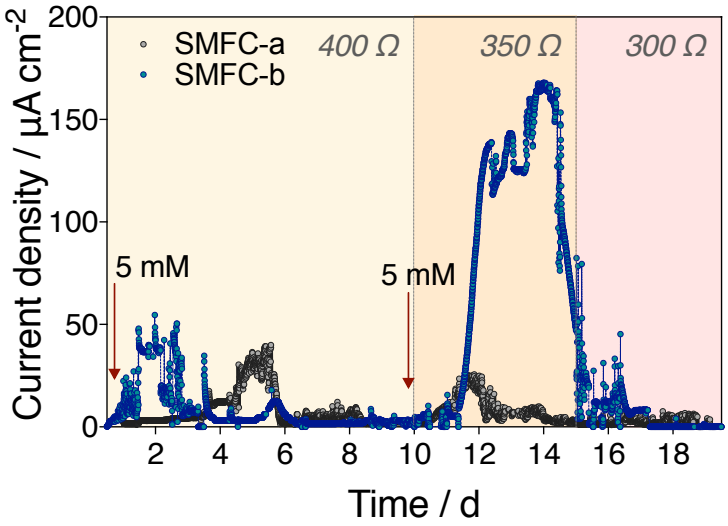

Figure 4.9 *SMFC-a and -b current density profiles during the closed circuit test, with an external resistance of 400, 350 and 300 Ω.*

As for SMFC-a, current density reached the highest value after 4 days: the maximum current density was about 40 µA cm^{-2} (net voltage production of 64 mV) under an external resistance of 400 Ω. This peak in the current production corresponded to the high consumption of Phe at the beginning of the experimental phase. A second lower peak corresponded to the second addition of sodium acetate (day 9); at the end of the phase, current density reached 0 µA cm^{-2}, indicating the complete consumption of the sodium acetate. The highest current output was achieved in SMFC-b: here, current density reached the maximum of 165 µA cm^{-2} (net voltage production of 230 mV) under an external load of 350 Ω, in the second half of the phase, after the second sodium acetate addition (day 9). The maximum current output achieved in SMFC-b was more than four time higher than the maximum value reached in SMFC-a, thereby indicating that more electrons reached the anode when SRB were inhibited: these results suggested a role of sulphate reducing bacteria in Phe degradation, hence a possible interference with the bioelectrochemical process. Another possible interference with the electrical current production, that is consequent to sulphate reduction, is the possible oxidation of sulphide (end product of this process) to elemental sulphur: sulphur, obtained either biotically (Rabaey *et al.*, 2006) or abiotically (Dutta *et al.*, 2008), is an insulative product whose precipitates over the anodic surface can possibly deactivate the electrode (Dutta *et al.*, 2008). Under the hypothesis that the total sulphate consumed in 20 days by SRB (Table 4.4) was reduced completely to hydrogen sulphide, and that the overall H_2S went to elemental sulfur, the amount of S generated

would have been 477 mg in SMFC-1a and 390 mg in SMFC-2a. Considering, for example, the sulphur produced by SMFC-1a (*i.e.*, the highest possible S production achieved in this study), and that S density is 1,960 kg m^{-3}, this quantity would have corresponded to the production of a sulphur volume of 0.26 cm^3. Assuming the same graphite felt specific surface hypothesized above (see section 4.2.1.3), the total anodic surface available for sulphur deposition would have been 440 cm^2. In the study of Dutta *et al.* (2009), sulphur deposits were about 10 µm thick; using the same value in the current study, the surface occupied by deposits would have been about 26 cm^2, one order of magnitude lower than the hypothesized specific surface of the electrode. Therefore, even if the hypothesis of sulphide oxidation to elemental sulphur was valid, a large portion of the anodic surface would have been still available for the bioelectrochemical process, hence for current production.

The discussions about current density reported in the previous study are still valid here (see section 4.2.1.3): the constant presence of an electrical activity in both SMFCs suggested that an electroactive biomass had developed at the anode; results were then corroborated by tests of cyclic voltammetry, reported herein. Moreover, the improvement of SMFC-b electrical performance was coherent with a different use of the anode in partially inhibited and not inhibited sulphate reducing conditions.

Biocatalytic activity assessment. In order to characterize the microbial electrocatalysis, linear sweep voltammetries of the SMFCs (Figure 4.10) were recorded. The voltammetric behavior of the biofilms developed over the anodic surfaces was monitored at day 0 (turnover conditions) and day 19 (non-turnover conditions, in acetate depleted medium), as displayed in Figure 4.11.

Maximum power densities and optimal current densities achieved in SMFC-a and -b were about 0.5 and 3.2 µW cm^{-2}, and 4.2 and 25 µA cm^{-2}, respectively. Maximum OCVs were 0.52 and 0.73 V; anodic potentials measured at OCV were -0.34 and -0.44 V, respectively. Anodic potentials showed an increased catalysis associated with SMFC-b, in accordance with higher electrical activity obtained in that cell (Figure 4.9). At the same time, SMFC-b polarization curve shape showed higher activation losses than SMFC-a: higher overpotentials were required to start the electron transfer in SMFC-b. As expected from profiles of current density *vs* time (Figure 4.9), the internal resistance of SMFC-b was lower than SMFC-a (1.3 and 6.7 kΩ, respectively), and confirmed the better overall performances in terms of current output when a

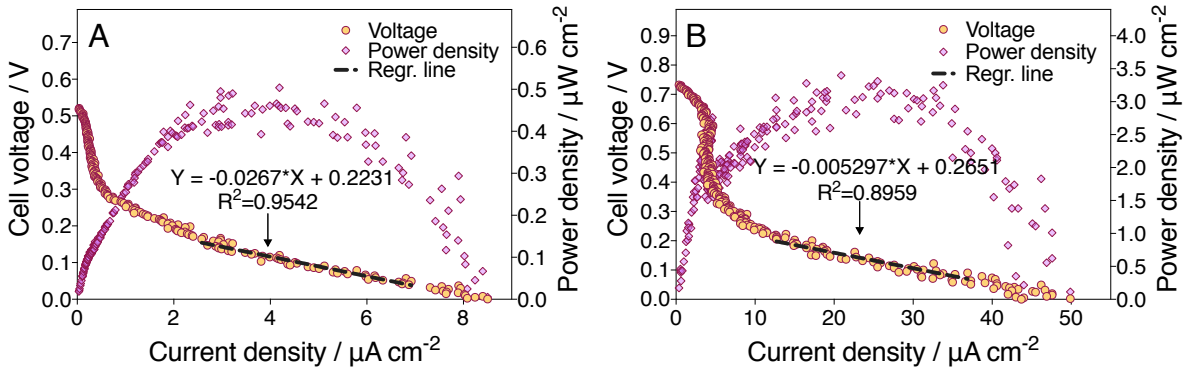

Figure 4.10 *Polarization curves (orange) and power curves (violet) of A) SMFC-a and B) SMFC-b. Reported straight linear equations indicate the slope of polarization curves.*

specific inhibitor of sulphate reduction was added, but also indicated the presence of mass transfer limitations under this range of currents, in both cases.

Observing representative voltammograms of SMFC-a (Figure 4.11 A) and -b (Figure 4.11 C) recorded in the closed circuit test at day 19, shapes suggested, in both cases, the presence of *Geobacter* spp. in the anodic biofilm, which have grown after addition of sodium acetate; in fact, most of the microorganisms within *Geobacteraceae* were isolated from anoxic sedimentary environments and are able to form biofilms (Holmes *et al*. 2004, Greene *et al*. 2009). Moreover, higher biocatalysis is evident in Figure 4.11 C, supporting the higher current production achieved in SMFC-b (Figure 4.9). This different behaviour might be associated to a differentiation of the microbial community composition developed on the anodic surface, as reported in the previous study of Hamdan *et al.* (2017): in this study, microbial community analysis of microorganisms developed on the anodic surface, both in closed (with and without partial SRB inhibition) and open circuit tests, revealed that a similar microbial community composition was present on the anode of the open circuit Control and on the anode of the closed circuit SMFC without SRB inhibition; as expected, a different community composition was found on the anodic surface of closed circuit SMFC whit temporary SRB inhibition; nevertheless, the closed circuit conditions enhanced biodegradation process in both cases, with and without partial SRB inhibition.

It is worth noting that turnover cyclic voltammetry recorded at day 0 in SMFC-b (Figure 4.11 B) indicated deposition of molybdenum oxides deriving from ammonium molybdate on the anodic surface, in the range of potentials applied (Petrova and Bojinov, 2011). However, the length of cyclic voltammetry recording, and the range of currents produced during this test corresponded to the consumption of a very low amount of the ammonium molybdate added to

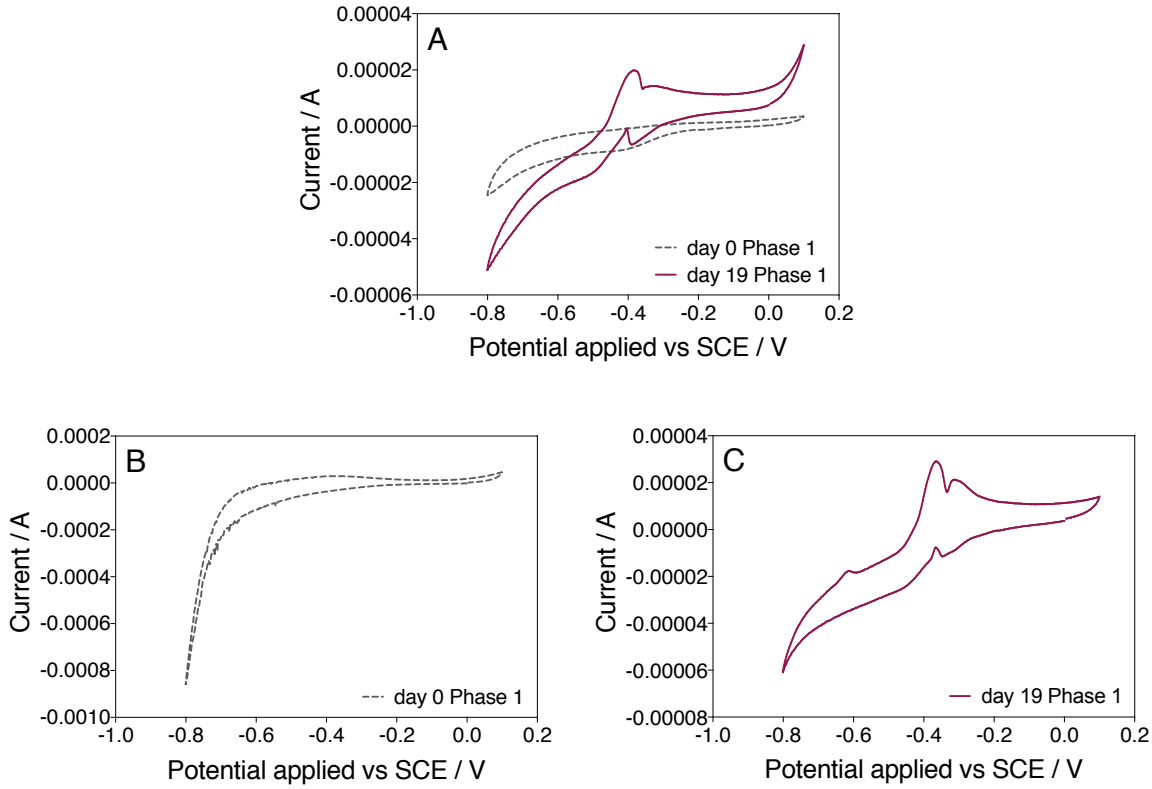

Figure 4.11 *Representative voltammograms recorded at 1 mV s^{-1} scan rate of A) SMFC-a: turnover CV, day 0 (grey dotted line), and non-turnover CV, day 19 (plum straight line); B) SMFC-b: turnover CV, day 0 (grey dotted line); C) SMFC-b: non-turnover CV, day 19 (plum straight line).*

the anolyte, which remained therefore available for SRB inhibition. This phenomenon was not observed in the cyclic voltammetry recorded in the same SMFC at day 19 (Figure 4.11 C), thereby confirming that molybdate had been fully metabolized by the biomass.

In general, voltammograms, recorded at the end of each test and shown in Figure 4.11, indicated the development of a biofilm on the anodic surface with an established electricity generation ability.

4.2.2.4 Conclusions

Results achieved in this study suggested that sulphate was probably used as terminal electron acceptor when Phe was oxidised in anaerobic conditions, in the absence of SRB inhibition; this hypothesis is well-related to the good removal efficiencies achieved in the open circuit Control test in this experiment and in the previous one (section 4.2.1). Profiles of current density *vs* time, LSVs and CVs recorded at closed circuit, confirmed that biomass growing on the anodic surface used differently the anode if ammonium molybdate was added as specific inhibitor of sulphate reduction: when the activity of SRB was temporary inhibited (SMFC-a), the system reached higher current densities and showed higher biocatalysis than in not inhibited conditions.

However, the addition of ammonium molybdate did not influence significantly Phe biodegradation: both, SMFC-a and SMFC-b, operated in closed circuit, respectively without and with SRB inhibition, achieved high removal efficiencies (which were only slightly higher in SMFC-b). These values were higher than values achieved in the open circuit Control, thereby indicating that the presence of the anode effectively promoted Phe removal, despite SRB inhibition. As observed in the previous study, current densities and power densities were low. However, the bioelectrochemical process promoted the effective bioremediation of sediments, which was the main goal of the experiment, and fastened degradation otherwise achieved in the open circuit Control.

4.2.3 Increase of electronic conductivity of porous soils and bioelectrochemical degradation capacity by reduction of graphene oxid

4.2.3.1 Introduction

Bioremediation relies on the microbial destruction of contaminants and is increasingly the chosen treatment even for contaminations by toxic organic compounds (see section 1.6). Conversely, the necessity to continuously supply electron acceptors (*e.g.*, oxygen) to promote the microbial metabolism usually translates into high operating costs. In this scenario, an alternative treatment solution could potentially be offered by microbial electrochemical technologies such as sediment bioelectrochemical systems, as extensively discussed in section 4.1 of the current Chapter. In these devices, electrodes (*e.g.*, graphitic material in the form of rods or felt) are used as inexhaustible sink of electrons to promote oxidation reactions, thereby overcoming the need for continuous supply of soluble electron acceptors. Nevertheless, current outputs in SBES are often hindered by the generally limited mass transport of contaminants towards the electrode surface, and by limited interfacial and long-range electron transfer kinetics, which altogether translate into a limited *radius of influence* of the bioelectrochemical treatment.

In contrast, the incorporation of conductive nanomaterials within soils and sediment particles may help improving the conductivity of porous soils and therefore resolve the drawbacks of traditional SBES configurations. Along these lines is the use of graphene, a two-dimensional carbon material characterized by an outstanding electric conductivity, excellent mechanical properties, high specific surface area, and biocompatibility. A previous study demonstrated that graphene produced by the biological reduction of graphene oxide, self-assembles with microbial cells to form thick biofilms with superior electrocatalytic properties due to the large packing of cells and the increased conductivity resulting from the inclusion of graphene within the biofilm structure (Virdis and Dennis, 2017). Here, under a similar rationale, synthetic porous soil was amended with graphene oxide and inoculated with an enriched culture of electroactive microorganisms. On the other hand, Hilder *et al.* (2011) demonstrated that GO suspensions can be conveniently electrochemically reduced to rGO by applying a fixed potential *vs* reference (see below). Therefore, in the current study, electrochemical reduction was investigated in parallel to biological reduction, by adopting the same set up (amending GO solution without adding electroactive microorganisms). Measurements of electric resistance were performed using 2-probe DC (*i-V*) method performed on the porous soils after reduction.

Since electrochemical reduction resulted in higher conductivities than biological reduction, and achieved reduction in a significantly shorter time length, GO-amended systems formed after electro-reduction were used to assess their bioelectrochemical degradation capacity: percolating[22] bioanodes were supplemented with an inoculum of electroactive microorganisms and metabolic electron donor acetate in order to test the hypothesis that a larger volume of soil could contribute to the catalytic current production in the GO-amended system.

4.2.3.2 Materials and methods

Electroactive microorganisms. Electroactive microorganisms were cultured in a sterile single-chambered bioelectrochemical system (parent BES) equipped with four carbon rods (short-circuited together) serving as working electrode (WE; Morgan AM&T, Australia), a piece of reticulated vitreous carbon (RVC) (dimension 1x1x2 cm, 45 pores per inch, Duocel, ERG Materials and Aerospace Corporation) serving as counter electrode (CE), and an Ag/AgCl reference electrode in 3 M KCl (MF-2052, Basi, USA, +0.210 V vs the standard hydrogen electrode, SHE). All potentials herein are reported with respect to Ag/AgCl reference electrode. The electrodes were immersed into 300 mL sterile anaerobic media (composition provided below) purged with pure nitrogen for at least 30 minutes to ensure anoxic conditions. The parent BES was inoculated with 10 mL of mixed liquor from a domestic activated sludge plant (Luggage Point WWTP, Brisbane, Australia). 40 mM of sodium acetate (CH_3COONa) was used as metabolic substrate. The working electrodes were poised at 0 V vs Ag/AgCl using a multichannel potentiostat (Potentiostat/Galvanostat VMP3, BioLogic Science Instruments, France). The growth of electroactive biofilms (*i.e.*, aggregates of electroactive microorganisms embedded in a matrix of extracellular polymeric substances) was monitored by measurement of bioelectrocatalytic current production (current *vs* time) resulting from the oxidation of the metabolic carbonaceous electron donor (*i.e.*, the acetate) and the resulting reduction of the extracellular electron acceptor (*i.e.*, the electrodes). Routinely, the media was completely replaced with fresh autoclaved media (usually once per week). When necessary, the rods serving as working electrodes were removed from the incubation cell and the biofilms were scraped off using a sterile blade, resuspended in phosphate buffer solution (PBS) and used as inoculum for the experiments requiring biocatalysts (see below).

[22] The word 'percolating' indicates the movement of electrons through a porous matrix.

Culturing media. The growth medium consisted of autoclaved reverse osmosis (RO) water containing: Na_2HPO_4 (6.0 g L^{-1}), KH_2PO_4 (3.0 g L^{-1}), NH_4Cl (0.1 g L^{-1}), NaCl (0.5 g L^{-1}), $MgSO_4 \cdot 7H_2O$ (0.1 g L^{-1}), $CaCl_2 \cdot 2H_2O$ (0.015 g L^{-1}), CH_3COONa (3.28 g L^{-1}, equivalent to 40 mM), trace elements solution (1 mL L^{-1}, composition in Lu *et al.,* 2006), and vitamin solution (1 mL L^{-1}, composition in Wolin *et al.,* 1963).

Model soil. Unless stated otherwise, quartz sand (sand, white quartz, 50-70 mesh, Sigma-Aldrich) was used in all experiments reported herein to simulate a porous aquifer.

Assessment of the effect of different GO concentrations on the electric conductivity in tests tubes. In order to directly investigate the effect of the presence of biologically- or electrochemically-reduced GO on the conductivity of the model soil, 30 mL of liquid containing GO suspensions (concentrations provided below) were poured into 70 mL sterile containers (Sarstedt AG & Co., Germany), modified to accommodate two carbon rods at a fixed distance between each other of approximately 2 cm (note that the exact distance between the rods varied depending on the manufacture of the rods), one titanium wire, and one reference electrode to allow for measurement of electric conductivity (see below). Each tube was partially filled with 30 g of the quartz sand, occupying approximately 20 mL of the tube. Rods portions 1.2 cm high were buried in the porous soil, while the upper portions, in contact with the electrolyte solution, were insulated by sticking the rods in a piece of tube (height of 3.6 cm, Norprene tubing, Masterflex®, Cole-Parmer), in order to avoid reduction effects in the supernatant. Different volumes of a concentrated GO suspension (4 g L^{-1}, water dispersion, Graphenea, Spain) were dosed to yield the following GO concentrations in the medium poured into test-tubes: 10, 50, 100, 200, 500, 1,000, 2,000 mg_{GO} L^{-1} (these values are equivalent in number to the GO load per kg of sand, *i.e.* per kg of dry weight). One additional SBES not amended with GO was used as a control. Unless otherwise indicated, tests were performed in triplicates. Prior to start with the reduction process, the ionic conductivity of the electrolyte and the pH were assessed for each test-tube, by using respectively a pH-meter (HANNA instruments, 2020-02 EDGE) and a conductivity meter (Hach, HQ30d flexi).

- *Biological GO reduction*. To test the effect of the presence of biologically-reduced GO on the conductivity of the soil, in addition to the GO solution, the test-tubes were filled with culturing media (composition provided above). Each test-tube was inoculated with 1 mL of inoculum scraped off four rods of the parent BES and resuspended in 15 mL PBS. The tubes were then sealed and incubated at 35° C for two weeks inside an

anaerobic chamber, to allow the complete reduction of GO into rGO (as proven by preliminary assessment in serum bottles, see below). Prior and after the incubation, measurements of conductivity were performed on the model soil according to the methods described below. Biological tubes set up is shown in Figure 4.12.

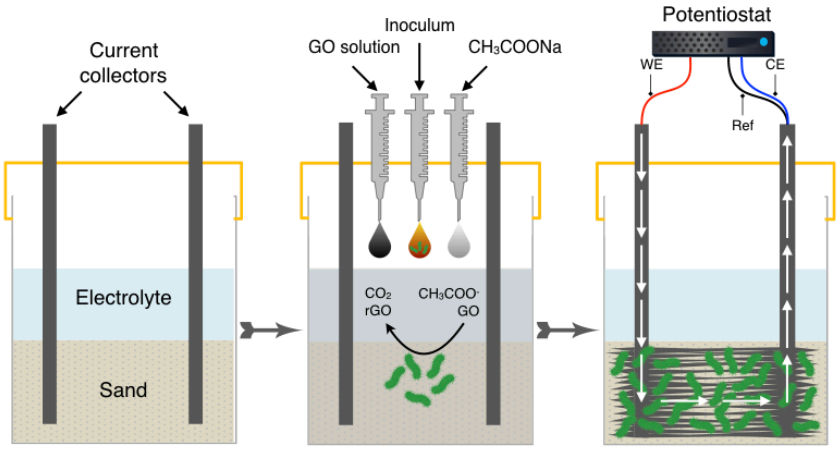

Figure 4.12 *Experimental set up of biological tubes. Tubes were filled with GO solution, culturing media and inoculated with inoculum from the parent BES; reduction of GO solution to rGO was biologically induced. Prior and after the incubation, measurements of conductivity were performed on the model soil, according to methods described in this section.*

- *Electrochemical GO reduction.* To test the effect of the presence of electrochemically-reduced GO on the conductivity of the model soils, the medium in the test-tubes was modified to contain, in addition to the GO suspensions, 5.8 g L^{-1} NaCl in RO water, according to Hilder *et al.* (2011). The tubes were then sealed, and the electrodes connected to the potentiostat. The two carbon rods were short-circuited and served as working electrode, while the titanium wire served as counter electrode. The electrochemical GO reduction was done according to Hilder *et al.* (2011). Briefly, a potential of -1.2 V vs Ag/AgCl was applied to the working electrode for a total period of 60 hours. Conductivity measurements were performed prior to the electrochemical reduction, and then after 12 hours, 36 hours and 60 hours according to the methods described below. Electrochemical tubes set up is shown in Figure 4.13.

- *Serum bottles.* In order to assess the possible toxicity of increasing GO concentrations to the biomass and to evaluate the GO reduction rate, 7 serum bottles were filled with the same GO concentrations amended to test-tubes, with culturing media (composition provided above) and, in addition, were seeded with 0.66 mL of inoculum scraped off four rods of the parent BES and resuspended in 15 mL PBS; 40 mM of sodium acetate were added to each bottle as metabolic substrate (the total volume filled to the serum

bottles was 20 mL). Moreover, an abiotic control containing acetate and GO (control #1) as well as a biotic control containing microorganisms and GO (control #2) were also included to prove that GO reduction is microbially mediated and that GO acted as the electron sink during acetate metabolism. Serum bottles were then sealed and incubated at 35° C inside an anaerobic chamber. 15 days allow the complete reduction of GO into rGO (see below).

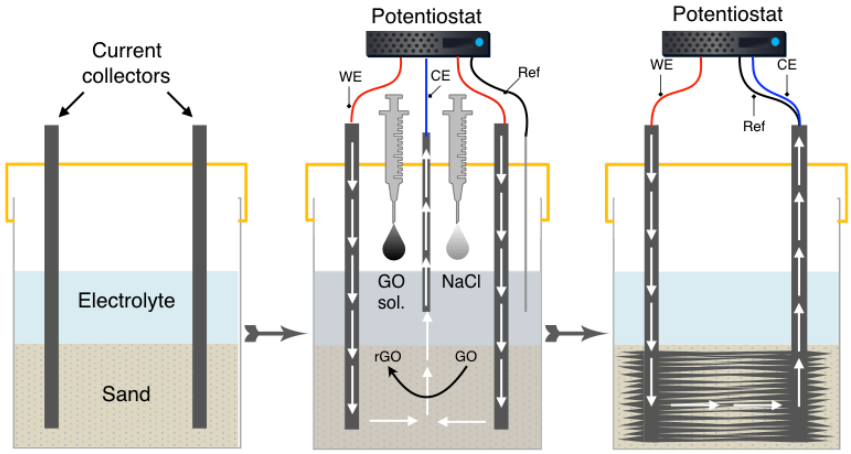

Figure 4.13 *Experimental set up of electrochemical tubes. Tubes were filled with GO solution and reduction of GO solution to rGO was electrochemically induced. Prior and after the electrochemical reduction, measurements of conductivity were performed on the model soil, according to methods described in this section.*

Measurements of electric conductivity.

- *Two-probe DC Current-Voltage (i-V) method.* Measurements of electronic resistance were performed applying a fixed voltage (bias) over a ramp between 0 and ±0.5 V with steps of 0.050 V (except for the time 0, i.e., before reduction, when it was performed between 0 and ±0.3 V) across the two carbon rods inserted in the sand. In order to maintain the structure of the rGO network within the sand, the measurements were done in the electrolyte. The applied voltage bias was appropriately low to ensure the linearity of the i-V profile, hence to determine the conductivity in the ohmic regime (Malvankar and Lovley, 2015). In general, electron transfer and ion diffusion can both contribute to the measured DC conductivity: in order to minimise the contribution of ion diffusion to the total current profile, and since the ionic conductivities measured in both experiments were similar (ranging between 9.95 mS cm-1 and 11 mS cm-1, as shown in Table 4.5), each bias was maintained for a total of 300 s and the current was measured every second in both, bio-reduction and electro-reduction; time-averaged current values were then evaluated by averaging the data collected in the last 60 s, when the current profiles

reached steady state, as confirmed by assessment of the variation of the current per minute below < 20 μA min^{-1} measured when applying the highest biases (0.5/-0.5 V, and 0.3/-0.3 V at time 0). Time-averaged steady-state current for each fixed bias was used to create *i-V* profiles. The *i-V* profiles were fitted with a linear function to extract the slope, whose inverse represents the electric resistance, according to Ohm's law (see Equation 4.1). Representative *i-V* profiles as well as fittings are reported herein.

Table 4.5 *Summary of the electrolyte ionic conductivity measured in each test-tube in biological and electrochemical tests, respectively. Values are reported as averages and standard deviations (n=2).*

GO levels [mg_{GO} kg_{dw}^{-1}]	Ionic conductivity [mS cm^{-1}] Biological medium	Electrochemical medium
0	10.965±0.004	11±0
10	10.915±0.004	10.68±0.02
50	10.860±0.007	11±0
100	10.780±0.007	10.575±0.004
200	10.810±0.007	10±0
500	10.720±0.007	10.705±0.004
1,000	10.575±0.004	9.95±0.02
2,000	10±0	10±0
Reverse osmosis water (*)	1.57±0.05	1.57±0.05

(*) = these values are expressed in μS cm^{-1}.

- *Two-probe AC electrochemical impedance spectroscopy method*. To provide an independently additional method to probe the electronic resistance across the two carbon rods, alternate (AC) impedance spectroscopy was applied, which, contrary to DC current-Voltage measurements, can more accurately distinguish between ionic conductivity and redox charge transfer processes. Impedance measurements were performed using a frequency response analyser associated to the multichannel VMP3 Potentiostat/Galvanostat (BioLogic Science Instruments, France). The impedance response was characterised from 100 kHz to 1 mHz using an AC amplitude of 100 mV imposed over the open circuit voltage across the rods. No amplitude dependency was observed over a range between 10 and 500 mV, thus demonstrating linearity of the impedance response and justifying the choice of 100 mV amplitude. Validity of the EIS data was checked using Kramers-Kronig transforms (Dominguez-Benetton *et al.*, 2012). Prior to each measurement, the electrochemical system under investigation was kept at open circuit for at least 15 minutes. EIS measurements were then performed only after the open circuit voltage across the two rods reached steady state, as confirmed by variation of the OCV below 310 μV min^{-1}. Nyquist plots depicting real and imaginary

components of the impedance were fitted using a semicircle function (EC-Lab® software, Version 11.12, BioLogic Science Instruments, France). Charge transfer resistance R_{CT}, was determined as the diameter of the semicircle, while electrolyte resistance was determined as the intercept of the real impedance axis at high frequencies ($\omega \rightarrow \infty$).

- *Determination of electronic conductivity*. The values of resistance evaluated according to the two methods described above were used to calculate the electronic resistivity according to the following Equation 4.3:

Equation 4.3 $$\rho = \frac{R \cdot A}{100 \cdot l}$$

where ρ is the electronic resistivity of the sample (Ω m), R is the resistance determined from the DC i-V method or the AC EIS method (Ω), A is the projected sectional area of the rods (cm^2), l is the distance between the rods (cm). According to Equation 4.4, S represents the shape factor (cm^{-1}):

Equation 4.4 $$S = \frac{A}{l}$$

The electronic conductivity σ (mS cm^{-1}), is then defined as the inverse of the resistivity, as reported in Equation 4.5:

Equation 4.5 $$\sigma = \frac{1}{\rho}.$$

Assessment of the electrocatalytic properties of percolating rGO-sand composite electrodes in bench-scale bioelectrochemical systems. To test the performance of the percolating rGO-sand composite as electrodes in SBES, two bench-scale systems were assembled consisting of tubular glass vessels (internal volume of ≅ 450 mL), namely rGO1 and rGO2, equipped with 3 graphite rods serving as WE and current collectors (rods portions of 3 cm were buried in the porous soil, while the upper parts, in contact with the electrolyte solution, were insulated with a 2-layers of parafilm wrapping), one piece of RVC with dimensions 1x1x2 cm serving as CE, and an Ag/AgCl reference electrode. The systems were filled with 250 g of sand, and 250 mL of electrolyte, composed by 125 mL of the saline medium (5.8 g L^{-1} of NaCl in RO water) and 125 mL of GO solution (to yield a GO concentration of 2,000 mg_{GO} kg_{dw}^{-1} in the vessel). Electro-reduction of the GO was obtained as detailed above: the 3 graphite rods of both SBES, rGO1 and rGO2, were short-circuited and connected to a potentiostat which controlled the potential of the working electrode at -1.2 V vs Ag/AgCl. To avoid oxidation of the RVC, a platinum wire was used as counter electrode during the preparation of the composites. The

electro-reduction was sustained for a total period of about 70 hours to allow maximum reduction of the GO provided, based on our knowledge of the system[23]. Conductivity measurements were performed as described above, before and after the electro-reduction; conductivity was assessed at each time between two of the three rods (three measurements), and then, an average value of conductivity was calculated.

After the electro-reduction and the conductivity measurements, the saline medium was drained from the BESs and replenished with 150 mL of culturing medium (composition provided above) containing 40 mM of sodium acetate. Additional 500 mL of medium was recirculated through the sand bed at a flow rate of 103.8 mL h^{-1} using a peristaltic pump (323S Watson-Marlow Pty Limited NSW, Australia). Two additional identical systems were set up without the amendment of GO and served as controls (herein referred to as C-1 and C-2). SBES adopted in this study are shown in Figure 4.14.

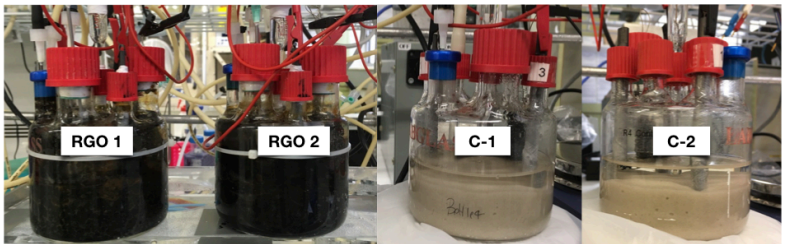

Figure 4.14 *Photograph of bench-scale reactors used in the study to assess the performance of rGO-sand composites to act as anodes in SBES: rGO1 and rGO2 represent the GO-amended systems (left), while C-1 and C-2 represent the controls not amended with GO (right). The digital picture was taken after GO reduction to rGO (as shown by the black colour of the material inside rGO1 and rGO2).*

All four BESs were immersed in a water bath set at a temperature of 35° C and inoculated with 2.50 mL each of biomass scraped off the four rods of the parent BES and resuspended in 12.5 mL PBS. The three rods in each reactor were short-circuited and connected to a potentiostat which controlled the potential of the working electrode 0 V *vs* Ag/AgCl. After 20 days of incubation, the performance of the systems was evaluated by measuring electric current production and acetate consumption during 8-hours batch tests (repeated in triplicate). Liquid samples were periodically collected for acetate analysis, filtered at 0.22 µm and then analysed via gas chromatography using an Agilent Technologies 7890A GC System (Agilent, USA)

[23] According to Hilder *et al.* (2011) GO can exchange 1 mol e^- for each 4 mol C; in the same study, carbon content of air-dried GO was determined in 69.3%. Based on this data, cumulative charge required for achieving the full reduction of the GO suspension inserted in the bench-scale reactors to rGO, was about 10x lower than the actual cumulative charge produced in almost 70 hours of reduction. Therefore, even considering that an important quantity of charge was due to hydrogen production, it can be said that 70 hours were enough to assume complete GO reduction to rGO.

equipped with a polar capillary column (DB-FFAP 30 m × 0.53 mm × 1.0 μm) and flame ionisation detector (make-up flow: 10 mL min^{-1} N_2; 250ºC).

Confocal Raman Microscopy (CRM) and Scanning Electron Microscopy (SEM). Confocal Raman Microscopy measurements were performed at 22±1° C using an Alpha 300 Raman/AFM (WITec GmbH, Ulm, Germany) equipped with a frequency-doubled continuous-wave Nd:YAG laser to obtain a 532 nm excitation line. The laser beam was focused by an objective lens (Nikon 40X, N.A. 0.6, CFI S Plan Fluor ELWD objective). The back-scattered Raman light from the sample was collected with a 100 μm optical fibre employing a Raman spectrometer (1800 grooves per mm grating) with a charge-coupled device (EMCCD) spectroscopic detector. Project FOUR software (WITec GmbH, Ulm, Germany) was used for spectra processing and image reconstruction. SEM images were obtained using a XL30 Philips (LaB6 source electron gun) Scanning Electron Microscope, on a freeze-dried sample (24 hours; sample was then stored at -18°C prior the scan).

Biomass sampling and sequencing.

- *DNA Extraction and 16S rRNA Amplicon Sequencing*. DNA was extracted from 200 mg of raw sample using the DNeasy PowerSoil Kit (Qiagen #12888-100). The manufacturer's protocol was followed except for one modification wherein the sample was heated at 65°C for 10 minutes just before bead beating. DNA concentration was measured using a Qubit high sensitivity assay (ThermoFisher Scientific; Qubit 3.0 and #Q32854) and was adjusted to a concentration of 5 ng μl^{-1} for 16S rRNA amplification. Illumina sequencing of the 16S rRNA gene, PCR amplified using iTAG 16S 926F and 1392wR primers (Engelbrektson *et al*., 2010), was then performed by the Australian Centre for Ecogenomics (The University of Queensland, Brisbane, Australia).
- *Community profiling.* Community structure was determined from amplicon reads using QIIME 2 v2017.10 (Caporaso *et al*., 2010). Features (formerly OTUs) were generated using 'deblur', with reads truncated to 200 base pairs. Features making up <0.01% relative abundance within the total set were discarded. Remaining features were then blasted against the Silva 132 database at 99% similarity using 'feature-classifier' to generate taxonomic labels, which were truncated at the genus level. Taxonomic lineages with the same labels were numbered sequentially from highest to lowest total sample set abundance, starting from 1. Taxonomically labelled features were then evenly rarefied based on the lowest sample feature count (19,000) using the

'rarefy_even_depth' function of the Ampvis package in R (Albertsen *et al*., 2015). Taxonomic labels were then aggregated at the genus level before generating the heatmap using Graphpad Prism.

4.2.3.3 Results and discussion

GO reduction into rGO, the biological and the electrochemical routes. Two approaches were used to achieve the reduction of GO into rGO and infer electrical properties to the model porous soil: biological (or microbial), and electrochemical ones. To achieve the biological reduction, systems were operated under the rationale that microorganisms can use GO as electron acceptor to support respiration (Salas *et al.*, 2010; Jiao *et al.*, 2011; Wang *et al.*, 2011; Tanizawa *et al.*, 2012), thereby producing insoluble and highly conductive rGO. Previously, Virdis and Dennis (2017) demonstrated that biologically reduced GO and microbial cells self-assemble into aggregates with superior catalytic properties due to the inclusion of rGO particles within the biological structures. Using a similar approach, the model soil was inoculated with an inoculum containing electrochemically active microorganisms enriched with acetate and amended with levels of GO ranging between 10 and 2,000 mg_{GO} kg_{dw}^{-1}. The biological test-tubes were incubated at 35° C for 15 days. Preliminary tests conducted in anaerobic serum bottles containing the same medium but lacking the sand, suggested that this incubation time was sufficient to allow the conversion of GO and produce a clear solution and a separated aggregate of graphitic black material, presumably rGO (Figure 4.15).

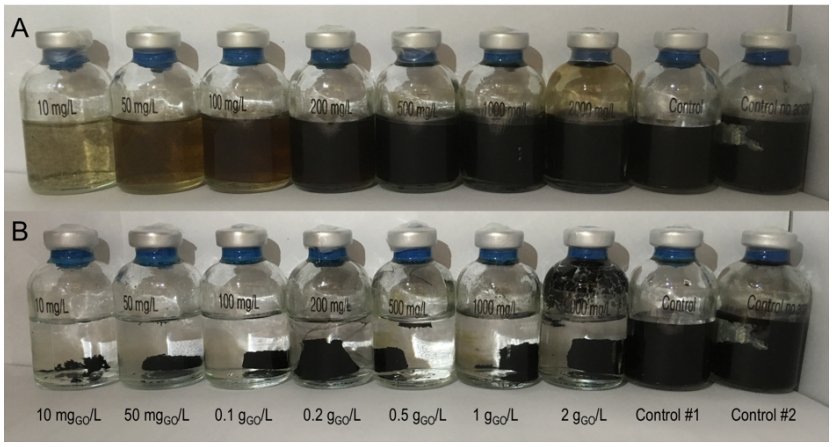

Figure 4.15 *Digital photographs of prepared graphene oxide dispersions (concentrations as indicated) seeded with electroactive microorganisms and amended with 40 mM acetate as metabolic substrate. Photographs were taken A) on the first day, and B) after 15 days of incubation at 35°C. An abiotic control containing acetate and GO (Control #1) as well as a biotic control containing microorganisms and GO (Control #2) were also included to prove that GO reduction is microbially mediated and that GO acted as the electron sink during acetate metabolism.*

Conversely, the electrochemical reduction of GO was achieved using similar test-tubes, this time under abiotic conditions and by poising the two current collectors (graphite rods) at the electrochemical potential of -1.2 $V_{Ag/AgCl}$ for a period of 60 hours to induce the reduction of GO (Figure 4.16). A similar approach was used by Hilder *et al.* (2011). The formation of black aggregates within the porosity of the medium was visible for both biological and electrochemical systems after the reduction, suggesting the formation of solid insoluble rGO.

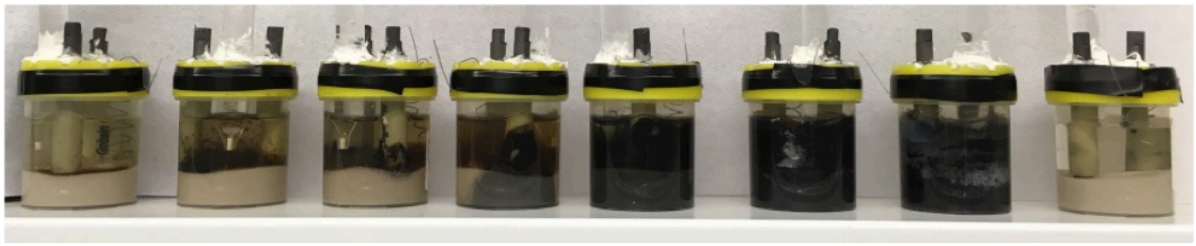

Figure 4.16 *Digital picture of a representative test of electro-reduction (after 60 hours); from the left to the right: test-tubes amended with GO concentrations from 10 mg_{GO} kg_{dw}^{-1} to 2,000 mg_{GO} kg_{dw}^{-1}, and control without GO amendment (last tube on the right). The picture shows that, in this specific configuration, GO concentrations below 500 mg_{GO} kg_{dw}^{-1} were not enough to create a visible reduction in the whole volume.*

Confocal Raman microscopy was used to assess the graphitic material formed during the biological and electrochemical reduction. The results are reported in Figure 4.17. The Raman scattering of graphene typically exhibit two main bands designated as the G- and the 2D at around 1,580 and 2,700 cm^{-1}, respectively. A third band designated as the D-band is often observable at around 1,350 cm^{-1} and is associated with defects within the carbon (Cançado *et al.*, 2011). All three bands are clearly visible in all spectra determined in our samples, including the GO (Figure 4.17 A), as well as spectra of the material obtained after the biological (Figure 4.17 B) and the electrochemical (Figure 4.17 C) reduction of the GO, hence taken after 15 days of incubation and after 60 hours of electrochemical reduction, respectively. These spectra show a very pronounced D-band, indicating a high level of structural disorder, probably ascribed to a multi-layered structure typical of the formation conditions. The formation of rGO from the reduction of GO is confirmed by the change in relative intensity of the G- and D-bands. In fact, the ratio of the intensities of these two bands (I_D/I_G) is typically higher in rGO than it is in GO due to the increase in structural defects (resulting in the increase in the intensity of the D-band) and the disruption of the sp^2 bonds of the carbon in rGO (resulting in a decrease in the intensity of the G-band) (Moon *et al.*, 2010; Cançado *et al.*, 2011). Figure 4.17 shows that after the reduction, spectra collected from the test-tubes present I_D/I_G of 1.19±0.06 and 1.70±0.03 for biological and electrochemical reduction, respectively, both higher than that measured on the GO solution (0.86±0.004), thus indicating the formation of new graphitic domains (smaller in

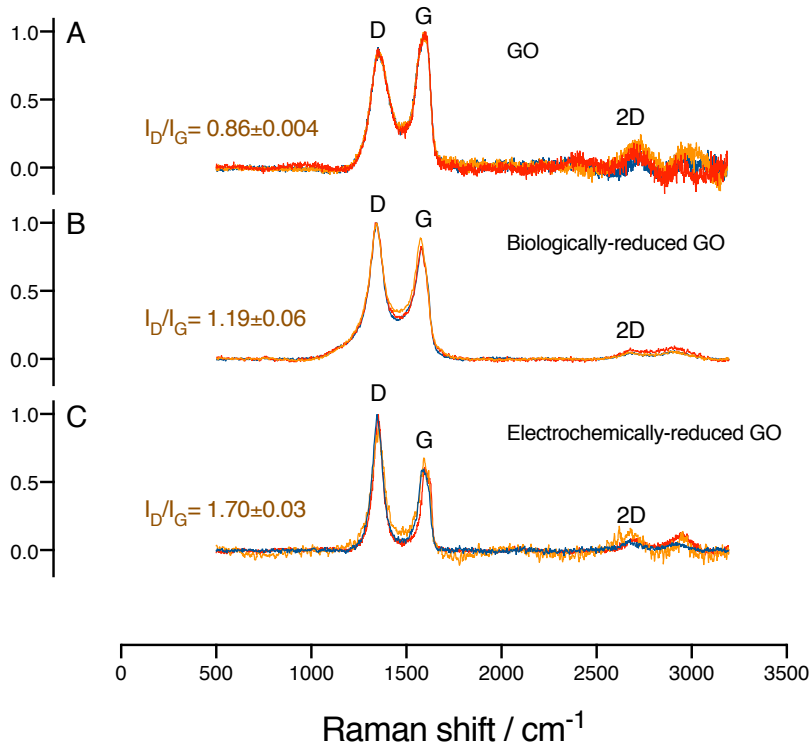

Figure 4.17 *Normalized and background subtracted Raman spectra. A) spectra of the GO solution as provided by the manufacturer, B) spectra of the graphitic material present after the biological reduction, and C) spectra of the graphitic material present after the electrochemical reduction.*

size and higher in number than those present in GO before reduction) and good reduction efficiency (Stankovich *et al*., 2007). Moreover, the higher increase in the ratio might indicate a better reduction degree obtained by the electrochemical reduction, compared with the biological route (Cançado *et al.*, 2011; Eigler *et al.*, 2012).

The disordered structure typical of rGO is evident in SEM micrographs (Figure 4.18 A and C) made on a representative sample of a bio-reduction test (2,000 $mg_{GO}\,kg_{dw}^{-1}$), collected after the 15 days incubation and afterwards freeze-dried. In Figure 4.18 B, the presence of bacteria is indicated: they were, in fact, responsible of rGO flakes formation in anaerobic conditions.

Analysis of the microbial community (Figure 4.19) was performed on samples collected from the test-tubes after the incubation time of 15 days to verify whether the exposure to GO solution would infer any significant change in the microbiome. While the inoculum prevalently contained the class *Deltaproteobacteria* (mostly of the family *Geobacteriaceae)*, which is not surprising considering the inoculum was collected from the anodic terminal of a bioelectrochemical cell oxidizing acetate, the samples collected from the test-tubes showed a minimal presence of the same class.

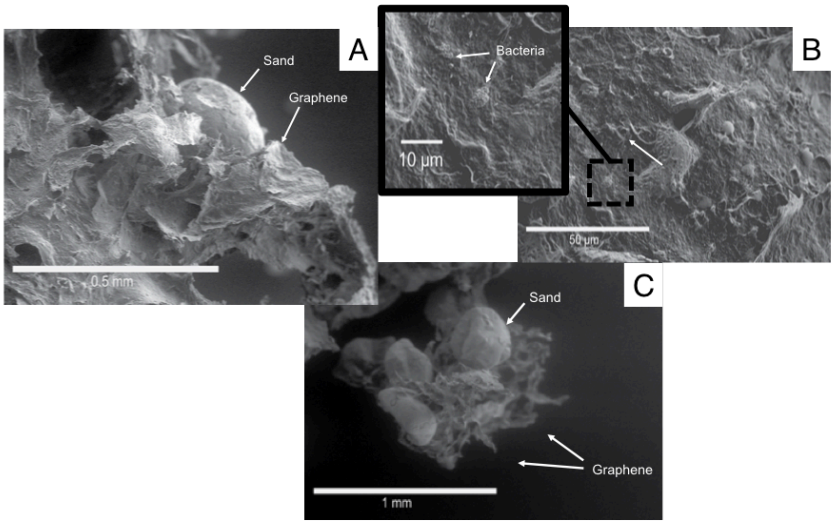

Figure 4.18 *SEM micrographs on a representative bio-reduced sample (2,000 mg_{GO} kg_{dw}^{-1}), previously freeze-dried. A) and C) rGO-sand aggregates: the disordered rGO structure is clearly showed in the mm scale. B) detail of portion of rGO (in the 50 µm scale); the presence of bacteria which formed the rGO flakes is indicated in the magnification.*

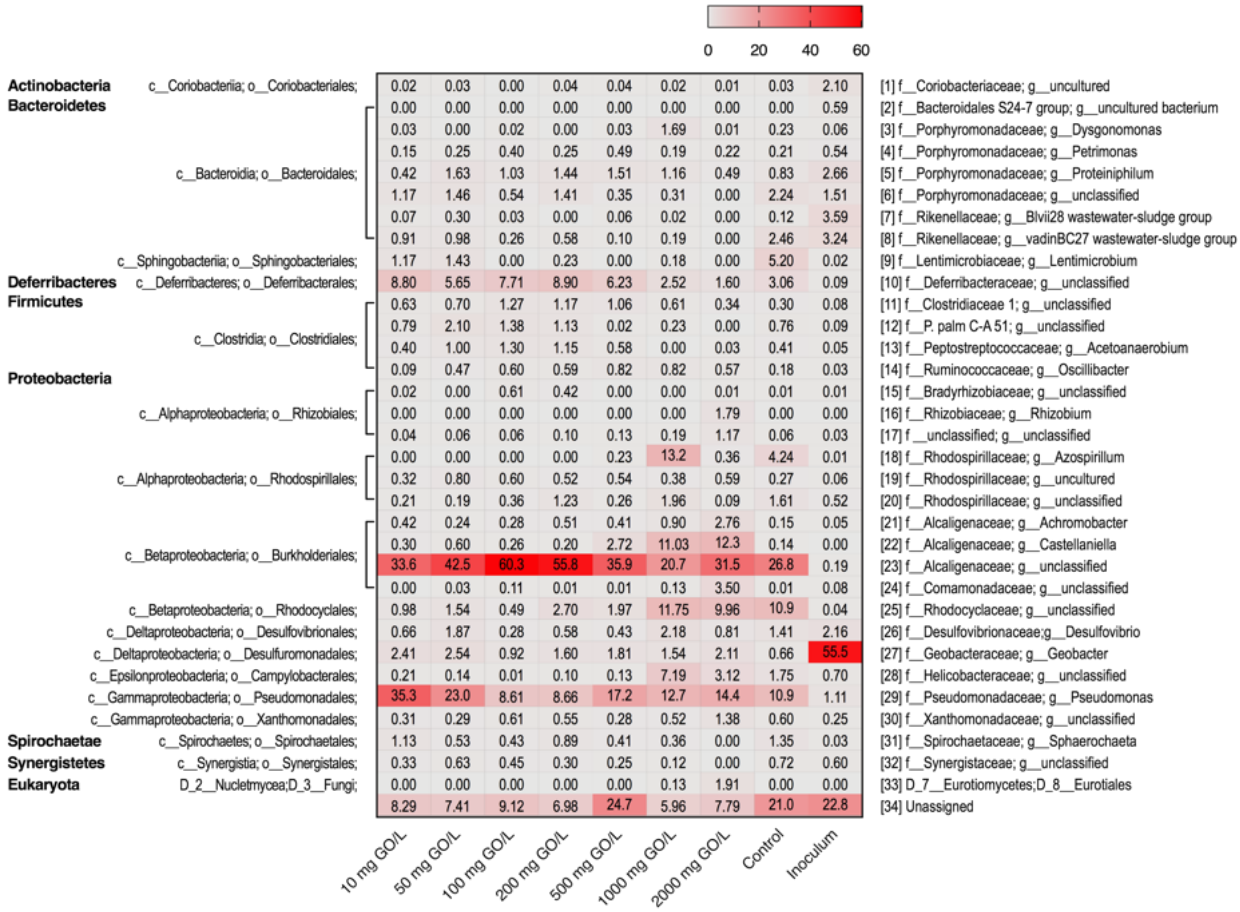

Figure 4.19 *Heatmap summarizing the abundance of the most dominant populations associated with the GO-amended test-tubes, the control, and the inoculum collected from a bioelectrochemical system performing anodic acetate oxidation using the anode as the sole electron acceptor. The numbers in square brackets are OTU IDs.*

Instead, GO-amended tubes showed an enrichment of *Betaproteobacteria*, mostly belonging to the order *Burkholderiales* (mostly of the family *Alcaligenaceae),* which accounted for at least the 20% of the community at all GO levels; although the highest relative abundance was shown in 100 mg_{GO} kg_{dw}^{-1} (60.5%), all samples showed this enrichment as the dominant. *Burkholderiales* were found also in the control test without GO amendment (26.8%). The second class for relative abundance was represented by *Gammaproteobacteria* belonging to the order *Pseudomonadales* and accounting for the highest relative abundance in 10 mg_{GO} kg_{dw}^{-1} test-tube (35.3%). To be noted the presence of not negligible percentages of the order *Deferribacterales* belonging to the class *Deferribacteres* (> 5% of the relative abundance until 500 mg_{GO} kg_{dw}^{-1}) and of *Betaproteobacteria* belonging to the order *Rhodocyclales* (approx. 10%) in 1,000 mg_{GO} kg_{dw}^{-1}, 2,000 mg_{GO} kg_{dw}^{-1} and in the control test. A not negligible relative abundance of unassigned bacteria was present in each sample. These results suggested that the presence of GO had the effect of pushing the community towards species that might be more tolerant to the GO presence than *Geobacter*, perhaps capable of reducing GO from the metabolism of acetate. Interestingly, the presence of the family *Alcaligenaceae* was also observed in Virdis and Dennis (2017) and might suggest that these organisms have a high tolerance to GO.

Electrical conductivity in the biologically-reduced versus electrochemically-reduced GO. To assess the electrical conductivity of the rGO-sand composites the DC i-V method was applied. Figure 4.20 shows i-V plots obtained on the biological (panels A, B and C) and electrochemical (panels C, D and E) reduction methods and representative of measurements made at the end of each reduction process (15 days for biological reduction and 60 hours for electrochemical reduction, respectively). The same profiles (not shown) were recorded also at time 0, in both experiments, and at 12 and 36 hours for electrochemical reduction. The i-V showed a linear response of the current at increasing biases, which is indicative of conductive material. Observing i-V profiles (Figure 4.20) it is evident that forward and biases backward lead to similar responses, hence verifying the ohmic contact existent within the graphite rods (Malvankar and Lovley, 2015). Shape factors, listed in Table 4.6 for each test-tube and calculated for each replicate (according to Equation 4.4) were used to determine average resistivities (Table 4.7) and conductivities (Table 4.8), associated to the i-V profiles measured at day 0 and 14 for the bio-reduction, and at 0, 12, 36 and 60 hours for the electro-reduction.

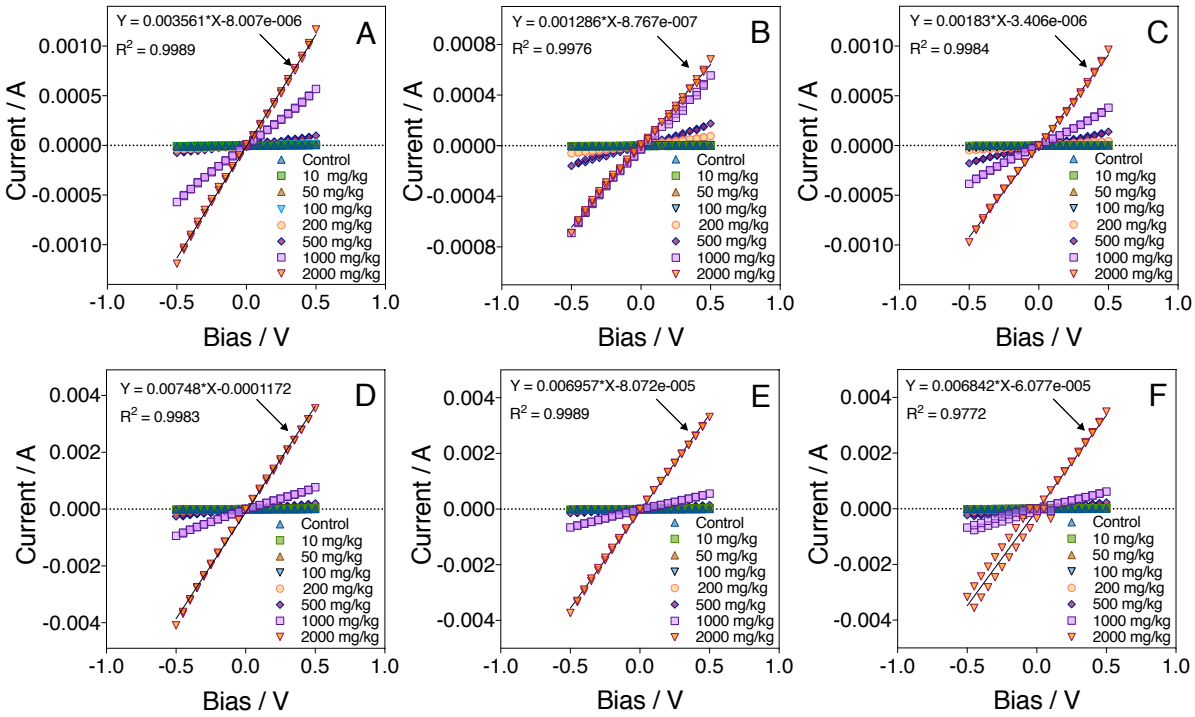

Figure 4.20 *Measurements of electric resistance based on 2-probe DC current-voltage (i-V) method, recorded after biological reduction (15 days) in A) Test 1, B) Test 2 and C) Test 3, and after electrochemical reduction (60 hours) in D) Test 1, E) Test 2 and C) Test 3.*

Conductivities calculated during the experiments are shown in Figure 4.21 A and B for bio- and electro-reduction, respectively; the pH values measured prior to start the reduction in each test-tube have been associated to each panel. Although the different pH measured in bio- and electro-reduction (stable around 7 in the buffered medium used for bio-reduction, and variable between 5.5 and 2.7 in the electrolyte used for electro-reduction) might have influenced the reductive process (the investigation on this specific effect lied outside the purposes of this study), the i-V measurements are independent from pH values. Moreover, despite different pH values the ionic conductivity of the electrolytes were similar (Table 4.5).

Table 4.6 *Shape factors calculated for each test-tube in each test replicate of biological reduction and electrochemical reduction. Shape factor was used for conductivity and resistivity calculations.*

GO levels [mg_{GO} kg_{dw}^{-1}]	Shape factor S [cm^{-1}]			
	Biological reduction			Electrochemical reduction
	TEST 1	TEST 2	TEST 3	EACH TEST
0	2.21	2.44	2.63	2.80
10	2.80	2.79	2.75	2.85
50	2.84	2.60	2.71	2.87
100	2.87	2.72	2.76	2.88
200	2.88	2.83	2.95	2.65
500	2.65	2.87	2.99	2.58
1,000	2.58	2.76	2.90	2.71
2,000	2.71	2.63	3.06	2.18

Table 4.7 *Summary of the resistivities of each test-tube, obtained with the application of the i-V method: values are representative of the situation before, during and after the application of the reduction process to rGO (ended in 15 days for the biological reduction and in 60 hours for the electrochemical reduction, respectively). Values are presented as averages and standard deviations (n=3).*

GO levels [$mg_{GO}\ kg_{dw}^{-1}$]	Resistivity ρ [kΩ·cm]					
	Biological reduction		Electrochemical reduction			
	day 0	day 14	0 hours	12 hours	36 hours	60 hours
0	544±343	[-]	454±53	[-]	[-]	[-]
10	784±592	80±52	155±111	9±0.9	8.4±0.3	8.1±0.2
50	767±455	81±45	198±124	7.2±0.4	6.50±0.02	6.24±0.05
100	447±261	18±5	237±134	7.2±0.7	6.1±0.6	5.9±0.7
200	283±183	4±1	115±76	6.0±0.8	4.2±0.7	4±1
500	366±231	1.5±0.7	119±71	1.0±0.3	0.9±0.1	1.0±0.3
1,000	787±635	0.38±0.08	120±71	0.21±0.03	0.22±0.03	0.28±0.05
2,000	1206±1022	0.21±0.08	56±25	0.040±0.005	0.042±0.009	0.052±0.002

Table 4.8 *Summary of the conductivities of each test-tube, obtained with the application of the i-V method: values are representative of the situation before, during and after the application of the reduction process to rGO (ended in 15 days for the biological reduction and in 60 hours for the electrochemical reduction, respectively). Values are presented as averages and standard deviations (n=3).*

GO levels [$mg_{GO}\ kg_{dw}^{-1}$]	Conductivity σ [mS cm^{-1}]					
	Biological reduction		Electrochemical reduction			
	day 0	day 14	0 hours	12 hours	36 hours	60 hours
0	0.003±0.003	0.003±0.003	0.0022±0.0002	0.0022±0.0002	0.0022±0.0002	0.0022±0.0002
10	0.004±0.005	0.02±0.02	0.009±0.004	0.11±0.01	0.119±0.005	0.124±0.003
50	0.002±0.002	0.02±0.01	0.007±0.004	0.138±0.008	0.1538±0.0004	0.160±0.001
100	0.003±0.001	0.06±0.02	0.005±0.002	0.14±0.01	0.16±0.02	0.17±0.02
200	0.006±0.005	0.27±0.09	0.011±0.005	0.17±0.02	0.24±0.04	0.26±0.07
500	0.005±0.004	0.7±0.3	0.011±0.006	1.0±0.3	1.2±0.2	1.1±0.3
1,000	0.004±0.006	2.7±0.6	0.011±0.006	4.8±0.7	4.5±0.6	3.6±0.6
2,000	0.004±0.007	5.0±1.5	0.012±0.007	25±3	25±5	19.3±0.9

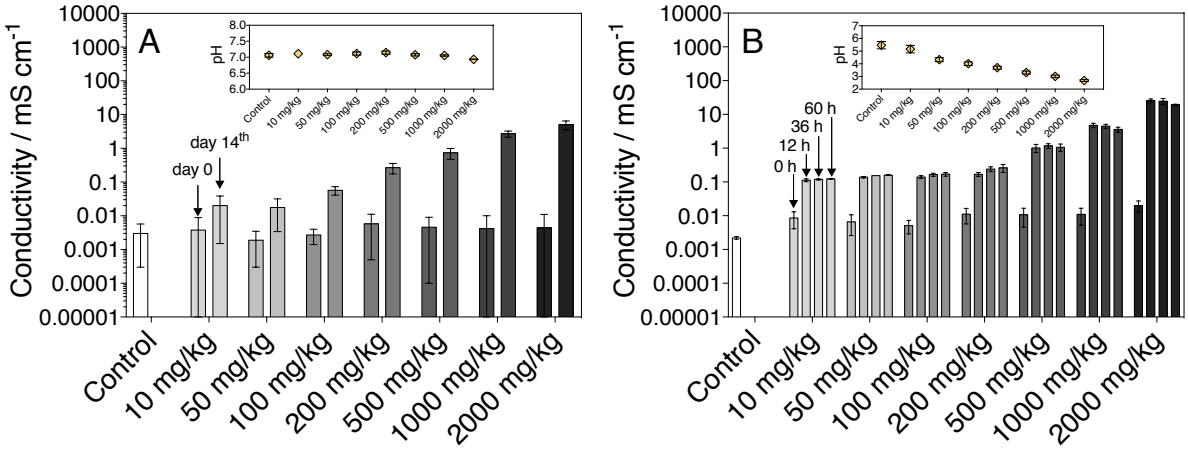

Figure 4.21 *Conductivities measured A) before and after biological reduction and B) before, during and after electrochemical reduction; values are displayed according to the increase concentration of GO amended to each test-tube. Panels show the pH profile measured in each test-tube before reduction.*

Both methods of GO reduction achieved a significant reduction of the electric resistance. Even the application of 10 mg_{GO} kg_{dw}^{-1} resulted in higher conductance of the composites relatively to the non-GO-amended controls after both the biological and the electrochemical reduction. Importantly, the increase in conductivity is positively correlated to the concentration of GO in the medium, hence the highest conductivities were reached in both experiments in test-tubes at 2,000 mg_{GO} kg_{dw}^{-1}. Although until 1,000 mg_{GO} kg_{dw}^{-1} both experiments showed a comparable increase in conductivities, the difference between the two reduction methods became higher in 2,000 mg_{GO} kg_{dw}^{-1} test-tubes (Figure 4.22): electro-chemical reduction achieved 19.3±0.9 mS cm^{-1}, almost four times higher than the conductivity obtained through the biological reduction method (5.0±1.5 mS cm^{-1}). These results are more remarkable considering the different time lengths used for achieving the reduction to rGO (15 days *vs* 60 hours). Moreover, Figure 4.21 B shows that very high conductivities were already obtained after 12 hours in electro-reduction tests, and that these values did not change significantly in the next reduction steps.

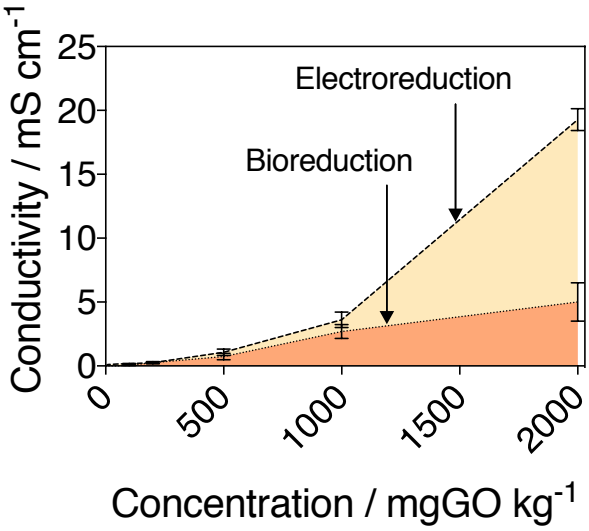

Figure 4.22 *Measurements of average conductivities calculated from the i-V method applied to bio-reduction and electro-reduction tests at the end of the reduction period (15 days and 60 hours, respectively).*

In order to confirm the results achieved with the i-V method, EIS measurements were applied (Figure 4.23), as indicated in section 4.2.3.2. Analysis of the impedance behaviour of the rGO-sand composites is consistent with charge transfer limitations dominating the electrochemical response. Each curve in the -Im(Z) *vs* Re(Z) Nyquist plots was fitted with a semicircle function to extract information on the polarization resistance (Figure 4.23 A and D). The intercept of the semicircles with the real impedance axis at low frequencies ($\omega \rightarrow 0$) assumed progressively smaller values at increasing levels of GO, indicating that the presence of rGO in the soil pores resulted in a large reduction of the polarization/charge transfer resistance (R_{CT}). The intercept

of the semicircles at high frequencies (ω→∞), which is a measurement of the ohmic resistance of the electrolyte, did not vary significantly between measurements made in both, bio-reduction and electro-reduction, indicating that the conductivity was induced by the presence of graphene and not by the properties of the electrolyte (Figure 4.23 B and E), which values of ionic conductivities were similar in each test-tube (Table 4.5). The highest conductivities of 4±1 mS cm^{-1} and 25.7±0.9 mS cm^{-1} were measured for GO levels of 2,000 mg_{GO} L^{-1} (equivalent to 2,000 mg_{GO} kg_{dw}^{-1}), respectively in bio-reduced and electro-reduced test-tubes; these values achieved with EIS are statistically similar to the value achieved with the i-V method (Figure 4.23 C and F), hence the former method fully validated the latter one.

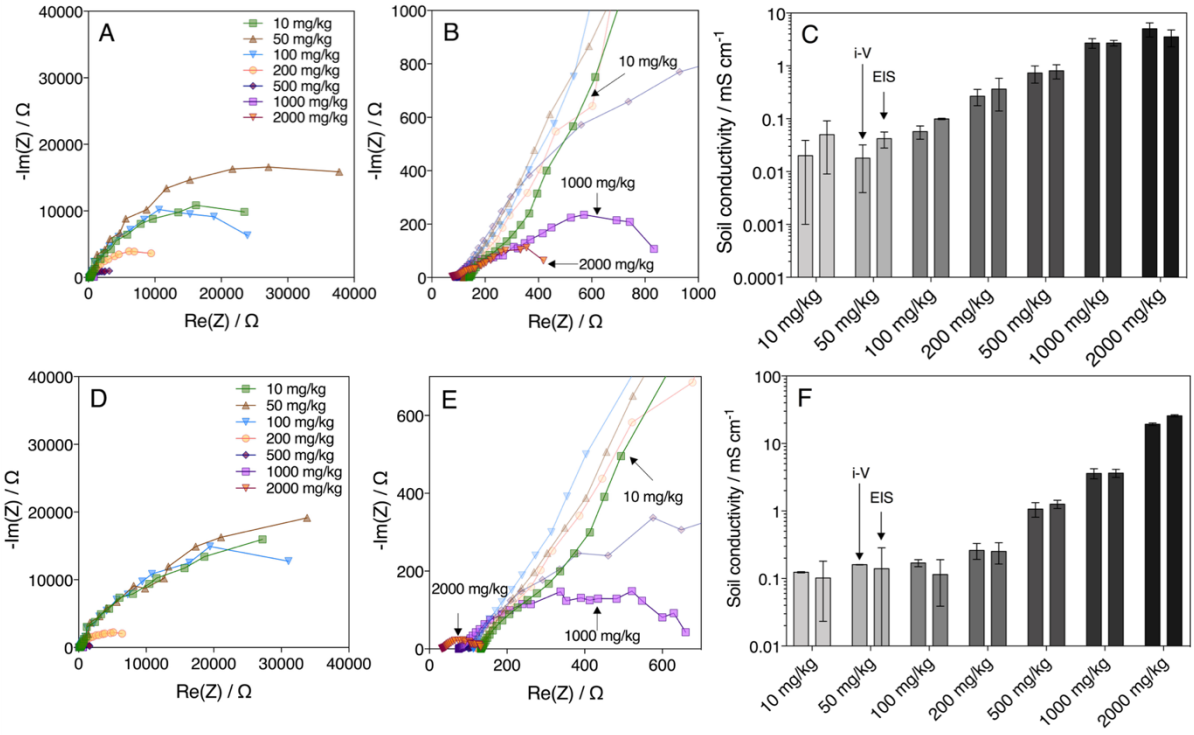

Figure 4.23 *Nyquist plots obtained with 2-probe AC impedance spectroscopy in a representative test of A) bio-reduction and D) electro-reduction; magnification on the test at 2,000 mg_{GO} kg_{dw}^{-1} in B) bio-reduction and E) electro-reduction; comparison between conductivities evaluated using the i-V method versus the EIS method in C) bio-reduction and F) electro-reduction.*

Enhancement of degradation capacity in porous soils modified with electrochemically reduced GO. Provided the very high conductivities achieved in miniature-scale SBES when 2,000 mg_{GO} kg_{dw}^{-1} were electrochemically reduced to rGO, this method was chosen to form percolating rGO-sand composites electrodes (Figure 4.24) in two bench-scale systems (rGO1 and rGO2) and prove the enhancement of degradation capacity in porous soils, when these electrodes were working as bioanodes, with respect to controls without the amendment of GO (C-1 and C-2).

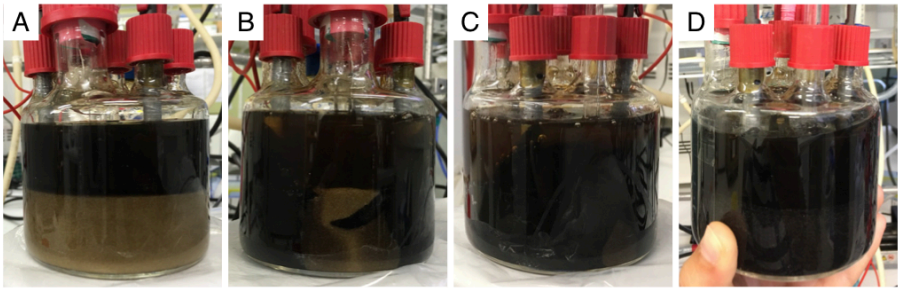

Figure 4.24 *Representative steps of the GO reduction to rGO in bench-scale reactors: A) system before reduction, B) after 24 hours, C) after 36 hours; D) after 70 hours. As evidenced in the digital pictures, rGO deposited within the soil pores covering completely the sand and, as proved by conductivity measurements (see below), inducing electrical properties to an otherwise insulating material.*

Conductivities of each bench-scale reactor were determined according to the geometry of the system, as averages and standard deviations of the conductivities calculated with the i-V method between three couple of rods. After the reduction, applied for 70 hours, conductivities of rGO1 and rGO2 were 42±5 mS cm^{-1} and 35±6 mS cm^{-1}, respectively. Conductivities measured in C-1 and C-2 were, instead, 0.0026±0.0006 mS cm^{-1} and 0.0021 ±0.0007 mS cm^{-1}.

The bioanodes delivered a current output of 105.30 mA, equivalent to 551.74 A m^{-3} soil, outperforming the control not amended with GO by 30 times (Figure 4.25 A and B). This is the highest current reported for a SBES and can be ascribed to larger volume of the soil contributing to current production in the GO amended soil.

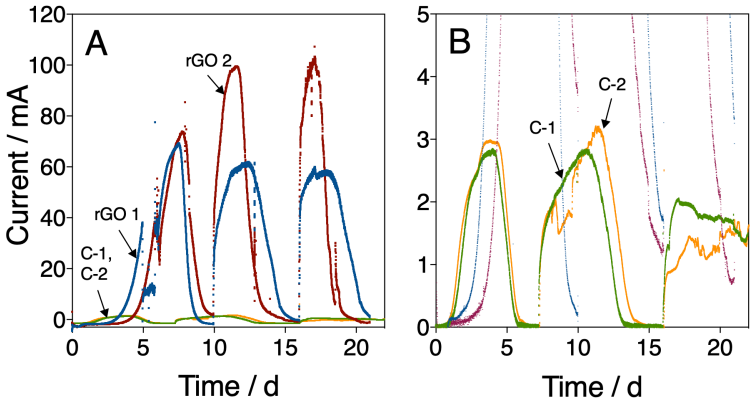

Figure 4.25 *A) Electric current vs time traces of duplicate reactors (rGO1 and rGO2), and controls not amended with GO (C-1 and C-2); B) magnification of the current vs time trace reported to show the comparison of current output of the control systems. The SBES were fed with 40 mM of sodium acetate as metabolic electron donor, and the electrodes were poised at 0 V vs Ag/AgCl.*

Moreover, due to this significant increase in electrode size achieved by the presence of graphene, the percolating electrodes were able to remove a model contaminant (sodium acetate)

at a maximum rate of 2.7±0.8 g_{COD} (L d)$^{-1}$, yielding to a Coulombic efficiency of 77±2% (Figure 4.26 A and B).

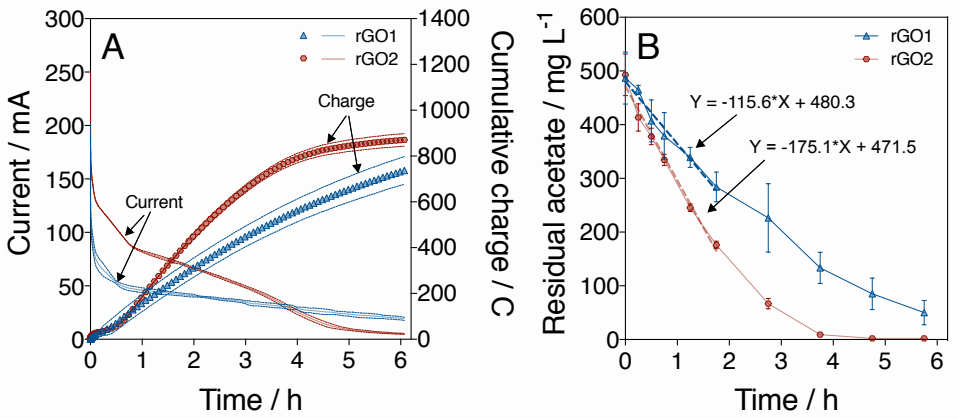

Figure 4.26 *A) Electric current and cumulative charge and B) acetate concentration profiles (average±standard deviation, n=3) observed during short-term batch tests performed on reactors rGO1 and rGO2 amended with 10 mM of sodium acetate; linear regression of the linear part of the acetate consumption profiles are also reported as dashed lines.*

4.2.3.4 Conclusions

The results obtained in this study highlight the possibility to exploit microbial metabolism and electrochemical reduction to achieve reduction of soluble GO into insoluble rGO, thereby inducing electrical properties in non-conductive soils by forming an interconnected network of electrically conductive particles extended several centimetres from the current collectors: while the microbes were able to reduce GO within 15 days soluble, electrochemical reduction achieved high electric conductivities within 60 hours (thereby significantly shortening the time length required for biological reduction). Electrochemical measurements revealed an increase in electric conductivity by more than 1,500 times after bio-reduction and by more than 8,500 times after electro-reduction relative to their respective controls. Since the electrochemical reduction allowed to achieve approx. 4 times higher conductivities than biological reduction, and in a significantly shorter time, the first one was the preferred method of percolating bioanodes preparation. When tested for its ability to act as inexhaustible electrode sink for the bioelectrochemical decontamination of the model organic contaminant sodium acetate, the rGO-sand electrodes showed impressive performances by delivering over 30 times more electric current than the controls and by removing the contaminant at the rate of approximately 3 kg_{COD} m^{-3} d^{-1}. These values are higher than typically reported in sediment bioelectrochemical systems and suggest that this easy-to-apply and cost-effective method has the potential to expand the current horizon of application of SBES. In fact, the electrochemical reduction of

GO could be useful for *ex-situ* bioelectrochemical treatments, and can also represent the preferred method of soil-electrode preparation in cases in which there is no sufficient carbon donor available *in situ* and in which bio-reduction might depend on the oxidation kinetics of slowly biodegradable organics such as, for instance, PAHs or BTEXs: in fact, relying on biological reduction when the only carbon donor *in situ* is represented by a recalcitrant substrate can possibly cause GO dispersions out of the contaminated site, hence a more difficult and slow-going electrode formation. In the case of *in situ* applications, percolating bioanodes could be easily colonised by the autochthonous microorganisms (which might not be, putatively, affected by the presence of GO, since it was proven not to be toxic for microorganisms, also at high concentrations, through bio-reduction tests). Moreover, given the extended volume of soil hypothetically contributing to the current production, this method might allow to treat contemporarily large portions of a contaminated site and, thanks to the high current outputs, to easy monitor decontamination processes.

Part of these results were published as proceedings at the European Conference of the International society for microbial electrochemistry and technology (Camedda and Virdis, 2018).

4.2.4 Preliminary assessment of the biodegradation capacity of percolating rGO-soil composite bioanodes on toxic organic contaminants

4.2.4.1 Introduction

Percolating rGO-sand composites bioanodes, obtained after electrochemical reduction of GO amended to a model soil (quartz sand), achieved extremely high current output and yielded a very good Coulombic efficiency by oxidising the model contaminant sodium acetate; these composite electrodes outperformed the controls not amended with GO, since the whole contaminated volume concurred to the bioelectrochemical process (section 4.2.3). In this way, typical drawbacks of SBES, such as difficult long-range electron transfer and a hindered mass transport, which limited the *radius of influence* of the bioelectrochemical process, were overcome. Moreover, the very high current recorded, suggested the possibility to achieve high current outputs in the presence of recalcitrant compounds such as PAHs and BTEX, therefore increasing their usually low signal-to-noise ratio.

In this framework, percolating bioanodes were tested on the degradation of two different organic contaminants used as models in order to simulate contaminations typical of real soils and sediments, *i.e.* toluene (which is relatively soluble in water) and phenanthrene. The degradation of toluene (150 mg L^{-1}) was assessed in a short-term test (14 days) made at AWMC (Brisbane, Australia), using one of the bioelectrochemical systems previously employed for sodium acetate consumption. Instead, the degradation of Phe (6 mg_{Phe} kg_{dw}^{-1}) was assessed at DICAAR laboratories (Cagliari) *versus* two control tests, an abiotic control and an open circuit control (53 days). Here, the rGO-soil composite bioanodes were obtained by using a slightly different model soil: the 95% (w/w) of artificial sand was mixed with the 5% (w/w) of raw sediment (previously, tests with different sand and sediment percentages were done in order to simulate different real sediment compositions).

4.2.4.2 Materials and methods

Test of toluene degradation

- *Assessment of toluene degradation by using percolating rGO-sand composite electrodes in bench-scale SBES.* To test the performance on the treatment of toluene with percolating rGO-sand bioanodes, the same bench-scale system used in the previous study (rGO2, which was delivering 105.30 mA, equivalent to 551.74 A m^{-3} soil, whilst removing the model contaminant sodium acetate) was here adopted. For the description of SBES configuration and the detail of GO electro-reduction, see section 4.2.3.2.

Before feeding toluene to rGO2, the bench-scale reactor was completely drained in order to eliminate any trace of acetate and replenished with 150 mL of culturing medium (composition provided above) containing 150 $mg_{toluene}$ L^{-1}. Toluene was incubated for 14 days, and the performance of the system was evaluated by measuring electric current production and toluene consumption at the end of this period. Liquid samples for toluene determination were filtered at 0.22 μm and then analysed via GC using an Agilent Technologies 7890A GC System (Agilent, USA) equipped with a polar capillary column (DB-FFAP 30 m × 0.53 mm × 1.0 μm) and flame ionisation detector (make-up flow: 10 mL min^{-1} N_2; 250°C).

Test of phenanthrene degradation

- *Biomass growth.* Microorganisms capable to degrade Phe were cultured in sterile 20 mL serum flasks. Sterile media (composition provided below) was purged with nitrogen for at least 30 minutes to ensure anoxic conditions; moreover, flasks were sealed with Viton stoppers (13x19xH12mm, Rubberbv). Two parent serum flasks were inoculated with 1 g of dry sediment per each one (Cagliari sediment, see Table 4.1), and filled with 18 mL of culturing media. 1 mL of GO concentrated suspension (4 g L^{-1}, water dispersion, Graphenea, Spain), equivalent to 200 mg_{GO} L^{-1}, was dosed in two times (at the start-up, and after 7 days, following the complete reduction of the GO initially provided), and served as the electron acceptor for ensuring bacterial growth (according to previous tests, microorganisms are able to biologically reduce GO to rGO; see section 4.2.3.2). Sediments were spiked with 50 mg_{Phe} kg_{dw}^{-1}, and Phe was the only carbon source fed to the system. When the GO was totally reduced to rGO (after 15 days of incubation), two new daughter serum flasks were derived from each parent serum flask: each one was filled with 12 mL of culturing media, 2 mL of liquid inoculum collected with a syringe from the parent serum flasks, and 1.5 mL of GO solution (equivalent to 400 mg_{GO} L^{-1}) (Figure 4.27). 250 mg_{Phe} L^{-1} were added to the anaerobic medium. The GO solution was added in three times, at regular intervals of three days. Once GO was totally reduced to rGO, the inoculum for the bench-scale systems was taken from the daughter serum flasks.
- *Culturing media.* The growth medium had the composition reported in section 4.2.1.2. Artificial seawater, used in the growth medium, had the same composition reported in 4.2.2.2, except for Na_2SO_4 (4.008 g L^{-1}), whose addition was avoided since it constitutes

a conspicuous extra source of sulphate (in fact, approx. 12 mg of sulphate per g of dry sediment were already filled to the system, coming from the sulphate sediment content and from the magnesium sulphate present in the growth medium itself).

- *Model soil.* Tests of GO reduction to rGO were attempted with different sediment concentrations: 5%, 10%, 25%, 50%, 75% of raw sediment (sieved at 2 mm) were mixed with Fontainebleau sand (sand, white quartz, VWR) to simulate a real soil/sediment. Given the results of these tests (see below), 5% sediment mixed with 95% sand was the composition of the model sediment used in the bench-scale systems.
- *Tests of GO reduction to rGO.* In order to directly investigate the effect of the presence of real sediments mixed with artificial sand on the conductivity of the model sediment, amended with 2,000 mg_{GO} kg_{dw}^{-1}, test-tubes were prepared according to the previous study (see section 4.2.3.2). Due to activation polarisation issues related with the decreased porosity of the model soil when sediment was added, a platinum counter electrode was used in order to guarantee the application of -1.2V *vs* Ag/AgCl. Each test was performed in triplicate along 36 hours reduction. Conductivity measurements were performed as described in section 4.2.3.2.

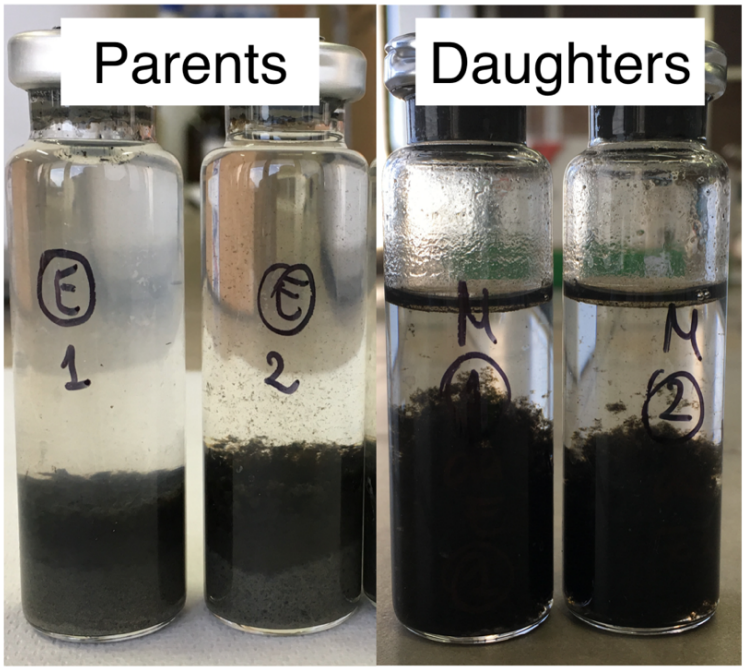

Figure 4.27 *To the left, parents serum flasks filled with contaminated Phe sediment (50 mg_{Phe} kg_{dw}^{-1}) and 200 mg_{GO} L^{-1}; to the right, example of two daughters serum flasks: 2 mL of inoculum were taken from the parents serum flasks, then solid Phe (250 mg_{Phe} L^{-1}) and 400 mg_{GO} L^{-1} were added to each serum flask. Digital pictures were taken after GO reduction to rGO.*

- *Assessment of phenanthrene degradation by using percolating rGO-soil composite electrodes in bench-scale SBES.* Bench-scale vessels and percolating rGO-soil composite formation were the same adopted in the previous study (see section 4.2.3.2); the only exception was represented by the model soil adopted in the current study (already described): percolating bioanodes for a closed circuit SBES (rGO-cc) and an open circuit control (rGO-oc) were both prepared by filling the glass vessel with 235 g of sand and 12.5 g of raw sediment, while the bioanode for an open circuit abiotic control (rGO-ab) was prepared by adding 114 g of sand plus 6 g of raw sediment (the sand/raw sediment ratio was the same as rGO-cc and rGO-oc tests). Sediments were previously contaminated with a Phe acetone-based stock solution, in order to reach 6 mg_{Phe} kg_{dw}^{-1} in each vessel (apart from the contribution deriving from sediments, dry weight is calculated considering the amount of sand and rGO). This very low contamination, if compared to the previous studies (see section 4.2.1 and 4.2.2), was adopted in order to avoid toxic effects on the unacclimated biomass already colonising the sediment, which was directly spiked with the Phe stock solution and then inserted into the glass vessels. 10 mL of inoculum taken from daughter serum flasks were added to rGO-cc and rGO-oc, prior to start with percolating bioanode formation. This inoculum served to fasten the biomass growth within the SBESs, since in the presence of the sole Phe as carbon source it could have been quite slow. Conductivity measurements were performed as described in section 4.2.3.2. After the electro-reduction and the conductivity measurements, the saline medium was drained from the BESs and replenished with 200 mL of culturing medium in rGO-cc and rGO-oc, and 100 mL of culturing medium in rGO-ab (composition provided above). In addition, 5% v/v of glutaraldehyde was added to rGO-ab in order to kill the biomass within the reactor (Erby *et al.*, 2015), hence quantify the removal of Phe not associated to a biological process. All three SBESs were incubated at 30° C and operated for 53 days. WE of rGO-cc was poised at 0 $V_{Ag/AgCl}$ for 33 days, and then at 0.4 $V_{Ag/AgCl}$ for 20 days. SBESs adopted in this study are shown in Figure 4.28.

  Solid samples were taken at day 0 and day 52: Phe extraction and analysis were performed according to section 4.2.1.2.

Figure 4.28 *Digital picture of the SBESs adopted in this study: rGO-cc was operated in closed circuit, while rGO-oc and rGO-ab were operated in open circuit (glutaraldehyde was added to rGO-ab in order to kill the biomass within the reactor).*

4.2.4.3 Results and discussion

Toluene degradation assessment and current profile. As to toluene degradation, results are displayed in Figure 4.29.

Removal efficiency achieved in only 14 days of operation was equal to 72%, hence indicating that biomass, which have grown attached to the percolating bioanode and developed in the presence of sodium acetate (as described in section 4.2.3.2) was able to degrade hydrocarbons. Previous experiments demonstrated, in fact, that *Geobacter metallireducens*, grown in the presence of acetate, could readily be adapted to work on benzoate, and then toluene (Zhang *et al.*, 2010).

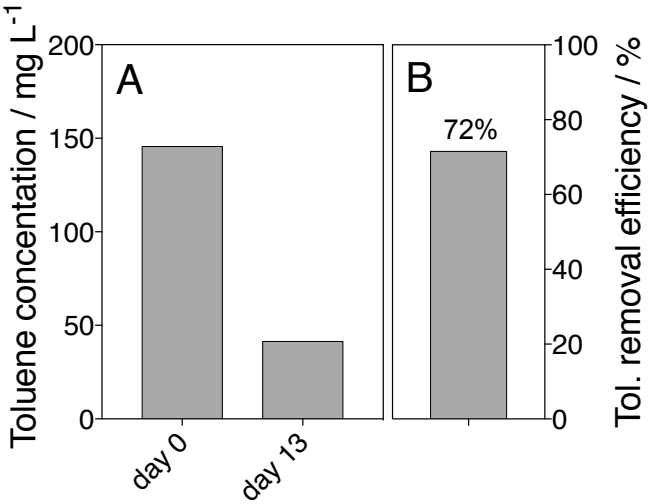

Figure 4.29 *A) Toluene concentration in rGO2 measured at day 0 and at day 13 (when the reactor was stopped); B) toluene removal efficiency after 14 days operation.*

Current output associated to toluene degradation was equal to an average value of 2.2 mA (or 11.5 A m^{-3}) and resulted in a cumulative charge of 2,598 C (eliminating the current amount associated to the initial discharge, which is capacitive current) (Figure 4.30). However, the stoichiometric cumulative charge that would have been associated to toluene consumption was 944 C. The Coulombic efficiency of the system resulted in approximately 404%. This result indicated that the one recorded is not the actual current associated to toluene degradation, but rather a current background generated by the system: in fact, in the previous study and in the presence of acetate, rGO2 was delivering 105 mA. Higher toluene concentrations would have been probably required to achieve higher current outputs not hidden by the background signal.

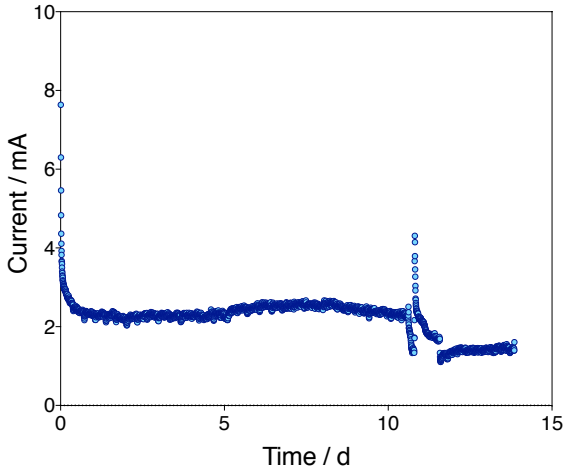

Figure 4.30 *Current output recorded during toluene degradation assessment. The average value was 2.2 mA, corresponding to 11.5 A* m^{-3}.

Tests of GO reduction to rGO with a model soil formed by sediment mixed with sand. While in the previous study only quartz sand was used as model soil (see section 4.2.3), here, according to the necessity to adapt percolating bioanodes to a real sediment composition, tests using different raw sediment percentages mixed with artificial sand were done (Figure 4.31).

The decreased porosity of the system induced by the presence of sediments hindered the rGO formation, likely due to mass transfer issues. The 5% sediment test-tube achieved the highest electrical conductivity (3±1 mS cm^{-1}), which was one order of magnitude higher than the other conductivities displayed in Figure 4.31. Conductivity of this test-tube was also over 8 times lower than the value achieved after 36 hours reduction with the 2000 mg_{GO} kg_{dw}^{-1} test-tube filled only with quartz sand, in the previous study (see section 4.2.3.3). This result indicated that, under the hypothesis of a real application of this bioremediation method, the formation of

rGO-soil or sediment composite bioanodes should be carefully evaluated in advance; in fact, if the porosity becomes too low, the percolating bioanode formation could not be effective.

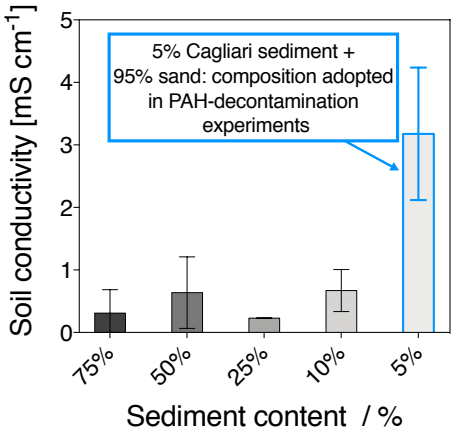

Figure 4.31 *Soil conductivities of different model soils calculated following the application of the i-V method (after 36 hours of electrochemical reduction). Conductivities were reported as averages and standard deviations (n=3). Model soils were obtained by adding different raw sediment percentages to quartz sand. 5% sediment and 95% sand was the composition adopted in Phe-degradation experiments, due to the highest value of conductivity that was achieved after reduction.*

Therefore, given the difficulty to induce a high conductivity in the presence of certain percentages of sediment, and according to the primary aim of this study, which was to investigate Phe degradation using the percolating bioanode composite (hence excluding the effect of the model soil adopted within the system), the soil composition with 5% sediment and 95% sand was preferred to the others.

Phenanthrene degradation assessment and current profile. In order to assess Phe degradation, three SBESs were assembled. After approx. 70 hours reduction, soil conductivities were 1.5±0.1 mS cm^{-1} in rGO-cc, 6.7±3.3 mS cm^{-1} in rGO-oc and 5.2±1.3 mS cm^{-1} in rGO-ab. These variations are in line with the typical variation of conductivity that was observed when sediment was added to sand (see also Figure 4.31).

Figure 4.32 shows that the highest Phe removal efficiency was achieved in the closed circuit system (53%). However, in line with results obtained in the previous studies (see sections 4.2.1 and 4.2.2), although the bioelectrochemical process enhanced the degradation, only slightly lower removal efficiencies were achieved in the open circuit control (rGO-oc). The presence of sulphate in the system was, in fact, high enough to achieve complete degradation of the very low quantity of phenanthrene spiked to the sediments: stoichiometric calculations showed that

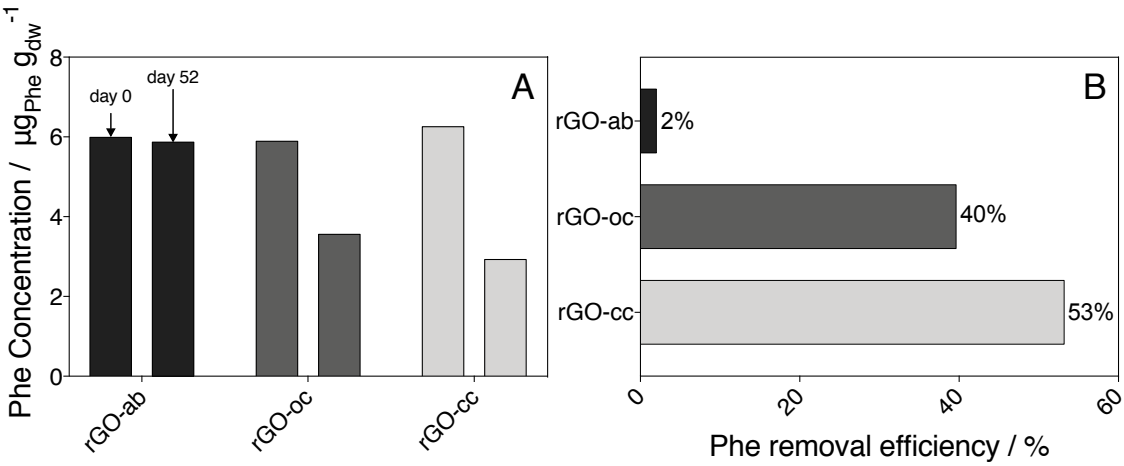

Figure 4.32 *A) Phe concentrations measured in each SBES at day 0 and day 52 (end of the experiment); B) Phe removal efficiencies achieved within the systems.*

sulphates were able to take 4.70 mmol e^- *vs* 0.05 mmol e^- released by Phe consumption associated to rGO-oc. Although an effect of sulphate on the Phe degradation in rGO-cc could not be excluded, the current output delivered by the closed circuit system could be putatively associated to the bioelectrochemical process (see below). As to rGO-ab, Phe removal efficiency was only 2%, thereby indicating that no abiotic losses occurred within the SBES.

The current profile associated to rGO-cc is displayed in Figure 4.33. In the first part of the experiment, the potential applied *vs* Ag/AgCl was set at 0 V, according to the previous study (section 4.2.3). Since biological activity in rGO-cc could rely only on the biomass added with the sediments (12.5 g of raw sediment) and with the inoculum of rGO flakes (coming from serum flasks), and since the only carbon donor added to the system was Phe (whose removal rate is slower than sodium acetate), the bacterial growth was expected to be slow. Therefore, the potential was maintained for 33 days. However, current remained constantly equal to 0 μA.

Therefore, during the last 20 days of experiment, 0.4 $V_{Ag/AgCl}$ were imposed to the WE, and the average current associated to this potential was 21.3 μA, equal to 0.11 A m^{-3}. The Coulombic efficiency calculated accounting for the removed Phe was 116% therefore the current recorded was only slightly higher than the hypothetical value that would have been associated to Phe degradation fully due to the bioelectrochemical process. The overestimation of the current output could be putatively related to the presence of a capacitive current associated to the high volume-electrode (likely discharged in the first part of the profile). However, discarding the first part, the current recorded was probably higher than the signal-to-noise ratio. Indeed, since the performance of the closed circuit SBES was enhanced compared to the open circuit system

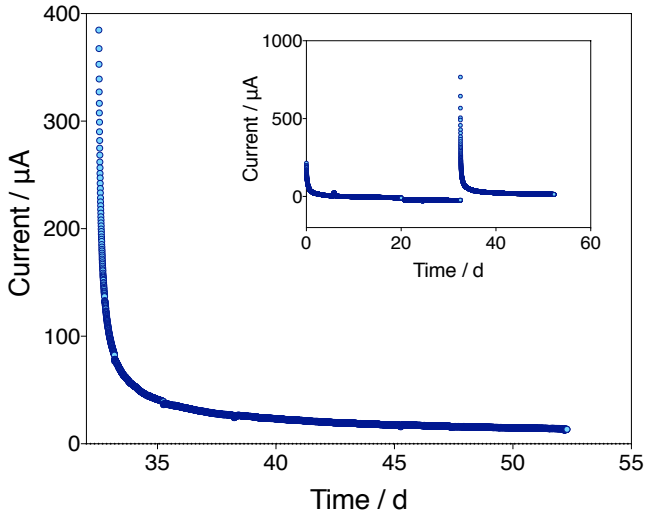

Figure 4.33 *Current profile recorded when 0.4 $V_{Ag/AgCl}$ were imposed to the bioanode: not considering the capacitive current recorded in the first part of the profile, the average current associated to Phe removal was 21.3 µA, equal to 0.11 A m^{-3}. The graph placed at the top, in the right corner, shows the complete current profile: 0 $V_{Ag/AgCl}$ were applied during the first 33 days of operation; this value was chosen according to the previous study (section 4.2.3), in order to allow biomass growth within the system; however, since current output was stable at 0 µA, a slightly higher potential (i.e., 0.4 $V_{Ag/AgCl}$) was applied subsequently.*

(Figure 4.32), the positive current associated to rGO-cc suggested that the degradation achieved within rGO-cc was at least partially associated to the bioelectrochemical process.

4.2.4.4 Conclusions

Although the experimental work presented in this section had a very preliminary connotation, the results achieved within both experiments were encouraging: both systems reached high organic compounds removal efficiencies. While toluene degradation was due to the presence of an abundant biomass grown with acetate, which was previously inoculated from a parent BES (see section 4.2.3.2), Phe degradation was associated only to the autochthonous biomass living in the sediment (which was also the same inoculated to serum flasks for achieving GO reduction to rGO while using Phe as the sole carbon donor; rGO flakes were then inoculated to the SBESs). This result indicated the possibility to effectively use bioanodes without an inoculum of specifically grown electroactive bacteria, since real soils and sediments are rich in a broad variety of microorganisms, which could possibly be electroactive, and also be able to degrade recalcitrant organic compounds.
Moreover, despite the very low Phe concentration fed to rGO-cc in the second study, a current higher than the signal-to-noise ratio was putatively related to this degradation.

The promising results achieved in this study suggested further investigations: 1) since tests of GO reduction made in the presence of different percentages of sediments indicated that porosity

is a key parameter to consider in the application of this composite electrodes, the possibility to apply GO reduction should be evaluated in order to better discriminate when the process is effectively applicable (the sediment used in this study came from a specific site, but maybe the use of another sediment, with other physical characteristics and composition, would have led to different results); 2) bioremediation performances in the presence of high contaminants concentrations should be evaluated; 3) the possibility to apply GO reduction *in situ* should be carefully explored, evaluating *in situ* specific conditions (*e.g.*, apart from the already described soil or sediment composition, hydraulic dynamics of the subsurface can as well influence the rGO network formation). In fact, if applied *in situ,* this system could serve to treat large portions of contaminated sites and could also be able to degrade contaminated groundwater fluxes, hence simulating a permeable reactive barrier.

CONCLUSIONS

Until now, bioremediation approaches have mainly addressed to the removal of recalcitrant organic compounds (such as PAHs) with aerobic treatments, due to the faster kinetics than anaerobic treatments: for instance, 60 days oxidation were necessary for the complete mineralisation of added phenanthrene (1.3 g L^{-1}) under sulphate reducing conditions and in the presence of a biomass incubated from a heavily PAHs-contaminated site, already able to work on these compounds (Coates *et al.,* 1996), while, following 3-5 hours lag phase, an aerobic mixed culture collected from known sites of continuous petrochemical effluent discharge and adapted to work on Phe as carbon source, completely degraded 5 mg_{Phe} L^{-1} within 28 hours (Yuan *et al.*, 2000). Anaerobic PAH degraders growth, in general, is very slow, with doubling times from 1-2 weeks up to months (Meckenstock *et al.*, 2016). Of course, it must be noted that both kinetics can be significantly reduced in the presence of an aged contamination and of mixed PAHs.

Therefore, in the first part of this study, since it is a well-established treatment for recalcitrant fluxes, the use of a conventional aerobic bioremediation treatment, *i.e.* SS-SBR technology, was explored. The aim of this experimental part was to investigate which setting of the process parameters could guarantee the best performances while treating sediments from Cagliari port (SBR-C) spiked with 4-mixed PAHs (fluorene and phenanthrene, 3-ring compounds, and fluoranthene and pyrene, 4-ring PAHs), when microbes were biostimulated (through the adjustment of nutrients and the addition of saponins as surfactants) and the SBR was bioaugmented. Moreover, in order to test if the same reactor configuration could work on sediments coming from different sites (hence characterised by diverse compositions and inhabited by a different biomass), another SS-SBR (SBR-EK) operated biostimulation (in this case through the adjustment of nutrients and the addition of sodium acetate as co-substrate) on sediments coming from El Kantaoui port (Tunisia). SBR-EK activity was followed for nearly one year, while SBR-C operated for approximately 2 years; both reactors were working in 5 days cycles. To the knowledge of the author, time length of 5 days is the shortest applied in SS-SBR treating marine sediments contaminated by PAHs.

Since the sediments used came from touristic ports, and a very low PAHs-contamination was measured in the site of origin, the autochthonous biomass was not already used to work with these compounds; however, both SBRs showed high removal efficiencies during their whole

experimental campaigns. Nevertheless, these efficiencies were not always coupled to the compliance with threshold levels of Italian regulations (*i.e.*, the target of this thesis, whose compliance corresponds to a sediment suitable for specific reuse or disposal). In fact, considering SBR-C, L_2 levels were met for each compound only during Phase A, when S/L ratio was 0.1, PAHs concentration did not overcome 200 $mg_{PAHs}\,kg_{dw}^{-1}$ and the vOLR was 0.4 $mg_{PAHtot}\,L^{-1}\cdot d^{-1}$. The increase of PAHs fed to the system (halving the S/L ratio and keeping constant the vOLR) and the increase of vOLR (by increasing the VER), they both ended in a general worsening of the process performance; the following inoculum of a specific strain isolated from Cagliari sediments, and able to work on pyrene removal, was not able to restore a good reactor operation. Not surprisingly, pyrene was the most difficult compound to treat, especially when the reactor was working under the highest vOLR; the difficulty to degrade more than 3-ring PAHs and to degrade mixed PAHs was already discussed in section 1.6. Interestingly, despite the significant differences in sediments characteristics and initial operating conditions, very good process performances were achieved also in SBR-EK when the same total PAHs concentration, S/L and vOLR, which had led to the best results in SBR-C, were applied.

This study confirms that SS-SBR is a suitable treatment to bioremediate solid matrixes polluted by recalcitrant compounds. The results achieved in both reactors lead to a few remarks:

- apart from applying the biostimulation through regulation of nutrients and oxygen (or the addition of other electron acceptors), the addition of surfactants or a co-substrate, appear recommended and must be suitably evaluated case by case basis (depending on the characteristics of the sediment to be treated, which must be always evaluated in advance);
- the maximum suitable S/L ratio to work with is 0.1 (or a ratio not too much higher than 0.1);
- too high PAHs concentration could be toxic for the microorganisms, if the biodegradative capability of the biomass is overcome;
- once known the inlet PAHs concentration and set the S/L ratio, the VER must be decided in order to avoid an excessive increase of the vOLR;
- despite the results achieved in this experimental work, the opportunity to apply effectively bioaugmentation could be considered and investigated.

On the other hand, the use of SS-SBR treatment entails a number of costs that cannot be avoided:

- the technology is *ex-situ* (or *ad site*), applied in bioreactors (which allow an accurate control of the process parameters), so it involves the investment cost of the reactor and costs related to the excavation or dredging of the contaminated matrix (even if the dredging can be necessary for practical reasons);
- continuous aeration (if required), mixing and pH control are important operating costs;
- since the treatment is applied to slurries, pre-treatments of the matrix (such as sieving) and the addition of huge quantities of water must be considered;
- nutrients and, if necessary, surfactants or co-substrates must always be regulated, thereby representing other operating costs.

In this context, the application of microbial electrochemical technologies, which are not considered a conventional process for bioremediation of toxic organic compounds, should be appropriately considered. This process is operated in reducing conditions, hence it does not require oxygen regulation nor amendment of other chemicals that would constitute terminal electron acceptors for pollutants (such as PAHs) oxidation and that must inevitably be replenished: indeed, the anodes used in the process replace the necessity for oxygen or other chemicals amendment, since they constitute an inexhaustible sink for electrons. Moreover, this process does not require nutrients addition and should not implicate bioaugmentation, since soils and sediments are already enriched in electroactive microbial communities (which were shown to be spread in natural environments). Electrodes, membranes and current collectors implicate costs, which have noticeably decreased in the last decade: nowadays, membranes and electrodes costs are ~50 US$ m^{-2} and ~15 US$ m^{-2}, respectively; conversely, costs reported by Rozendal *et al.* (2008) were about 10 times higher. If operated as SMFCs, BESs do not require energetic costs, because the process is self-sustained. On the other hand, if the process is not spontaneous, small voltages or currents are applied in order to sustain the process (in this case, the process entails also the operative cost for the electrical energy necessary to sustain a power source). Moreover, if the aim is to monitor the effectiveness of a bioremediation process, the use of a data logger could be a valid help to monitor continuously its performances (hypothetically also from remote sites), thanks to the presence of a current output.

The use of SMFCs to preliminarily assess the feasibility of phenanthrene degradation was here investigated. Phenanthrene was spiked to the same marine sediments used in SBR-C (coming

from Cagliari port). Although sulphates (which composed the sediment and were added with the biological medium used in the experiments) probably played a role in the degradation process, the presence of the anode fastened the removal compared to open circuit controls, hence indicating the successful development and maintenance of a phenanthrene degrading biomass in the system. Nevertheless, in this system current outputs were low, as is typical for sediment bioelectrochemical systems, especially when operating on slowly biodegradable compounds (see below).

The peculiar geometrical configuration adopted in these SMFCs (a bottle, constituting the anodic chamber, with a PVC tube inserted in the cap, separated from the anodic chamber by a membrane, which was instead the cathodic chamber), wherein the sediment was inserted as a slurry and which operated in well-mixed conditions, makes them particularly suitable for their integration in *on-site* slurry bioreactors. However, since mechanical stirring was still applied, the only advantage of these SMFCs compared with SS-SBR, was the absence of aeration costs and of costs for nutrients regulation and saponins dosing. In addition, SMFCs involved membrane and electrodes investments costs. A careful evaluation of the electrode and membrane surfaces required for implementing this kind of reactors in a larger scale should be done, in order to compare the costs of the two processes in a real scale.

Considering, instead, removal rates, the aerobic process resulted, as expected, in higher kinetics: taking one of the profiles obtained in SBR-C when the reactor was giving its best performances, and the degradation profile obtained in SMFC-a (in the presence of acetate dosed to enhance microbial growth), and fitting both degradation profiles with a one phase decay kinetic, k was -8.781 d^{-1} in the aerobic process and -0.9443 d^{-1} in the anaerobic one. However, since SMFC-a worked in a 20 days test, the system was probably still in its start-up when degradation was considered; therefore, the removal rate might have been slightly higher in the presence of a completely developed biofilm.

The results achieved with SMFCs highlighted, from one side, the possibility to degrade recalcitrant compounds from marine sediments with BESs, but on the other side, the existence of a gap between SS-SBR and the use of this specific SMFCs configuration. Therefore, under the hypothesis to render the bioelectrochemical process competitive with the aerobic bioslurry treatment, this PhD research focussed on find solutions to overcome some drawbacks typical of SBES.

As already discussed, BESs applied to soils and sediments suffer from low signal-to-noise ratios that makes it difficult to couple current outputs to the removal of a specific contaminant. In

fact, low current outputs are often determined by limited mass transport of contaminants towards the electrode surface and by limited interfacial and long-range electron transfer kinetics, which together limit the *radius of influence* of the bioelectrochemical treatment; low currents are also determined by the slow biodegradability of certain contaminants such as PAHs. In addition, contrary to processes occurring in liquid phase, the presence of soil particles and the absence of mixing conditions (in general SBES are characterised by the absence of stirring), contribute to generate strong concentration gradients around the electrodes, which limit the kinetics of the remediation process. Therefore, due to these considerations, the bioelectrochemical process could lose his characteristic to be easy-to-monitor, which constitutes instead one of his main strengths. Moreover, although bioelectrochemical systems applied with bioremediation purposes can be hypothetically deployed *ex-situ* or *in situ*, the limited *radius of influence* make the application *in situ* unsuitable.

In order to overcome the discussed drawbacks, the possible solutions already outlined in this thesis are:

- use of materials suitable for catalyzing bacteria activity;
- increase of ionic conductivity, thereby improving the mass transport;
- increase of the specific surface that constitutes the site for reactions, thereby extending the long-range electron transfer distance (*i.e.*, increase of the soil conductivity).

Along these lines was the formation of percolating bioanodes obtained with the electrochemical reduction of a graphene oxide dispersion within the pores of a model soil (quartz sand), hence inducing electrical properties to an otherwise insulating material. Reduced GO is similar to pristine graphene, which is a 2-dimensional carbon material with outstanding electric conductivity, excellent mechanical properties and biocompatibility. In general applications, the main advantage given by the use of graphene oxide is the possibility to amend this material in the form of liquid dispersions to soil, that allows an easier distribution through its porosity.
When reduced for 60 hours in test-tubes, a solution containing 2000 mg_{GO} L^{-1} increased the electric conductivity of the model soil not amended with GO by four orders of magnitude. Interestingly, when supplemented with an inoculum of electroactive microorganisms and metabolic electron donor acetate, after electrochemical reduction, GO-amended systems outperformed the controls by delivering more than 30 times higher current, indicating that probably a much larger volume of soil contributed to the catalytic current production. These results suggested the possibility to apply this easy and cost-effective method to real soils, hence

overcoming the main drawbacks typical of SBES stated before. Moreover, the same system was tested with a toluene contamination: in only 13 days the percolating bioanode achieved the removal of the 72% of toluene.

However, when quartz sand was mixed with different percentages of real sediment in order to simulate different real soils, the formation of percolating bioanodes resulted more difficult due to mass transfer issues; this result indicated that soil porosity is a key factor to be considered when deciding to apply this technology.

In the end of this PhD, a percolating bioanode formed by mixing the 5% sediment with the 95% sand was used to test phenanthrene degradation. Although the initial Phe concentration was quite low, bacteria growing on the anodic surface were capable to use phenanthrene as the sole carbon donor and to degrade the 53% of the spiked compound within 53 days, and also the system was able to deliver a current probably higher than the signal-to-noise ratio. Indeed, the actual process performance could have been underestimated: since the autochthonous biomass was growing without the addition of a readily degradable co-substrate (able to promote the start-up of the system), 53 days could have been a short time for the electrode surface to be fully covered by an electroactive biofilm, thereby the system might not have been working at steady state. However, this preliminary study elucidated the possibility to effectively degrade phenanthrene within this SBES configuration, though bioremediation performances in the presence of high contaminants concentrations should be next assessed.

Clearly, the possibility to compare process performances of the conventional SS-SBR treatment and the percolating bioanodes is still far away. Before, it would be recommended to assess if the process of electro-reduction of GO within a real matrix is effectively feasible: the sediment used in this study came from a specific site, but maybe the use of another sediment, with other physical characteristics (hence a different porosity, given by a high percentage of sand), or the use of a porous soil, could have led to different conductivities. In addition, the possibility to apply the GO reduction *in situ* is another interesting option that should be carefully explored: this system could serve, in fact, to treat contemporarily large contaminated volumes, avoiding the continuous replenishment of chemicals (that once in the subsurface are depleted and can also diffuse away from the site of injection); rGO-soil composite could also be able to treat contaminated groundwater fluxes, hence simulating a permeable reactive barrier. In both cases, together with the soil or sediment composition, also the hydraulic dynamics of the subsurface can influence the rGO network formation.

Besides, an economic assessment including installation, operational and monitoring costs would be required in order to compare different treatment technologies. However, given the preliminary connotation of the experiments regarding microbial electrochemical technologies, a detailed budget evaluation which compares conventional and innovative treatments is beyond the purposes of this PhD thesis. As to bioslurry reactors, treatment costs indicated in literature ranged from 130 to 200 US$ m^{-3} of soil, while capital, equipment, design and construction costs ranged between 125,000 US$ and 2,000,000 US$ (Khan *et al.*, 2004). Given the novelty of the remediation solution proposed here, data involving the use of rGO-soil composite electrodes are still not available in literature. However, an assessment of electrodes' building costs and an evaluation of the hypothetic operational costs for the treatment of a real case contamination are reported herein. Nowadays graphene oxide is only employed for research and development purposes, hence the cost for building rGO electrodes is still very high (1,000 US$ per kilogram of dry weight); future projections, which consider a high volume graphene oxide production, estimate that its cost will reach 25 US$ kg_{dw}^{-1} (Ekhlasi *et al.*, 2018; https://www.graphene-info.com/abalonyx-sees-go-production-cost-reaching-22-eurokg-high-volumes). Considering forming a rGO-soil composite electrode (volume of 1 m^3) with 2,000 mg_{GO} kg_{dw}^{-1} (as described above), and assuming as soil the quartz sand used in the previous electro-reduction experiments (density of about 1.5 kg dm^{-3}) (see section 4.2.3) the quantity of graphene oxide dosed per cubic meter would be equal to 3,000 g_{GO}: the cost for the electrode building would be today 3,000 US$ m^{-3}, whereas according to future predictions, the cost will decrease to 75 US$ m^{-3}. Under the hypothesis that this cubic meter of soil is contaminated by Phe (150 mg_{Phe} kg_{dw}^{-1}), and that the contamination can be removed through a bioelectrochemical process in 50 days, the theoretical current produced by this process would be 1.86 A. Now considering a conservative value of cell voltage of 2 V, the power produced by the SBES in 50 days would be 4.464 kWh. The average cost of electrical current in Europe, calculated in 2017, was 0.204 € per kWh of electrical current, *i.e.*, 0.23 US$ kWh^{-1} (https://1-stromvergleich.com/electricity-prices-europe/): it means that, under the hypothesis done above, the operational cost of the system would be 1.04 US$ m^{-3} of contaminated soil treated, which would represent today only the 0.035% of the electrode building cost and the 1.4 % considering, instead, future cost previsions (*i.e.*, building rGO-soil composite electrodes represents the major SBES cost item). Therefore, reaching a low graphene oxide cost is essential in order to render the treatment applicable also in the large scale. However, given the encouraging results obtained in this study with rGO-soil composite electrodes, the possible applications at reasonable costs in the future, and the growing interest for two-dimensional carbon-based materials (for example in the field of

groundwater remediation), the one proposed here seems to represent an interesting solution for future applications, which deserves for further investigations.

References

Abbondanzi, F., L. Bruzzi, T. Campisi, A. Frezzati, R. Guerra, and A. Iacondini. 2006. Biotreatability of polycyclic aromatic hydrocarbons in brackish sediments: Preliminary studies of an integrated monitoring. International Biodeterioration and Biodegradation 57:214–221.

Abdel-Shafy, H. I., and M. S. M. Mansour. 2016. A review on polycyclic aromatic hydrocarbons: Source, environmental impact, effect on human health and remediation. Egyptian Journal of Petroleum 25:107–123.

Albertsen, M., S. M. Karst, A. S. Ziegler, R. H. Kirkegaard, and P. H. Nielsen. 2015. Back to basics–the influence of DNA extraction and primer choice on phylogenetic analysis of activated sludge communities. PloS one 10:e0132783.

Alexander, M. 1999. Biodegradation and bioremediation. Gulf Professional Publishing.

Alvarez, P., and W. Illman. 2005. Bioremediation and Natural Attenuation. Vol. 27. John Wiley & Sons.

Ambrosoli, R., L. Petruzzelli, J. L. Minati, and F. A. Marsan. 2005. Anaerobic PAH degradation in soil by a mixed bacterial consortium under denitrifying conditions. Chemosphere 60:1231–1236.

ANPA. 2001. Metodi di Analisi del compost. Manuali e Linee guida 3:55–70.

Aulenta, F., A. Canosa, P. Reale, S. Rossetti, S. Panero, and M. Majone. 2009. Microbial reductive dechlorination of trichloroethene to ethene with electrodes serving as electron donors without the external addition of redox mediators. Biotechnology and Bioengineering 103:85–91.

Bamforth, S. M., and I. Singleton. 2005. Bioremediation of polycyclic aromatic hydrocarbons: Current knowledge and future directions. Journal of Chemical Technology and Biotechnology 80:723–736.

Boldrin, B., A. Tiehm, and C. Fritzsche. 1993. Degradation of phenanthrene, fluorene, fluoranthene, and pyrene by a Mycobacterium sp. Applied and Environmental Microbiology 59:1927–1930.

Bonanni, P. S., D. Massazza, and J. P. Busalmen. 2013. Stepping stones in the electron transport from cells to electrodes in Geobacter sulfurreducens biofilms. Physical Chemistry

Chemical Physics 15:10300–10306.

Bond, D. R., D. E. Holmes, L. M. Tender, and D. R. Lovley. 2002. Electrode-Reducing Microorganisms That Harvest from Marine Sediments 295:483–485.

Bond, D. R., and D. R. Lovley. 2003. Electricity Production by Geobacter sulfurreducens Attached to Electrodes Electricity Production by Geobacter sulfurreducens Attached to Electrodes. Applied and Environmental Microbiology 69:1548–1555.

Bond, D. R., and D. R. Lovley. 2005. Evidence for involvement of an electron shuttle in electricity generation by Geothrix fermentans. Applied and environmental microbiology 71:2186–2189.

Bortone, G. 2007. Sediment Treatment – a General Introduction. Pages 1–10 *in* P. Bortone, editor. Sediment and Dredged Material Treatment. Elsevier Science.

Boyd, D. A., R. M. Snider, J. S. Erickson, J. N. Roy, S. M. Strycharz-Glaven, and L. M. Tender. 2015. Theory of Redox Conduction and the Measurement of Electron Transport Rates Through Electrochemically Active Biofilms. Pages 177–210. Biofilms in Bioelectrochemical Systems: From Laboratory Practice to Data Interpretation.

Buchanan, J. B. 1984. Sediment analysis. 41-45. Methods for the study of marine benthos. Blackwell. Londres.

Bulleri, F., and M. G. Chapman. 2010. The introduction of coastal infrastructure as a driver of change in marine environments. Journal of Applied Ecology 47:26–35.

Camedda, C., and B. Virdis. 2018. Percolating bioanodes achieve high current output in sediment bioelectrochemical systems:4072.

Cançado, L. G., A. Jorio, E. H. M. Ferreira, F. Stavale, C. A. Achete, R. B. Capaz, M. V. O. Moutinho, A. Lombardo, T. S. Kulmala, and A. C. Ferrari. 2011. Quantifying defects in graphene via Raman spectroscopy at different excitation energies. Nano letters 11:3190–3196.

Caporaso, J. G., J. Kuczynski, J. Stombaugh, K. Bittinger, F. D. Bushman, E. K. Costello, N. Fierer, A. G. Pena, J. K. Goodrich, and J. I. Gordon. 2010. QIIME allows analysis of high-throughput community sequencing data. Nature methods 7:335.

Cassidy, D. P., S. Efendiev, and D. M. White. 2000. A comparison of CSTR and SBR bioslurry reactor performance. Water Research 34:4333–4342.

Chandrasekhar, K., and S. Venkata Mohan. 2012. Bio-electrochemical remediation of real field

petroleum sludge as an electron donor with simultaneous power generation facilitates biotransformation of PAH: Effect of substrate concentration. Bioresource Technology 110:517–525.

Chang, I.-S., H.-S. Moon, O. Bretschger, J.-K. Jang, H.-I. Park, K. H. Nealson, and B.-H. Kim. 2006. Electrochemically active bacteria (EAB) and mediator-less microbial fuel cells. Journal of Microbiology and Biotechnology 16:163–177.

Chaudhuri, S. K., and D. R. Lovley. 2003. Electricity generation by direct oxidation of glucose in mediatorless microbial fuel cells. Nature biotechnology 21:1229.

Chiavola, A., R. Baciocchi, and R. Gavasci. 2010. Biological treatment of PAH-contaminated sediments in a Sequencing Batch Reactor. Journal of Hazardous Materials 184:97–104.

Coates, J. D., R. T. Anderson, D. R. Lovley, J. D. Coates, and R. T. Anderson. 1996. Oxidation of Polycyclic Aromatic Hydrocarbons under Sulfate-Reducing Conditions . These include : Oxidation of Polycyclic Aromatic Hydrocarbons under Sulfate-Reducing Conditions 62:1099–1101.

Coates, J. D., J. Woodward, J. Allen, P. Philp, and D. R. Lovley. 1997. Anaerobic degradation of polycyclic aromatic hydrocarbons and alkanes in petroleum-contaminated marine harbour sediments. Applied and Environmental Microbiology 63:3589–3593.

Cookson Jr, J. T. 1995. Bioremediation engineering: Design and application. McGraw-Hill, Inc.

Couling, N. R., M. G. Towell, and K. T. Semple. 2010. Biodegradation of PAHs in soil: Influence of chemical structure, concentration and multiple amendment. Environmental Pollution 158:3411–3420.

Creasey, R. C. G., A. B. Mostert, T. A. H. Nguyen, B. Virdis, S. Freguia, and B. Laycock. 2018. Microbial nanowires – Electron transport and the role of synthetic analogues. Acta Biomaterialia 69:1–30.

Daghio, M., F. Aulenta, E. Vaiopoulou, A. Franzetti, J. B. A. Arends, A. Sherry, A. Suàrez-Suàrez, I. M. Head, G. Bestetti, and K. Rabaey. 2017. Electrobioremediation of oil spills. Water Research 114:351–370.

Dean-Ross, D. 2005. Biodegradation of selected PAH from sediment in bioslurry reactors. Bulletin of Environmental Contamination and Toxicology 74:32–39.

Dean-Ross, D., J. Moody, and C. E. Cerniglia. 2002. Utilization of mixtures of polycyclic

aromatic hydrocarbons by bacteria isolated from contaminated sediment. FEMS Microbiology Ecology 41:1–7.

Decreto 15 luglio 2016, n. 173. Regolamento recante modalità e criteri tecnici per l'autorizzazione all'immersione in mare dei materiali di escavo di fondali marini.

Dennis, P. G., B. Virdis, I. Vanwonterghem, A. Hassan, P. Hugenholtz, G. W. Tyson, and K. Rabaey. 2016. Anode potential influences the structure and function of anodic electrode and electrolyte-associated microbiomes. Scientific Reports 6:1–11.

Dheilly, A., I. Linossier, A. Darchen, D. Hadjiev, C. Corbel, and V. Alonso. 2008. Monitoring of microbial adhesion and biofilm growth using electrochemical impedancemetry. Applied microbiology and biotechnology 79:157–164.

Dominguez-Benetton, X., S. Sevda, K. Vanbroekhoven, and D. Pant. 2012. The accurate use of impedance analysis for the study of microbial electrochemical systems. Chemical Society Reviews 41:7228–7246.

Domínguez-Garay, A., A. Berná, I. Ortiz-Bernad, and A. Esteve-Núñez. 2013. Silica colloid formation enhances performance of sediment microbial fuel cells in a low conductivity soil. Environmental Science and Technology 47:2117–2122.

Dreyer, D. R., S. Park, C. W. Bielawski, and R. S. Ruoff. 2010. Graphite oxide. Chemical Society Reviews 39:228–240.

Duran, R., and C. Cravo-Laureau. 2016. Role of environmental factors and microorganisms in determining the fate of polycyclic aromatic hydrocarbons in the marine environment. FEMS Microbiology Reviews 40:814–830.

Dutta, P. K., J. Keller, Z. Yuan, R. A. Rozendal, and K. Rabaey. 2009. Role of sulfur during acetate oxidation in biological anodes. Environmental Science and Technology 43:3839–3845.

Dutta, P. K., K. Rabaey, and Z. Yuan. 2008. Spontaneous electrochemical removal of aqueous sulfide 42:4965–4975.

EEA. 2018. European Union emission inventory report 1990-2016.

Ehlers, L. J., and R. G. Luthy. 2003. Contaminant bioavailability in improving risk assessment and remediation rests on better understanding bioavailability. Environmental Science & Technology 37:295–302.

Eigler, S., C. Dotzer, and A. Hirsch. 2012. Visualization of defect densities in reduced graphene

oxide. Carbon 50:3666–3673.

Ekhlasi, L., H. Younesi, and A. Rashidi. 2018. Populus wood biomass-derived graphene for high CO 2 capture at atmospheric pressure and estimated cost of production. Process Safety and Environmental Protection 113:97–108.

Engelbrektson, A., V. Kunin, K. C. Wrighton, N. Zvenigorodsky, F. Chen, H. Ochman, and P. Hugenholtz. 2010. Experimental factors affecting PCR-based estimates of microbial species richness and evenness. The ISME journal 4:642.

Erby, G., A. Nieddu, M. Piredda, C. Ruggeri, L. Serreli, E. Tamburini, and A. Carucci. 2014. Batch tests for the optimization of PAH bioremediation in Mediterranean Tourist Port Sediments. Page I2SM 2014 4th International Symposium on Sediment Management. MAGGIOLI SpA.

Erby, G., E. Tamburini, C. Ruggeri, E. Bullita, and A. Carucci. 2015. Bioaugmentation tests for PAH bioremediation in Mediterranean tourist port sediments. Crete:601–605.

Eweis, J. B., S. J. Ergas, D. P. Y. Chang, and E. D. Schroeder. 1998. Bioremediation principles. McGraw-Hill Book Company Europe.

Freguia, S. 2009. Organics oxidation. Pages 225–242 *in* K. Rabaey, L. Angenent, U. Schroder, and J. Keller, editors. Bioelectrochemical systems. IWA publishing.

Freguia, S., K. Rabaey, Z. Yuan, and J. Keller. 2007. Electron and carbon balances in microbial fuel cells reveal temporary bacterial storage behavior during electricity generation. Environmental science & technology 41:2915–2921.

Freguia, S., B. Virdis, F. Harnisch, and J. Keller. 2012. Bioelectrochemical systems: Microbial versus enzymatic catalysis. Electrochimica Acta 82:165–174.

Friman, H., A. Schechter, Y. Nitzan, and R. Cahan. 2012. Effect of external voltage on Pseudomonas putida F1 in a bio electrochemical cell using toluene as sole carbon and energy source. Microbiology 158:414–423.

Gan, S., E. V. Lau, and H. K. Ng. 2009. Remediation of soils contaminated with polycyclic aromatic hydrocarbons (PAHs). Journal of Hazardous Materials 172:532–549.

Gil, G.-C., I.-S. Chang, B. H. Kim, M. Kim, J.-K. Jang, H. S. Park, and H. J. Kim. 2003. Operational parameters affecting the performannce of a mediator-less microbial fuel cell. Biosensors and Bioelectronics 18:327–334.

Giordano, A., L. Stante, F. Pirozzi, R. Cesaro, and G. Bortone. 2005. Sequencing batch reactor

performance treating PAH contaminated lagoon sediments. Journal of Hazardous Materials 119:159–166.

Girguis, P. R., M. E. Nielsen, and C. E. Reimers. 2009. Fundamentals of benthic microbial fuel cells. Pages 327–346 *in* K. Rabaey, L. Angenent, U. Schroder, and J. Keller, editors. Bioelectrochemical systems. IWA Publishing.

Gonzàlez-Garcia, J., P. Bonete, E. Exposito, V. Montiel, A. Aldaz, and R. Torregrosa-Macià. 1999. Characterization of a carbon felt electrode: structural and physical properties ´. J. Mater. Chem.:419–426.

Greene, A. C., B. K. C. Patel, and S. Yacob. 2009. Geoalkalibacter subterraneus sp. nov., an anaerobic Fe (III)-and Mn (IV)-reducing bacterium from a petroleum reservoir, and emended descriptions of the family Desulfuromonadaceae and the genus Geoalkalibacter. International journal of systematic and evolutionary microbiology 59:781–785.

Grifoll, M., M. Casellas, J. M. Bayona, and A. M. Solanas. 1992. Isolation and characterization of a fluorene-degrading bacterium: identification of ring oxidation and ring fission products. Applied and environmental microbiology 58:2910–2917.

Hamdan, H. Z., D. A. Salam, A. R. Hari, L. Semerjian, and P. Saikaly. 2017. Assessment of the performance of SMFCs in the bioremediation of PAHs in contaminated marine sediments under different redox conditions and analysis of the associated microbial communities. Science of the Total Environment 575:1453–1461.

Haritash, A. K., and C. P. Kaushik. 2009. Biodegradation aspects of Polycyclic Aromatic Hydrocarbons (PAHs): A review. Journal of Hazardous Materials 169:1–15.

Hilder, M., B. Winther-Jensen, D. Li, M. Forsyth, and D. R. MacFarlane. 2011. Direct electro-deposition of graphene from aqueous suspensions. Physical Chemistry Chemical Physics 13:9187–9193.

Holmes, D. E., D. R. Bond, R. A. O'Neil, C. E. Reimers, L. R. Tender, and D. R. Lovley. 2004. Microbial communities associated with electrodes harvesting electricity from a variety of aquatic sediments. Microbial Ecology 48:178–190.

Hutchinson, A. J., J. C. Tokash, and B. E. Logan. 2011. Analysis of carbon fiber brush loading in anodes on startup and performance of microbial fuel cells. Journal of Power Sources 196:9213–9219.

IRSA-CNR. 2005. Gli ecosistemi e i sedimenti: Caratterizzazione dei sedimenti:91–98.

Irvine, R. L., P. S. Yocum, J. P. Early, and R. Chozick. 1993. Periodic processes for in situ and on-site bioremediation of leachates and soils. Water science and technology 27:97–104.

Isa, M. H., and G. K. Anderson. 2005. Molybdate inhibition of sulphate reduction in two-phase anaerobic digestion. Process Biochemistry 40:2079–2089.

de Jesus, E. B., L. R. P. de Andrade Lima, L. A. Bernardez, and P. F. Almeida. 2015. Inhibition of Microbial Sulfate Reduction By Molybdate. Brazilian Journal of Petroleum and Gas 9:95–106.

Jiao, Y., F. Qian, Y. Li, G. Wang, C. W. Saltikov, and J. A. Granick. 2011. Deciphering the electron transport pathway for graphene oxide reduction by Shewanella oneidensis MR-1. Journal of bacteriology:JB-00201.

Johnsen, A. R., L. Y. Wick, and H. Harms. 2005. Principles of microbial PAH-degradation in soil. Environmental Pollution 133:71–84.

Johnson, K., and S. Ghosh. 1998. Feasibility of anaerobic biodegradation of PAHs in dredged river sediments. Water Science and Technology 38:41–48.

Kato Marcus, A., C. I. Torres, and B. E. Rittmann. 2007. Conduction-based modeling of the biofilm anode of a microbial fuel cell. Biotechnology and Bioengineering 98:1171–1182.

Kato, S., K. Hashimoto, and K. Watanabe. 2012. Microbial interspecies electron transfer via electric currents through conductive minerals. Proceedings of the National Academy of Sciences 109:10042–10046.

Kennish, M. J. 2000. Practical handbook of marine science. crc press.

Kester, D. R., I. W. Duedall, D. N. Connors, and R. M. Pytkowicz. 1967. Preparation of artificial seawater. Limnology and oceanography 12:176–179.

Khan, F. I., T. Husain, and R. Hejazi. 2004. An overview and analysis of site remediation technologies 71:95–122.

Kim, B. H., T. Ikeda, H. S. Park, H. J. Kim, M. S. Hyun, K. Kano, K. Takagi, and H. Tatsumi. 1999. Electrochemical activity of an Fe (III)-reducing bacterium, Shewanella putrefaciens IR-1, in the presence of alternative electron acceptors. Biotechnology Techniques 13:475–478.

Kronenberg, M., E. Trably, N. Bernet, and D. Patureau. 2017. Biodegradation of polycyclic aromatic hydrocarbons: Using microbial bioelectrochemical systems to overcome an impasse. Environmental Pollution 231:509–523.

Kuppusamy, S., P. Thavamani, K. Venkateswarlu, Y. B. Lee, R. Naidu, and M. Megharaj. 2017. Remediation approaches for polycyclic aromatic hydrocarbons (PAHs) contaminated soils: Technological constraints, emerging trends and future directions. Chemosphere 168:944–968.

Laufer, K., J. M. Byrne, C. Glombitza, C. Schmidt, B. B. Jørgensen, and A. Kappler. 2016. Anaerobic microbial Fe(II) oxidation and Fe(III) reduction in coastal marine sediments controlled by organic carbon content. Environmental Microbiology 18:3159–3174.

Launen, L. A., V. H. Buggs, M. E. Eastep, R. C. Enriquez, J. W. Leonard, M. J. Blaylock, J. W. Huang, and M. M. Haggblom. 2002. Bioremediation of polyaromatic hydrocarbon-contaminated sediments in aerated bioslurry reactors. Bioremediation Journal 6:125–141.

Lee, J. Y., T. S. Kwon, and Y. C. Lee. 2017. Removal of polycyclic aromatic hydrocarbons from contaminated soil in a two-phase partitioning bioreactor. Korean Journal of Chemical Engineering 34:2418–2422.

Lei, L., A. P. Khodadoust, M. T. Suidan, and H. H. Tabak. 2005. Biodegradation of sediment-bound PAHs in field-contaminated sediment. Water Research 39:349–361.

Li, X., X. Wang, Y. Zhang, L. Cheng, J. Liu, F. Li, B. Gao, and Q. Zhou. 2014. Extended petroleum hydrocarbon bioremediation in saline soil using Pt-free multianodes microbial fuel cells. RSC Advances 4:59803–59808.

Li, X., X. Wang, Y. Zhang, Q. Zhao, B. Yu, Y. Li, and Q. Zhou. 2016. Salinity and Conductivity Amendment of Soil Enhanced the Bioelectrochemical Degradation of Petroleum Hydrocarbons. Scientific Reports 6:1–11.

Logan, B. E., D. Call, S. Cheng, H. V. M. Hamelers, T. H. J. A. Sleutels, A. W. Jeremiasse, and R. A. Rozendal. 2008. Microbial Electrolysis Cells for High Yield Hydrogen Gas Production from Organic Matter. Environmental science & technology 42:8630–8640.

Logan, B. E., and K. Rabaey. 2012. Conversion of Wastes into Bioelectricity and Chemicals by Using Microbial Electrochemical Technologies Conversion of Wastes into Bioelectricity and Chemicals by Using Microbial Electrochemical Technologies 337.

Lovley, D. R. 2012. Electromicrobiology. Annual Review of Microbiology 66:391–409.

Lu, H., A. Oehmen, B. Virdis, J. Keller, and Z. Yuan. 2006. Obtaining highly enriched cultures of Candidatus Accumulibacter phosphates through alternating carbon sources. Water Research 40:3838–3848.

Lu, L., H. Yazdi, S. Jin, Y. Zuo, P. H. Fallgren, and Z. J. Ren. 2014. Enhanced bioremediation of hydrocarbon-contaminated soil using pilot-scale bioelectrochemical systems. Journal of Hazardous Materials 274:8–15.

Madigan, M. T., K. S. Bender, D. H. Buckley, W. M. Sattley, and D. A. Stahl. 2017. Brock Biology of microorganisms. Page (Pearson, Ed.). 15th edition.

Madrid, F., M. Rubio-Bellido, J. Villaverde, M. Tejada, and E. Morillo. 2016. Natural attenuation of fluorene and pyrene in contaminated soils and assisted with hydroxypropyl-β-cyclodextrin. Effect of co-contamination. Science of the Total Environment 571:42–49.

Majone, M., R. Verdini, F. Aulenta, S. Rossetti, V. Tandoi, N. Kalogerakis, S. Agathos, S. Puig, G. Zanaroli, and F. Fava. 2015. In situ groundwater and sediment bioremediation: Barriers and perspectives at European contaminated sites. New Biotechnology 32:133–146.

Malvankar, N. S., J. Lau, K. P. Nevin, A. E. Franks, M. T. Tuominen, and D. R. Lovley. 2012. Electrical conductivity in a mixed-species biofilm. Applied and environmental microbiology 78:5967–5971.

Malvankar, N. S., and D. R. Lovley. 2015. Electronic Conductivity in Living Biofilms: Physical Meaning, Mechanisms, and Measurement Methods. Page *in* H. Beyenal and J. Babauta, editors. Biofilms in Bioelectrochemical Systems: From Laboratory Practice to Data Interpretation. John Wiley & Sons, Inc.

Malvankar, N. S., M. Vargas, K. P. Nevin, A. E. Franks, C. Leang, B.-C. Kim, K. Inoue, T. Mester, S. F. Covalla, J. P. Johnson, V. M. Rotello, M. T. Tuominen, and D. R. Lovley. 2011a. Tunable metallic-like conductivity in microbial nanowire networks. Nature Nanotechnology 6:573–579.

Malvankar, N. S., M. Vargas, K. P. Nevin, A. E. Franks, C. Leang, B. Kim, K. Inoue, T. Mester, S. F. Covalla, J. P. Johnson, M. Rotello, M. T. Tuominen, and D. R. Lovley. 2011b. Tunable metallic-like conductivity in microbial nanowire networks Supplementary figures:1–12.

Manap, N., and N. Voulvoulis. 2015. Environmental management for dredging sediments - The requirement of developing nations. Journal of Environmental Management 147:338–348.

MAPMED - ENPI CBCMED Project “Management of port areas in the Mediterranean sea Basin” 2015a. Site Characterization Report: Cagliari Port-Sardinia, Italy.

MAPMED - ENPI CBCMED Project “Management of port areas in the Mediterranean sea

Basin" 2015b. Site Characterization Report: El Kantaoui Port-Tunisia.

McFarland, M. J., and R. C. Sims. 1991. Thermodynamic Framework for Evaluating PAH Degradation in the Subsurface.

Mcnally, D. L., I. J. R. Mihelcic, and D. R. Lueking. 1999. Biodegradation of mixtures of polycyclic aromatic hydrocarbons under aerobic and nitrate-reducing conditions. Chemosphere 38:1313–1321.

Mcnally, D. L., J. R. Mihelcic, and D. R. Lueking. 1998. Biodegradation of three- and four-ring polycyclic aromatic hydrocarbons under aerobic and denitrifying conditions. Environmental Science and Technology 32:2633–2639.

Meckenstock, R. U., M. Boll, H. Mouttaki, J. S. Koelschbach, P. Cunha Tarouco, P. Weyrauch, X. Dong, and A. M. Himmelberg. 2016. Anaerobic degradation of benzene and polycyclic aromatic hydrocarbons. Journal of Molecular Microbiology and Biotechnology 26:92–118.

Milia, S., C. Camedda, G. Erby, and A. Carucci. 2017a. Effects of different operating conditions on sediment slurry sequencing batch reactors treating marine port sediments contaminated by PAHs.

Milia, S., C. Camedda, G. Erby, M. Mascia, B. Virdis, and A. Carucci. 2017b. Preliminary evaluation of microbial fuel cells applicability to bioremediate marine sediments contaminated by polycyclic aromatic hydrocarbons.

Miller, R. M. 1995. Surfactant-Enhanced Bioavailability of Slightly Soluble Organic Compounds 1. Bioremediation: science and applications:33–54.

Millo, D. 2012. Spectroelectrochemical analyses of electroactive microbial biofilms. Biochemical Society Transactions 40:1284–1290.

Mohan, S. V., and K. Chandrasekhar. 2011. Self-induced bio-potential and graphite electron accepting conditions enhances petroleum sludge degradation in bio-electrochemical system with simultaneous power generation. Bioresource Technology 102:9532–9541.

Moon, I. K., J. Lee, R. S. Ruoff, and H. Lee. 2010. Reduced graphene oxide by chemical graphitization. Nature Communications 1:1–6.

Morris, J. M., and S. Jin. 2012. Enhanced biodegradation of hydrocarbon-contaminated sediments using microbial fuel cells. Journal of Hazardous Materials 213–214:474–477.

Mueller, J. G., P. J. Chapman, and P. H. Pritchard. 1989. Creosote-contaminated sites. Their

potential for bioremediation. Environmental science & technology 23:1197–1201.

Nemati, M., T. J. Mazutinec, G. E. Jenneman, and G. Voordouw. 2001. Control of biogenic h2s production with nitrite and molybdate. Journal of Industrial Microbiology and Biotechnology 26:350–355.

Nichols, G. 2009. Sedimentology and stratigraphy. Page Journal of Chemical Information and Modeling.

Nielsen, L. P., N. Risgaard-Petersen, H. Fossing, P. B. Christensen, and M. Sayama. 2010. Electric currents couple spatially separated biogeochemical processes in marine sediment. Nature 463:1071–1074.

Oldeman, L. R., R. T. A. Hakkeling, and W. G. Sombroek. 1991. Glasod world map of the status of human-induced soil degradation. ISRIC, Wageningen UNEP, Nairobi.

Park, D. H., and J. G. Zeikus. 2000. Electricity Generation in Microbial Fuel Cells Using Neutral Red as an Electronophore Electricity Generation in Microbial Fuel Cells Using Neutral Red as an Electronophore 66:1292–1297.

Petrova, M., and M. Bojinov. 2011. Electrodeposition kinetics of molybdenum oxides from ammonia-molybdate electrolyte. Bulletin of alloy phase diagrams 11:96–99.

Pfeffer, C., S. Larsen, J. Song, M. Dong, F. Besenbacher, R. L. Meyer, K. U. Kjeldsen, L. Schreiber, Y. A. Gorby, M. Y. El-Naggar, K. M. Leung, A. Schramm, N. Risgaard-Petersen, and L. P. Nielsen. 2012. Filamentous bacteria transport electrons over centimetre distances. Nature 491:218–221.

Pirbadian, S., and M. Y. El-Naggar. 2012. Multistep hopping and extracellular charge transfer in microbial redox chains. Physical Chemistry Chemical Physics 14:13802–13808.

Pisciotta, J. M., and J. J. Dolceamore Jr. 2016. Bioelectrochemical and Conventional Bioremediation of Environmental Pollutants. Journal of Microbial & Biochemical Technology 8:327–343.

Prasanna, D., S. Venkata Mohan, B. Purushotham Reddy, and P. N. Sarma. 2008. Bioremediation of anthracene contaminated soil in bio-slurry phase reactor operated in periodic discontinuous batch mode. Journal of Hazardous Materials 153:244–251.

Predicala, B., M. Nemati, S. Stade, and C. Laguë. 2008. Control of H2S emission from swine manure using Na-nitrite and Na-molybdate. Journal of Hazardous Materials 154:300–309.

Rabaey, K., N. Boon, M. Höfte, and W. Verstraete. 2005a. Microbial phenazine production

enhances electron transfer in biofuel cells. Environmental Science and Technology 39:3401–3408.

Rabaey, K., W. Ossieur, M. Verhaege, and W. Verstraete. 2005b. Continuous microbial fuel cells convert carbohydratesto electricity. Water Science and Technology 52:515–523.

Rabaey, K., K. Van de Sompel, L. Maignien, N. Boon, P. Aelterman, P. Clauwaert, L. De Schamphelaire, H. T. Pham, V. Jan, M. Verhaege, P. Lens, and W. Verstraete. 2006. Microbial Fuel Cells for Sulfide Removal. Environ Sci Technol. 40:5218–5224.

Reimers, C. E. 2001. Harvesting Energy from the Marine Sediment - Water Interface 35:192–195.

Richardson, D. J. 2000. Bacterial respiration: A flexibe process for a changing environment. Microbiology 146:551–571.

Robles-González, I. V., F. Fava, and H. M. Poggi-Varaldo. 2008. A review on slurry bioreactors for bioremediation of soils and sediments. Microbial Cell Factories 7:1–16.

Rothermich, M. M., L. A. Hayes, and D. R. Lovley. 2002. Anaerobic, sulfate-dependent degradation of polycyclic aromatic hydrocarbons in petroleum-contaminated harbor sediment. Environmental Science and Technology 36:4811–4817.

Rouse, J. D., D. A. Sabatini, J. M. Suflita, and J. H. Harwell. 1994. Influence of surfactants on microbial degradation of organic compounds. Critical Reviews in Environmental Science and Technology 24:325–370.

Rozendal, A., H. V. M. Hamelers, K. Rabaey, J. Keller, and C. J. N. Buisman. 2008. Towards practical implementation of bioelectrochemical wastewater treatment.

Salas, E. C., Z. Sun, A. Lu, and J. M. Tour. 2010. Reduction of Graphene Oxide via. ACS nano 4:4852–4856.

Salomons, W., and J. Brils. 2004. Contaminated Sediments in European River Basins. European Sediment Research Network:71.

Samanta, S. K., O. V. Singh, and R. K. Jain. 2002. Polycyclic aromatic hydrocarbons: Environmental pollution and bioremediation. Trends in Biotechnology 20:243–248.

Schauer, R., N. Risgaard-Petersen, K. U. Kjeldsen, J. J. Tataru Bjerg, B. B. Jørgensen, A. Schramm, and L. P. Nielsen. 2014. Succession of cable bacteria and electric currents in marine sediment. ISME Journal 8:1314–1322.

Schröder, U. 2007. Anodic electron transfer mechanisms in microbial fuel cells and their energy efficiency. Physical Chemistry Chemical Physics 9:2619–2629.

Schulz, H. D. 2006. Quantification of early diagenesis: dissolved constituents in pore water and signals in the solid phase. Pages 73–124 Marine Geochemistry. Springer.

Semple, K. T., K. J. Doick, L. Y. Wick, and H. Harms. 2007. Microbial interactions with organic contaminants in soil: Definitions, processes and measurement. Environmental Pollution 150:166–176.

Shen, H. 2016. Polycyclic Aromatic Hydrocarbons. Page Ecotoxicology Essentials.

Shen, H., Y. Huang, R. Wang, D. Zhu, W. Li, G. Shen, B. Wang, Y. Zhang, Y. Chen, Y. Lu, H. Chen, T. Li, K. Sun, B. Li, W. Liu, J. Liu, and S. Tao. 2013. Global atmospheric emissions of polycyclic aromatic hydrocarbons from 1960 to 2008 and future predictions. Environmental Science and Technology 47:6415–6424.

Sherafatmand, M., and H. Y. Ng. 2015. Using sediment microbial fuel cells (SMFCs) for bioremediation of polycyclic aromatic hydrocarbons (PAHs). Bioresource Technology 195:122–132.

Shi, L., H. Dong, G. Reguera, H. Beyenal, A. Lu, J. Liu, H. Q. Yu, and J. K. Fredrickson. 2016. Extracellular electron transfer mechanisms between microorganisms and minerals. Nature Reviews Microbiology 14:651–662.

Shi, L., D. J. Richardson, Z. Wang, S. N. Kerisit, K. M. Rosso, J. M. Zachara, and J. K. Fredrickson. 2009. The roles of outer membrane cytochromes of Shewanella and Geobacter in extracellular electron transfer. Environmental Microbiology Reports 1:220–227.

Shuttleworth, K. L., and C. E. Cerniglia. 1995. Environmental Aspects of PAH Biodegradation. Applied Biochemistry and Biotechnology 54:291–302.

Snider, R. M., S. M. Strycharz-Glaven, S. D. Tsoi, J. S. Erickson, and L. M. Tender. 2012. Long-range electron transport in Geobacter sulfurreducens biofilms is redox gradient-driven. Proceedings of the National Academy of Sciences 109:15467–15472.

Stankovich, S., D. A. Dikin, R. D. Piner, K. A. Kohlhaas, A. Kleinhammes, Y. Jia, Y. Wu, S. B. T. Nguyen, and R. S. Ruoff. 2007. Synthesis of graphene-based nanosheets via chemical reduction of exfoliated graphite oxide. Carbon 45:1558–1565.

Straube, W. L., C. C. Nestler, L. D. Hansen, D. Ringleberg, P. H. Pritchard, and J. Jones-

Meehan. 2003. Remediation of polyaromatic hydrocarbons (PAHs) through landfarming with biostimulation and bioaugmentation. Acta Biotechnologica 23:179–196.

Stringfellow, W. T., and M. D. Aitken. 1995. Competitive metabolism of naphthalene, methylnaphthalenes, and fluorene by phenanthrene-degrading pseudomonads. Applied and environmental microbiology 61:357–362.

Stucki, G., and M. Alexander. 1987. Role of dissolution rate and solubility in biodegradation of aromatic compounds. Applied and Environmental Microbiology 53:292–297.

Stumm, W., and J. J. Morgan. 1996. Aquatic chemistrychemical equilibria and rates in natural waters.

Syama, S., and P. V. Mohanan. 2016. Safety and biocompatibility of graphene: A new generation nanomaterial for biomedical application. International Journal of Biological Macromolecules 86:546–555.

Tanizawa, Y., Y. Okamoto, K. Tsuzuki, Y. Nagao, N. Yoshida, R. Tero, S. Iwasa, A. Hiraishi, Y. Suda, and H. Takikawa. 2012. Microorganism mediated synthesis of reduced graphene oxide films. Page 12011 Journal of Physics: Conference Series. IOP Publishing.

Tender, L. M., C. E. Reimers, H. A. Stecher, D. E. Holmes, D. R. Bond, D. A. Lowy, K. Pilobello, S. J. Fertig, and D. R. Lovley. 2002. Harnessing microbially generated power on the seafloor. Nature Biotechnology 20:821–825.

Todaro, F., S. De Gisi, and M. Notarnicola. 2016. Contaminated Marine Sediments : Waste or Resource ? Procedia Environmental Science, Engineering and Management 3:157–164.

Torres, C. I., A. K. Marcus, P. Parameswaran, and B. E. Rittmann. 2008. Kinetic experiments for evaluating the Nernst− Monod model for anode-respiring bacteria (ARB) in a biofilm anode. Environmental science & technology 42:6593–6597.

Townsend, G. T., R. C. Prince, and J. M. Suflita. 2003. Anaerobic Oxidation of Crude Oil Hydrocarbons by the Resident Microorganisms of a Contaminated Anoxic Aquifer. Environmental Science and Technology 37:5213–5218.

UNI EN 15105. 2011. Biocombustibili solidi - Metodi per la determinazione del contenuto di cloro, sodio e potassio solubili in acqua.

USEPA. 1990. Engineering Bulletin: Slurry Biodegradation. Cincinnati, OH.

USEPA. 2014. Priority Pollutant List. Effluent Guidelines:2.

Vagge, G., L. Cutroneo, M. Castellano, G. Canepa, R. Maria, and M. Capello. 2018. The effects of dredging and environmental conditions on concentrations of polycyclic aromatic hydrocarbons in the water column. Marine Pollution Bulletin 135:704–713.

Venkata Mohan, S., D. Prasanna, B. Purushotham Reddy, and P. N. Sarma. 2008. Ex situ bioremediation of pyrene contaminated soil in bio-slurry phase reactor operated in periodic discontinuous batch mode: Influence of bioaugmentation. International Biodeterioration and Biodegradation 62:162–169.

Viggi, C. C., E. Presta, M. Bellagamba, S. Kaciulis, S. K. Balijepalli, G. Zanaroli, M. P. Papini, S. Rossetti, and F. Aulenta. 2015. The "Oil-Spill Snorkel": An innovative bioelectrochemical approach to accelerate hydrocarbons biodegradation in marine sediments. Frontiers in Microbiology 6:1–11.

Virdis, B., and P. G. Dennis. 2017. The nanostructure of microbially-reduced graphene oxide fosters thick and highly-performing electrochemically-active biofilms. Journal of Power Sources 356:556–565.

Virdis, B., D. Millo, B. C. Donose, Y. Lu, D. J. Batstone, and J. O. Krömer. 2016. Analysis of electron transfer dynamics in mixed community electroactive microbial biofilms. RSC Advances 6:3650–3660.

Virdis, B., K. Rabaey, Z. Yuan, R. A. Rozendal, and J. Keller. 2009. Electron Fluxes in a Microbial Fuel Cells Performing Carbon and Nitrogen Removal.pdf. Environmental Science & Technology 43:5144–5149.

Volkering, F., A. M. Breure, A. Sterkenburg, and J. G. van van Andel. 1992. Microbial degradation of polycyclic aromatic hydrocarbons: effect of substrate availability on bacterial growth kinetics. Applied Microbiology and Biotechnology 36:548–552.

Walker, H. J. 2012. Artificial structures and shorelines. Springer Science & Business Media.

Walter, U., M. Beyer, J. Klein, and H.-J. Rehm. 1991. Degradation of pyrene byRhodococcus sp. UW1. Applied Microbiology and Biotechnology 34:671–676.

Wang, G., F. Qian, C. W. Saltikov, Y. Jiao, and Y. Li. 2011. Microbial reduction of graphene oxide by Shewanella. Nano Research 4:563–570.

Wang, H. X., and P. F. Andutta. 2013a. Sediment Transport Dynamics in Ports, Estuaries and Other Coastal Environments. Pages 2–3 *in* I. Sediment Transport Andrew Manning, editor. Sediment Transport Processes and Their Modelling Applications.

Wang, H. X., and P. F. Andutta. 2013b. Sediment Transport Dynamics in Ports, Estuaries and Other Coastal Environments. Pages 2–3 *in* I. Sediment Transport Andrew Manning, editor. Sediment Transport Processes and Their Modelling Applications.

Wang, X., Z. Cai, Q. Zhou, Z. Zhang, and C. Chen. 2012. Bioelectrochemical stimulation of petroleum hydrocarbon degradation in saline soil using U-tube microbial fuel cells. Biotechnology and Bioengineering 109:426–433.

Weissenfels, W. D., M. Beyer, and J. Klein. 1990. Degradation of phenanthrene, fluorene and fluoranthene by pure bacterial cultures. Applied Microbiology and Biotechnology 32:479–484.

White, D. 1995. The Physiology and Biochemistry of Prokaryotesny. New York: Oxford University Press, NY (US).

Wick, A. F., N. W. Haus, B. F. Sukkariyah, K. C. Haering, and W. L. Daniels. 2011. Remediation of PAH-contaminated soils and sediments: A literature review. CSES Department, internal research document.

Wolin, E. A., M. Wolin, and R. S. Wolfe. 1963. Formation of methane by bacterial extracts. Journal of Biological Chemistry 238:2882–2886.

Yan, Z., N. Song, H. Cai, J. H. Tay, and H. Jiang. 2012. Enhanced degradation of phenanthrene and pyrene in freshwater sediments by combined employment of sediment microbial fuel cell and amorphous ferric hydroxide. Journal of Hazardous Materials 199–200:217–225.

Yuan, S. Y., S. H. Wei, and B. V. Chang. 2000. Biodegradation of polycyclic aromatic hydrocarbons by a mixed culture. Chemosphere 41:1463–1468.

Zacharoff, L. A., and M. Y. El-Naggar. 2017. Redox conduction in biofilms: From respiration to living electronics. Current Opinion in Electrochemistry 4:182–189.

Zappi, M. E., B. A. Rogers, C. L. Teeter, D. Gunnison, and R. Bajpai. 1996. Bioslurry treatment of a soil contaminated with low concentrations of total petroleum hydrocarbons. Journal of Hazardous Materials 46:1–12.

Zhang, L., P. Li, Z. Gong, and X. Li. 2008. Photocatalytic degradation of polycyclic aromatic hydrocarbons on soil surfaces using TiO2 under UV light. Journal of Hazardous Materials 158:478–484.

Zhang, T., S. M. Gannon, K. P. Nevin, A. E. Franks, and D. R. Lovley. 2010. Stimulating the anaerobic degradation of aromatic hydrocarbons in contaminated sediments by providing

an electrode as the electron acceptor. Environmental Microbiology 12:1011–1020.

Zhang, Y., and S. Tao. 2009. Global atmospheric emission inventory of polycyclic aromatic hydrocarbons (PAHs) for 2004. Atmospheric Environment 43:812–819.

Zhang, Z., and I. M. C. Lo. 2015. Biostimulation of petroleum-hydrocarbon-contaminated marine sediment with co-substrate: involved metabolic process and microbial community. Applied Microbiology and Biotechnology 99:5683–5696.

Zheng, Z., Y. Zhang, X. Su, and X. Cui. 2016. Responses of hydrochemical parameters, community structures, and microbial activities to the natural biodegradation of petroleum hydrocarbons in a groundwater–soil environment. Environmental Earth Sciences 75:1–13.

Zhou, L., D. Deng, D. Zhang, Q. Chen, J. Kang, N. Fan, and Y. Liu. 2016. Microbial Electricity Generation and Isolation of Exoelectrogenic Bacteria Based on Petroleum Hydrocarbon-contaminated Soil. Electroanalysis 28:1510–1516.

https://definedterm.com/biological_pump

http://ec.europa.eu/environment/water/water-framework/info/intro_en.htm

http://www.imo.org/en/OurWork/Environment/LCLP/Pages/default.aspx

https://www.graphene-info.com/abalonyx-sees-go-production-cost-reaching-22-eurokg-high-volumes

https://1-stromvergleich.com/electricity-prices-europe/